

---

[All ETDs from UAB](#)

[UAB Theses & Dissertations](#)

---

2007

## **Dysregulated ENAC and NHE Function in Cilium-Deficient Renal Collecting Duct Cell Monolayers, a Model of Polycystic Kidney Disease**

Dragos S. Olteanu

Follow this and additional works at: <https://digitalcommons.library.uab.edu/etd-collection>

---

### **Recommended Citation**

Olteanu, Dragos S., "Dysregulated ENAC and NHE Function in Cilium-Deficient Renal Collecting Duct Cell Monolayers, a Model of Polycystic Kidney Disease" (2007). *All ETDs from UAB*. 6718.  
<https://digitalcommons.library.uab.edu/etd-collection/6718>

This content has been accepted for inclusion by an authorized administrator of the UAB Digital Commons, and is provided as a free open access item. All inquiries regarding this item or the UAB Digital Commons should be directed to the [UAB Libraries Office of Scholarly Communication](#).

DYSREGULATED ENAC AND NHE FUNCTION IN CILIUM-DEFICIENT RENAL  
COLLECTING DUCT CELL MONOLAYERS, A MODEL OF POLYCYSTIC  
KIDNEY DISEASE

by

DRAGOS S. OLTEANU

ERIK M. SCHWIEBERT, COMMITTEE CHAIR  
MARK O. BEVENSEE  
JOHN P. CLANCY  
PETER R. SMITH  
BRADLEY K. YODER

A DISSERTATION

Submitted to the graduate faculty of the University of Alabama at Birmingham,  
in partial fulfillment of the requirements for the degree of  
Doctor of Philosophy

BIRMINGHAM, ALABAMA

2007

DYSREGULATED ENAC AND NHE FUNCTION IN CILIUM-DEFICIENT RENAL  
COLLECTING DUCT CELL MONOLAYERS, A MODEL OF POLYCYSTIC  
KIDNEY DISEASE

DRAGOS S. OLTEANU

CELLULAR AND MOLECULAR PHYSIOLOGY

ABSTRACT

Polycystic kidney disease in both its recessive and dominant forms involves the remodeling of the kidney and extra-renal tissues where parts of the tissue break contact with the normal tissue as “pseudocysts” or fully encapsulated and fluid-filled cysts. Once this remodeling into “cystic” tissue has occurred, the secondary progression of the disease is influenced dramatically by salt and water transport and by autocrine and paracrine factors that become trapped in these abnormal cystic microenvironments. During this progression, hypertension develops ahead of renal decline. In recessive PKD (ARPKD), there is early onset hypertension in neonatal and pediatric patients that is severe and debilitating. My research has focused on cilium-deficient cortical collecting duct principal cell models of PKD from the  $Tg737^{orpK}$  mouse. My work is being extended to conditional cilium-deficient cell models as well as the mouse models from which these cells were derived. I have found that ENaC is 4-fold upregulated in cilium-deficient versus cilium-competent cell monolayers. This upregulation may be central to the rapid development of hypertension. In parallel, there is inappropriate mislocalization of sodium/hydrogen (Na/H) exchange (NHE) in the apical membrane of cilium-deficient cell monolayers versus controls. Together, apical NHE activity with ENaC upregulation may contribute marked  $Na^+$  hyperabsorption leading to hypertension in ARPKD and, perhaps, ADPKD patients. This cilium-deficient pathology creates an intriguing

pathophysiology where NHEs and ENaC are in the same apical membrane domain in principal cells. Apical NHE activity would fuel ENaC activity via extracellular acidification and intracellular alkalization. Metabolic pH measurements of freshly voided urine showed enhanced acidification in the mutant mice at all ages between 1 and 4 weeks. Metabolic alkalosis developed at 4 weeks of age. My future work will seek to understand why the loss of a sensory organelle, the primary or central monocilium, leads to upregulation of salt and water reabsorption in terms of epithelial cell pathophysiology. Steps designed to quell salt hyperabsorption may be beneficial in controlling the establishment and progression of cystic kidney disease in humans.

## DEDICATION

This thesis is dedicated to my beloved wife Melinda and my daughter Andra. I thank them for their continued support and encouragement through these past four years. This work is also dedicated to my parents for their guidance and support of my career. Last but not least, I would like to thank my teachers and professors throughout the years who believed in me, helping me to reach my goals, without giving up on me.

## ACKNOWLEDEMENTS

I would like to thank and acknowledge Erik M Schwiebert, Mark O Bevensee, Bradley K Yoder, Peter Komlosi, James Fortenberry, Elisabeth Welty, Nai-Lin Cheng, Clintoria Williams, Venus Childress Roper, and Mandy Croyle for their help and assistance in my graduate studies, as well as their contributions to this work. I would like to express appreciation and thanks to my committee members Erik M Schwiebert, Mark O Bevensee, Bradley K Yoder, Peter R Smith and John P Clancy who offered their time and expertise. I would also like to thank Dale Benos, Lisa M Schwiebert, Peter R Smith, Shawn Galin, Patricia Matthews, and Kathy McConnell as a part of the Cellular and Molecular Physiology graduate program. Finally, I would especially like to thank my mentor, Erik Schwiebert who believed in me and had patience when times were hard. His support and guidance have been invaluable.

## TABLE OF CONTENTS

	<i>Page</i>
ABSTRACT.....	ii
DEDICATION.....	iv
ACKNOLEGEMENTS.....	v
LIST OF TABLES.....	ix
LIST OF FIGURES .....	x
INTRODUCTION .....	1
SODIUM AND WATER REABSORPTION ALONG THE NEPHRON .....	2
Proximal Tubule.....	2
Loop of Henle .....	3
Distal Tubule.....	4
Cortical Collecting Duct .....	4
EPITHELIAL SODIUM CHANNEL (ENaC) .....	7
Subunits and Structure .....	7
Regulation.....	8
Expression Along the Nephron.....	10
ENaC-Related Kidney Diseases .....	12
ENaC-Related Lung Disorders .....	13

## TABLE OF CONTENTS (CONTINUED)

	<i>Page</i>
SODIUM/HYDROGEN EXCHANGERS (NHEs) .....	14
Structure, Isoforms and Cellular Localization .....	14
Molecular Physiology and Pharmacology .....	16
Tissue Localization, Regulation and Function.....	17
PRIMARY CILIA, POLYCYSTIC KIDNEY DISEASE, AND DYSREGULATION OF SALT AND WATER BALANCE .....	25
Primary Cilia Structure .....	25
Implications of Cilia in Cystic Diseases .....	27
Salt and Water Balance Dysregulation in Cystic Diseases.....	28
POLYCYSTIC KIDNEY DISEASES .....	29
Autosomal Dominant Polycystic Kidney Disease (ADPKD).....	30
Autosomal Recessive Polycystic Kidney Disease (ARPKD).....	36
SUMMARY .....	40
HEIGHTENED ENAC-MEDIATED SODIUM ABSORPTION IN A MURINE POLYCYSTIC KIDNEY DISEASE MODEL EPITHELIUM LACKING APICAL MONOCILIA .....	42
INAPPROPRIATE SODIUM/HYDROGEN EXCHANGE ON THE APICAL SURFACE OF A CILIUM-DEFICIENT CORTICAL COLLECTING DUCT PRINCIPAL CELL MODEL OF POLYCYSTIC KIDNEY DISEASE .....	93
DISCUSSION.....	150
THE FUNDAMENTAL QUESTION .....	151
HYPOTHESES .....	153



## TABLE OF CONTENTS (CONTINUED)

	<i>Page</i>
FUTURE DIRECTIONS .....	155
SUMMARY OF APPROACH .....	170
FUTURE LINES OF INVESTIGATION.....	177
CONCLUSIONS.....	182
GENERAL LIST OF REFERENCES .....	183
APPENDICES	
A MEMORANDUM.....	224
B NOTICE OF APPROVAL .....	226

## LIST OF TABLES

*Table*

*Page*

## FUTURE DIRECTIONS

1. NHE Primers.....	175
---------------------	-----

## LIST OF FIGURES

<i>Figure</i>	<i>Page</i>
INTRODUCTION	
1. Sodium Handling Along the Nephron .....	6
2. Cortical Collecting Duct Principal Cells versus Intercalated Cells .....	11
3. Distribution of Sodium-Hydrogen Exchangers Along The Nephron .....	24
HEIGHTENED ENAC-MEDIATED SODIUM ABSORPTION IN A MURINE POLYCYSTIC KIDNEY DISEASE MODEL EPITHELIUM LACKING APICAL MONOCILIA	
1. Transepithelial Voltage Is Enhanced Markedly in Mutant <i>orp</i> <i>k</i> Collecting Duct Principal Cell Clones Grown as Well-Polarized Monolayers.....	85
2. Heightened Transepithelial Voltage Is a Consistent and Reproducible Phenotype in Mutant <i>orp</i> <i>k</i> Collecting Duct Principal Cell Clones Grown as Well-Polarized Monolayers and Studied in Parallel to Counterpart Controls.....	86
3. Heightened Transepithelial Voltage in Mutant <i>orp</i> <i>k</i> Collecting Duct Principal Cell Monolayers and Measurable Voltage in Genetically Rescued <i>orp</i> <i>k</i> Monolayers Is Inhibited in a Dose-Dependent Manner by Amiloride.....	87
4. Heightened Transepithelial Short-Circuit Current in Mutant <i>orp</i> <i>k</i> Collecting Duct Principal Cell Monolayers and Measurable Current in Genetically Rescued <i>orp</i> <i>k</i> Monolayers Is Inhibited in a Dose-Dependent Manner by Amiloride.....	88
5. Cell Culture Conditions and the Dynamics of Electrical Measurements Affect Transepithelial Voltage and Current in Mutant and Rescued <i>orp</i> <i>k</i> Collecting Duct Principal Cell Monolayers Profoundly .....	89

## LIST OF FIGURES (CONTINUED)

<i>Figure</i>	<i>Page</i>
6. The ENaC-selective Amiloride Analog, Benzamil, Inhibits Transepithelial Voltage and Current Markedly But Not Completely in Mutant <i>orpk</i> Collecting Duct Principal Cell Monolayers .....	90
7. Additional Amiloride Analogs, EIPA and DMA, Also Inhibit Upregulated $V_{TE}$ in Mutant Monolayers: Additive Inhibition with Different Pairs of Analogs .....	91
8. Protease Inhibitors Attenuate Transepithelial Voltage and Current in Mutant <i>orpk</i> Collecting Duct Principal Cell Monolayers, Suggesting ENaC Hyperactivity.....	92
<p>INAPPROPRIATE SODIUM/HYDROGEN EXCHANGE ON THE APICAL SURFACE OF A CILIUM-DEFICIENT CORTICAL COLLECTING DUCT PRINCIPAL CELL MODEL OF POLYCYSTIC KIDNEY DISEASE</p>	
1. Proton Pseudoflux Measurements and Calculations.....	136-137
2. Flow Chamber and Early $Na^+$ Removal and Re-Addition Protocols .....	138-139
3. Multiple Mutant Cell Clones Display this Mislocalized Apical NHE Activity in Addition to Normal Basolateral-exclusive NHE Activity Displayed in Multiple Rescued Cell Clones.....	140-141
4. Lower and Faster Acidification, Higher Alkalinization and Higher Apical Acid Extrusion Capacity in Mutant versus Rescued Cells Monolayers.....	142-143
5. Pharmacological Assessment of Apical NHE Activities .....	144
6. Pharmacological Assessment of Basolateral NHE Activities.....	145-146
7. $pHi$ Dependencies of Cariporide-Sensitive Acid Extrusion .....	147
8. Imaging of the Ciliary Status and the Cystic Nature of Kidneys in the HoxB7 Cre-Lox Kidney-specific Conditional Cilium knockout Mouse Model; Urinary and Blood pH. Metabolic Measurements of Fresh Urine and Plasma Samples Reveals Acid-Base Balance Anomalies in Cilium-deficient PKD Mouse Models.....	148-149

## LIST OF FIGURES (CONTINUED)

<i>Figure</i>	<i>Page</i>
---------------	-------------

### DISCUSSIONS

4. Differences in Renal Tubule Re-Modeling in ARPKD versus ADPKD .....	152
5. Compensatory Overexpression and Redistribution .....	154
6. Dysregulation due to Loss of Cilium-derived Signal.....	156
7. Dysregulation due to a Change in Localization.....	160
8. The ENaC Upregulation Problem.....	163
9. The Apical NHE Problem.....	165
10. The Apical NHE-ENaC Crosstalk Problem.....	167

### FUTURE DIRECTIONS

11. ENaC RT-PCR Products.....	172
12. NHE RT-PCR Products .....	176

## INTRODUCTION

Recent discoveries from candidate gene analysis, positional cloning, proteomic analysis, and cellular and molecular biology have revealed that most protein products of human cystic kidney disease genes (as well as several homolog genes found in experimental models) are localized, at least in part, to the primary cilia, basal body or centrosomal region (Refs. 1, 2). Primary cilia may act as flow sensors and, possibly, as chemosensors or osmosensors along the nephron (Refs. 3). Cilia may initiate signal transduction which affects cell cycle regulation, tubular differentiation, epithelial cell polarity and cell secretion (Ref. 2). Cystic epithelial cells continue to transport chloride ( $\text{Cl}^-$ ), bicarbonate ( $\text{HCO}_3^-$ ), potassium ( $\text{K}^+$ ),  $\text{Na}^+$  and  $\text{H}^+$  across the cell membrane in a manner similar to that of the nephron segment from which they are derived. However, because of the changes in cell polarity and kidney architecture, absorption and secretion of stimulatory or inhibitory factors, and modifications of gene expression, dysregulated transport of electrolytes within cystic kidney tissues may contribute to the progression of the disease and, more precisely, may primarily contribute to the development of profound hypertension early in ARPKD and during ADPKD (Refs. 4, 5, 6). The work of my thesis dissertation seeks to define the dysregulation of sodium and water transport in cilium-deficient “cystic” epithelial cell models from the renal collecting duct versus cilium-competent controls. My results may explain the underlying pathophysiology that leads

to cystic disease progression and hypertension in ARPKD.

## SODIUM AND WATER REABSORPTION ALONG THE NEPHRON

Water and  $\text{Na}^+$  transport processes and how they influence salt and water balance are critical in maintaining homeostasis and blood pressure control (Ref. 7). The kidney plays a major role in balancing the daily intake of fluid and salt with urinary  $\text{Na}^+$  and water excretion. Under normal circumstances, when blood pressure increases, the kidney begins to excrete sodium and water at a higher rate. As a result, the extracellular fluid volume decreases causing blood pressure to drop. Hypertension develops when the kidney requires higher than normal blood pressure to maintain the balance between intake and excretion of sodium and water (Ref. 7). Sodium and water are freely filtered at the glomeruli. Normally, approximately 99% of filtered sodium is reabsorbed through various  $\text{Na}^+$ -selective transporters located along the nephron (Ref. 8).

### Proximal Tubule

The proximal tubule reabsorbs roughly 50% of the filtered  $\text{Na}^+$  and 70-90% of  $\text{HCO}_3^-$  (via basolateral  $\text{Na}^+/\text{HCO}_3^-$  cotransporter) but causes only minor changes in fluid composition (Ref. 8). Because the apical membrane contains multiple microvilli, the capacity for volume transport across the proximal tubule is greatly increased. The transport systems reabsorb electrolytes at a high rate, but because the proximal tubule has a high water permeability and a high paracellular conductance, there are only small osmotic gradients across the tubular cells (Ref. 8). There are multiple  $\text{Na}^+$  transporters in

the apical membrane and most of them are coupled with substrates such as carbohydrates and amino acids. These types of transporters account for a small fraction of sodium reabsorption; however, the majority of sodium reabsorption is mediated by Na/H exchangers (NHEs) (Ref. 8). The activity of apical NHEs are coupled with the basolateral  $\text{Na}^+/\text{K}^+$  ATPase pump which produces a chemical gradient for  $\text{Na}^+$ , causing  $\text{Na}^+$  to travel from the luminal membrane into the peritubular capillary stream (Ref. 8). Inside the cell, carbonic anhydrase transforms water and  $\text{CO}_2$  into protons ( $\text{H}^+$ ) and bicarbonate anions ( $\text{HCO}_3^-$ ) (Ref. 8). As a result of proton secretion, NHEs play a major role in  $\text{HCO}_3^-$  reabsorption.  $\text{Na}^+$  and  $\text{HCO}_3^-$  exits across the basolateral membrane into the blood stream via the sodium bicarbonate cotransporter (NBC) (Ref. 8). Water is reabsorbed mainly through the aquaporin 1 water channel (AQP1) (Ref. 8). The proximal tubule can be the site of impaired  $\text{Na}^+$  reabsorption (Fanconi syndrome, nephrotic syndrome) or enhanced  $\text{Na}^+$  reabsorption (congestive heart failure, cirrhosis) (Ref. 9).

### Loop of Henle

The loop of Henle reabsorbs 30-40% of filtered  $\text{Na}^+$ . Special permeabilities for  $\text{Na}^+$  and water along the different segments of the loop of Henle provide an ingenious mechanism for regulating salt and water excretion (Ref. 8). There is no active transport of  $\text{Na}^+$  and water in the thin descending limb and the thin ascending limb. In the thick ascending limb (TAL), sodium is transported across the apical membrane mainly by  $\text{Na}^+/\text{K}^+/\text{2Cl}^-$  cotransporter and secondarily by NHE which may also contribute  $\text{Na}^+$  and  $\text{HCO}_3^-$  reabsorption (Ref. 8). An electroneutral NBC present in the apical membrane of TAL cells also contributes to  $\text{Na}^+$  and  $\text{HCO}_3^-$  reabsorption. The driving force



coordinating the  $\text{Na}^+$  transport across the loop of Henle is due to the  $\text{Na}^+/\text{K}^+$  ATPase pump. This segment is the site of action for “loop diuretics,” which inhibit  $\text{Na}^+$  reabsorption via the  $\text{Na}^+/\text{K}^+/\text{2Cl}^-$  cotransporter. This is also the site of Bartter’s syndrome, a mutation of the  $\text{Na}^+/\text{K}^+/\text{2Cl}^-$  cotransporter, characterized by  $\text{Na}^+$ ,  $\text{Cl}^-$  and  $\text{K}^+$  wasting and an inability to produce concentrated urine (Ref. 10).

### Distal Tubule

The distal tubule is responsible for reabsorption of 5% of the filtered sodium. In the distal tubule,  $\text{Na}^+$  is transported across the apical membrane primarily by the  $\text{Na}^+/\text{Cl}^-$  cotransporter and secondarily by NHEs (Ref. 8). Loss of  $\text{Na}^+/\text{Cl}^-$  cotransporter function due to a genetic disease (Gitelman's syndrome) or by inhibition with the thiazide class of diuretics, causes a mild degree of  $\text{Na}^+$  and water wasting (Ref. 10). The late distal tubule and connecting tubule reabsorb  $\text{Na}^+$  in a manner similar to the cortical collecting duct (Ref. 8).

### Cortical Collecting Duct

The cortical collecting duct (CCD) is responsible for the fine-tuning of  $\text{Na}^+$  (~3-5% of filtered sodium) and water reabsorption. The CCD contains two types of cells: principal cells and intercalated cells (Ref. 8). Functionally, intercalated cells are implicated in acid-base homeostasis (Ref. 8). Principal cells reabsorb  $\text{Na}^+$  via epithelial sodium channels (ENaC) under the control of aldosterone and vasopressin (Ref. 8). These cells also secrete potassium through an inwardly rectifying  $\text{K}^+$  channel (ROMK) (Ref. 8). The driving force sustaining the function of these channels is due to the  $\text{Na}^+/\text{K}^+$  ATPase

pump, located on the basolateral side. The importance of ENaC in  $\text{Na}^+$  regulation in the CCD is demonstrated by two genetic disorders. Liddle's syndrome is described as a monogenic, hypertensive disorder involving a gain-of-function mutation in ENaC subunits, whereas autosomal recessive pseudohypoaldosteronism type I is a salt-wasting disease with a loss-of-function mutation in ENaC subunits (Ref. 11). The collecting ducts are the chief sites for regulation of water reabsorption. Water permeability in principal cells is low but it can be increased to very high levels when stimulated with vasopressin (ADH - Antidiuretic Hormone). Aquaporin 2 (AQP 2), on the apical side, and aquaporins 3 and 4 on the basolateral side are involved in water reabsorption (Ref. 12). Loss of water due to the dysfunction of AQP 2 is described in some forms of diabetes insipidus and in the syndrome of inappropriate antidiuretic hormone secretion (SIADH) (Ref. 12). Please refer to figure 1 for sodium handling along the nephron.

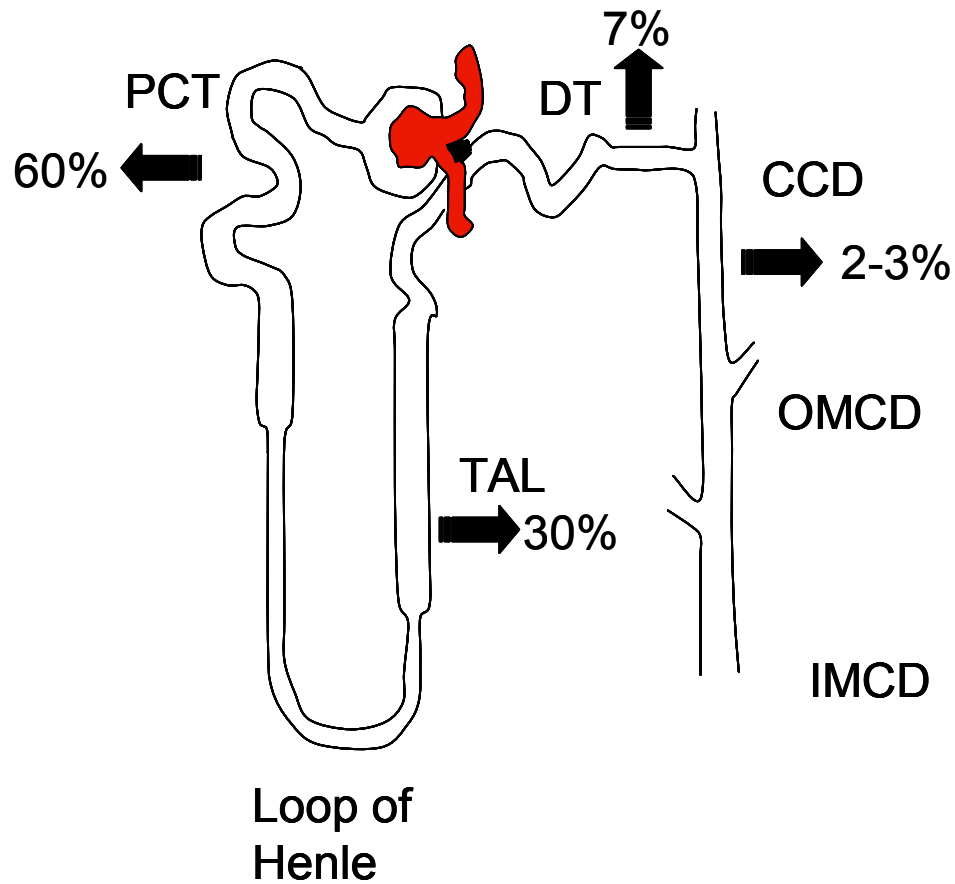


**Figure 1. Sodium Handling Along the Nephron**

With a GFR of 180 L/day and each liter of plasma containing 140 mmol/L  $\text{Na}^+$  then 25,000mmol of  $\text{Na}^+$  are filtered every day. If we take into account that a normal person with a dietary sodium of 200-250mmol excretes 150-200mmol of  $\text{Na}^+$  daily then the fraction of filtered load excreted will be  $\sim 0.6\text{-}0.8\%$ . More than 99% of the filtered sodium is reabsorbed,  $\sim 60\%$  in the proximal tubule,  $\sim 30\%$  in the loop of Henle,  $\sim 7\%$  in distal tubule and about 2-3% in the collecting duct.

## EPITHELIAL SODIUM CHANNEL (ENaC)

### Subunits and Structure

The epithelial sodium channel (ENaC) is a member of a superfamily of ion channels called ENaC/DEG (degenerin) channels. This family is found in mammals, mollusks, nematodes and insects, where it plays roles in electrolyte transport, mechanosensation and neurotransmission (Ref. 13). ENaC is the rate-limiting step in transepithelial sodium reabsorption in the collecting duct, as well as in the respiratory and gastrointestinal tracts (Ref. 13). It can also be found in the salivary and sweat ducts, keratinocytes, taste buds, cochlea, and retina (Ref. 13). It has been proposed that ENaC functions as a mechanoreceptor, which senses both touch and blood pressure (Refs. 14-16). Within the ENaC subfamily, five subunits have been cloned:  $\alpha$ ,  $\beta$ ,  $\gamma$ ,  $\delta$  and  $\epsilon$ -ENaC. The stoichiometry of the channel is still a matter of debate. It is largely accepted that co-expression of  $\alpha$ -ENaC with  $\beta$ -ENaC and  $\gamma$ -ENaC is sufficient to obtain maximal channel current (Ref. 17). ENaC is thought to be a tetrameric structure composed of 2 alpha subunits facing each other, one beta subunit and one gamma subunit (Refs. 18, 19). Others have proposed a hetero-oligomer of eight or nine subunits (Refs. 20-22). The  $\delta$ -ENaC subunit can substitute for the  $\alpha$ -ENaC as the  $\text{Na}^+$  conducting subunit, and it is highly expressed in the human brain, testis, ovary and pancreas (Ref. 23). It is also localized in the neurons of the monkey (Ref. 24) and the rabbit (Ref. 25). From a phylogenetic standpoint, human  $\delta$ -ENaC is more closely related to  $\alpha$ -ENaC, whereas  $\beta$ -ENaC is more closely related to  $\gamma$ -ENaC. The  $\epsilon$ -ENaC subunit was cloned from *Xenopus laevis* (Ref. 26) and it has a high amino acid homology to both  $\alpha$ -ENaC and  $\delta$ -ENaC. All

ENaC subunits possess a large extracellular loop, two short membrane-spanning domains and short cytoplasmic N and C termini (Ref. 27). A unique proline-rich domain, called the PY domain, is found in the carboxyl termini of  $\alpha$ -,  $\beta$ - and  $\gamma$ -ENaC subunits. The PY domain found in  $\alpha$ -ENaC is responsible for apical localization of the channel (Ref. 28), whereas the PY domains found in  $\beta$  and  $\gamma$  subunits are responsible for endocytosis of the channel (Ref. 29). The alpha subunit is required for anchoring the channel to the cytoskeleton (Refs. 30, 31) and for the intracellular pH sensitivity of the channel (Ref. 32). The delta ENaC is shown to be stimulated by an acidic extracellular pH (Ref. 33).

## Regulation

In the polarized cells, ENaC is located on the apical membrane where it mediates vectorial  $\text{Na}^+$  absorption. ENaC has a higher affinity for  $\text{Na}^+$  and  $\text{Li}^+$  than for  $\text{K}^+$  indicating a higher level of selectivity than the voltage-gated  $\text{Na}^+$  channels (Ref. 34). Amiloride, a non-specific  $\text{Na}^+$  transporter blocker, decreases channel conductance and blocks ENaC at submicromolar concentrations (Ref. 13). It is speculated that amiloride may competitively interact with  $\text{Na}^+$  for the same binding site on ENaC (Ref. 34). Based on the pH dependence of the channel and the fact that amiloride is a weak base, it is suggested that during a hyperpolarized membrane state, an ionized form of amiloride would enhance channel blockage (Refs. 35, 36). Membrane hyperpolarization (Ref. 37), stretch (Ref. 38), and flow (Refs. 39, 40) increase ENaC activity, whereas intracellular  $\text{Na}^+$  (Ref. 41),  $\text{Ca}^{2+}$  (Ref. 41) and low pH inhibit ENaC (Ref. 32). There may also be an “ENaC self inhibition” phenomena that appears after rapid  $\text{Na}^+$  addition or amiloride removal (Ref. 26). It is influenced paradoxically by temperature: low temperature

stimulates the channel whereas high temperature inhibits the current (Refs. 43-45). ENaC activity and expression also increased by a short-term, low  $\text{Na}^+$  diet (Refs. 46, 47). Treatment with different enzymes such as trypsin and serine proteases (elastase, prostasin and channel activating proteins (CAP)) stimulate channel activity whereas treatment with aprotinin and leupeptin, protease inhibitors, reduces transepithelial sodium transport (Refs. 48-51). Epidermal growth factor is a potent inhibitor of ENaC (Refs. 52, 53). Phosphatidylinositol 4,5-bisphosphate ( $\text{PIP}_2$ ) is required to maintain ENaC activity (Ref. 54). It is speculated that G proteins stimulate ENaC, while  $\text{P2Y}$  purinergic receptors and EGF receptors inhibit ENaC activity by modulating  $\text{PIP}_2$  levels (Ref. 55).

ENaC expression and function is upregulated by the hormones aldosterone, angiotensin II, vasopressin (ADH) and insulin, whereas atrial natriuretic factor (ANF) downregulates ENaC (Refs. 56-60). The classic response of ENaC to aldosterone is the transcriptional activation of ENaC subunits and of genes whose protein products regulate ENaC positively (see below). Following this pathway, ENaC activity reaches a maximum 24 hours after aldosterone or glucocorticoid treatment (Ref. 61). An alternate, faster pathway for ENaC activation by steroid hormones has been described, where ENaC activity is stimulated not due merely to an increase in mRNA or protein levels but most likely from redistribution from the cytoplasmic pool to the apical plasma membrane (Refs. 62, 63). Aldosterone rapidly (in as early as 30 min) increases the mRNA level of the serum and glucocorticoid regulated kinase 1 (SGK-1) (Ref. 64). Co-expression of SGK with ENaC in heterologous systems was found to stimulate ENaC activity markedly (Refs. 65-67). SGK-1 may exert its effects on ENaC activity through direct phosphorylation of the C-terminus of alpha ENaC (Ref. 68) or through phosphorylation

of regulatory proteins, like Nedd4 (Refs. 69, 70). ENaC channels can be removed from the apical surface by Nedd4 mediated ubiquitination (Ref. 71) and clathrin mediated endocytosis (Ref. 72). Vasopressin mediates the increase in ENaC activity and the redistribution of aquaporine 2 (AQP2) to the apical membrane of the principal cells via the cAMP and PKA mechanisms (Ref. 73).

#### Expression Along the Nephron

Even though mRNA encoding all three subunits (alpha, beta and gamma) was detected in the proximal tubule using RT-PCR (Ref. 74), no protein signal was detected using immunocytochemistry and no mRNA was found *in vivo* via in situ hybridization (Ref. 75). Expression of ENaC mRNA and protein has not been detected in the loop of Henle (Refs. 75, 76). Presence of both ENaC mRNA and protein have been found in the distal convoluted tubule (DCT), connecting tubule (CNT), cortical collecting duct (CCD) outer medullary collecting duct (OMCD) (Ref. 75) and in the inner medullary collecting duct (IMCD) (Refs. 77, 78)

There is a suggestion of axial heterogeneity of ENaC expression along the nephron. The expression of ENaC is higher in more superficial cortical regions like the connecting tubule or CCD, whereas the distal convoluted tubule and the medullary collecting duct contain less ENaC expression (Ref. 13). ENaC is present on the luminal surface of principal cells in the CCD. Please refer to figure 2.

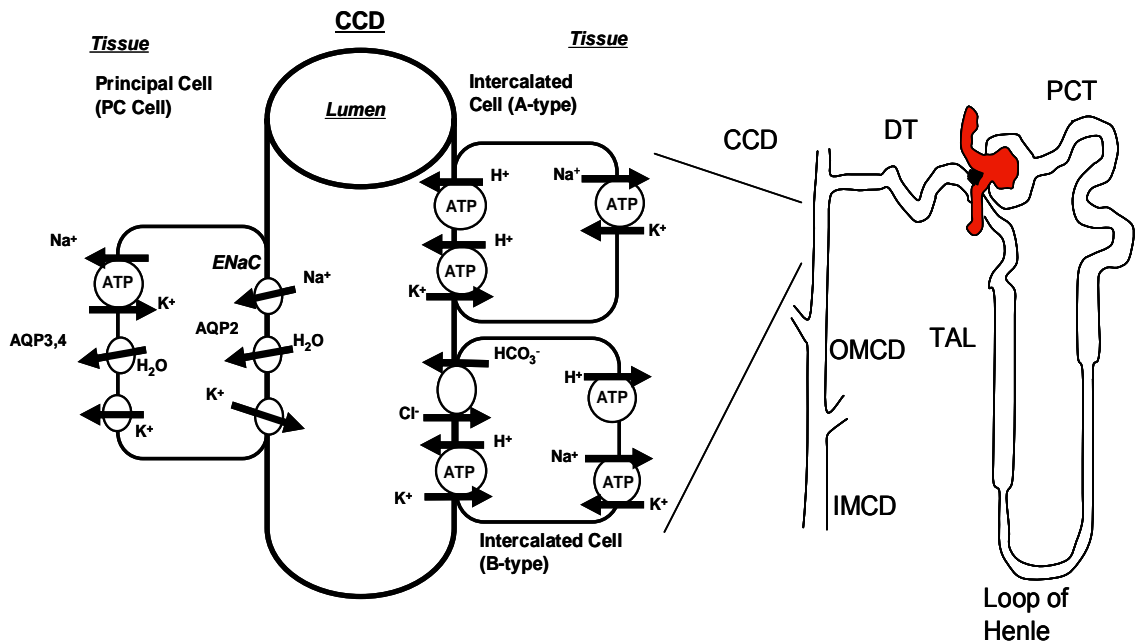


**Figure 2. Cortical Collecting Duct Principal Cells versus Intercalated Cells**

Principal cells account for 70-90% of the cells in CCD and are characterized by hormonally regulated  $\text{Na}^+$  absorption and water permeability. Epithelial sodium channels (ENaC) and aquaporin 2 (AQP2) are localized to the apical membrane of principal cells (PC) and represent the rate limiting step in  $\text{Na}^+$  and water reabsorption at the CCD level. Intercalated cells account for 10-30% of the cells in the collecting duct and are responsible for  $\text{H}^+/\text{HCO}_3^-$  excretion in the distal nephron.



## ENaC- Related Kidney Diseases

### *Liddle's Syndrome.*

Liddle's syndrome is an autosomal dominant form of early onset and severe hypertension, characterized by metabolic alkalosis, hypokalemia, hyporeninemia and low aldosterone secretion. This syndrome was first described by Liddle *et al.* (Ref. 79) in 1963. Thirty years later, it was found that this disorder is connected with a truncation of the carboxy terminus in the  $\beta$ - or  $\gamma$ -ENaC subunits (Refs. 80, 81). These are gain-of-function mutations that cause constitutive activation of ENaC on the apical surface of the CCD via retention of the channels. The site of truncation in the carboxy terminus implicates the conserved proline-rich domain, called the PY motif, in the retention of the channel at the cell surface. Two mechanisms have been proposed to explain ENaC retention. Normally, Nedd4, an ubiquitin ligase that contains multiple tryptophan rich domains, binds the PY domain of the ENaC subunits leading them to degradation (Ref. 82). The first mechanism implies that the interaction between ENaC and Nedd4 is altered, resulting in an impairment of channel internalization (Ref. 83). The second proposed mechanism implies a defect in the clathrin-mediated endocytosis of ENaC. This is based on the fact that the PY domain also contains an endocytic signal (Ref. 84).

### *Autosomal Recessive Pseudohypoaldosteronism Type I.*

The autosomal recessive form of pseudohypoaldosteronism (PHA) type I is a loss-of-function mutation which can occur in  $\alpha$ -,  $\beta$ - or  $\gamma$ -ENaC subunits (Ref. 13). The clinical symptoms of PHA type I are quite severe and include hypotension, hyponatremia,

hyperkalemia, and metabolic acidosis. PHA type I is also associated with elevated renin and aldosterone levels (Ref. 85).

#### ENaC-Related Lung Disorders

ENaC has an important role in mediating salt reabsorption along the airway epithelia, maintaining the composition and volume of the airway surface liquid (ASL) bathing beating respiratory cilia (Ref. 86). Normally, ENaC activity is suppressed by the cystic fibrosis transmembrane conductance regulator (CFTR) (Ref. 87). In cystic fibrosis (CF), with a  $\Delta F508$  mutation within CFTR, there is increased ENaC activity, sodium hyperabsorption and decreased ASL volume, without any elevation in the number of the ENaC subunits (Refs. 88, 89). There are no abnormalities in  $\text{Na}^+$  transport in the kidney in CF (Ref. 87). In contrast to CF, patients with PHA type I have diminished  $\text{Na}^+$  absorption and increased ASL volume (Ref. 90).

ENaC subunits increase in their expression levels during the very last part of fetal life, during birth, and in the first part of the neonatal life when the airway epithelium becomes an absorptive epithelium, helping the lung to clear the amniotic liquid that fills the airways and air spaces (Ref. 91). In ARPKD, there is a high rate of death within the first month of life due to respiratory distress syndrome and subsequent complications (Ref. 6). The main cause of respiratory distress syndrome is inadequate lung development caused by oligohydroamnios (Ref. 6). Oligohydroamnios are speculated to develop and accumulate due to decreased kidney output. A viable secondary cause of respiratory hypoplasia and respiratory distress in ARPKD could be inappropriately present and hyperactive ENaC function that would promote absorption of  $\text{Na}^+$  and water when fetal

lung liquid secretion is preferred to fill the branching airways with fetal lung fluid *in utero*. (Ref. 92)

## SODIUM/HYDROGEN EXCHANGERS (NHEs)

### Structure, Isoforms and Cellular Localization

Mammalian  $\text{Na}^+/\text{H}^+$  exchangers (NHE) are part of a large family of proteins that transport sodium in exchange for protons. This large family of antiporters has been detected in almost all organisms from simple prokaryotes to the highest eukaryotes (Ref. 93). In mammalian cells, NHEs are classified as secondary active transporters because the driving force that generates the electroneutral exchange derives from the sodium electrochemical gradient across the membrane established by the  $\text{Na,K-ATPase}$  pump. In mammals, NHEs mediate physiological processes including transepithelial sodium movement, intracellular pH regulation, acid-base and fluid volume homeostasis, cell cycle and cell proliferation (Refs. 94, 95), cell death and survival (Ref. 96), cell volume regulation, and vesicle trafficking (Refs. 97-99). In humans, the NHE gene family is called *SLC9A*, and 11 subtypes have been found so far (PubMed NM\_178527). Related to the research of the second paper, it is of note that the mouse NHE gene family has only 10 identified subtypes; the gene family is called *Slc9a*. Based on their primary structure, all NHE subtypes predict a common membrane topology. The N-terminus is cytoplasmic and quite long. There are 10-12 rather conserved membrane spanning segments that are involved in  $\text{Na/H}$  exchange function (Ref. 93). The C-terminus is localized intracellularly and is more variable among different subtypes. It is involved mainly in regulatory

function of the NHE. Depending on their localization in the cell, members of NHE family can be divided into plasma membrane isoforms and intracellular isoforms. Plasma membrane forms (NHE1-NHE5) show subtype-specific tissue expression, whereas organellar subtypes (NHE6-NHE9) are ubiquitous expressed (Ref. 100). There is a longer carboxylic terminus in plasma membrane subtypes than in organellar subtypes, suggesting a tighter regulatory function as well as the additional presence of cell membrane targeting motifs (Ref. 93). NHEs 1, 2 and 4 reside at the plasma membrane, whereas NHE3 and NHE5 are classified as plasma membrane isoforms but they can also be translocated to and from the membrane in the recycling endosomes (Refs. 101, 102). NHE6 is located mainly in endosomes, and it may appear transiently on the plasma membrane (Refs. 103-105). NHE7 is localized in the trans-Golgi network and associated endosomes (Ref. 106). NHE8 localization is not clear. It is found intracellularly in the trans-Golgi compartments but it also can be detected in isolated brush-border membrane vesicles of the proximal tubule in the kidney (Refs. 100, 107). NHE9 is also classified as an intracellular subtype that can appear transiently on the plasma membrane (Ref. 105). Mouse NHE10 is a plasma membrane subtype that is specific to the sperm and localized mainly to the flagellum (Refs. 108, 109). Only the primary structure of NHE11 predicts that it is part of the NHE family. It is only found in humans thus far, and it is not yet well characterized (PubMed NM\_178527). Taken together, the NHE superfamily is composed of an intriguing set of membrane transport proteins with diverse distribution and cellular localization.

## Molecular Physiology and Pharmacology

Each mammalian NHE isoform is characterized by the transport of one  $\text{Na}^+$  ion in exchange for one  $\text{H}^+$  ion. However, affinity for ions, kinetics, and pharmacological sensitivity makes each isoform unique. Plasma membrane isoforms (NHE1-NHE5) are highly selective for  $\text{Na}^+$ , whereas organellar isoforms (NHE6-NHE9) are thought to transport either  $\text{Na}^+$  or  $\text{K}^+$  in exchange for  $\text{H}^+$  (Ref. 93). However, taking in account the intracellular concentrations of the two ions, organellar subtypes seem to rely more on the  $\text{K}^+$  gradient (Ref. 110).

NHE dependence on extracellular  $\text{Na}^+$  conforms to simple Michaelis-Menten kinetics, exhibiting a hyperbolic nature for NHE1-3 and NHE5 (Ref. 111). This indicates that there is no cooperativity for extracellular sodium binding. However, NHE4 may show either a hyperbolic dependence (Ref. 112) or a sigmoidal dependence in transfected fibroblasts (Ref. 113), suggesting cooperative kinetics for external sodium in the latter case. NHE8 activity is  $\text{Na}^+$  dependent, displaying a sigmoidal relationship that suggests cooperativity in extracellular sodium binding (Ref. 114).

NHE dependence on intracellular pH indicates that NHE1-3 subtypes are sensitive to low pH. The Hill coefficient for these subtypes may vary between 1.5 and 2, suggesting allosteric modulation at the intracellular  $\text{H}^+$  binding site (Ref. 115). The NHE4 subtype displays low affinity for intracellular  $\text{H}^+$  and cooperativity at the  $\text{H}^+$ -binding site (Ref. 112). The NHE5 isoform exhibits a first order dependence (Ref. 116).

Several classes of NHE inhibitory drugs have been developed but those used most frequently are amiloride-based compounds (dimethyl amiloride (DMA), ethylisopropyl amiloride (EIPA), methylisobutyl amiloride (MIBA), hexamethylene amiloride (HMA))

and benzoylguanidine-based compounds (HOE694, cariporide (HOE642), eniporide) (Refs. 93, 117). Cimetidine, clonidine and harmaline are also reported to be weak and non-specific inhibitors for NHEs (Refs. 93, 117). In general, the affinity for the above inhibitors is the following: NHE1 > NHE2 > NHE5 > NHE3 > NHE4 (Ref. 93). When expressed on the apical surface of rat polarized kidney epithelial cells, NHE8 activity is highly sensitive to 5-(N-ethyl-n-isopropyl)-amiloride (EIPA) (Ref. 114). It has been suggested that plasma membrane NHEs have a higher sensitivity to amiloride and its derivatives than organellar NHEs (Ref. 110). Transmembrane segments 4 and 9 are considered important for inhibitor interaction with  $\text{Na}^+/\text{H}^+$  exchangers because they are important in both drug recognition and cation translocation (Refs. 93, 118).

Hypertonic medium activates NHE4 and NHE1 acutely; but, paradoxically, it inhibits NHE3 and NHE5 (Refs. 113, 119, 120). The activity of NHE2 is reported to be activated by hypertonic stress (Refs. 121-124), but NHE2 can also be inhibited by this stress when heterologously expressed in PS120 fibroblasts (Ref. 119).

ATP dependence is also different among the different subtypes. Cellular depletion of ATP reduces the activity of NHE1 and NHE2 and abolishes the activity of NHE3 and NHE5 almost completely (Refs. 111, 125). cAMP metabolism is impaired in spermatozoa lacking the sperm specific NHE10 isoform (Ref. 108). However, NHEs neither bind nor consume ATP directly.

#### Tissue Localization, Regulation and Function

The NHE1 isoform is expressed in virtually all cells and tissue (Refs. 93, 118). It is, therefore, thought of as the “housekeeping” NHE isoform throughout the body. In

polarized epithelial cells, NHE1 is mostly restricted to the basolateral side (Ref. 126), but it can also be found on the apical side of opossum kidney (OK) or Madin-Darby canine kidney (MDCK) cells (Ref. 127). The main function of NHE1 is in maintaining cytoplasmic acid-base balance. However, recent studies have implicated NHE1 in cell proliferation (Ref. 125), cell survival (Ref. 128), adhesion and migration, and as acting as a plasma membrane anchor for the actin-based cytoskeleton (Ref. 129). NHE1 has great importance in the function of the mammalian circulatory system and heart (Ref. 130). NHE1 inhibitors have proved to be protective in ischemia (Ref. 131). NHE1 interacts with calmodulin (Ref. 132), calcineurin homologous protein (Ref. 133), carbonic anhydrase II (Ref. 134), PIP<sub>2</sub> (Ref. 135) and cytoskeletal proteins via PDZ-binding proteins and ezrin/radixin/moesin (ERM) proteins (Ref. 136). Angiotensin II, EGF, endothelin and insulin stimulate NHE1 activity (Refs. 137-140). In the kidney, the main function of NHE1 is to regulate intracellular pH and cell volume (Ref. 93).

Along the nephron, NHE1 may co-exist with NHE4 on the basolateral side in multiple segments. However, NHE1 can also be coupled with the apical isoforms, NHE2 and NHE3 (Ref. 141). NHE1 enhances bicarbonate absorption in the thick ascending limb (Refs. 142, 143), an effect mediated by coupling Na<sup>+</sup>/H<sup>+</sup> exchange from the apical side with the one found on the basolateral side (Ref. 141). There are extensive studies implicating NHE1 in hypertension (Ref. 144). Transgenic mice overexpressing NHE1 exhibit decreased urinary excretion and elevated systolic blood pressure after excessive salt intake (Ref. 145). Cultured cells from the proximal tubule of spontaneously hypertensive rats (SHR) show increased NHE1 activity. It is suggested that the increased activity results from a posttranslational processing mechanism because neither the mRNA

nor the protein levels are increased (Ref. 146). These findings are not restricted only to the kidney. NHE activity is increased in vascular smooth muscle tissue (Ref. 132) and skeletal muscle tissue in humans with essential hypertension (Ref. 147). Increased NHE activity has been reported in freshly isolated erythrocytes, platelets, neutrophils, and lymphocytes from SHR animals and in immortalized blood cells derived from patients with essential hypertension (Ref. 148). The latter fact is important, because it shows that the phenotype is preserved even in the absence of external factors. The fact that increased NHE1 activity does not exist in all persons with essential hypertension makes it unlikely that NHE1 activity increases secondarily to hypertension.

The NHE2 isoform is mainly restricted to the apical side of the intestine and kidney, but it has been reported on the basolateral side in IMCD cells (Ref. 121). NHE2 is found predominantly in the thick ascending limb, macula densa, distal convolute tubule and connecting tubule (Refs. 149-151). Localization of NHE2 to the proximal tubule is not clear, but studies in mice with deleted NHE genes demonstrate that NHE3 is responsible for  $\text{HCO}_3^-$  absorption in the proximal tubule, not NHE2 (Refs. 152, 153). However, NHE2 co-expression with NHE3 has been detected in the thin limbs of the loop of Henle and on the apical membrane of the thick ascending limb (Refs. 150, 154). NHE2 activity is stimulated by EGF and angiotensin II (Refs. 155, 151) and is inhibited by calmodulin (Ref. 156). The function of NHE2 has not been studied extensively. It is reported that NHE2 contributes to  $\text{Na}^+$  absorption in distal convoluted tubules where it is co-expressed with the  $\text{Na}^+/\text{Cl}^-$  cotransporter (NCC) (Refs. 150, 157). NHE2 also modulates bicarbonate reabsorption in the distal tubules (Ref. 158) as well as cell proliferation (Ref. 159). In fibroblasts transfected with NHE-2, only cell acidification



(but not extracellular sodium removal) translocates the exchanger to the plasma membrane (Ref. 160). NHE2 seems to be protective for gastric parietal cells, and a disruption mutation within this isoform causes loss of acid secretion (Ref. 161).

The carboxy terminus of NHE2 contains 2 proline-rich domains called SH3 domains. These regions seem to be unique in the NHE family and resemble proline-rich domains found to target epithelial  $\text{Na}^+$  channels to the apical membrane by binding the cytoskeletal protein, alpha-spectrin (Ref. 28). Deletion of a region of the SH3 domain known to specifically bind to alpha-spectrin, does not influence NHE2 function, but it does cause mis-targeting of the protein to the basolateral membrane (Refs. 116, 122). Cytoskeletal interactions with ENaC and NHEs in conjunction with the absence or presence of the monocilium may be the basis of my findings in this thesis dissertation. This theme will be recurrent and will be discussed below.

The NHE3 isoform is expressed on the apical side of the polarized epithelial cells in the intestine and the kidney (Ref. 93). It is the predominant isoform in the proximal tubule but is also expressed to a lesser extent in the thick ascending limb (Ref. 154). The expression of NHE3 in the distal tubule is controversial (Refs. 162-164). NHE3 is the major player in  $\text{Na}^+$  and  $\text{HCO}_3^-$  reabsorption across the proximal tubule. It is reported that hormonal regulation of NHE3 is mainly due to PKA mediated phosphorylation (Ref. 93). Angiotensin II, aldosterone, endothelin, EGF and insulin increase NHE3 activity, whereas dopamine and parathyroid hormone decrease its activity (Refs. 165-171). Because NHE3 is also found in recycling vesicles, it is likely to participate in the pH-sensitive regulation of endocytosis and exocytosis of other proteins that undergo recycling. This hypothesis is dependent upon the fact that NHE3 regulates albumin and

albumin receptor recycling (Refs. 172-174). Calmodulin inhibits NHE3 under basal conditions (Ref. 175). Cyclic AMP-mediated inhibition of NHE3 occurs via large protein complexes that include NHERF1/NHERF2 and ezrin (Refs. 176, 177). Flow requires an intact actin cytoskeleton to modulate proximal tubule NHE3 activity (Ref. 178). In fibroblasts transfected with NHE3, removal of external  $\text{Na}^+$  (but not a decrease in intracellular pH) translocates the exchanger to the plasma membrane (Ref. 160). Being highly regulated by hormones, growth factors, and other agonists or ligands, NHE-3 is also implicated in hypertension in the SHR model (Refs. 146, 179, 180). In the proximal tubule of hypertensive rats, NHE3 protein expression is increased (Ref. 146). In the phenol injury model, there is a rapid redistribution of NHE3 from the intracellular pool to the apical membrane which may contribute to the creation of  $\text{Na}^+$  hyperabsorption and a rapid and persistent hypertension (Refs. 181, 182). NHE3 knockout mice have metabolic acidosis and hypotension and perish on a low sodium diet (Refs. 183, 184). As with NHE2, NHE3 upregulation has been linked to the development of hypertension and vascular disease.

The NHE4 isoform is localized to the basolateral surface in most epithelial cell models (Refs. 112, 151, 185, 186). It is abundant in the stomach and is present in lower levels in kidney, pancreas, salivary glands and hippocampus. The precise localization of NHE4 along the nephron is controversial. NHE4 is the main isoform expressed on the basolateral side of macula densa where it is stimulated by angiotensin II (Ref. 151), but it has also reported to be expressed in thick ascending limb and collecting ducts (Ref. 112). NHE4 function remains unclear at the present. In the stomach, NHE4 modulates normal levels of gastric acid secretion (Ref. 187). Because of its low affinity for intracellular  $\text{H}^+$ ,

NHE4 was proposed to contribute to acid-base regulation by exchanging  $\text{NH}_4^+$  for  $\text{Na}^+$  (Ref. 112). However, it also seems to have a different role than the other NHEs because it is highly stimulated by osmotic cell shrinkage. Thus, it is likely that NHE4 plays a prominent role in regulating cell volume when cells are exposed to hyperosmolarity (Refs. 113, 186).

The NHE5 isoform has been detected mainly in the brain but also in testis, spleen, and skeletal muscle by Northern blot analysis (Ref. 188). However, NHE5 expression has been found to be highly restricted to neural tissue. Disruption of the actin cytoskeleton elevates NHE5 activity (Ref. 189). NHE5 has a significant resistance to amiloride, more than NHE1 but less than NHE3 (Refs. 117, 188). NHE5 is downregulated by both PKC and PKA (Ref. 120). The expression and function of NHE5 in the kidney are unknown at present.

The NHE8 isoform is classified as being rather unique among the intracellular NHE isoforms (Ref. 110). NHE8 transcripts are expressed ubiquitously. NHE8 is expressed abundantly in the proximal tubule (Ref. 107) and it translocates to the apical membrane of the proximal tubule, where it exchanges  $\text{Na}^+$  for  $\text{H}^+$  only (Ref. 114). In rat kidney, the apical membrane of the adult proximal tubule has a lower abundance of NHE8 than the apical membrane of the same segment in the neonate (Refs. 190, 191).

The NHE6, 7 and 9 isoforms are also expressed across a wide variety of tissues, if not, ubiquitously. These isoforms are localized intracellularly and are thought to regulate organellar volume and pH, maintaining a favorable environment for processes such as protein maturation, endoprotease activity and receptor-ligand dissociation (Ref. 100).

NHE6 has been shown to form protein complexes with the angiotensin II receptor (Ref. 192).

The NHE10 isoform is a plasma membrane exchanger specific to sperm. It forms protein complexes with soluble adenylyl cyclase and it is thought that, together, they facilitate sperm motility regulation (Refs. 108, 109).

Taken together, the NHEs represent a fascinating superfamily of membrane transport proteins. This entire family needs to be presented and discussed in the context of my thesis studies, because most of the NHE isoforms are expressed in our renal epithelial cell models at the mRNA level. While it is likely that NHEs 1, 2, and 4 play prominent roles in our cell models, I cannot rule out the involvement of additional NHE isoforms when presenting my findings below. Please refer to figure 3 for the distribution of NHE isoforms along the nephron.

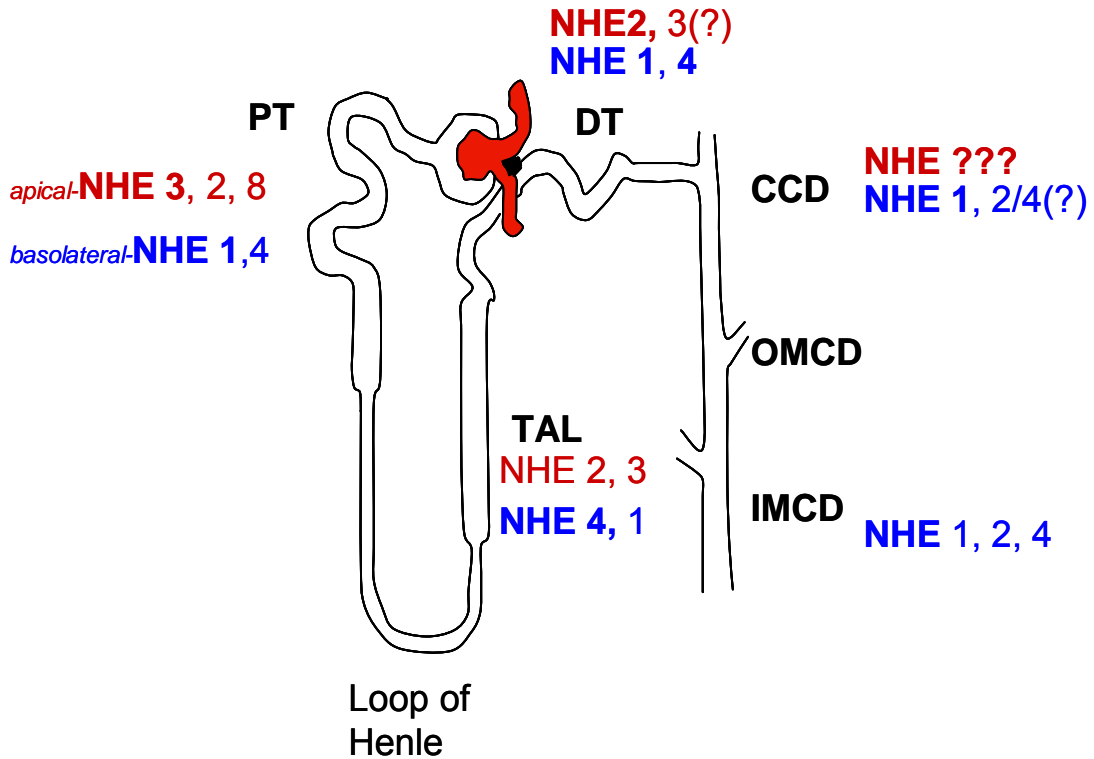


**Figure 3. Distribution of Sodium-Hydrogen Exchangers Along The Nephron**

In the proximal tubule (PT), NHE3 is the predominant isoform, but NHE2 and NHE8 are also present on the apical membrane. In the TAL, NHE2 and NHE3 are present on the apical membrane. In the distal tubule (DT) NHE2 is the apical predominant isoform; Depending on the specie, NHE3 may be also present (NHE2 is on the apical and NHE4 is on the basolateral side in maculla densa cells). Principal cells in CCD have basolateral NHE activity. Because scarce evidences are brought, the presence of apical NHE in PC is controversial. NHE1, 2 and 4 are expressed in the IMCD on the basolateral side. NHE 1 and 4 are expressed on the basolateral side along the multiple segments of the nephron. NHE4 is predominantly expressed in the TAL and DT.

## PRIMARY CILIA, POLYCYSTIC KIDNEY DISEASE, AND DYSREGULATION OF SALT AND WATER BALANCE

The primary cilia were first described in 1898 and since then scientists have documented their presence on almost every mammalian cell type (Ref. 2). The only cell lineage where primary cilia are absent is cells of the hematopoietic system. Until recently, the primary cilium was thought to be a vestigial structure with no relevant function in physiological processes. Functional characterization of the primary cilium did not begin until the 1990s. Since then, a large body of data has been gathered to show that primary cilia are sensory organelles that play a critical role in health and disease (Ref. 2).

### Primary Cilia Structure

Primary cilia are long and thin tubular structures that appear as single projections on the surface of cells. They are longer than microvilli or microplcae and they are the same length as beating cilia on the surface of respiratory epithelial cells. They consist of a ciliary membrane that is contiguous with the plasma membrane and the central axoneme (Refs. 1, 2). Unlike the axonemes from motile or beating cilia, the primary cilium axoneme is made from nine pairs of microtubules displayed in the form of a hollow cylinder (9+0 pattern), which lacks the central pair of single microtubules that allow cilia to beat (Ref. 2). This 9+0 structure does not confer movement, as is classically seen in motile cilia. Some primary cilia, like nodal cilia found in the embryonic node, have the ability to move in a circular fashion (Ref. 193). The primary cilium originates from a modified centriole called the basal body.

During the mitotic phase, the primary cilium disassembles but then reassembles early in interphase when the centriole moves to the plasma membrane, transforms into the basal body and starts the nucleation of the axoneme (Ref. 1). Intact intraflagellar transport (IFT) machinery is required for the assembly and maintenance of the cilia (Refs. 2, 194). Because the cilium is not able to synthesize proteins, ciliary components are synthesized in the cell body, assembled at the base of the cilium, transported to the distal end of this organelle where cilium assembly occurs (Ref. 194). The cargo molecules are transported in an anterograde direction by kinesin-II motors and a retrograde direction by dynein motors (Ref. 2). These motor molecules can also transport sensory signals from the tip of the cilia to the cell body. The primary cilia are maintained and become fully developed during cell differentiation (Ref. 3). It is widely held that ciliary assembly is the terminal step in ciliated epithelial cell polarity generation and differentiation (Refs. 2, 3).

During mitosis, the centrosome contains 2 centered centrioles (a mature centriole called the mother centriole and an immature centriole called the daughter centriole) surrounded by pericentriolar material. The role of the centrosome is to organize the mitotic spindle and to form the microtubule-organizing center during interphase (Ref. 195). The primary cilium is built from the mother centriole, which is distinguished by the presence of distal and subdistal appendages that are thought to anchor the centriole to the plasma membrane during the ciliogenesis (Ref. 195). The pericentriolar material, the terminal plate at the distal end of the basal body and transitional fibers at the base of the cilium may form a special environment that may regulate the molecules that can pass into or out of the cilium (Ref. 1). The ciliary membrane is thought to be separated from the plasma membrane by a necklace associated with cytoskeletal elements. All these unique

arrangements make the primary cilium a special structure that can function not only as a sensor, but can also control processes on the apical plasma membrane adjacent to the cilium (Refs. 1, 196). On epithelial cells, primary cilia play an important role in proliferation, polarization, differentiation and membrane ion transport. With the exception of intercalated cells, primary cilia have been documented on all segments of the nephron from the Bowman's capsule to the collecting ducts (Refs. 197, 198). In the cortical collecting duct, the primary cilium was a known biomarker of the principal cell (PC cell) that differentiated it from the intercalated cells covered by "ridge-like" microplicae (Ref. 8).

#### Implications of Cilia in Cystic Diseases

Many of the polycystic kidney disease (PKD) relevant proteins mutated in human and animal forms of the disease are localized at least in part to the cilia, basal body or centrosome (Ref. 2). In humans, polycystins (ADPKD), fibrocystin/polyductin (ARPKD), and the nephronocystins (nephronophthisis) are localized in part or exclusively to the cilia (Ref. 2). The BBS (Bardet-Biedl Syndrome) proteins 1-8 are localized to the cilia and basal body (Ref. 2). The OFD1 (Oral-facial-digital syndrome type 1) protein is localized to the basal body, whereas the Hamartin (Tuberous Sclerosis Complex 1) protein is localized in the centrosome (Refs. 2, 199). Tuberin (Tuberous Sclerosis Complex 2) is shown to interact with the polycystin-1 tail (Ref. 200) and patients with deletions in both adjacent genes, PKD1 and TSC2, suffer from early onset PKD (Ref. 201). There are mouse models which support the ciliary hypothesis of PKD. Most notably, polaris (Tg737<sup>orp<sup>k</sup></sup> mouse), inversin (*inv* mouse), cystin (*cpk* mouse),



polycystin 1 and 2 (pkd1 KO and pkd2 KO mouse), and kinesin-II 3a (kif3a) are known to be localized in the primary cilium (Ref. 2). The list of proteins found to be localized in the primary cilium/basal body/centrosome continues to grow.

### Salt and Water Balance Dysregulation in Cystic Diseases

Abnormalities in gene expression, proliferation, apoptosis, cell polarity and the extracellular matrix are reported in PKD (Ref. 202). Another abnormality found within the cystic kidney is dysregulation of salt and water balance. ENaC is reported to be expressed in the cilia and is thought to participate in electrical depolarization (Ref. 203) and mechanosensation (Ref. 204) of the primary cilia. In the proximal tubule, NHE3 and the angiotensin receptor are co-localized in condensed apical recycling endosomes in proximity to the primary cilium (Refs. 196, 205). Systemic hypertension, developed before renal impairment, is common among ADPKD patients (Refs. 4, 5). Mislocalized  $\text{Na}^+$ ,  $\text{K}^+$ ,  $2\text{Cl}^-$  co-transporter (NKCC) on the basolateral side together with normal apically localized cystic fibrosis transmembrane conductance regulator (CFTR) are thought to participate in fluid secretion and cyst enlargement in ADPKD (Ref. 206). Patients with normal glomerular filtration rate have a reduced ability to concentrate urine (Ref. 206). Early and severe hypertension is common in children and infants with ARPKD and appears well in advance of renal insufficiency (Ref. 6). Enhanced transepithelial sodium reabsorption has been shown in monolayers of human ARPKD cyst cells (Ref. 207). I published that ENaC activity is upregulated in cilium deficient versus cilium competent CCD principal cell monolayers from the  $\text{Tg737}^{orpK}$  mouse model of ARPKD (Chapter 2). I have also found inappropriate NHE activity in the apical

membrane of the same cilium-deficient cell monolayers (Chapter 3). Enhanced fluid movement was observed from the apical to the basolateral side in cilium deficient monolayers (D. Olteanu and EM Schwiebert, unpublished observation). The earliest symptoms of nephronophthisis are polyuria, polydipsia and decreased urinary concentrating capacity (Ref. 208). Patients with Bardet-Biedl syndrome and normal renal function are reported with hypertension and the inability to concentrate urine (Ref. 209). Since Bardet-Biedl syndrome is an autosomal recessive disease, relatives of patients with Bardet-Biedl syndrome, who are carriers of the mutated gene, are also predisposed to hypertension (Refs. 210, 211). Among patients with Tuberous Sclerosis who have cystic disease, hypertension may occur before renal failure (Ref. 212), but in general it is difficult to define the cause of the hypertension due to the fact that tuberous sclerosis is a systemic disease.

## POLYCYSTIC KIDNEY DISEASES

Polycystic kidney disease (PKD) is a disorder characterized by growth of numerous fluid-filled cysts in both kidneys. The cysts enlarge over a period of years which leads to a decline in renal function mainly due to the compression and progressive destruction of normal tissue (Ref. 202). More than 600,000 people in the US (Ref. 213) and an estimate of 12.5 million people worldwide suffer from PKD. It is the fourth leading cause of kidney failure, accounting for 6-10% of end stage renal disease (ESRD). It is the most common genetic cause of renal failure and subsequent dialysis and transplantation. In the US, PKD affects more people than cystic fibrosis, sickle cell

anemia, hemophilia, Huntington's disease, Down's syndrome and muscular dystrophy combined (Ref. 214).

Depending on the cause, cystic kidney diseases can be divided in multiple subcategories: hereditary, congenital (associated with malformative syndromes), acquired and still unknown (medullary sponge kidney) (Ref. 202). Acquired forms are characterized by single or multiple cysts in one or both kidneys and are associated with long-term damage and severe scarring (glomerulonephritis, diabetic nephropathy) (Ref. 202). Multiple cysts are most common in patients with chronic renal failure, especially those undergoing hemodialysis, but may appear as a consequence of drug and hormone therapy (Ref. 202). The congenital forms of cystic kidney disease are associated with malformative syndromes, such as Bardet-Biedl syndrome and Tuberous Sclerosis Complex, and can be transmitted as autosomal recessive or autosomal dominant traits (Refs. 2, 199). The hereditary forms include nephronthisis and medullary cystic kidney disease; however, the forms which are the most well researched are Autosomal Dominant Polycystic Kidney Disease (ADPKD) and Autosomal Recessive Polycystic Kidney Disease (ARPKD) (Ref. 202).

#### Autosomal Dominant Polycystic Kidney Disease (ADPKD)

ADPKD is known as the most common, single gene inherited disorder in humans, affecting men and women equally regardless of race, age or ethnic origin, with a slow progression to renal failure. It occurs in 1:500 to 1:1000 live births (Refs. 202, 206),

affecting around 500,000 persons in the US and 6 million worldwide. The disease is characterized by gradual, massive kidney enlargement that culminates with renal insufficiency in the majority of individuals by the fifth or sixth decade. However, the disease can be symptomatic in childhood and even in infancy (Refs. 215-217). Cysts develop from multiple nephron segments and they can reach impressive dimensions up to 10 to 20 cm (Ref. 202). ADPKD is genetically heterogenous and results from mutations in at least two genes: PKD1 and PKD2. The mutation of PKD1, located on chromosome 16, accounts for approximately 85% of cases, whereas the mutation in PKD2, located on chromosome 4, is responsible for the remaining 15% of cases (Refs. 202, 206). Even if renal and extrarenal manifestations are identical in both types of ADPKD, patients with mutations in PKD2 have a longer survival rate and fewer complications (Refs. 202, 206). However, patients with mutations of both PKD1 and PKD2 have a more severe presentation than those with only one mutation type (Ref. 218). In a very small percent of patients with a similar ADPKD phenotype, no mutation in either of the two genes above was found (Refs. 202, 206). This leaves room for the possibility of other gene candidates. New mutations in PKD genes are thought to appear relative rarely (5% for PKD1) (Ref. 219).

The PKD1 gene product, polycystin-1 (PC1), is a large membrane protein with 11 membrane-spanning domains, a large extracellular amino-terminal region and a short intracellular carboxy-terminus (Ref. 219). The extracellular region contains several protein motifs that are potential sites for protein-protein and protein-carbohydrate interactions. The intracellular domain contains a coiled-coil region that interacts with polycystin-2 (PC2) (Refs. 155, 220). It also contains many sites of potential

phosphorylation by protein kinases as well as additional domains or motifs that could activate intracellular signaling pathways (Ref. 219). PKD2 gene encodes polycystin-2, a protein that shares sequence homology with the transient receptor potential (TRP) superfamily of  $\text{Ca}^{2+}$ -permeable non-selective cation channels (Refs. 221, 222). Intriguingly, TRP channels have been implicated in store-operated  $\text{Ca}^{2+}$  entry and in sensory physiology in numerous different cell types through the body (Ref. 223). It is currently hypothesized that the PC1-PC2 complex may participate in flow-induced mechanosensation in the primary cilium of the renal cells; however, this idea is a matter of current debate (Ref. 224)

#### *Potential Implications of ENaC Dysregulation in ADPKD*

The leading cause of death in ADPKD patients is cardiovascular complications (Refs. 225, 226), and hypertension is an important risk factor. Hypertension is an early finding in ADPKD, and it is observed in approximately 60% of the patients before they reach renal failure (Refs. 4, 5). Even if hypertension plays a major role in morbidity and mortality of ADPKD patients, the cause has not been pursued extensively. Several potential causes are implied for hypertension, including: activation of renin-angiotensin-aldosterone system (RAAS) (Refs. 227, 228), a hyperactive sympathetic nervous system (Refs. 229, 230), an increased level of endothelin (Refs. 231, 232) and an increased level of vasopressin (Ref. 217 233). Activation of RAAS is the most studied cause to date. In a report of Harrap *et al* (Ref. 227), young normotensive ADPKD patients, with no significant impairment in renal function, were compared with unaffected matched family

members. It was shown that total exchangeable sodium, plasma renin and aldosterone levels are significantly higher in ADPKD patients when compared with controls. Even if these findings are largely accepted, other studies showed inconsistent findings along these lines, showing only subtle sodium excretion abnormalities (Ref. 234). This was puzzling to the field until two studies succeeded to establish evidence for local production of renin in ADPKD cysts (Refs. 235, 236). Renin was produced by dilated tubules and cysts derived from the distal nephron, whereas angiotensinogen was produced by dilated tubules and cysts derived from the proximal nephron (Ref. 236). Angiotensin-converting enzyme (ACE), angiotensin II and angiotensin II type 1 receptor are found in multiple segments of the nephron (Refs. 236-239). It is speculated that hypertension, in the early course of the disease, is due to the local production of renin and angiotensinogen (Refs. 235, 236). This could lead to increased concentration of angiotensin II and consequently excessive  $\text{Na}^+$  reabsorption. There are two types of cysts in ADPKD: nongradient or proximal cysts and gradient or distal cysts. High concentrations of angiotensin II, accumulated in proximal dilated tubules or cysts, by direct secretion or by activation of RAAS (renin can be filtered), may inhibit  $\text{Na}^+$ ,  $\text{HCO}_3^-$  and fluid reabsorption (Refs. 240, 241) which matches the definition of a nongradient cyst (normal  $\text{Na}^+$  concentration, normal pH, osmolality close to plasma osmolality) (Refs. 242-244). These cysts account for two-thirds of the total population of cysts (Refs. 245, 246) and may play a leading role in renal enlargement. Instead, accumulation of angiotensin II in dilated tubules and cysts derived from the distal nephron may stimulate  $\text{Na}^+$  channels,  $\text{N}^+/\text{H}^+$  exchange (Refs. 247, 248) and fluid reabsorption, features that match the definition of a gradient cyst (low  $\text{Na}^+$  concentration, low pH and slightly

higher osmolality than plasma) (Ref. 244). ENaC is known to be stimulated by angiotensin II (Ref. 56) and may be a potent player in fluid reabsorption in the distal nephron.

A great deal of effort has been devoted to elucidating the mechanisms involved in cystic dilatation, while few studies have been dedicated to understanding the hypertension problem. Cysts may absorb or secrete electrolytes depending on the absence or presence of secretagogues. Ye *et al* (Ref. 249) compared weight gain in intact cysts loaded with native cyst fluid versus cysts loaded with incubation media. Cysts containing native cyst fluid gained weight, in contrast with the majority of cysts containing incubation media which lost weight due to fluid reabsorption (Ref. 249). Once forskolin, known to stimulate cAMP secretion and consequently  $\text{Cl}^-$  secretion, was added to the bathing media, the cysts loaded with incubation media began to gain weight. Grantham *et al.* (Ref. 250) studied polarized monolayers of epithelial cells derived from human ADPKD cysts. These monolayers absorbed fluid in the absence of cAMP agonists. Once forskolin was added, the monolayers began to secrete fluid. However, amiloride, known to inhibit  $\text{Na}^+$  channels and  $\text{Na}^+/\text{H}^+$  exchanger, was not used to prevent fluid absorption. Perrone *et al.* (Ref. 251) mounted pieces of human cyst wall in Ussing chambers and found that gradient cysts had elevated transepithelial voltage and short-circuit current, in comparison with non-gradient cysts. Using  $^{22}\text{Na}$ , authors were able to show the existence of an active, unidirectional NaCl transport from the mucosal to serosal side that was reversibly inhibited by adding 10 $\mu\text{M}$  amiloride, a dose known to inhibit sodium channels (Ref. 251). Forskolin was not used in this study.

Elevated levels of vasopressin and endothelin, two ligands which were reported as possible causes of hypertension in ADPKD, also stimulate epithelial sodium channels in the kidney (Refs. 252, 253). Vasopressin also stimulates AQP-2 that is expressed on the apical side of the principal cell and contributes to water reabsorption. Taken together, the above evidence indicates that ENaC may be implicated in  $\text{Na}^+$  and fluid hyperabsorption that leads to hypertension in ADPKD, but this hypothesis needs further investigation.

#### *Potential NHE Implications in ADPKD*

An increased NHE activity can be speculated as a secondary mechanism in  $\text{Na}^+$  reabsorption in ADPKD. Wilson *et al.* reported that the apical to basal flux of  $^{22}\text{Na}^+$  was inhibited by 100 $\mu\text{M}$  Amiloride in ADPKD monolayers. These authors suggested that NHE was generating the flux (Ref. 254). As described earlier in the  $\text{Na}^+/\text{H}^+$  exchanger section above, NHEs are widely expressed along the nephron and highly regulated by different hormones that are also reported to be increased in ADPKD. Angiotensin II stimulates NHE1-4 activities along the nephron (Refs. 137, 151, 166). EGF receptors are mislocalized and hyperactive on the apical side on the cyst epithelia (Ref. 255) and may contribute to increased NHE activity (Refs. 138, 165, 256). Increased endothelin in ADPKD stimulates NHE1 and NHE3 (Refs. 139, 167). NHERF2, a regulatory factor for NHE3, is located on chromosome 16 very close to the PKD1 gene (Ref. 257). Chromosomal deletion in some of the ADPKD patients, which include both genes, may be implicated in loss of NHE3 inhibition from other proteins that interact with this isoform via NHERF (Ref. 257). The roles of ENaC and NHEs in ADPKD remain to be



fully investigated. Inhibitors of these Na<sup>+</sup> transport proteins may be beneficial in controlling the progression of ADPKD.

#### Autosomal Recessive Polycystic Kidney Disease (ARPKD)

ARPKD is the most common heritable renal cystic disease occurring in infancy and childhood, often leading to death in the first month of life (Ref. 6). It is characterized by the presence of renal cysts, biliary dysgenesis and portal tract fibrosis (Ref. 6). ARPKD has an incidence of approximately 1 in 20,000 live births (Ref. 6). The mortality rate is very high during the first month of life, as 30-50% of neonates die shortly after birth due to pulmonary hypoplasia (Refs. 6, 258-261). This is due to poor fetal urine production and formation of oligohydroamnious. At birth, ARPKD patients may present with bilaterally enlarged echogenic kidneys, Potter facies and respiratory distress syndrome (Ref. 6). Most of the children who survive the neonate period develop early and severe hypertension, renal insufficiency and portal tract hypertension (Ref. 6). Cysts in ARPKD are multiple and do not exceed a few millimeters, arising only from the collecting duct. The gene responsible for the disease, PKHD1, is a very large gene (~470kb) located on the short arm of chromosome 6 (Ref. 262). The product of the PKHD1, termed polyductin or fibrocystin, is predicted to be a membrane protein with a large extracellular domain and a single transmembrane segment and a short carboxyl terminal tail (Ref. 262). Recently, a homologue gene PKHDL1 was identified in multiple tissues, but was only detected in blood cell lines, especially T lymphocytes, a finding that suggests a role in cellular immunity (Ref. 262). Polyductin/ fibrocystin is localized to the ciliary axoneme and basal body in MDCK cells and IMCD3 cells, as well as in human

adult and embryonic kidney cells (Refs. 258-260, 263). Cystic cells derived from human ARPKD patients as well as in mouse models of ARPKD (*orpk*, *bpk*, *cpk*, *Pkd1*, *Kif3A*) express the EGF receptor on the apical side instead of or as well as the basolateral side (Refs. 261, 264, 265). The  $\alpha 1$  and  $\beta 2$  subunits of the Na/K-ATPase are mislocalized to the apical membrane of collecting duct cysts in tissue sections of human fetal ARPKD (Ref. 207); however, it is not clear whether functional Na/K-ATPase pump becomes mislocalized to the apical cell membrane to affect vectorial movement of  $\text{Na}^+$  across cystic epithelia.

#### *Evidence for ENaC Implications in ARPKD*

Cysts in ARPKD are dilated collecting ducts that remain connected to the remaining nephron and allow urine to flow freely throughout the nephron. Studies in ARPKD kidney cysts show that the amount of sodium inside the cysts is reduced relative to plasma levels (Refs. 266, 267). Rohatgi *et al.* (Ref. 207) reported that immortalized cells, derived from collecting ducts of human fetal ARPKD kidneys, absorb sodium at a rate 50% greater than the age matched collecting tubule (HFCT) cells. These authors showed a two fold greater expression of alpha ENaC subunit mRNA and protein expression by Northern blot analysis of whole kidney and in Western blot analysis from ARPKD cells. I have also found (Chapter 2) that principal cells, from the collecting duct of a *Tg737<sup>orpk</sup>* mouse model of ARPKD lacking the proper length of the primary monocilium, present with 4-fold elevated transepithelial voltage and short circuit current, compared with cells in which the length of the primary monocilium was genetically

rescued. Amiloride and its analogs inhibited the transepithelial current. In my unpublished observations using RT-PCR, I found that  $\beta$ -ENaC expression in cilium deficient cells is greater than in cilium competent cells (see Future Directions section). Veizis *et al.* (Ref. 268) reported reduced  $\text{Na}^+$  absorption in a *bpk* mouse model of ARPKD. However, these authors grew their monolayers in the presence of significant EGF, which is known to inhibit ENaC (Refs. 269, 270). They removed the EGF 24 hours before their experiments. Recently, Loghman-Adham *et al.* (Ref. 271) published evidence for local, intrarenal expression of components of RAS in ARPKD. Angiotensin II binds to specific receptors found in collecting ducts (Ref. 56). In the model proposed by Loghman-Adham *et al.*, this pathway would stimulate ENaC and consequently heighten the reabsorption of sodium and water that may result in chronic hypertension.

#### *Evidence for NHE Implications in ARPKD*

Evidence for acid-base dysregulation in ARPKD was recently shown by Banizs *et al.* (Ref. 272). These authors reported that choroid plexus epithelium in a *Tg737<sup>orpk</sup>* mutant mouse have lower intracellular pH and higher  $\text{Na}^+$ -dependent  $\text{HCO}_3^-$  transport activity when compared with wild-type choroid plexus epithelium. Furthermore, as presented in Chapter 3, I have the first evidence of a NHE transport abnormality within collecting duct principal cells from a *Tg737<sup>orpk</sup>* mutant mouse. Normally, in the collecting duct, principal cells do not participate in acid-base regulation; rather, the intercalated cells are responsible for this function. I have found inappropriate NHE activity on the apical side of the cilium-deficient cells, activity that was missing in cilium-competent cells. Amiloride analogs, as well as more specific inhibitors (HOE-694 and cariporide),

were used to define the pharmacological properties of the NHE activity. In my preliminary experiments attempting to define which NHE or NHEs are mislocalized or improperly expressed on the apical side of the membrane, I found using RT-PCR that NHE2 had a greater expression in cilium deficient cells than in cilium competent cells. I also found that urine in HoxB7-Cre Tg737<sup>flox/Δ</sup> mice, lacking proper length of the cilium, was more acidic than their age-matched controls. Metabolic alkalosis had also developed at 4 weeks of age in the mutant animals when compared to littermate controls.

Intriguingly, Rohatgi *et al.* (Ref. 207) used <sup>22</sup>Na to measure Na<sup>+</sup> absorption flux in immortalized cells, derived from collecting ducts of human fetal ARPKD. Transepithelial sodium absorption was partially inhibited with 100 μM amiloride added on the apical side, a dose known to be at the upper limit of ENaC inhibition. Because Na<sup>+</sup> flux was not influenced by adding apical ouabain, an inhibitor of the mislocalized apical Na,K ATPase pump, the authors proposed that a non-classical ENaC subunit composition and/or function mediated Na<sup>+</sup> absorption. However, an alternative possibility would be an associated and inappropriate apical NHE activity. Rohatgi *et al* were measuring Na<sup>+</sup> flux, not short circuit currents. Because NHE is electroneutral, it does not participate in membrane potential or current, but it participates in transmembrane Na<sup>+</sup> flux. The partial inhibition of the Na<sup>+</sup> flux by 100 μM amiloride is comparable to the range of amiloride sensitivity for NHEs. Interestingly, the amiloride-sensitive NHE1 isoform was not detected, leading the authors to conclude that participation of this isoform in transepithelial Na<sup>+</sup> transport was unlikely. However, the expression of additional more amiloride-resistant isoforms was not examined.

Loghman-Adham *et al.* (Ref. 271) suggested that angiotensin II, produced by intrarenal components of RAS found in ARPKD, stimulates NHE and triggers  $\text{Na}^+$  and water reabsorption by the proximal tubule. Elevated basal intracellular  $\text{Ca}^{2+}$  found in cilium deficient CCD principal cells from the *orpk* mouse model of ARPKD (B. Siroky and P. Darwin Bell, unpublished observations; Ref. 273) could activate  $\text{Ca}^{2+}$ -calmodulin that binds to the NHE1 autoinhibitory regions, thereby activating the exchanger (Refs. 118, 144, 274). Actin disruption found in the *orpk* mouse (B Siroky and P. Darwin Bell, unpublished observations) may also compromise the function of ion channels and transporters that are linked to the cytoskeleton (Refs. 28, 129, 176, 178, 275).

## SUMMARY

Below, I present evidence that both ENaC- and NHE-mediated  $\text{Na}^+$  absorption are upregulated in a cilium-deficient renal epithelial cell model of polycystic kidney disease. Coupled with this defect, I also have found upregulated NHE-mediated acid-base transport *in vitro* and *in vivo*, as evidenced by an acidified urine as early as 1 week of age (likely due to excessive  $\text{H}^+$  secretion and subsequent excretion) and the development of metabolic alkalosis at 4 weeks of age. These cellular mechanisms may underlie and be primarily responsible for the development of hypertension in both forms of PKD. They may also contribute to the progression of the disease in general in both the kidney and in extra-renal tissues. The molecular mechanisms whereby the loss of the primary cilium leads to upregulated ENaC and upregulated and mislocalized NHE activities is a matter for on-going and future investigation. I seek to connect the primary cilium to these

membrane transport proteins in an effort to understand how the cilium governs transepithelial salt, acid-base, and water transport in normal and diseased renal cells and tissues.

HEIGHTENED ENAC-MEDIATED SODIUM ABSORPTION IN A MURINE  
POLYCYSTIC KIDNEY DISEASE MODEL EPITHELIUM LACKING APICAL  
MONOCILIA

by

DRAGOS OLTEANU<sup>1</sup>, BRADLEY K. YODER<sup>2</sup>, WEN LIU<sup>5</sup>, MANDY J. CROYLE<sup>2</sup>,  
ELISABETH A. WELTY<sup>1</sup>, KELLEY ROSBOROUGH<sup>2</sup>, J. MICHAEL WYSS<sup>2</sup>, P.  
DARWIN BELL<sup>1,3</sup>, LISA M. GUAY-WOODFORD<sup>2,3,4</sup>, MARK O. BEVENSEE<sup>1</sup>, LISA  
M. SATLIN<sup>5</sup> AND ERIK M. SCHWIEBERT<sup>1,2,3</sup>.

Departments of Physiology and Biophysics<sup>1</sup> and of Cell Biology<sup>2</sup> and the Divisions of  
Nephrology<sup>3</sup> and Genetics and Translational Medicine<sup>4</sup> in the Department of Medicine,  
University of Alabama at Birmingham, 1918 University Blvd.,  
Birmingham, AL, 35294-0005

*American Journal of Physiology* 290(4):C952-63, 2006

Copyright

2006

by

The American Physiological Society

Used by permission

Format adapted for dissertation

## ***Abstract***

The Tg737<sup>orpk</sup> autosomal recessive polycystic kidney disease (ARPKD) mouse carries a hypomorphic mutation in the Tg737 gene. Due to the absence of its protein product Polaris, the non-motile primary monocilium central to the luminal membrane of ductal epithelia such as the cortical collecting duct (CCD) principal cell (PC) is malformed. While functions of the renal monocilium remain elusive, primary monocilia or flagella on neurons act as sensory organelles. Thus, we hypothesize that the PC cell monocilium functions as a cellular sensor. To this end, we assessed the contribution of Polaris and cilium structure and function to renal epithelial ion transport electrophysiology. Properties of Tg737<sup>orpk</sup> mutant CCD PC clones were compared with clones genetically rescued with wild-type Tg737 cDNA. All cells were grown as polarized cell monolayers with similar very high transepithelial resistance ( $R_{TE}$ ) on permeable filter supports. Three to 4-fold elevated transepithelial voltage ( $V_{TE}$ ) and short-circuit current ( $I_{SC}$ ) was measured in mutant *orpk* monolayers versus rescued controls. Pharmacological and cell biological examination of this enhanced electrical endpoint in mutant monolayers revealed that ENaC sodium ( $Na^+$ ) channels were upregulated. Amiloride, ENaC-selective amiloride analogs (benzamil, phenamil), and protease inhibitors (aprotinin and leupeptin) attenuated heightened transepithelial voltage and current. Higher concentrations of additional amiloride analogs (ethylisopropylamiloride, dimethylamiloride) also revealed inhibition of  $V_{TE}$ . Cell culture requirements and manipulations were also consistent with heightened ENaC expression and function. Taken together, these data suggest that ENaC expression and/or function is upregulated in the luminal membrane of mutant, cilium-deficient *orpk* CCD PC cell monolayers versus cilium-competent controls. When the



genetic lesion causes loss or malformation of the monocilium, ENaC-driven  $\text{Na}^+$  hyperabsorption may explain the rapid emergence of severe hypertension in a majority of human ARPKD patients.

## ***Introduction***

Little is known about the transport properties of dilated collecting tubule-lining renal epithelial cells in ARPKD. In this study, we wished to investigate whether ion transport and cell signaling abnormalities exist in autosomal recessive polycystic kidney disease (ARPKD). In a murine mouse model of ARPKD, the Oak Ridge Polycystic Kidney (Tg737<sup>orp<sup>k</sup></sup>) mouse, ductal epithelia from multiple tissues lack a well-formed central monocilium in the apical membrane (Refs. 52, 63). The central monocilium is a key defining morphological feature of the CCD PC (Ref. 32). Malformation of this non-motile cilium is due to the lack of a key protein, Polaris (encoded by the Tg737 gene). Polaris is normally located at the basal body and base of the cilium at the point of attachment to the luminal or apical membrane and along the cilia axoneme (Ref. 63). Without functional Polaris serving as a key structural protein for the cilium, a well-formed central monocilium cannot be built.

The primary cilium is a relatively obscure organelle and its function in the kidney remains largely unknown. In tissues from lower organisms, cilia found on neurons in *C. elegans* are important in sensory perception (Ref. 22). The *C. elegans* gene homolog for Tg737 is *OSM5*, a gene involved in *C. elegans* chemosensation within its flagella (Ref. 22). In this light, recent data from Praetorius and Spring suggest that the renal cilium may be a mechanosensitive organelle that initiates a calcium spark and wave in MDCK epithelia caused by fluid flow or mechanical bending of the cilium (Refs. 39, 40). The cilium also modulates secretory potassium channels in MDCK cells (Ref. 38). In addition to the mechanosensory role, it is possible that the cilium of the CCD PC cell might be involved in osmosensation as seen in olfactory cilia or in flagella in *C. elegans* (Refs. 3,

4, 22, 24). Moreover, original studies on the Tg737<sup>orpk</sup> mouse revealed that the urine/plasma osmolarity ratio as well as the urine specific gravity was much lower in mutant *orpk* versus genetically rescued or wild-type mice (Refs. 60-62). A defect in the urine concentrating mechanisms and/or hyperabsorption of a key osmole could underlie this difference and be a key contributor to cystic disease.

It is important to note that ARPKD and ADPKD differ greatly with regard to the type of tissue remodeling and its impact upon transepithelial salt and water transport and vice versa (Refs. 11, 18-21). In ADPKD, closed fluid-filled cysts that are encapsulated by a single monolayer of cystic epithelial cells occur along multiple nephron segments. Chloride and fluid secretion into the cyst as well as trapped autocrine and paracrine growth factor and autacoid signaling then contribute detrimentally to cyst volume expansion and growth (Refs. 11, 18, 19). In ARPKD, collecting duct segments dilate but they never “close off” or encapsulate (Refs. 20, 21). As such, there are likely unstirred layers of tubular fluid and turbulent flow within the collecting ducts of ARPKD kidneys; however, the tubular fluid is never trapped. Ions, solutes and water are still freely reabsorbed and secreted along diseased ARPKD collecting ducts, and ARPKD nephron tubular fluid does eventually constitute the final urine. These dilated collecting ducts are often referred to as “pseudocysts” (Refs. 20, 21). However, this can be misleading because ARPKD pseudocysts are merely dilated renal tubules rather than fully encapsulated *bona fide* cysts observed routinely in ADPKD. The term “pseudocyst” also appears to refer more to such structures in the gastrointestinal tract in general and the pancreas in particular (Ref. 34).

Herein, we report the electrophysiological analysis of mutant Tg737<sup>orpk</sup> CCD PC cells with defects in the formation of the central cilium. We compared results obtained from mutant clones to clones that were genetically rescued by expression of the wild-type Tg737 cDNA, previously shown to correct the renal pathology *in vivo* in Tg737<sup>orpk</sup> mutant mice (Refs. 60-62). This panel of cells is an excellent tool to study the role of Polaris and the structural and functional integrity of the monocilium in ductal epithelial cell function in a well-polarized cell monolayer. Our results reveal a markedly elevated transepithelial voltage and current in the mutant *orpk* monolayers, despite comparable transepithelial resistance. Although we first suspected enhanced chloride secretion (based on our ADPKD studies) (Ref. 47), pharmacological and cell biological examination of this enhanced ion transport revealed that ENaC Na<sup>+</sup> channels were upregulated. Manipulations of defined cell culture conditions also suggest primary ENaC involvement. As such, we hypothesize that Polaris and the central monocilium normally act to limit apical ENaC-mediated Na<sup>+</sup> absorptive pathways. When this cilium-mediated inhibition is lost, Na<sup>+</sup> transport becomes dysregulated and hyperabsorption results, producing an underlying primary etiology of early onset and severe hypertension in the majority of human ARPKD patients.

## ***Methods and Materials***

### *Generation of Collecting Duct Principal Cell Clones from Mutant and Genetically Rescued orpk Mice by Genetic Cross with the Immortomouse*

The details of tubule dissection, clonal selection, and characterization of the cilia defect in the original mutant ("Mutant 1") and genetically rescued collecting duct principal cell clones ("Rescued 1" and "Rescued 2") was published previously in detail (Ref. 63). The details of genetic rescue of the *ork* mouse were also published (Refs. 60-62). These studies led to the generation of these clones that are excellent tools to study the contribution of Polaris and of non-motile central cilia on ductal epithelial cell function. Current work is designed to establish similar cell models in ductal epithelia from other tissues.

In this study, we isolated two additional mutant clones ("Mutant 2" and "Mutant 3"). This was accomplished by clonal dilution of the mixed mutant CCD cell population that was expanded from the 94D CCD individually dissected from the kidney of an animal that was generated from an *ork*<sup>Tg737</sup> and *Immortomouse* cross. We also expanded and studied this original mixed mutant 94D CCD cell population grown in the PC cell defined medium above. In addition, we also studied a third genetically rescued clone from a separate individually dissected CCD, 94E, that will be referred to as the genetically rescued clone, "Rescued B2." Mutant 1, Rescued 1, Rescued 2, and Rescued B2 were grown under G418 selection (Mutant 1 is transfected with pcDNA 3.1 empty vector without the Tg737 cDNA; the three rescued clones stably express the Tg737

cDNA). The mixed mutant 94D CCD cell population, Mutant 2, and Mutant 3 are not selected in G418.

#### *Cell Culture and Seeding of Filter Supports for Transepithelial Electrophysiology*

Mixed mutant CCD cells and mutant and genetically rescued collecting duct clones were grown initially under non-polarized conditions and at a permissive temperature of 33 °C in collagen-coated tissue culture flasks. The medium used for this initial culture was a defined collecting duct (CD) medium. It's recipe included DMEM-F12 supplemented with 10% FBS, 10 U/ml interferon-gamma (IFN- $\gamma$ ), 1.3  $\mu$ g/L sodium selenite, 1.3  $\mu$ g/L triiodothyronine (T3), 5 mg/L insulin, 5 mg/L transferrin, 5  $\mu$ M dexamethasone, 2.5 mM L-glutamine, 100 U/ml penicillin, and 100  $\mu$ g/ml streptomycin in a humidified 5% CO<sub>2</sub> incubator. These conditions are known to upregulate ENaC expression. No epidermal growth factor was present at any time during the culture, because it is known to inhibit ENaC (Refs. 15, 49) and stimulate an aberrantly hyperactive EGF receptor signaling cascade in PKD cells (Refs. 41, 54). For this and other reasons, EGF was excluded from the defined and supplemented medium. G418 (200  $\mu$ g/ml) was present in the medium throughout 33 °C culture to continually select the clones bearing pcDNA 3.1 vector without or with the Tg737 cDNA cassette. G418 was left out of the medium for the mixed uncloned CCD cells and mutant clones "Mutant 2" and "Mutant 3." Cells were then lifted in minimal trypsin-EDTA solution and were seeded onto 6.5 mm diameter Costar Transwell filter supports (polycarbonate filter, 0.45  $\mu$  pore size) coated with diluted Vitrogen 100 solution (1:15 dilution with CaMg-free

PBS) at a density more than adequate to cover the entire filter at Day 0 (the seeding day). Cells were then grown in the same defined CD medium at 39 °C but without IFN- $\gamma$ . Cells were all grown at similar passage numbers and were passed a minimum of 10 times without any change in morphological or functional phenotypes. All monolayers were fed one day prior to the experiment.

### *Transepithelial Electrophysiology*

*Open-Circuit Measurements with Millipore VoltOhmmeter*  $R_{TE}$  and  $V_{TE}$  were measured after Day 2 following seeding with a Millipore VoltOhmmeter using Ag-AgCl chopstick electrodes.  $V_{TE}$  readings were quite stable in these mutant and rescued model renal epithelia, because the  $R_{TE}$  values achieved by these clones grown as monolayers were very high (near or  $\geq 20,000 \Omega \cdot \text{cm}^2$  after 4-6 days on filters). All such readings were made in the defined CD medium. All monolayers were fed one day prior to the experiment. When  $R_{TE}$  and  $V_{TE}$  reached stable values (between Days 4 and 6), open-circuit measurements were performed in CD medium in unstirred conditions before and at defined timepoints after application of inhibitors or agonists.

*Short-Circuit Current Analysis in Ussing Chambers* Ussing chamber recordings of short-circuit current ( $I_{SC}$ ) were performed as described previously (Ref. 47) in a homemade system designed to accommodate 6.5 mm diameter Transwell filter supports. All monolayers were fed one day prior to the experiment. Because the defined CD medium was found to be critical in maintaining at least part of the large transepithelial

current and voltage in mutant and rescued monolayers, these recordings were also performed in the CD medium bubbled with 5% CO<sub>2</sub> in a circulating system warmed to 37 °C. The only difference between these recordings and open-circuit readings was that the medium was devoid of FBS in the Ussing chamber. A voltage pulse was injected by the amplifier periodically during most recordings to gauge resistance (see Results), and inhibitors were added only after a stable baseline was achieved.

#### *Data Analysis and Statistics*

I<sub>SC</sub> data were converted to  $\mu\text{A per cm}^2$  filter support surface area by multiplying that area (0.33 cm<sup>2</sup>) by 3. Data are expressed as mean  $\pm$  SEM. Differences before and after application of a drug were assessed by paired Students' t-test ( $P < 0.05$  as a significance level). Differences between mutant and rescued or wild-type monolayers were assessed by ANOVA ( $P < 0.05$  as a significance level).

#### *Materials*

Hormone supplements for the defined CD medium, amiloride and amiloride analogs, and protease and protease inhibitors were obtained from Sigma. Vitrogen 100 was obtained from Cohesion, and filter supports were purchased from Costar through Fisher Scientific.



## **Results**

*V<sub>TE</sub> is elevated in mutant orpk CCD principal cell monolayers versus genetically rescued CCD principal cell monolayers, despite similar R<sub>TE</sub>*

Transepithelial resistance (R<sub>TE</sub>) was measured on Day 2 for each monolayer, two days after seeding at confluence on Day 0, to allow the cells to attach to the filter support and to initiate monolayer formation. After Day 2, the R<sub>TE</sub> was assessed frequently thereafter until a plateau was measured for both R<sub>TE</sub> and V<sub>TE</sub>. This plateau was reached routinely on Day 5 and remained stable on Days 6 and 7. In general and despite equivalent R<sub>TE</sub> values, there was a 3- to 6-fold augmented V<sub>TE</sub> in mutant monolayers versus rescued monolayers. The overall summary of all V<sub>TE</sub> measurements for this panel of mutant and genetically rescued CCD PC cell models is provided in Figure 1. Taken together and despite equivalent R<sub>TE</sub> for both mutant and genetically rescued monolayers that approached or exceeded 20 k $\Omega$ •cm<sup>2</sup>, mutant *orkp* CCD PC cell monolayers had a profoundly upregulated V<sub>TE</sub> due to a heightened activity in one or more ionic conductances.

The very large R<sub>TE</sub> achieved by these clones grown as monolayers and the upregulated V<sub>TE</sub> in the mutant *orkp* cell monolayers versus counterpart control monolayers necessitated verification and constant and reproducible comparison between mutant and genetically rescued clones. As such, several different investigators in the laboratory performed open-circuit measurements of R<sub>TE</sub> and V<sub>TE</sub> in mutant (“M”) versus rescued (“R”) monolayers with the Millipore open-circuit assay (Figure 2). The first data

set showed the development of  $V_{TE}$  as the monolayers matured from Day 4 to Day 7 to Day 10 (Figure 2). Subsequent data sets were measured on Day 5 and/or Day 6 where the  $V_{TE}$  and  $R_{TE}$  were most stable. In each data set, mutant and rescued cell monolayers were compared routinely. In all data sets and over at least 10 passages, mutant monolayers lacking a well-formed apical central cilium (defined as “cilium-deficient”) had an augmented  $V_{TE}$  versus genetically rescued monolayers (controls defined as “cilium-competent”). Figure 2 also demonstrates again the difference in morphological phenotype of the central monocilium for mutant and genetically rescued PC cell clones. Examples of this phenotype were published previously (Ref. 63); however, we provide this additional and more recently gathered data set of better images for full presentation. It should be noted that cilium length in the rescued monolayers is 2-3  $\mu\text{m}$ , whereas the malformed cilium in mutant monolayers is less than 0.5  $\mu\text{m}$  in length. It should also be noted that these are maximal monocilium length in matured monolayers. In contrast, MDCK cell monolayers express monocilia that grow longer and longer as the monolayers age (Ref. 39). This is not the case in these mouse PC cells derived from individually dissected CCDs. Taken together, these data show a reproducible and upregulated ionic conductance in the apical membrane of mutant *orpk* mixed CCD cells and in CCD PC cell clones grown as monolayers and deficient in an apical central monocilium.

< Figures 1 and 2 HERE >

*Elevated  $V_{TE}$  and  $I_{SC}$  in mutant monolayers is inhibited in a dose-dependent manner by amiloride, an inhibitor of  $Na^+$  transport*

Based on our experience with ADPKD epithelial cell models (Ref. 47), we first tested the hypothesis that secretory chloride ( $Cl^-$ ) current was upregulated, causing the enhanced  $V_{TE}$  and  $I_{TE}$  observed in mutant *orpk* monolayers. Experiments with apical  $Cl^-$  channel blockers (DIDS, DPC, and glibenclamide) as well as basolateral  $Na,K,2Cl^-$  cotransporters (bumetanide) were without effect (data not shown). This is not surprising, because CCD PC cells are not thought to be capable of much or any  $Cl^-$  secretion under basal conditions (Refs. 29, 32, 33, 45).

Therefore, because PC cells are primarily  $Na^+$ -absorbing and  $K^+$ -secreting cells within the CCD under normal conditions, we postulated that  $Na^+$  absorption across the apical membrane of mutant *orpk* ARPKD PC cell monolayers may be upregulated. Figure 3 shows the sensitivity of  $V_{TE}$  in mutant and rescued cell clones grown as monolayer to apical application of 50  $\mu M$  amiloride. Both the greatly enhanced  $V_{TE}$  in mixed mutant CCD PC cells from the *orpk* mouse and mutant *orpk* PC cell clones and the reduced but significant  $V_{TE}$  in the genetically rescued clones was highly sensitive to amiloride. Apical application of amiloride to mutant and rescued cells inhibited the  $V_{TE}$  virtually completely within 5 minutes (Figure 3). Taken together, these data further confirm that these cell models derived originally from individually dissected CCD segments are  $Na^+$ -absorbing PC cells and that a  $Na^+$  absorptive transport mechanism appeared upregulated in mutant versus rescued *orpk* PC cell monolayers.

< Figure 3 HERE >

To examine this Na<sup>+</sup> transport mechanism more deeply and to confirm that it was electrogenic, we performed electrophysiological analysis of I<sub>SC</sub> in mutant versus rescued *orpk* PC cell monolayers mounted in Ussing chambers. Despite equivalent R<sub>TE</sub> (as indicated by the voltage pulses causing brief current deflections at fixed times on the raw traces), amiloride-sensitive I<sub>SC</sub> was upregulated approximately 4-fold in mutant monolayers versus rescued monolayers (Figure 4). Basal I<sub>SC</sub> in both mutant and rescued monolayers was inhibited markedly by 10 μM amiloride (Figure 4). In correlative V<sub>TE</sub> measurements, the IC<sub>50</sub> for amiloride was approximately 1 μM, while maximal inhibition was achieved at 10 μM or greater (Figure 4). These initial data suggested that ENaC may be upregulated in this murine model of ARPKD; however, the small residual V<sub>TE</sub> and I<sub>SC</sub> resistant to amiloride suggested that other Na<sup>+</sup> transport pathways might be present.

< Figure 4 HERE >

#### *Cell culture requirements are consistent with ENaC expression and function*

Analysis of the initial cell culture findings and responses to assay modifications also provided insight into the identity of the Na<sup>+</sup> transport mechanisms responsible for this pathophysiological phenotype. V<sub>TE</sub> was lost within 24 to 48 hours from mutant and rescued monolayers to zero, if the monolayers were switched out of their defined CD medium and into a more standard FBS-containing medium without hormonal supplements. Figure 5 shows these data using the Mutant 1 clone grown as well polarized monolayers because of the upregulated V<sub>TE</sub> signal. The upregulated V<sub>TE</sub> was also lost

transiently (over a period of 5-12 hours) when the apical medium was aspirated and replaced (Figure 5). In contrast, replacement of the basolateral medium fueled  $V_{TE}$  within 30 minutes (Figure 5). The difference in electrophysiological phenotype was also most dramatic in the unstirred, open-circuit measurements of  $V_{TE}$ . Curiously, in standard Ringers for Ussing chambers, the upregulated  $V_{TE}$  and short-circuit current ( $I_{SC}$ ) was lost completely during the 15 minute time lag during set-up and stabilization of the  $V_{TE}$  and  $I_{SC}$  under clamped conditions. In fact,  $I_{SC}$  decayed over time before our eyes while waiting for the basal  $I_{SC}$  to stabilize in these renal cell monolayers. This loss in  $I_{SC}$  (versus calculated  $I_{TE}$  from open-circuit measurements) was prevented partially by performing Ussing chamber experiments in defined CD medium without FBS or in an OptiMEM-1 serum-free medium or Ringers supplemented with insulin (at the same concentration as the defined culture medium; Figure 5). Importantly, Ringers supplemented with insulin that lacked  $Na^+$  (replaced by NMDG) could not support  $I_{SC}$  (Figure 5). Taken together, these data suggest that amiloride-sensitive  $V_{TE}$  and  $I_{SC}$  are quite sensitive to cell culture conditions and are mediated by electrogenic  $Na^+$  transport mechanisms, likely ENaC, in a polarized cell monolayer system.

< Figure 5 HERE >

These data also show that hormonal supplements (dexamethasone and insulin, in particular) support overall ENaC expression and function in renal epithelia. However, these data also suggest that the renal epithelium itself secretes stimulatory factors that support ENaC activity acutely and independently of the defined culture medium. One possible candidate for this acute stimulation of ENaC is a secreted protease that cleaves

the extracellular domain of the ENaCs to keep ENaC open. A protease or another factor may be removed by changing the medium or washed away and/or diluted when exposed to the circulating conditions of the Ussing chamber. It should be noted emphatically that these properties do not affect the overall difference in activity observed in cilium-deficient versus cilium-rescued monolayers. Rather, these observations and factors merely support the idea that it is ENaC activity that is being measured in these studies and the data are consistent with the hormonal requirements, properties and regulation of ENaC described in the literature (Refs. 6, 28). These data led us to a primary focus on ENaC.

*ENaC-selective amiloride analogs inhibit the elevated  $V_{TE}$  and  $I_{SC}$  in mutant monolayers*

Because amiloride at higher doses can inhibit multiple  $Na^+$  transporters as well as multiple  $Na^+$  and cation channels that might be involved in  $Na^+$  absorption, we tested ENaC-selective amiloride analogs. Further proof of ENaC involvement in this phenotype was provided by inhibition of the majority of the upregulated  $V_{TE}$  and  $I_{SC}$  with apical benzamil (Figure 6). Phenamil was also effective at nanomolar concentrations with an  $IC_{50}$  of approximately 200 nM (data not shown). These amiloride analogs are more selective for ENaC. The  $IC_{50}$  for benzamil was approximately 50 nM (Figure 6), consistent with a more potent effect of benzamil over amiloride known to exist for ENaC (Refs. 6, 28). Taken together, these data led us to a focus on ENaC as a mediator of electrogenic  $Na^+$  hyperabsorption in mutant models of ARPKD grown as well polarized monolayers and lacking apical central cilia.

< Figure 6 HERE >

As internal controls for this amiloride analog pharmacology, we also tested ethylisopropylamiloride (EIPA) and dimethylamiloride (DMA), analogs that are less selective for ENaC channels and more selective for Na/H exchangers at low micromolar concentrations (Ref. 37). To our initial surprise, EIPA also inhibited the  $V_{TE}$  with an  $IC_{50}$  of approximately 2  $\mu$ M (Figure 7). DMA inhibited as well with an  $IC_{50}$  of approximately 20  $\mu$ M (Figure 7). It should be noted, however, that apical application of ouabain (100  $\mu$ M) was without effect, ruling out a role for mislocalized Na,K-ATPase pumps in this  $Na^+$  hyperabsorption (data not shown). Although these data suggest a possible parallel role for NHE exchangers in sodium absorption, the activity of such exchangers should not affect  $V_{TE}$  because of their universally shared 1:1 stoichiometry of cation exchange (Ref. 37). Moreover, further examination of the ENaC literature showed that a rank order potency of benzamil > amiloride > DMA has been published for ENaC (Ref. 12). However, we also evaluated EIPA effects in our studies, which is a key and most highly selective amiloride analogs at lower doses for NHE exchange versus ENaC. While our rank order potency is similar to that above, it is also more comprehensive (benzamil > amiloride  $\geq$  EIPA > DMA). Taken together, we conclude that ENaC upregulation likely underlies the upregulated  $V_{TE}$  and  $I_{SC}$  observed in mutant cilium-deficient cells. Nevertheless, we cannot rule out the fact that parallel and upregulated NHE exchange activity may stimulate ENaC through effects on external apical pH (Refs. 27, 58), intracellular pH (Ref. 13), or both.

*Proteases influence upregulated ENaC-mediated  $I_{SC}$  or  $V_{TE}$  in the mutant monolayers*

In the light of a primary role for ENaC in upregulated amiloride-sensitive  $V_{TE}$  and  $I_{SC}$  in cilium-deficient PC cells, we tested whether endogenous secreted or membrane-bound proteases were active in the regulation of ENaC in this model epithelium. Such proteases are thought to recognize Kunitz-like domains in the cysteine-rich regions of the extracellular domain of ENaC and activate ENaC channels in epithelia specifically through direct protease-dependent cleavage (Refs. 8, 10, 25, 51, 53, 56). We also used protease inhibitors as another diagnostic, cell biological tool to implicate ENaC in this dysregulated ion transport phenotype in the mutant monolayers. Aprotinin is a protease inhibitor used widely in these ENaC studies (Refs. 8, 10, 25, 51, 53, 56). While aprotinin lowered the current only slightly in the rescued monolayers, it had a significant inhibitory effect on Ussing chamber  $I_{SC}$  in mutant monolayers that was inhibited further by benzamil (Figure 8). If left on the apical side of the mutant monolayers longer in open-circuit experiments (10 minutes versus 5 minutes in the Ussing chamber), the inhibitory effect of aprotinin was more robust (Figure 8).  $V_{TE}$  was virtually abolished in the mutant Tg737<sup>orpk</sup> monolayers by 1 and 10  $\mu$ g/ml aprotinin, after 30 minutes (Figure 8). The inhibitory effect was diluted away by diluting the protease inhibitor to ng/ml amounts. Leupeptin, another broad specificity serine protease inhibitor, also inhibited the  $V_{TE}$  driven by ENaC (data not shown). Taken together, protease inhibitors attenuate ENaC activity in the mutant *orpk* cell monolayers. We speculate that secreted proteases may be responsible for keeping ENaC active at the membrane. They may be washed away upon a medium change, upon transfer from unstirred to stirred conditions, or upon exposure of



the monolayer to a 20-fold larger volume of medium bathing its apical surface in the Ussing chamber (10 mls) versus in a apical cup of a filter support (0.5 mls). Other locally released factors may also be necessary to gate or maintain ENaC activity and cannot be discounted. Nevertheless, these data provide another diagnostic piece of evidence implicating ENaC channels in this enhanced  $I_{SC}$  and  $V_{TE}$  phenotype and agree with similar work performed by multiple laboratories in human primary and immortalized airway epithelial cell monolayers (Refs. 8, 51, 53).

< Figure 8 HERE >

### ***Discussion***

We hypothesized that ion transport across the apical membrane of PC cells lacking well-formed apical monocilia might be abnormal, based on evidence implicating non-motile cilia and flagella as sensory organelles in neurons (Refs. 3, 4, 22, 24). While the apical central monocilium might be a flow sensor in renal tubules with higher flow rates such as the proximal tubule, its role in the collecting duct may be different in a region of lower flow of tubular fluid. Along these lines, we speculate that the apical central monocilium could be an “osmosensor” or “chemosensor” for the CCD PC cells and, if lost, may affect ductal epithelial ion transport in the renal collecting duct and in tubules and ducts from extrarenal tissues.

Based upon the aforementioned data, we have formed working hypotheses concerning the cellular and molecular mechanisms of ENaC upregulation in the face of the loss of a fully formed apical central monocilium. These postulates are most germane to this mouse model of ARPKD. However, they also agree with findings in a human

ARPKD cell model (Ref. 42) and with early onset hypertension in the majority of human ARPKD patients (Ref. 20). First, it is possible that ENaC channel proteins are localized normally on or near the monocilium in a limited and highly localized pattern. When the cilium is lost, the PC cell may overexpress ENaC in the apical membrane in a compensatory manner. Data from Satlin and coworkers in human ARPKD cell models documented a modest yet significant upregulation in alphaENaC mRNA and protein (Ref. 42). Second, we hypothesize that an inhibitory signal that normally originates from the monocilium ( $\text{Ca}^{2+}$  spark and wave, phospholipids, cilium-specific protein kinase, etc.) tonically inhibits ENaC-mediated  $\text{Na}^+$  absorption. Autocrine purinergic signaling could drive one or more of these inhibitory signals as could other ligands such as growth factors and hormones whose receptors localize to the luminal membrane of ductal epithelia. When the monocilium is lost, this inhibitory signal is lost, leading to resultant upregulation of ENaC activity. Early data suggests that ATP release is impaired in mutant, cilium-deficient cell monolayers versus cilium-competent controls (A Fintha, EL Hanson, D. Olteanu, PD Bell and EM Schwiebert, unpublished observations). Third, we postulate that the loss of the apical central monocilium causes a redistribution of ENaC from a primarily intracellular location to the plasma membrane. An effect on the microfilament- or microtubule-based cytoskeleton due to the absence of the monocilium could affect ENaC protein distribution in the apical pole of the polarized CCD PC cells (Refs. 50, 64). ENaC localization and/or function is also affected by actin (Refs. 50, 64). Fourth, our amiloride analog pharmacology data do not discount the possibility that there may be parallel upregulation of Na/H exchangers or NHEs. We speculate that loss of a well-formed monocilium may cause upregulation of NHEs and either acidification of the

tubular fluid bathing the apical membrane or alkalinization of the cytosol in a cilium-deficient cell and potentiate ENaC activity (Refs. 13, 27, 58). Early data suggest that NHE activity may also be present and/or upregulated in both the apical and basolateral membranes *in vitro* and *in vivo* in *orpk* cilium-deficient cell monolayers and isolated perfused tubules, respectively (D Olteanu, W Liu, M Bevensee, LM Satlin, BK Yoder and EM Schwiebert, unpublished observations). We are keeping an open mind to all possible models above and are cognoscente to the fact that a combination of the working hypotheses and postulates formed above may ultimately contribute to the observed  $\text{Na}^+$  hyperabsorption phenotype.

In light of the fourth postulate immediately above, extracellular  $[\text{H}^+]$  is known to affect BNaCs, ASICs, and the topologically related P2X purinergic receptor channels (Refs. 1, 5, 35, 46, 48). Human  $\delta\text{ENaC}$  is stimulated by extracellular protons (acidic pH,  $\text{EC}_{50}$  @ 5.0) and has been shown to be expressed in human kidney and elsewhere (Ref. 58). This effect on  $\delta\text{ENaC}$ , co-expressed with  $\beta\text{ENaC}$  and  $\gamma\text{ENaC}$  in *Xenopus* oocytes, was also confirmed by Ji and Benos and is conferred by degenerin domains within  $\delta\text{ENaC}$  (Ref. 27). A mouse ortholog has not been found but will likely emerge in the near term.  $\delta\text{ENaC}$ , as part of a novel or additional ENaC heteromultimeric channel in renal collecting duct, may be critical in this disease paradigm and may sense and be upregulated by the NHE-dependent acidification of the tubular fluid. To our knowledge, the effect of extracellular pH on the other ENaC subunits has not been addressed. Alternatively, profound intracellular alkalinization due to upregulated NHE activity in the apical and basolateral membranes of PC cell monolayers may potentiate ENaC. Stanton, Benos and colleagues in *Xenopus* oocytes and in planar lipid bilayers showed that

intracellular alkalinization stimulates various ENaC heteromultimers (due specifically to the presence of  $\alpha$ -ENaC) and that intracellular acidification did the opposite (Ref. 13). We are currently pursuing these early observations on NHE function and its effects on ENaC activity in our native mouse CCD PC model epithelia. We also cannot discount the possible upregulation of additional types of cation channels that are sensitive to amiloride such as cyclic nucleotide-gated non-selective cation channels expressed in collecting duct epithelial cell models (Refs. 30, 31, 42).

It is important to draw key distinctions now between ADPKD and ARPKD. We and others have proposed that ion, solute and water secretion into encapsulated ADPKD cysts contributes to and is detrimental to expansion of cyst volume and size over time (Refs. 11, 18, 19, 47). Particular attention has been paid to chloride secretion via CFTR and other chloride channels (Refs. 11, 18, 19, 47). Curiously, cystic epithelia in both forms of the disease, ARPKD and ADPKD, either never fully differentiate or revert to an undifferentiated, “fetal-like” phenotype. In this sense, cystic cells from ARPKD and ADPKD share this trait. As such, any and all ENaC subunits may be expressed in the mutant monolayers in a way that may differ from controls. It is likely, however, that ENaC subunits are exclusively apical in both mutant and control monolayers. This is a universally accepted fact in all absorptive epithelia (Ref. 6). It is opposite in highly secretory epithelia like choroid plexus of the brain and ciliary process of the eye (see below) (Ref. 9). However, it may their relative abundance and/or their function that may be upregulated at the mRNA, protein and/or cell surface level. Again, we have designed RT-PCR primers and gathered antibodies to all relevant ENaC subunits to perform a thorough analysis of expression and localization of these  $\text{Na}^+$  transport proteins. This is a

separate study beyond the scope of this manuscript that requires collaboration with multiple laboratories.

Despite this similarity in undifferentiated cell phenotype, it is important to re-state that ARPKD and ADPKD are very different diseases in terms of how the architecture of the kidney is remodeled (Refs. 11, 18-21). The type of remodeling has profound implications for salt and water movement and the role of a diseased PKD kidney in salt and water balance. Encapsulated cysts arise mainly in ADPKD, where such drastic remodeling occurs throughout the nephron. Tubules along the entire nephron fully “pinch off” and cause the formation of fluid-filled cysts that are surrounded by a single cell monolayers of cystic epithelial cells. Tubules only dilate profoundly in ARPKD. This occurs mainly along the collecting duct and more rarely in proximal tubule. Importantly, ARPKD dilated tubules do not “pinch off” to form encapsulated cysts but merely create an unstirred environment within the renal parenchyma. Thus, in ARPKD,  $\text{Na}^+$  is likely hyperabsorbed based upon our results. Interestingly, early characterization of the *ork* mouse revealed a very low urine:plasma osmolality ratio (Refs. 60-62). This may be due to a lack of ability to concentrate the urine and/or hyperabsorption of a key osmole like  $\text{Na}^+$  or both. Similar data has been published by our co-authors showing hyperabsorption of  $^{22}\text{Na}^+$  in polarized monolayers of human ARPKD cells versus normal age-matched controls (Ref. 42). Data from this laboratory also suggest that  $\text{Na}^+$  absorptive mechanisms in addition to ENaC may contribute in their system, owing to a high  $\text{IC}_{50}$  for amiloride in these studies (Ref. 42). Tubular fluid collected from human ARPKD dilated ducts that resemble pseudocysts and destined to be part of the final urine at the time of nephrectomy pre- or at the time of transplant show extremely low  $[\text{Na}^+]$ , suggesting avid renal  $\text{Na}^+$

absorption (Ref. 43). They had very low Na (2-7 mM, average <5 mM), a [K] that was greater than that observed in plasma (8-9 mM). An important final point, however, is that hypertension in ARPKD is likely caused by a lesion that creates a primary or secondary defect in a Na<sup>+</sup> transport mechanism. This defect would be a “gain of function” lesion, and we hypothesize that this is likely the case with ENaC upregulation in the renal collecting duct in ARPKD.

Although ENaC hyperactivity and/or upregulation is consistent with human ARPKD and the early onset of hypertension (Ref. 20), hypertension is also present in ADPKD well before the onset of renal disease and insufficiency. In ADPKD clinical studies, it is thought to reflect the distortion/destruction of the normal renal parenchyma by the progressive expansion of cyst size, thereby activating the renin-angiotensin system. However, is this the sole cause? In ADPKD cysts, Na<sup>+</sup> may not be excreted because it fails to enter the urinary bladder. This effect would only be a minor contributing factor, because cysts only arise from 5-10% of nephron segments throughout the kidney. As such, could Na<sup>+</sup> hyperabsorption also occur in ADPKD and contribute to hypertension that arises prior to presentation of ADPKD kidney disease? Hypertension tends to arise ahead of significant kidney and extrarenal tissue dysfunction in ADPKD.

In this light and importantly, the [Na] in cyst fluids in ADPKD has been documented. Interestingly, [Na] in cyst fluids from the kidney and elsewhere in ADPKD is quite heterogeneous. Gardner and Grantham found a range of [Na] in 12 cyst fluids from 3.1 to 150 mEq/L (Ref. 17). They stated that the cyst fluids that had lower [Na] were likely of distal origin because of this and other attributes (Ref. 17). Proximal cysts likely had isotonic [Na] with respect to plasma or interstitium because of isotonic

reabsorption that occurs in proximal tubule segments (Ref. 17). Eckhardt et al. measured [Na] when assessing EPO production and expression in cysts (Ref. 16). There was a similar heterogeneity to that found in the study mentioned above and, again, a conclusion that cysts of distal nephron origin had low [Na] of 20-40 mM (some less than 20 mM), while cysts from proximal segments had high [Na] isotonic to plasma or interstitium (Ref. 16). A third study by Gardner and coworkers compared cyst fluid content in kidney cysts in ADPKD versus breast cysts in another disease (Ref. 26). There were again kidney and breast cysts with low and high [Na] content. Interestingly, those with low amounts of [Na] and other ions had a greater content of amino acids. Those with high content of [Na] and other ions had a low amino acid content. Both low and high [Na] cysts in kidney and breast were isotonic to plasma or interstitium because of this. It is difficult to know that cysts of distal nephron origin have low [Na] because of hyperabsorption or because the distal tubule and collecting tubular fluid have low [Na] to begin with because most of it is reabsorbed from the glomerular filtrate by this point in the nephron. However, these data and the pre-emergence of hypertension before renal decline in ADPKD suggest that Na transport pathways should also be assessed in ADPKD cystic epithelia versus controls.

Not only is there significant evidence for upregulation of ENaC in human collecting duct epithelia and, now, mouse ARPKD model epithelia, there is clinical and mouse model evidence in other tissues besides the kidney that hints of Na<sup>+</sup> transport dysregulation defects in ARPKD. In a significant percentage of ARPKD patients from multiple cohorts, there is profound pulmonary hypoplasia that causes respiratory insufficiency at birth and/or chronic lung disease that leads to significant mortality (Ref.

20). In salt and water transport physiology,  $\text{Na}^+$  absorption is absent during fetal lung development. Rather, secretion of an acidic and chloride-rich fluid is solely active. This allows for a fetal lung fluid to fill the developing lung and airways and allow optimal growth factor function (Ref. 7). Any  $\text{Na}^+$  absorption, hyperactive or not during this time in fetal lung development, could hamper normal development and lead to hypoplasia or incomplete branching of the airways and lung (Ref. 7). There are also reports in the human condition of low amniotic fluid during pregnancy (Ref. 14). Low fluid volume in the amniotic sac may suggest  $\text{Na}^+$  and water hyperabsorption. Similarly,  $\text{Na}^+$  hyperabsorption in gastrointestinal (GI) tissues such as pancreas and liver may hamper optimal secretion of anions such as bicarbonate and chloride that water follows (Refs. 2, 36, 44). Such an impairment of secretion due to the counteractive movement of  $\text{Na}^+$  absorption (which is normally less prominent in these two particular GI tissues) could be detrimental. Finally, the choroid plexus is a highly secretory organ where chloride and  $\text{Na}^+$  are secreted in parallel to fuel cerebrospinal fluid (CSF) secretion at high rates (Ref. 9). In this epithelium, ENaC is on the basolateral membrane as the entry step for  $\text{Na}^+$  secretion, while the Na,K-ATPase pump actively secretes  $\text{Na}^+$  out into the ventricles of the brain to help form the CSF.  $\text{Na}^+$  hypersecretion, with parallel movement of excessive chloride and water, could explain at least in part hydrocephalus in the *orpk* animal (Ref. 9).

Having said all that above, we do not intend to imply that  $\text{Na}^+$  hyperabsorption is a universal phenotype in all mouse models of ARPKD. It is also not universal in the human condition. These and other PKD mouse models have been generated by deletional, insertional, and chemical mutagenesis. The structural ciliary phenotype is quite dramatic



in the *orpk* mice; however, it is less dramatic or not present in other ARPKD mouse models such as *bpk* and *cpk* mice. It should be noted that Cotton and colleagues showed reduced ENaC-mediated Na<sup>+</sup> absorption in the *bpk* mouse model in mixed collecting duct cell monolayers (Ref. 55). This could have been due to the profound inhibitory effects of EGF on ENaC function and abnormal EGF signaling in cystic epithelia (Refs. 15, 41, 49), given that these monolayers were established in the presence of EGF (Ref. 55). Despite the overnight removal of EGF, EGF effects likely remained (Ref. 55). Nevertheless, protein products of genes mapped in humans and specific mouse models display shared localization in cilia (Refs. 23, 59). As such and given the similar phenotype of the Na<sup>+</sup> hyperabsorptive cyst-lining cell in *orpk* and human ARPKD collecting ducts, further investigation is warranted in this area of PKD.

Why would the non-motile monocilium central to the apical membrane of PC cells influence ENaC subunits or NHE subtypes? In the proximal tubule or in any duct with high flow rates, the apical central monocilium is ideally positioned to be a “flow sensor.” Flow has indeed been shown to influence Na<sup>+</sup> and K<sup>+</sup> transport in the CCD by our co-authors (Refs. 45, 57), and the luminal monocilium may play a critical role in transducing this mechanical signal. As likely, however, in ducts and tubules with lower flow rates such as the collecting duct of the kidney, the bile duct, the pancreatic duct, and elsewhere, the role of the non-motile monocilium may be different, not unlike that of an “osmosensor” or a “chemosensor.” It is intriguing to speculate that this monocilium sensor may sense the degree of diuresis versus antidiuresis or the balance between natriuresis and antinatriuresis. Each principal cell may need a way to sample the tubular fluid osmolality and transduce that information to the ion transport pathways within the

same cell. The same may be true for tubular fluid pH to sense states of acidosis versus alkalosis. Further studies in progress are addressing the possible cellular mechanism or mechanisms that connect the cilium to ENaC and other solute and water transport pathways. In this light, it would be intriguing to evaluate a possible connection between the functions of the polycystins on cilia and ENaC activity as well as ENaC activity in conditional knockouts of the cilium induced by affecting other ciliary proteins critical to cilia structure and function besides Polaris. Indeed, the similar Na<sup>+</sup> hyperabsorptive states reported in human ARPKD (Ref. 42) and in our *orpk* mouse cell models suggest that a hypertensive state is a general feature of ARPKD. Irregardless of the cellular and molecular mechanisms to be elucidated, upregulated ENaC-mediated hyperabsorption of Na<sup>+</sup> may be a primary underlying cause of profound hypertension in a majority of human ARPKD patients and should be contemplated as a target for clinical treatment.

### ***Acknowledgments***

This work was supported by R01 NIH grants DK67343 to EMS and DK55007 to BKY. Grants to PDB (DK71007), LMS (PO1 DK62345) and Fellowship grants to WL from the Polycystic Kidney Disease Research Foundation and the Revson Foundation are also acknowledged. Our chief collaborator in this ARPKD mouse model work at UAB is BKY. We collaborate with LMS and WL on isolated perfused collecting duct studies in these ARPKD animal models. We collaborate with PDB at UAB on ATP release dynamics and regulation in these cells and models. LGW is the very able Director of our Recessive PKD Core Center at UAB.

We thank Drs. Peter Smith and Dale Benos at UAB for agreeing to provide new reagents to assess ENaC expression and localization for future work. We thank Dr. Daniel Biemesderfer at Yale for agreeing to provide NHE subtype-specific antibodies to assess NHE expression and localization in cilium-deficient versus cilium-competent models for future work. Dr. J. Michael Wyss and Dr. Jim Schafer at UAB stand ready to collaborate in blood pressure telemetry measurements from ARPKD mouse models and in metabolic analyses from these mice, respectively.

## **References**

1. **Adams CM, PM Snyder, and MJ Welsh.** Paradoxical stimulation of a DEG/ENaC channel by amiloride. *J. Biol. Chem.* 274: 15500-15504, 1999.
2. **Ahn YJ, Brooker DR, Kosari F, Harte BJ, Li J, Mackler SA, and TR Kleyman.** Cloning and functional expression of the mouse epithelial sodium channel. *Am. J. Physiol.* 277: F121-F129, 1999.
3. **Bargmann CI, E Hartwig, and HR Horvitz.** Odorant-sensitive genes and neurons mediate olfaction in *C. elegans*. *Cell* 74(3): 515-527, 1993.
4. **Bargmann CI and HR Horvitz.** Chemosensory neurons with overlapping functions direct chemotaxis to multiple chemicals in *C. elegans*. *Neuron* 7(5): 729-742, 1991.
5. **Baron A, R Waldmann, and M Lazdunski.** ASIC-like, proton-activated currents in rat hippocampal neurons. *J. Physiol.* 539: 485-494, 2002.
6. **Benos DJ and BA Stanton.** Functional domains within the degenerin/epithelial sodium channel (Deg/ENaC) superfamily of ion channels. *J. Physiol. (London)* 520: 631-644, 1999.
7. **Bland RD.** Chapter 161. Fetal lung liquid and its removal near birth. In The Lung: Scientific Foundations; Eds. RG Crystal, JB West et al., Lippincott-Raven Publishers, Philadelphia, c1997.
8. **Bridges RJ, BB Newton, JM Pilewski, DC Devor, CT Poll, and RL Hall.** Sodium transport in normal and CF human bronchial epithelial cells is inhibited by BAY 39-9437. *Am. J. Physiol.* 277: F552-F559, 2001.

9. **Brown PD, Davies SL, Speake T, and ID Millar.** Molecular mechanisms of cerebrospinal fluid production. *Neuroscience* 129(4): 957-970, 2004.
10. **Caldwell RA, RC Boucher, and MJ Stutts.** Serine protease activation of near-silent epithelial Na<sup>+</sup> channels. *Am. J. Physiol.* 286(1): C190-C194, 2004.
11. **Calvet JP and JJ Grantham.** The genetics and physiology of polycystic kidney disease. *Semin. Nephrol.* 21(2): 107-123, 2001.
12. **Carr MJ, Gover TD, Weinreich D, and BJ Undem.** Inhibition of mechanical activation of guinea-pig airway afferent neurons by amiloride analogues. *Br. J. Pharmacol.* 133(8): 1255-1262, 2001.
13. **Chalfant ML, Denton JS, Berdiev BK, Ismailov II, Benos DJ, and BA Stanton.** Intracellular H<sup>+</sup> regulates the alpha-subunit of ENaC, the epithelial Na<sup>+</sup> channel. *Am. J. Physiol.* 276: C477-C486, 1999.
14. **D'Alton M, Romero R, Grannum P, DePalma L, Jeanty P, and JC Hobbins.** Antenatal diagnosis of renal anomalies with ultrasound. IV. Bilateral multicystic kidney disease. *Am. J. Obstet. Gynecol.* 154(3): 532-537, 1986.
15. **Deachapunya C and SM O'Grady.** Epidermal growth factor regulates the transition from basal sodium absorption to anion secretion in cultured endometrial epithelial cells. *J. Cell Physiol.* 186(2): 243-250, 2001.
16. **Eckhardt KU, Mollmann M, Neumann R, et al.** Erythropoietin in polycystic kidneys. *J. Clin. Invest.* 84: 1160-1166, 1989.
17. **Gardner KD and JJ Grantham.** Composition of fluid in 12 cysts of a polycystic kidney. *J. Am. Soc. Neph.* 9: 1965-1970, 1998.

18. **Grantham JJ.** Polycystic kidney disease: From the bedside to the gene and back. *Curr. Opin. Nephrol. Hypertens.* 10(4): 533-542, 2001.
19. **Grantham JJ and DP Wallace.** Return of the secretory kidney. *Am. J. Physiol.* 282: F1-F9, 2002.
20. **Guay-Woodford LM and RA Desmond.** Autosomal recessive polycystic kidney disease: the clinical experience in North America. *Pediatrics* 111(5): 1072-1080, 2003.
21. **Guay-Woodford LM.** Murine models of polycystic kidney disease: Molecular and therapeutic insights. *Am. J. Physiol.* 285: F1034-F1049, 2003
22. **Haycraft CJ, P Swoboda, PD Taulman, JH Thomas, and BK Yoder.** The *C. elegans* homolog of the murine cystic kidney disease gene *Tg737* functions in a ciliogenic pathway and is disrupted in *OSM-5* mutant worms. *Development* 128: 1493-1505, 2001.
23. **Hou X, M Mrug, BK Yoder, EJ Lefkowitz, G Kremmidiotis, P D'Eustachi, DR Beier, and LM Guay-Woodford.** Cystin, a novel cilia-associated protein, is disrupted in the *cpk* mouse model of polycystic kidney disease. *J. Clin. Invest.* 109: 533-540, 2002.
24. **Huangfu D, A Liu, AS Rakeman, NS Murcia, L Niswander, and KV Anderson.** Hedgehog signalling in the mouse requires intraflagellar transport proteins. *Nature* 426(6962): 83-87, 2003.
25. **Hughey RP, JB Bruns, CL Kinlough, KL Harkleroad, Q Tong, MD Carattino, JP Johnson, JD Stockand, and TR Kleyman.** Epithelial sodium channels are activated by furin-dependent proteolysis. *J. Biol. Chem.* 279(18): 18111-18114, 2004.

26. **Hurley DK, Bandy SM, Glew RH, Morris DM, and KD Gardner.** Kidney and breast cysts: A comparative study of fluids. *Nephron* 77: 304-308, 1997.
27. **Ji HL and DJ Benos.** Degenerin sites mediate proton activation of deltabetagamma-epithelial sodium channel. *J. Biol. Chem.* 279: 26939-26947, 2004.
28. **Kellenberger S and L Schild.** Epithelial sodium channel/degenerin family of ion channels: a variety of functions for a shared structure. *Physiol. Rev.* 82: 735-767, 2002.
29. **Kizer NL, B Lewis, and BA Stanton.** Electrogenic sodium absorption and chloride secretion by an inner medullary collecting duct cell line (mIMCD-K2). *Am. J. Physiol.* 268: F347-F355, 1995.
30. **Light DB, Schwiebert EM, Karlson KH, and BA Stanton.** Atrial natriuretic peptide inhibits a cation channel in renal inner medullary collecting duct cells. *Science* 243: 383-385, 1989.
31. **Light DB, Corbin JD, and BA Stanton.** Dual ion channel regulation by cyclic GMP and cyclic GMP-dependent protein kinase. *Nature* 344: 336-339, 1990.
32. **Madsen KM and CC Tisher.** Structural-functional relationship along the distal nephron. *Am. J. Physiol.* 250: F1-F15, 1986.
33. **McCoy DE, AL Taylor, BA Kudlow, KH Karlson, MJ Slattery, LM Schwiebert, EM Schwiebert, and BA Stanton.** Nucleotides regulate NaCl transport across mIMCD-K2 cells via P2X and P2Y purinergic receptors. *Am. J. Physiol.* 277: F552-F559, 1999.
34. **McFarlane ME.** The role of percutaneous drainage in the modern management of pancreatic pseudocysts. *Int. J. Clin. Pract.* 59(4): 383-384, 2005.

35. **North RA.** Molecular physiology of P2X receptors. *Physiol. Rev.* 82: 1013-1067, 2002.
36. **Novak I and MR Hansen.** Where have all the sodium channels gone? In search of functional ENaC in exocrine pancreas. *Biochim. Biophys. Acta* 1566: 162-168, 2002.
37. **Orlowski J and S Grinstein.** Diversity of the mammalian sodium/proton exchanger SLC9 gene family. *Pflugers Arch.* 447: 549-565, 2004.
38. **Praetorius HA, J Frokiaer, S Nielsen, and KR Spring.** Bending the primary cilium opens calcium-sensitive intermediate conductance potassium channels in MDCK cells. *J. Membr. Biol.* 191: 193-200, 2003.
39. **Praetorius HA and KR Spring.** Bending the MDCK cell primary cilium increases intracellular calcium. *J. Membr. Biol.* 184:71-79, 2001.
40. **Praetorius HA and KR Spring.** Removal of the MDCK cell primary cilium abolishes flow sensing. *J. Membr. Biol.* 191: 69-76, 2003.
41. **Richards WG, Sweeney WE, Yoder BK, Wilkinson JE, Woychik RP, and ED Avner.** Epidermal growth factor receptor activity mediates renal cyst formation in polycystic kidney disease. *J. Clin. Invest.* 101(5): 935-939, 1998.
42. **Rohatgi R, PD Wilson, C Burrow, and LM Satlin.** Sodium transport in autosomal recessive polycystic kidney disease (ARPKD) cyst lining epithelial cells. *J. Am. Soc. Neph.* 14: 827-836, 2003.
43. **Rohatgi R, B Zavilowitz, M Vergara, C Woda, P Kim, and LM Satlin.** Cyst fluid composition in human autosomal recessive polycystic kidney disease. *Pediatr. Nephrol.* 20(4): 552-553, 2005.



44. **Sakai H, Lingueglia E, Champigny G, Mattei MG, and M Lazdunski.** Cloning and functional expression of a novel degenerin-like Na<sup>+</sup> channel gene in mammals. *J. Physiol.* 519: 323-333, 1999.
45. **Satlin LM, S Sheng, CB Woda, and TR Kleyman.** Epithelial Na<sup>+</sup> channels are regulated by flow. *Am. J. Physiol. Renal Physiol.* 280(6): F1010-F1018, 2001.
46. **Schwiebert, E.M.,** Liang, L., Cheng, N.L., Olteanu D. Richards-Williams, C., Welty, E.A., and A. Zsembery. Extracellular ATP- and zinc-gated P2X receptor calcium entry channels: Physiological sensors and therapeutic targets. *Purinergic Signalling* In Press, 2005.
47. **Schwiebert EM, DP Wallace, GM Braunstein, SR King, J Peti-Peterdi, K Hanaoka, WB Guggino, LM Guay-Woodford, PD Bell, LS Sullivan, JJ Grantham, and AL Taylor.** A detrimental autocrine and paracrine purinergic signaling loop exists in epithelial cells derived from polycystic kidneys. *Am. J. Physiol. Renal Fluid Electrolyte Physiol.* 282: F763-F775, 2002.
48. **Schwiebert EM and A Zsembery.** Extracellular ATP as a signaling molecule for epithelial cells. *Biochim. Biophys. Acta* 1615: 7-32, 2003.
49. **Shen JP and CU Cotton.** Epidermal growth factor inhibits amiloride-sensitive sodium absorption in renal collecting duct cells. *Am. J. Physiol.* 284(1): F57-F64, 2002.
50. **Smith PR, G Saccomani, E-H Joe, K Angelides, and DJ Benos.** Amiloride-sensitive sodium channel is linked to the cytoskeleton in renal epithelial cells. *Proc. Natl. Acad. Sci. USA* **88**: 6971-6975, 1991.

51. **Swystun V, Chen L, Factor P, Siroky B, Bell PD and S Matalon.** Apical trypsin increases ion transport and resistance by a phospholipase C-dependent rise in cell calcium. *Am. J. Physiol.* 288: L820-L830, 2005.
52. **Taulman PD, CJ Haycraft, DF Balkovetz, and BK Yoder.** Polaris, a protein involved in left-right axis patterning, localizes to basal bodies and cilia. *Mol. Biol. Cell* 12: 589-599, 2002.
53. **Tong Z, B Illek, VJ Bhagwandin, GM Verghese, and GH Caughey.** Prostasin, a membrane-anchored serine peptidase, regulates sodium currents in JME/CF15 cells, a cystic fibrosis airway epithelial cell line. *Am. J. Physiol.* 287(5): L928-935, Epub 2004.
54. **Veizis IE and CU Cotton.** Abnormal EGF-dependent regulation of sodium absorption in ARPKD collecting duct cells. *Am. J. Physiol.* 288: F244-F254, 2004.
55. **Veizis EI, CR Carlin, and CU Cotton.** Decreased amiloride-sensitive  $\text{Na}^+$  absorption in collecting duct principal cells isolated from *BPK* ARPKD mice. *Am. J. Physiol.* 286(2): F244-F254, 2004.
56. **Vuagniaux G, V Vallet, NF Jaeger, C Pfister, M Bens, N Farman, N Courtois-Coutry, A Vandewalle, BC Rossier, and E Hummler.** Activation of the amiloride-sensitive epithelial sodium channel by the serine protease mCAP1 expressed in a mouse cortical collecting duct cell line. *J. Am. Soc. Neph.* 11: 828-834, 2000.
57. **Woda CB, A Bragin, TR Kleyman, and LM Satlin.** Flow-dependent  $\text{K}^+$  secretion in the cortical collecting duct is mediated by a maxi  $\text{K}^+$  channel. *Am. J. Physiol. Renal Physiol.* 280(5): F786-F793, 2001.

58. **Yamamura H, S Ugawa, T Ueda, M Nagao, and S Shimada.** Protons activate the  $\delta$ -subunit of the epithelial  $\text{Na}^+$  channel. *J. Biol. Chem.* 279: 12529-12534, 2004.
59. **Yoder BK, X Hou, and LW Guay-Woodford.** The polycystic kidney disease proteins, polycystin-1, polycystin-2, polaris, and cystin, are co-localized in renal cilia. *J. Am. Soc. Neph.* 13: 2508-2516, 2002.
60. **Yoder BK, WG Richards, C Sommardahl, WE Sweeney, EJ Michaud, JE Wilkinson, ED Avner, and RP Woychik.** Functional correction of renal defects in a mouse model for ARPKD through expression of the cloned wild-type Tg737 cDNA. *Kidney Int.* 50: 1240-1248, 1996.
61. **Yoder BK, WG Richards, C Sommardahl, WE Sweeney, EJ Michaud, JE Wilkinson, ED Avner, and RP Woychik.** Differential rescue of the renal and hepatic disease in an autosomal recessive polycystic kidney disease mouse mutant. A new model to study the liver lesion. *Am. J. Pathol.* 150: 2231-2241, 1997.
62. **Yoder BK, WG Richards, WE Sweeney, JE Wilkinson, ED Avner, and RP Woychik.** Insertional mutagenesis and molecular analysis of a new gene associated with polycystic kidney disease. *Proc. Assoc. Am. Physicians* 107: 314-323, 1995.
63. **Yoder BK, A Tousson, L Millican, JH Wu, CE Bugg, JA Schafer, and DF Balkovetz.** Polaris, a protein disrupted in *orpk* mutant mice, is required for assembly of renal cilium. *Am. J. Physiol. Renal Fluid Electrolyte Physiol.* 282: F541-F552, 2002.
64. **Zuckerman JB, X Chen, JD Jacobs, B Hu, TR Kleyman, and PR Smith.** Association of the epithelial sodium channel with Apx and alpha-spectrin in A6 renal epithelial cells. *J. Biol. Chem.* 274: 23286-23295, 1999.

### ***Figure Legends***

#### **Figure 1: Transepithelial Voltage Is Enhanced Markedly in Mutant *orpk* Collecting Duct Principal Cell Clones Grown as Well-Polarized Monolayers.**

Data summary of all measurements of  $V_{TE}$  measured by Millipore volttohmmeter chopstick electrodes. Data derived from mutant clones grown as monolayers are in the open bars. Data from genetically rescued clones are shown in the closed bars. Measurements were made on Day 5 or Day 6 following seeding of cells on filter supports at Day 0. The number of experiments for each clone was  $n=24$  for mixed mutant monolayers and 48-72 for all other clones. The asterisk reflects  $P < 0.05$  or lower by ANOVA or unpaired Student's  $t$  test as appropriate. The  $R_{TE}$  of these monolayers was routinely between 18 and  $20 \text{ k}\Omega\bullet\text{cm}^2$  and often exceeded  $20 \text{ k}\Omega\bullet\text{cm}^2$ , which is the highest value that the Millipore Volttohmmeter could measure.

#### **Figure 2: Heightened Transepithelial Voltage Is a Consistent and Reproducible Phenotype in Mutant *orpk* Collecting Duct Principal Cell Clones Grown as Well-Polarized Monolayers and Studied in Parallel to Counterpart Controls.**

Data are shown in this figure based on the subsets of mutant and genetically rescued clones measured and compared over time and in each data set. Multiple investigators assessed these monolayers blinded and unprompted to their identity. The number of experiments was 6-12 for each data set. The asterisk reflects  $P < 0.05$  or lower by ANOVA or unpaired Student's  $t$  test as appropriate. The  $R_{TE}$  of these monolayers was routinely between 18 and  $20 \text{ k}\Omega\bullet\text{cm}^2$  and often exceeded  $20 \text{ k}\Omega\bullet\text{cm}^2$ , which is the

highest value that the Millipore Voltohmmeter could measure. This upregulated  $V_{TE}$  phenotype (and  $I_{SC}$  phenotype, see below) remained consistent over at least 10 passages after clonal selection and cryopreservation. *Inset figure:* More recent analysis of monocilium morphology in the mutant 1 clone versus the rescued 2 clone. A malformed cilium is observed in the mutant monolayers (94D pcDNA 3.1), while a well-formed cilium is seen in the rescued 2 monolayers (94D Tg737-2). This is a newer data set done with cilium-specific tubulin antibodies to echo data already published on these cell models and to illustrate the morphological difference with specific to apical central monocilia in these PC clones. However, these data are already published and we did not want to recount them here (Ref. 63); the inset figure is only intended to remind the reader about the morphological difference. The mutant 1 clone was compared to the rescued 2 clone below in additional electrical experiments.

**Figure 3: Heightened Transepithelial Voltage in Mutant *orpk* Collecting Duct Principal Cell Monolayers and Measurable Voltage in Genetically Rescued *orpk* Monolayers Is Inhibited in a Dose-Dependent Manner by Amiloride.**

The effect of 50  $\mu$ M amiloride was examined on  $V_{TE}$  in both panels of mutant and genetically rescued clones grown as monolayers. All epithelial cell models are  $Na^+$  absorbing PC cells. This maximal dose of amiloride virtually abolished  $V_{TE}$  in all mutant and rescued clones, keeping in mind that the mutant monolayers had a 3- to 6-fold upregulated  $V_{TE}$ . The number of experiments is 12 for each set of data. The number of experiments is shown for the summary data for  $I_{SC}$  at the center of the figure.

**Figure 4: Heightened Transepithelial Short-Circuit Current in Mutant *orpk* Collecting Duct Principal Cell Monolayers and Measurable Current in Genetically Rescued *orpk* Monolayers Is Inhibited in a Dose-Dependent Manner by Amiloride.**

Original short-circuit current ( $I_{SC}$ ) traces are shown at *left*. Inhibition with 10  $\mu$ M amiloride is shown for mutant and rescued monolayers in these raw traces. Note the significantly larger amount of  $I_{SC}$  in the mutant monolayer, despite equivalent resistance. The spikes in the trace reflect the current deflections generated by a voltage pulse injected by the amplifier to monitor resistance. Ten micromolar was the dose used for amiloride to fully block the  $Na^+$  currents in  $I_{SC}$  recordings. At *center*, summary  $I_{SC}$  data is provided measured before and after addition of amiloride.  $I_{SC}$  is expressed as  $\mu A \bullet cm^2$ . The number of experiments is shown for the summary data for  $I_{SC}$  at the center of the figure. At *right*, open circuit  $V_{TE}$  data summary with a full dose-response assessment with amiloride is shown.  $N = 6$  to 12 for each clone in each data set. The  $IC_{50}$  for amiloride inhibition of the  $V_{TE}$  was determined to be approximately 1  $\mu$ M. \*  $P < 0.05$  or lower for  $I_{SC}$  data at *center*. \*  $P < 0.01$  or lower for open-circuit data at *right*.  $N$  is shown for  $I_{SC}$  data;  $n=12$  to 24 for the amiloride dose-response set of  $V_{TE}$ . Paired Student's  $t$  test was used to assess the amiloride inhibition.

**Figure 5: Cell Culture Conditions and the Dynamics of Electrical Measurements Affect Transepithelial Voltage and Current in Mutant and Rescued *orpk* Collecting Duct Principal Cell Monolayers Profoundly.**

Only data from mutant monolayers are shown because the electrical signal was larger; however, these maneuvers also affected voltage and current in rescued monolayers to the

similar degree (data not shown). **A.** Removal of the defined PC cell medium with 5% FBS and hormonal supplements into another basal medium with 5% FBS but without hormones caused a complete loss of amiloride-sensitive  $V_{TE}$ . **B.** Feeding the apical side of the monolayers with new defined PC cell medium caused a transient loss in amiloride-sensitive  $V_{TE}$  that returned after 7 hours. **C.** Feeding the basolateral side of the monolayers with fresh PC cell medium potentiated the  $V_{TE}$ . **D.** Transfer of the monolayers from open-circuit conditions where the  $V_{TE}$  and  $R_{TE}$  were measured (and the  $I_{TE}$  “calculated”) into the circulating Ussing chamber led to complete loss of amiloride-sensitive  $I_{SC}$  in Ringers of various formulation. This loss was partially prevented by performing the Ussing chamber  $I_{SC}$  recordings in the defined PC cell medium (without FBS) or in OptiMEM-I medium or Ringer with insulin. Ringer devoid of  $Na^+$  that also contained supplemental insulin failed to support  $I_{SC}$ . \*  $P < 0.05$  or lower.  $N = 12-24$  for each data set. ANOVA was used to compare the different experimental conditions where appropriate in A and D. Paired Student’s t test was used for data in B and C.

**Figure 6: The ENaC-selective Amiloride Analog, Benzamil, Inhibits Transepithelial Voltage and Current Markedly But Not Completely in Mutant *orpk* Collecting Duct Principal Cell Monolayers.**

Original short-circuit current ( $I_{SC}$ ) traces are shown at *left*, summary  $I_{SC}$  data in the *center*, and open circuit  $V_{TE}$  data summary for mutant monolayers assessing benzamil  $IC_{50}$  at *right*. This is a similar data presentation to Figure 4 above. Amiloride inhibits more than just  $Na^+$  channels involved in  $Na^+$  absorption. As such, we tested an expanded panel of amiloride analogs. Benzamil at 10  $\mu M$  inhibited the hyperactive absorptive  $Na^+$

current in the mutant monolayers as well as the low level of current in the rescued monolayer. Like Figure 3 above with amiloride, 10 micromolar benzamil was the dose used to fully block the  $\text{Na}^+$  currents in  $I_{\text{SC}}$  recordings. The number of experiments is shown for the summary data for  $I_{\text{SC}}$  at the center of the figure. At *right*, the  $\text{IC}_{50}$  for benzamil inhibition of the  $V_{\text{TE}}$  was determined to be approximately 50 nM. \*  $P < 0.05$  or lower for  $I_{\text{SC}}$  data at *left* and the open-circuit data at *right*. N is shown for  $I_{\text{SC}}$  data; n=12-24 for the  $V_{\text{TE}}$  data. A paired Student's t test was used to assess benzamil inhibition.

**Figure 7: Additional Amiloride Analogs, EIPA and DMA, Also Inhibit Upregulated  $V_{\text{TE}}$  in Mutant Monolayers: Additive Inhibition with Different Pairs of Analogs. A.** Dose-response relationship for EIPA to estimate the  $\text{IC}_{50}$  for inhibition of the upregulated  $V_{\text{TE}}$  in mutant monolayers. EIPA  $\text{IC}_{50}$  was approximately 2  $\mu\text{M}$ . **B.** Similar dose-response experiment with the more NHE-selective analog, DMA. DMA  $\text{IC}_{50}$  was approximately 20  $\mu\text{M}$ . **C and D.** Use of the  $\text{IC}_{50}$  doses for the four amiloride analogs used in this study to document additive inhibition of the upregulated  $V_{\text{TE}}$ . These data provide evidence for upregulated ENaC-mediated  $\text{Na}^+$  hyperabsorption in cilium-deficient *orpk* PC cells, although we cannot rule out that parallel NHE activity might modulate ENaC function in this model epithelium.

**Figure 8: Protease Inhibitors Attenuate Transepithelial Voltage and Current in Mutant *orpk* Collecting Duct Principal Cell Monolayers, Suggesting ENaC Hyperactivity.**

Endogenous secreted or membrane-bound proteases are thought to recognize Kunitz-like domains in the cysteine-rich regions of the extracellular domain of ENaC and activate



ENaC channels specifically. As such, aprotinin, a protease inhibitor used widely in these ENaC protease studies, was also tested for its inhibitory effect. While aprotinin lowered the current in the rescued monolayer, the protease inhibitor had a significant inhibitory effect on Ussing chamber short-circuit current in mutant monolayers that was inhibited further by benzamil. The number of experiments is shown for the summary data for  $I_{SC}$  at the center of the figure. If left on the apical side of the monolayer longer in open-circuit experiments (15-30 minutes versus 5 minutes in the Ussing chamber), the inhibitory effect of aprotinin was more robust.  $n=6$  to 12 for each clone in each data set. The asterisk reflects  $P < 0.05$  or lower by paired Student's  $t$  test as appropriate.

**Figure 1**

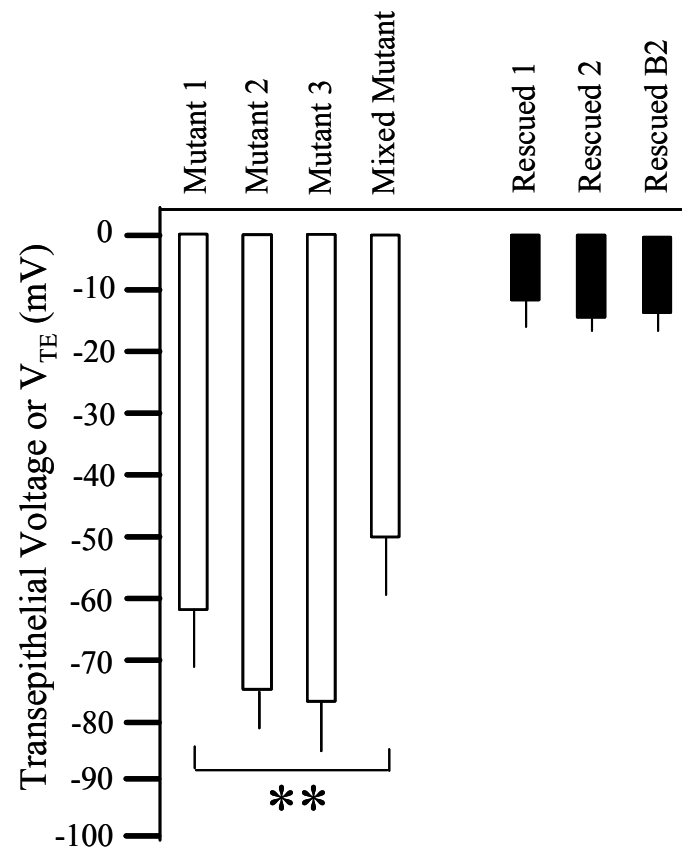


**Figure 2**  
**(NOTE: “Figure 2 Inset” Is in a Separate File Submitted in Support of the MS)**

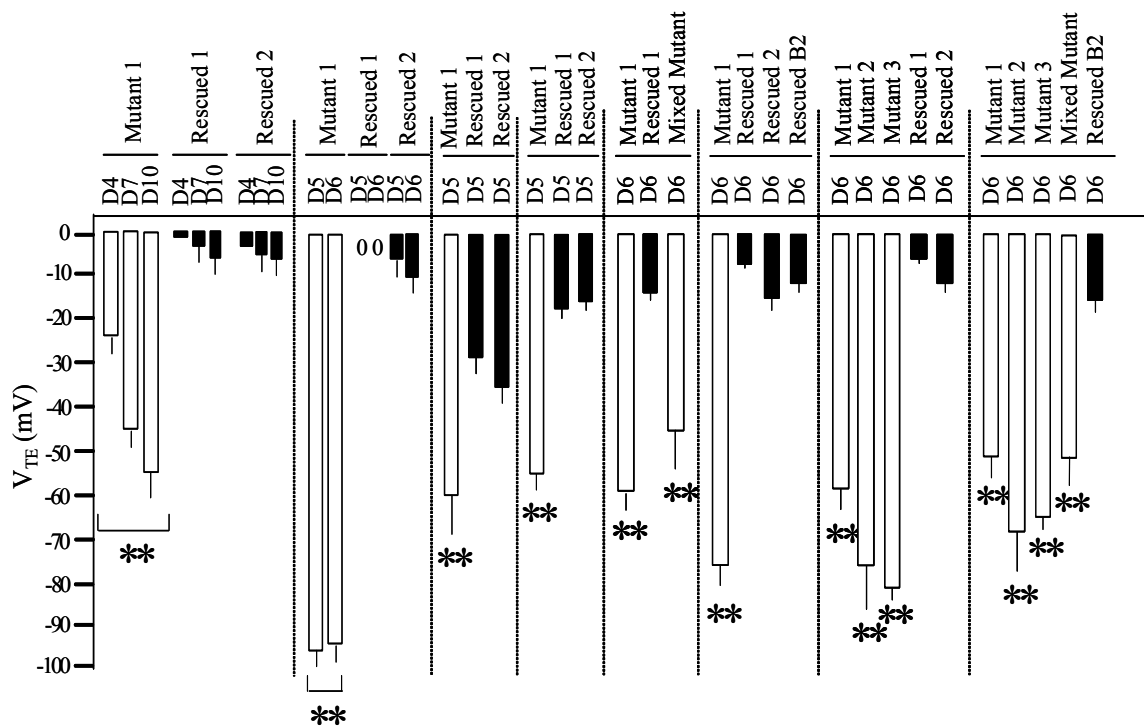


**Figure 3**

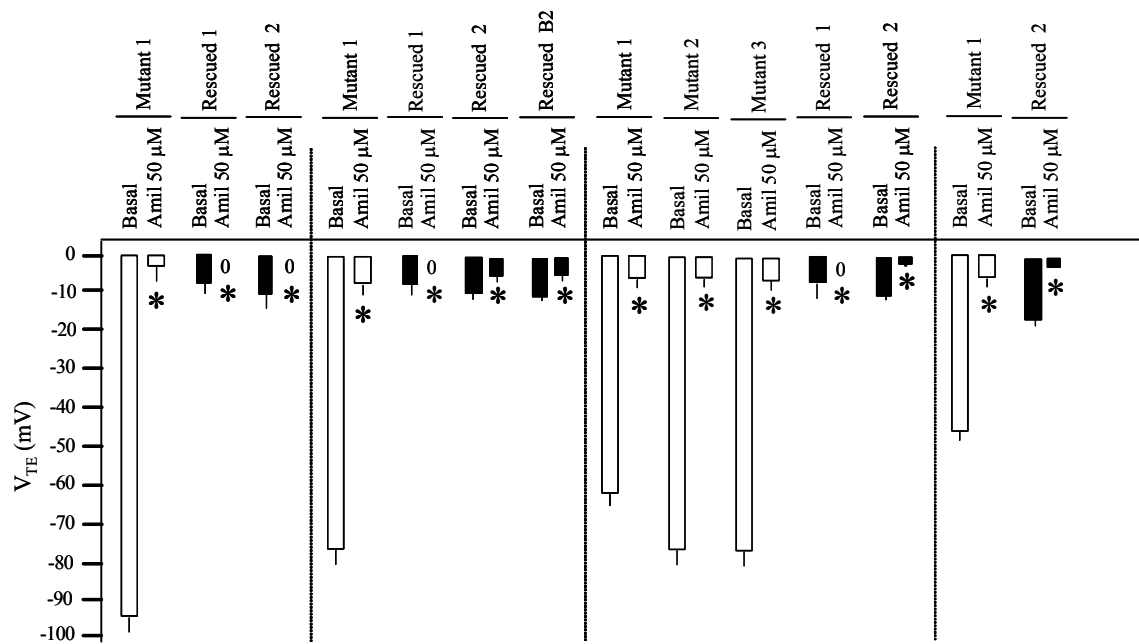


**Figure 4**

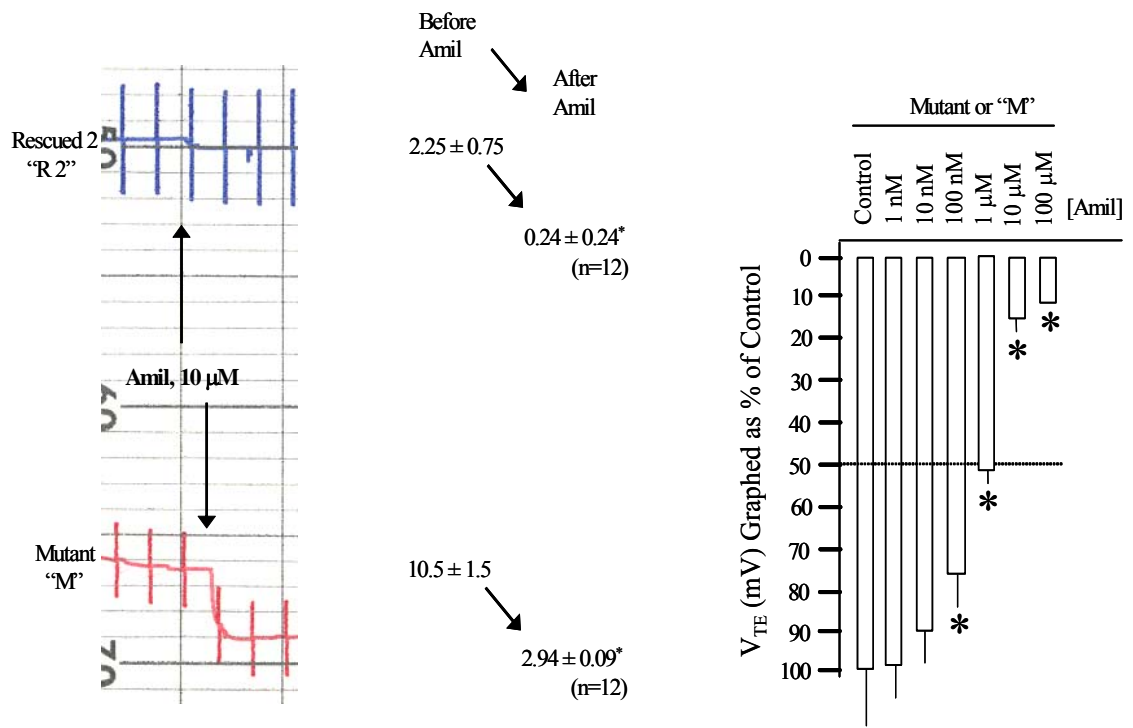


Figure 5

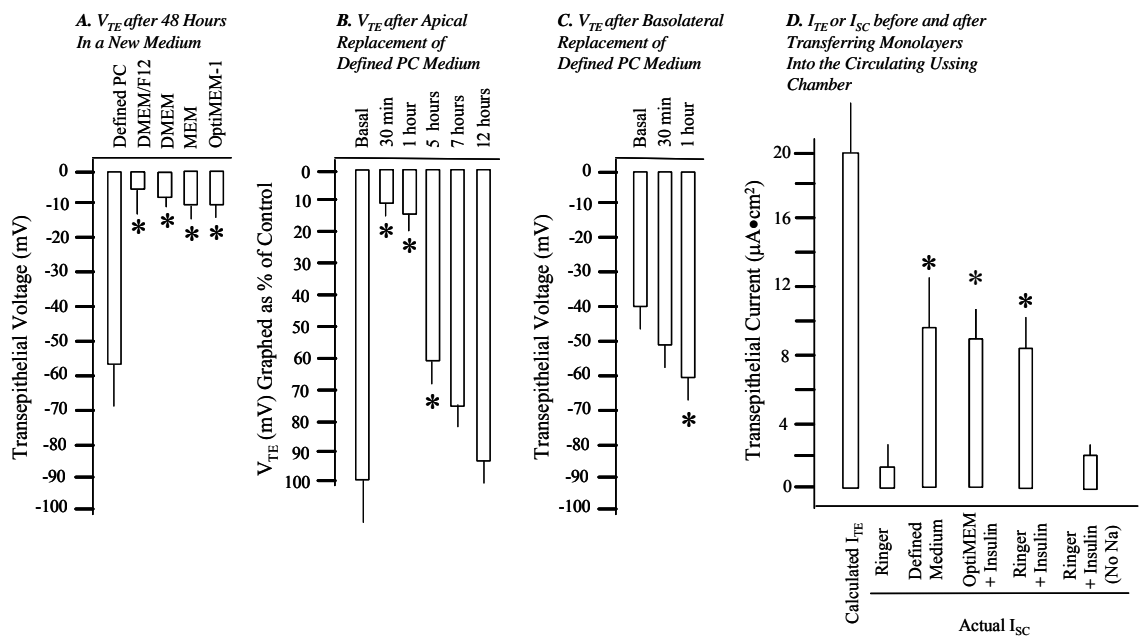
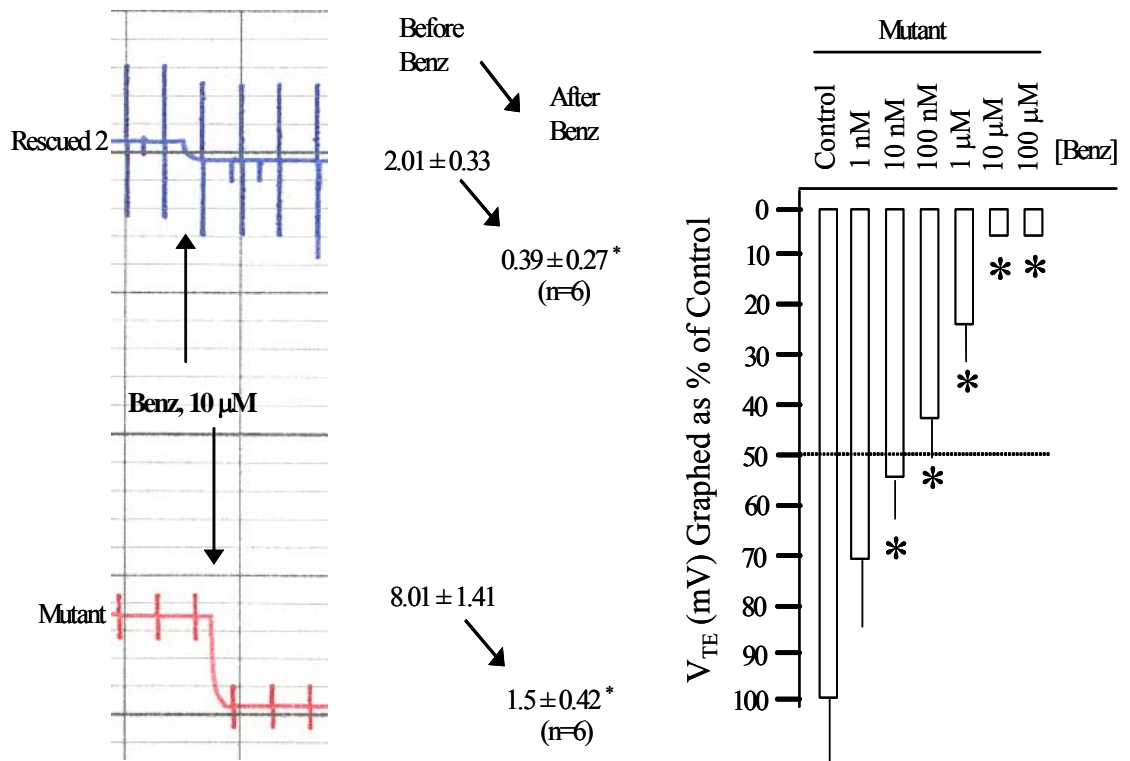
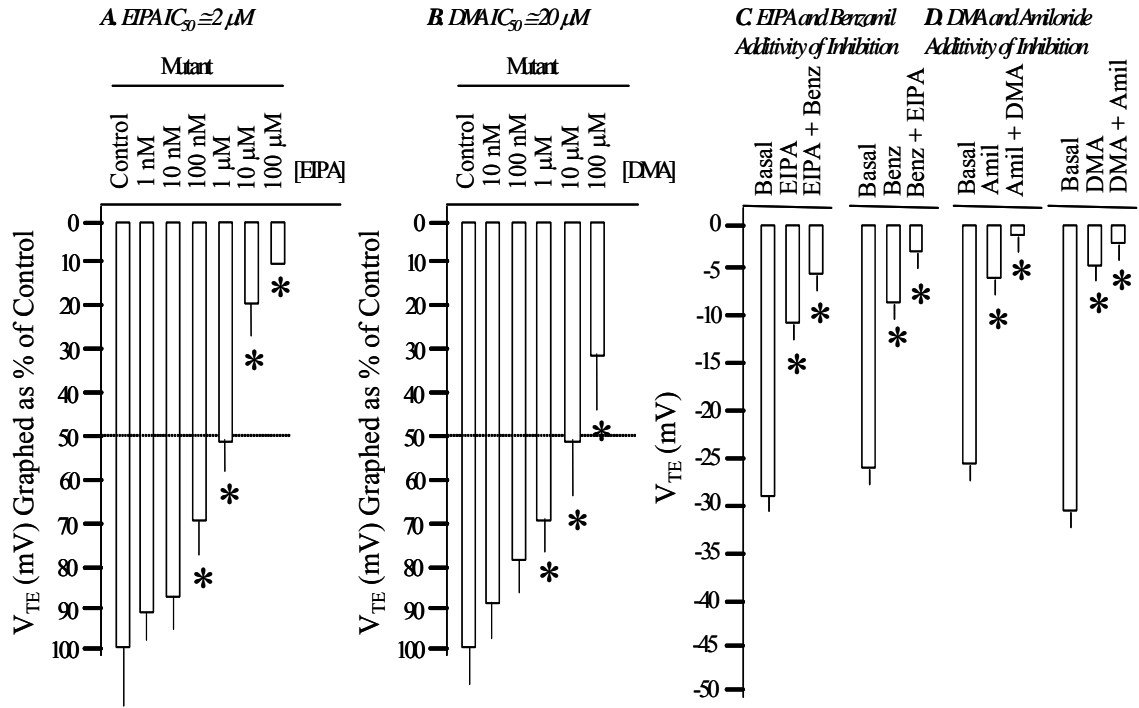


Figure 6

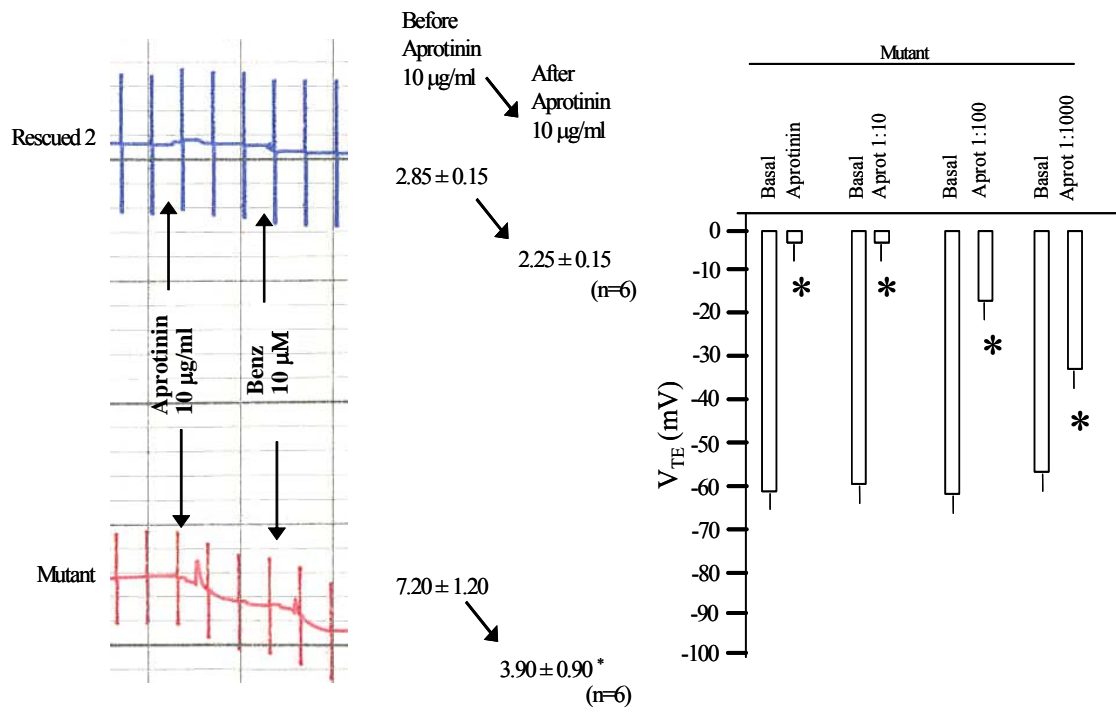


**Figure 7**





**Figure 8**



INAPPROPRIATE SODIUM/HYDROGEN EXCHANGE ON THE APICAL  
SURFACE OF A CILIUM-DEFICIENT CORTICAL COLLECTING DUCT  
PRINCIPAL CELL MODEL OF POLYCYSTIC KIDNEY DISEASE

by

DRAGOS OLTEANU<sup>1</sup>, VENUS C. ROPER<sup>2</sup>, NEERAJ SHARMA<sup>2</sup>, BRADLEY K.  
YODER<sup>2,3</sup>, MARK O. BEVENSEE<sup>1,4†</sup>, AND ERIK M. SCHWIEBERT<sup>1,2,3,†</sup>

Departments of Physiology and Biophysics<sup>1</sup> and of Cell Biology<sup>2</sup> and the Recessive PKD  
Translational and Research Core Centers<sup>3</sup> and the Nephrology Research Training  
Center<sup>4</sup>, University of Alabama at Birmingham, 1918 University Blvd., Birmingham, AL,  
35294-0005

††MOB and EMS should be considered as co-senior authors.

Submitted to *American Journal of Physiology-Cell Physiology*

Format adapted for dissertation

## ***Abstract***

Ductal epithelial cells regulate vectorial movement of ions, solutes, acids, bases and water into and out of tissues. In both forms of polycystic kidney disease, mutant ductal epithelia are less differentiated, leading to remodeling, mispolarity, dysregulated signal transduction, enhanced proliferation, dysregulated ion transport and modified gene expression. This myriad of pathophysiological anomalies may derive, at least in part, from impaired function or formation of the apical central monocilium of ductal epithelia. In the *Tg737<sup>orp</sup>* mouse and its immortalized cell models for the renal collecting duct, there is a malformed apical central monocilium. Recent studies by our laboratory and by others have shown dysregulated cell physiology in cilium-deficient cells. Use of a panel of amiloride analogs for inhibition of hyperabsorptive  $\text{Na}^+$  transport revealed that sodium/hydrogen exchange (Na/H exchange or NHE) activity may also be dysregulated in mutant monolayers versus genetically rescued controls, contributing to  $\text{Na}^+$  hyperabsorption. In normal collecting duct, NHE expression and function is primarily, if not exclusively, basolateral. To examine Na/H exchange function more closely, we examined well-polarized and BCECF-loaded cilium-deficient (“mutant”) and cilium-competent (“rescued”) cortical collecting duct (CCD) principal cell (PC cell) monolayers in a perfusion chamber where the apical and basolateral solutions could be manipulated separately. In  $\text{Na}^+$  removal and re-addition experiments and in ammonium chloride “prepulse” protocols, there was consistent and prominent appearance of apical NHE activity in cilium-deficient cell monolayers in addition to basolateral NHE function. In sharp contrast, cilium-competent cell monolayers had only basolateral NHE function.

Apical  $\text{Na}^+$ -induced  $\text{pH}_i$  recovery was significantly greater and overall NHE function was markedly augmented in cilium-deficient cell monolayers. Pharmacological analysis of the apical NHE activity in mutant cell monolayers and the basolateral NHE activity in both mutant and rescued cell monolayers revealed that cariporide and HOE-694 inhibited NHE function at low micromolar doses. Consistent with inappropriate expression of luminal NHEs along cystic collecting ducts, urinary pH from freshly voided samples from young cilium-deficient mice was more acidic than control littermates. There was also a trend toward metabolic alkalosis in younger mutant animals versus controls that became significant at 28 days of age in mutant animals. Taken together, this study provides the first description of dysregulated NHE function in any form of polycystic kidney disease and the first report of an acid-base anomaly in a primary organ affected by PKD.

***Keywords***

Polycystic kidney disease, cilia, acid-base transport, Na/H exchange, epithelia

## ***Introduction***

Polycystic kidney disease (PKD) cause a remodeling of the kidney and other tissues, leading to the dilatation of tubules and ducts and/or the full encapsulation of tubules and ducts into fluid-filled cysts (Ref. 33, 26, 11). The latter structures become isolated from the rest of the tissue, while dilated tubules remain contiguous with the tissue (Ref. 26). The autosomal recessive form of PKD (ARPKD) is a rarer genetic disorder that causes dilatation of tubules and ducts in the collecting duct system of the kidney and the bile duct of the liver in the human condition early in life (Ref. 18). If infants survive a curious phase of respiratory insufficiency that remains ill-defined, then they develop early-onset, severe and debilitating hypertension that can cause multiple deleterious effects leading to renal failure and vascular problems (Ref. 11). Autosomal dominant PKD (ADPKD) is more common than ARPKD, yet slower to progress (Ref. 26). ADPKD involves the formation of encapsulated cysts throughout the kidney and in the ductal systems of the liver and pancreas (Ref. 18). Vascular aneurysms are also prevalent in ADPKD, but they are difficult to study in animal models (Ref. 27). Similar to that seen in ARPKD, hypertension also precedes significant kidney remodeling and renal decline in ADPKD (Ref. 22). Our laboratories have become keenly interested in the mechanisms of  $\text{Na}^+$  hyperabsorption that may underlie this debilitating hypertensive phenotype found in both forms of PKD in addition to other chronic kidney diseases.

Our collaborative PKD research group studies cilium-deficient cell and tissue models of PKD in mice in an effort to understand the human disease. Recently, we

published the observation that ENaC-driven  $\text{Na}^+$  absorption was upregulated 4-fold in cilium-deficient CCD PC cell monolayers versus cilium-competent controls (Ref. 21). More recently, we have found that cilium-deficient cells exhibit impaired flow-induced calcium signaling—an observation made by many other laboratories (Ref. 15). However, in a novel twist, our laboratory showed that the cilium-driven calcium signal may require mechanically-induced ATP secretion into the apical medium (Ref. 15). Interestingly, stimulated ATP secretion into the apical medium is impaired in cilium-deficient cell monolayers versus cilium-competent controls. During the course of our initial ENaC study performed on well-polarized cell monolayers, we found that amiloride analogs, ethylisopropylamiloride (EIPA) and dimethylamiloride (DMA), inhibited  $\text{Na}^+$  hyperabsorption at concentrations more specific to NHEs than to ENaC (Ref. 21). Although one interpretation was that these analogs were indeed inhibiting mouse ENaC at low micromolar concentrations in a manner similar to amiloride, phenamil and benzamil, another hypothesis was that the analogs were inhibiting one or more NHEs, which contribute to  $\text{Na}^+$  hyperabsorption in cilium-deficient cell monolayers via one or more mechanisms (Refs. 9, 35).

To assess the expression and function of NHEs in cilium-deficient mutant monolayers and cilium-competent rescued monolayers, we established well-polarized and high resistance monolayers and inserted them into a homemade flow chamber where the apical and basolateral solutions could be changed and manipulated independently. Using ratiometric fluorescence imaging with the pH-sensitive dye BCECF, we examined the regulation of intracellular pH ( $\text{pH}_i$ ), as well as the presence and activities of NHEs on the

apical and basolateral membranes independently. We found that mutant CCD PC cells lacking a well-formed cilium compared to cells possessing a cilium display pronounced NHE activity on the apical membrane. This increased acid extrusion on the apical membrane correlates with high urinary pH and metabolic acidosis of the mutant mice. The co-localization of NHE and ENaC proteins in the apical membrane is not a normal physiological occurrence along the nephron (Refs. 25, 30). Increased alkalinization in the cytosol near the apical membrane may stimulate alpha-ENaC (Ref. 9). Extracellular acidification near the apical membrane may increase the open probability of delta-ENaC (Ref. 35). Due to these and other possible reasons, ENaCs and NHEs in the apical membrane of cystic epithelia may collaborate to confer Na<sup>+</sup> hyperabsorption and resultant hypertension in either or both forms of PKD.

## ***Materials and Methods***

*Generating Solutions* The standard  $\text{Na}^+$ -containing Ringer solution contains (in mM): 140 NaCl, 5 KCl, 1.5  $\text{CaCl}_2$ , 1.5  $\text{MgCl}_2$ , 10 HEPES, and NaOH necessary to titrate the solution to pH 7.4 at 37° C. In  $\text{Na}^+$ -free solutions,  $\text{Na}^+$  was substituted with equimolar *N*-methyl-D-glucammonium ( $\text{NMDG}^+$ ) and the solutions titrated with HCl to pH 7.4 at 37°C. In  $\text{Na}^+$ -free, 20 mM  $\text{NH}_3/\text{NH}_4^+$ -containing solutions, 20 mM NMDG-Cl was replaced with equimolar  $\text{NH}_4\text{Cl}$ . Nigericin (Sigma, St. Louis, MO) was prepared as a 10-mM stock solution in 100% ethanol. The high- $\text{K}^+$  solutions used for BCECF calibration contained (in mM) 130 KCl, 15 NMDG, 15 HCl, 1.5  $\text{CaCl}_2$ , 1.5  $\text{MgCl}_2$ , 10 HEPES and either KOH or HCl necessary to titrate each solution to the desired pH at 37°C. The 2', 7'-bis-(2-carboxyethyl)-5-(and-6)-carboxyfluorescein, acetoxymethyl ester (BCECF, AM) from Molecular Probes (Eugene, OR) was prepared as a 5-mM stock solution in dimethylsulfoxide (DMSO). HOE-694 and Cariporide (generous gifts from Aventis, Frankfurt, Germany) were prepared as 50-mM stock solutions in DMSO. All other chemicals were either obtained from either Sigma (St. Louise, MO) or Fisher (Fair Lawn, NJ).

*Culturing Cells* The collecting duct principal cells derived from an Oak Ridge polycystic kidney (*orpk*) mouse model of ARPKD and the genetically rescued cells with the wild type *orpk*<sup>Tg737</sup> gene were generous gifts from Dr. Bradley Yoder (Department of Cell Biology, University of Alabama at Birmingham). We previously described our approach for generating and culturing additional mutant and rescued cell clones (Ref. 21).



*Forming Monolayers* Cells were seeded onto 12-mm diameter Snapwell permeable filter supports (Corning Inc, Corning NY), each containing a membrane of 0.4  $\mu\text{m}$  pores. Cells were fed on both the apical and basolateral sides every 2 days, keeping the apical volume at minimum of 300  $\mu\text{l}$  and the basolateral volume at 2 ml. Experiments were conducted on both young (5-9 d) and old monolayers (35-40 d) with a high transepithelial resistance of greater than 5,000  $\Omega\text{cm}^2$ . Similar results were obtained from these monolayers and the results were pooled.

*Measuring  $\text{pH}_i$  in Polarized Cell Monolayers* Before each experiment, the monolayer was washed twice with Ringer solution and incubated for 20 min in Ringer solution containing 5  $\mu\text{M}$  BCECF-AM—the cell permeant form of the pH-sensitive dye BCECF. The monolayer was subsequently washed twice with Ringer solution to remove nonhydrolyzed dye, and then placed in Ringer solution for another 5-10 min. Each filter was snapped out from its support, placed in a double-sided perfusion flow chamber, and imaged using a 40 $\times$  PlanFl objective of an IX-70 inverted microscope (Olympus) equipped for fluorescence imaging. The monolayer was perfused continuously with solutions heated to  $37^\circ\text{C} \pm 0.5^\circ\text{C}$  by an automatic temperature controller (TC-344B, Warner Instruments). Intracellular dye was alternately excited with 495-nm and 440-nm light using a high-speed wavelength changer (Lambda DG-4, Sutter Instruments) and emitted light at 530 nm was captured by a digital CCD camera (Orca II, Hamamatsu). Because fluorescence from 495-nm excitation ( $I_{495}$ ) is pH sensitive and that from 440-nm excitation ( $I_{440}$ ) is relatively pH insensitive, the ratio ( $I_{495}/I_{440}$ ) is predominantly a function of  $\text{pH}_i$  and independent of changes in dye concentration, light path, etc. during

experiments.  $I_{495}$  and  $I_{440}$  values were corrected for background fluorescence from the dye-free monolayer and the baseline setting of the camera. MetaFluor software (Universal Imaging) was used for image and data acquisition. Each “n” represents 8-12 cells in one of 9 regions designated by a 3×3 grid of the entire field of cells.

*Calibrating BCECF*  $I_{495}/I_{440}$  values were converted to  $\text{pH}_i$  values using the high- $\text{K}^+$ /nigericin technique initially described by Thomas et al. (Ref. 28) and modified for a one-point calibration described by Boyarsky et al. (Ref. 7). At the end of “full-calibration” experiments, monolayers were perfused on both sides with 0  $\text{Na}^+$ /130 mM  $\text{K}^+$  solutions containing 5  $\mu\text{M}$  nigericin and different extracellular pH ( $\text{pH}_o$ ) varying from 5.5 to 8.5 (Fig. 1A). Functioning as a K-H exchange carboxylic ionophore, nigericin will set  $\text{pH}_i$  equal to  $\text{pH}_o$  if extracellular and intracellular  $\text{K}^+$  concentrations are equal. Steady-state  $I_{495}/I_{440}$  values obtained from each experiment were normalized to the ratio obtained at pH 7.0. As described by Boyarsky et al. (Ref. 7), normalized  $I_{495}/I_{440}$  data were fit using a non-linear least-squares method with the following pH-titration curve:

$$\frac{I_{490}}{I_{440}} = 1 + b \left[ \frac{10^{(\text{pH}-\text{pK})}}{1 + 10^{(\text{pH}-\text{pK})}} - \frac{10^{(7-\text{pK})}}{1 + 10^{(7-\text{pK})}} \right]$$

Where  $b$  and  $\text{pK}$  are  $1.611 \pm 0.007$  (SD) and  $7.212 \pm 0.005$  (SD), respectively, for cilium-competent cells, and  $1.302 \pm 0.007$  (SD) and  $7.095 \pm 0.006$  (SD), respectively for cilium-deficient cells. The best-fit titration curves (Fig. 1B) had lower and upper asymptotes (i.e.,  $R_{\min}$  and  $R_{\max}$ ) of 0.387 and 1.999, respectively, for cilium-competent cells, and 0.420 and 1.722, respectively for cilium-deficient cells. These titration-curve values allowed us to use the one-point calibration approach (Ref. 7) for all experiments.

At the end of each experiment, the monolayer was perfused on both sides with the high- $K^+$ /nigericin solution at pH 7.0. The  $I_{495}/I_{440}$  value obtained at pH 7.0 was used to normalize all  $I_{495}/I_{440}$  values ( $R_N$ ) of the experiment, and  $pH_i$  was computed using the equation:

$$pH_i = pK + \log \left[ \frac{(R_N - R_{\min})}{(R_{\max} - R_N)} \right]$$

*Computing Proton Pseudofluxes and Intrinsic Intracellular Proton Buffering Power.* As described in Bevensee and Boron (Ref. 5), proton pseudoflux ( $\phi$ ) in moles per unit cell volume per unit time (e.g.,  $\mu M s^{-1}$ ) is the product of the time-dependent change in  $pH_i$  (i.e.,  $dpH_i/dt$ ) and intrinsic  $H^+$  buffering power ( $\beta_i$ ) for cells in the nominal absence of an open buffering system such as  $CO_2/HCO_3^-$ :  $\beta_i$  was computed as  $\Delta[NH_4^+]_i/\Delta pH_i$  in experiments in which decreases in  $pH_i$  were elicited by stepwise decreases in the extracellular  $NH_3/NH_4^+$  concentration while both sides of the monolayer were exposed to a  $Na^+$ -free solution to minimize acid-base transporter activity (Ref. 7).  $\beta_i$  vs. the average  $pH_i$  before and after each step change in  $NH_3/NH_4^+$  exhibited a  $pH_i$  dependence that was best fit with the line  $\beta_i = -13.0 \times pH_i + 105.2$  for the cilium-deficient monolayer and  $\beta_i = -7.1 \times pH_i + 68.8$  for the cilium-competent monolayer (Fig. 1C). Although the slopes and y-intercepts were different for the two lines,  $\beta_i$  values were similar in the  $pH_i$  range during recoveries from acid loads.

***Figure 1: Proton Pseudoflux Measurements and Calculations***

*Designing Experimental pH Protocols* Two experimental protocols were used to examine  $\text{pH}_i$  regulation and NHE activity in the apical vs. basolateral membranes of the mutant and rescued monolayers. In one protocol, external  $\text{Na}^+$  was first removed from both sides of the monolayer —thereby causing a decrease in  $\text{pH}_i$  (e.g., Fig. 2B and 2C, point 2) due to reverse NHE activity or unmasked background acid loading— and then selectively added back to either the apical (e.g., Fig. 2B and 2C, point 3) or basolateral membrane to monitor the  $\text{Na}^+$ -dependent  $\text{pH}_i$  recovery. This protocol is more closely related to the technique used in isolated tubule perfusion, a procedure with which we intend to correlate with our findings in the future in PKD mouse models and cilium-deficient mice with our collaborators, Lisa Satlin and Wen Liu.

In another protocol, cells were acid loaded from both sides of the monolayer using the ammonium-prepulse technique (Ref. 6) in the absence of external  $\text{Na}^+$ . In these experiments, an initial steady-state  $\text{pH}_i$  was first obtained with both sides of the monolayer exposed to the  $\text{Na}^+$ -containing Ringer solution (e.g., Fig. 3, point 1). Then, the cells from both sides were exposed to a  $\text{Na}^+$ -free solution containing 20 mM  $\text{NH}_3/\text{NH}_4^+$  for 2 min (e.g., Fig. 3, segment 2-3).  $\text{pH}_i$  initially increases (e.g., Fig. 3, point 2) due to the rapid cellular influx of  $\text{NH}_3$ , which combines with intracellular  $\text{H}^+$  to form  $\text{NH}_4^+$ . This phase is followed by a slower acidification due to the stimulation of acid loading and/or influx of  $\text{NH}_4^+$ , which dissociates into  $\text{H}^+$  and  $\text{NH}_3$ . Removing the  $\text{NH}_3/\text{NH}_4^+$  solution (e.g., Fig. 3, point 3) causes  $\text{pH}_i$  to decrease below the initial steady-state as accumulated  $\text{NH}_4^+$  dissociates into both  $\text{NH}_3$ , which diffuses out of the cells, and  $\text{H}^+$ , which remains trapped in the cells.

After cells reached a near steady-state low  $\text{pH}_i$ , external  $\text{Na}^+$  was then selectively added back to either the apical or basolateral membrane to monitor the  $\text{Na}^+$ -dependent  $\text{pH}_i$  recovery. In other experiments designed to evaluate the influence of an NHE inhibitor on the  $\text{Na}^+$ -dependent  $\text{pH}_i$  recovery, cells were subjected to two acid loads; the first in the absence of the inhibitor, and the second in presence of the inhibitor added after the acid load, but 30 s before returning the external  $\text{Na}^+$ .

All  $\text{pH}_i$  experiments were performed in the nominal absence of  $\text{CO}_2/\text{HCO}_3^-$  to minimize the contribution of  $\text{HCO}_3^-$ -dependent transporters.

*Generating the HoxB7 Cre-Lox Kidney-specific Conditional Cilium Knockout Mouse Model* The generation of conditional  $Tg737(\text{IFT88})^{\text{lox}}$  mutant allele was described previously (Ref. 13). Kidney-specific mutant animals were established by first crossing heterozygous null  $Tg737$  ( $Tg737^{\text{WT/}}$ ) mutants with a transgenic line expressing Cre recombinase under the Hoxb7 promoter ( $Hoxb7\text{-cre}$ ) (Ref. 36). The  $Tg737^{\text{WT/}}$ ;  $Hoxb7\text{-Cre}$  males were then crossed with the homozygous flox mice ( $Tg737^{\text{flox/flox}}$ ). The resulting  $Tg737^{\text{flox/}}$ ;  $Hoxb7\text{-Cre}$  were used as experimental animals while the  $Tg737^{\text{WT/flox}}$ ;  $Hoxb7\text{-Cre}$  mice were used as littermate control. Mice were genotyped by PCR using primers designed to amplify a region of genomic DNA flanking one of the *loxP* sites (wild-type and flox alleles) or spanning the region deleted upon Cre-mediated recombination (null allele;  $Tg737$ ). Primer sequences are available on request. All mice were maintained in AALAC certified mouse facilities at UAB with protocols approved by the IACUC.

*Isolating Tubules and Performing Immunofluorescence.* Kidneys were dissected in cold PBS and cut into small pieces. Tubules were isolated by collagenase digestion in DMEM without serum at 37°C as previously described (Ref. 24). Tubules in solution were fixed in 4% paraformaldehyde with 0.2% Triton X-100, washed several times in PBS, blocked in 2% bovine serum albumin in PBS, and probed with 1:1,000 dilution of anti-acetylated- $\alpha$ -tubulin (Sigma, St Louis, MO) in 1% BSA. DNA was labeled with Hoechst (1:1,000, Sigma). Images were captured on a Nikon TE2000 microscope equipped with a CoolSnap HQ CCD camera.

*Performing Plasma and Urinary pH Measurements in Mice.* A pH electrode for small samples (9810BN from Thermo Orion, Beverly, MA) connected to a portable pH and pH/ISE meter (model 290Aplus from Thermo Orion) was used to measure both blood and urine pH. After mice were weighed and urine samples collected, they were intraperitoneally anesthetized with 50  $\mu$ l of a cocktail of 12.5% ketamine and 12.5% xylazine in PBS. Mice older than 7 d sometimes needed an additional 25-50  $\mu$ l to be fully anesthetized. The abdominal and thoracic cavities were then opened and fresh blood was extracted with a syringe from the cavities of the heart while it was still beating. Both blood and urinary pH were measured immediately after the samples were collected. Samples were obtained from mice at the following postnatal ages: day 7, day 14, day 21 (range: 19 to 23) and day 28.

*Performing Statistical Analyses.* Data are expressed as mean  $\pm$  standard deviation (SD) or standard error of the mean (SEM). For  $\text{pH}_i$  recoveries from acid loads,  $\text{pH}_i$  vs.

time traces were first fit with single exponentials. The  $\text{pH}_i$ -dependencies of  $d\text{pH}_i/dt$  values were then fit with third-order polynomials using Prism 5 (GraphPad Software, Inc.), and mean values in increments of 0.025 pH units were determined using a custom-written Excel macro by Dr. Christof J. Schwiening previously in the Boron laboratory (Department of Cellular and Molecular Physiology, Yale University). Slopes and y-intercepts of linear fits to data were obtained using the Regression function of Excel.

## **Results**

***Increased  $\text{Na}^+$ -dependent  $\text{pH}_i$  Regulation Across the Apical Membrane of Cilium-deficient vs. Cilium-competent CCD PC Cell Monolayers*** To study the relative activity of  $\text{Na}^+$ -dependent  $\text{pH}_i$  regulation across the apical versus basolateral membranes of well-polarized CCD PC cell monolayers, we used a flow chamber designed by Drs. Peter Komlosi and P. Darwin Bell to perfuse the apical and basolateral surfaces of these monolayers selectively. A schematic of the “sided” flow chamber is shown in Fig. 2A. In early protocols, we simply removed  $\text{Na}^+$  from both sides of the monolayer in both cilium-competent (“rescued”) monolayers (Fig. 2B, point 2) and cilium-deficient (“mutant”) monolayers (Fig. 2C, point 2) to acidify the cytosol.  $\text{Na}^+$  was subsequently re-introduced first to the apical side of the monolayer and then to the basolateral side to assess  $\text{Na}^+$ -dependent  $\text{pH}_i$  recoveries consistent with NHE activity. In cilium-competent monolayers (Fig. 2B), adding back apical  $\text{Na}^+$  at point 3 had little effect on  $\text{pH}_i$  but returning basolateral  $\text{Na}^+$  at point 4 elicited a full recovery of  $\text{pH}_i$  to the initial steady-state value. In cilium-deficient monolayers (Fig. 2C) however, adding back apical  $\text{Na}^+$  caused a pronounced increase in  $\text{pH}_i$  (point 3) which increased further to the initial steady-state value by returning basolateral  $\text{Na}^+$  at point 4. The  $\text{pH}_i$  increase elicited by returning apical  $\text{Na}^+$  shown in Fig. 2C is consistent with the induction of apical NHE activity in the cilium-deficient monolayers, but not cilium-competent, CCD PC cell monolayers.

***Figure 2: Flow Chamber and Early  $\text{Na}^+$  Removal and Re-Addition Protocols.***



***Inappropriate Apical NHE Functional Expression in Multiple Mutant Cell Clones in Comparison with Multiple Rescued Cell Clones that Display a Normal Basolateral-exclusive NHE Activity.*** To examine NHE activity in more detail, we first acid loaded cells using the ammonium prepulse technique (Ref. 6) in the absence of external  $\text{Na}^+$ , and subsequently examined  $\text{pH}_i$  recoveries elicited by returning either apical or basolateral  $\text{Na}^+$ . In our previous electrophysiologic studies on a panel of cilium-competent and cilium-deficient cell monolayers, we found an increase in ENaC-mediated transepithelial  $\text{Na}^+$  movement in the cilium-deficient cells (Ref. 21). We also studied each rescued and mutant clone as a polarized cell monolayer in our BCECF-based NHE characterization. Multiple rescued or cilium-competent cell clones were grown as well-polarized monolayers where the wild-type Tg737 gene and the normal Polaris protein were expressed. In cilium-competent cell clones (Fig. 3 A-C), returning apical  $\text{Na}^+$  had little effect on  $\text{pH}_i$  after the acid load (point 4). However, returning basolateral  $\text{Na}^+$  elicited a pronounced increase in  $\text{pH}_i$  (point 5) to the initial value. We obtained similar results with wild-type mCCD-K1 and mIMCD-K2 monociliated collecting duct cell models that were also derived from individually dissected collecting ducts from the Immortomouse (data not shown) (Ref. 17). These data support previous observations (Refs. 8, 10, 31, 32) that CCD PC cells with well-formed apical monocilia exhibit basolateral NHE activity. Different  $\text{Na}^+$ -elicited  $\text{pH}_i$  recoveries were obtained in the mutant clones (Fig. 3 D-F). Returning apical  $\text{Na}^+$  elicited a marked increase in  $\text{pH}_i$  (point 4) and accounted for the majority of the  $\text{Na}^+$ -induced  $\text{pH}_i$  recovery. Subsequently, returning basolateral  $\text{Na}^+$  elicited a smaller increase in  $\text{pH}_i$  back to the initial value (point 5). Figure 3 data are

consistent with apical NHE activity in cilium-deficient cell monolayers that is not present in cilium-competent cell monolayers.

***Figure 3: Multiple Mutant Cell Clones Display an Inappropriate Apical NHE Activity in Addition to Normal Basolateral-exclusive NHE Activity Displayed in Multiple Rescued Cell Clones***

***Cilium-deficient monolayers are characterized by higher alkalization, lower acidification and apical acid extrusion, if compared with cilium-competent monolayers***

An immediate and initial observation was that the mutant cell monolayers acidified faster than rescued cells monolayers. This aspect was observed first when we were using the Na removal protocol. Once the resting  $\text{pH}_i$  was recorded, Na containing Ringer solution was changed simultaneously on both sides with NMDG-containing solution. In the cilium-deficient cells, the  $\text{pH}_i$  dropped faster and to a lower value than in the cilium-competent cells (Fig. 4A). We also measured the “alkalinization peak” during the ammonium prepulse (the peak recorded between step 2 and 3 in Fig. 3) as well as the acidification point following the ammonium “washout” (the steady state value immediately before step 4 in Figure 3). These values were calculated as a difference from the resting  $\text{pH}_i$  and were plotted together in the same graph (Fig. 4B). Because the resting  $\text{pH}_i$  values were not different in mutant and rescued monolayers (7.21 and 7.20, respectively), we chose to plot the summarized data together against the pH 7.2 value only for sake of comparison. Mutant cell monolayers (n=59 traces) alkalized more vigorously and acidified more

vigorously than their rescued cell monolayer controls (n=45 traces). These values were significantly greater in mutant versus rescued cell monolayers (Fig. 4B).

From Figure 3 experiments, we used the rate of  $\text{pH}_i$  recovery elicited by adding  $\text{Na}^+$  back to the apical side to calculate the  $\text{pH}_i$  sensitivity of total acid extrusion, which is defined as the product of  $d\text{pH}_i/dt$  and intrinsic buffering power (see Methods). Cilium-deficient cell monolayers displayed 3- to 9-fold greater acid extrusion ( $\text{pH}_i$  range: 6.18–6.65) upon returning apical  $\text{Na}^+$  than cilium-competent cell monolayers (Fig. 4C)

***Figure 4: Lower and Faster Acidification, Higher Alkalinization and Higher Apical Acid Extrusion Capacity in Mutant versus Rescued Cells Monolayers***

#### ***Pharmacological Analysis of Apical NHE Function in Mutant Cell Monolayers***

To quantitate the contribution of NHE activity to  $\text{pH}_i$  recoveries following acid loads, we performed “Figure 3 type” experimental protocols and incorporated a panel of amiloride analogs and more specific NHE inhibitors. We found that amiloride, as well as amiloride analogs such as EIPA and DMA, inhibited the apical  $\text{Na}^+$ -induced  $\text{pH}_i$  recovery (data not shown). However, such inhibitors are not diagnostic among the most common NHE subtypes. As such, we focused on HOE-642 (cariporide) and HOE-694, two inhibitors that are more selective for NHE1 versus NHE2, NHE3 and NHE4 (Ref. 19). One caveat in our work and interpretation below is that HOE  $\text{IC}_{50}$  values for NHE 1 through 4 was determined in rat and rabbit preparations (Ref. 19). Our studies were performed on cells derived from transgenic mice. In addition to examining the effect of apical NHE

inhibitors, we also assessed the sensitivity of basolateral  $\text{Na}^+$ -induced  $\text{pH}_i$  recoveries to HOE inhibitors for comparative purposes.

Figure 5A contains three representative traces of apical  $\text{Na}^+$ -induced  $\text{pH}_i$  recoveries from ammonium prepulse experiments either in the absence or presence of two different concentrations of cariporide. For clarity, we only show the  $\text{pH}_i$  vs. time traces after the ammonium prepulse-induced acid loads. The inhibitors were added immediately prior to the curves plotted in Fig. 5A. Compared to the full  $\text{pH}_i$  recovery observed in the absence of inhibitor, the  $\text{pH}_i$  recovery was a little more than 50% inhibited by 1  $\mu\text{M}$  cariporide, and almost completely blocked by 50  $\mu\text{M}$  cariporide. From  $\text{pH}_i$  recoveries similar to those shown in Figure 5A, we computed the  $\text{pH}_i$  dependencies of apical acid extrusion. All three apical acid extrusion plots shown in Fig. 5B were linear over the reported  $\text{pH}_i$  ranges. Compared to apical total acid extrusion in the absence of inhibitor, 1  $\mu\text{M}$  cariporide (which completely inhibits NHE1 but not NHE2 in mice (Ref. 2)) reduced apical acid extrusion by 59-70% in the  $\text{pH}_i$  range 6.18-6.60. Thus, an apical NHE sensitive to low doses of cariporide is responsible for the majority of acid extrusion during the  $\text{Na}^+$ -stimulated recovery of  $\text{pH}_i$  from an acid load. Fifty  $\mu\text{M}$  cariporide (which inhibits NHE2 activity in mice (Ref. 2)) inhibited the remaining apical acid extrusion an additional 20% in a similar  $\text{pH}_i$  range of 6.23-6.68. The low apical acid extrusion remaining in the presence of 50  $\mu\text{M}$  cariporide is similar to the low apical total acid extrusion seen in the cilium-competent monolayers. The apical NHE phenotype in mutant cell monolayers was quite sensitive to low doses of HOE-694. A dose of 10  $\mu\text{M}$  HOE-694 inhibited the apical acid extrusion with 79-88% in the  $\text{pH}_i$  range of 6.23-6.6. These

data are consistent with the inappropriate expression of NHE1 and, possibly, NHE2 to the apical cell surface of cilium-deficient cell monolayers, in addition to their standard expression in the basolateral membrane of both mutant and rescued cells (see below).

***Figure 5: Pharmacological Assessment of Apical NHE Activities***

***Pharmacological Analysis of Basolateral NHE Function in Mutant and Rescued Cell Monolayers*** We examined cariporide and HOE-694 sensitivities of basolateral  $\text{Na}^+$ -induced  $\text{pH}_i$  recoveries from acid loads using the approach described for Figure 5. Pharmacological inhibitor sensitivity was similar in mutant and rescued cell monolayers with regard to basolateral  $\text{Na}^+$  re-addition and  $\text{pH}_i$  recovery. In Fig. 6A, we show three representative traces of basolateral  $\text{Na}^+$ -induced  $\text{pH}_i$  recoveries from ammonium prepulse experiments in cilium-deficient cells either in the absence or presence of cariporide. Compared to the full  $\text{pH}_i$  recovery observed in the absence of inhibitor, the  $\text{pH}_i$  recovery was inhibited ~50% by 1  $\mu\text{M}$  cariporide, and almost completely blocked by 10  $\mu\text{M}$  cariporide. Similar results on the cilium-deficient cells were obtained with higher concentrations (e.g., 10 and 100  $\mu\text{M}$ ) of HOE-694 (Fig. 6B). In addition, similar results (not shown) with both HOE compounds were obtained with cilium-competent cells.

From the  $\text{pH}_i$  recoveries, we computed the  $\text{pH}_i$  dependencies of basolateral acid extrusion. For both cilium-deficient and -competent cells, we observed two general differences between the acid extrusion plots from the basolateral vs. apical membranes.

First, basolateral acid extrusion was considerably greater than apical acid extrusion. For example, at  $\text{pH}_i \sim 6.0$ , total acid extrusion was  $\sim 4$ -fold greater on the basolateral membrane (Fig. 6C) vs. apical membrane (Fig. 5B) of cilium-deficient cells. Second, basolateral acid extrusion plots were more hyperbolic (Fig. 6C and 6D) compared to the apical plots, which were more linear (Fig. 5B).

Compared to basolateral total acid extrusion in the absence of inhibitor for cilium-deficient cells, 1  $\mu\text{M}$  cariporide reduced basolateral acid extrusion by 49-59% in the  $\text{pH}_i$  range 6.03-7.18, and 50  $\mu\text{M}$  cariporide reduced acid extrusion by 91-93% in the  $\text{pH}_i$  range 6.18-6.78 (Fig. 6C). Total acid extrusion across the basolateral membrane of mutant cell monolayers was also reduced by 10  $\mu\text{M}$  and 100  $\mu\text{M}$  HOE-694 (36-52% and 84-92%, respectively) in the  $\text{pH}_i$  range 6.2-6.8 (data not shown). Similar acid extrusion plots with cariporide were obtained with cilium-competent cells. Total acid extrusion across the basolateral membrane of rescued cell monolayers was reduced by 1  $\mu\text{M}$  and 50  $\mu\text{M}$  cariporide with 35-45% and 93-95%, respectively, over a  $\text{pH}_i$  range of 6.33-6.78 (Figure 6D). Furthermore, 10  $\mu\text{M}$  and 100  $\mu\text{M}$  of the second HOE compound, HOE-694, reduced the basolateral total acid extrusion by 76-79% and 95-97%, respectively, in the  $\text{pH}_i$  range 6.45-6.63 (data not shown). According to these data, the pharmacological profile of basolateral NHE activity is similar in mutant and rescued cell monolayers, and similar to apical NHE activity in the mutant cell monolayers.

***Figure 6: Pharmacological Assessment of Basolateral NHE Activities***

***Comparing the  $pH_i$  Dependencies of Apical and Basolateral NHE Activity in Cell Monolayers*** In the context of our studies above, inappropriate apical NHE activity in mutant cilium-deficient cell monolayers was different than basolateral NHE activity in mutant and rescued cell monolayers in at least two fundamental ways. To compare basolateral and apical NHE activities, we plotted the 50  $\mu$ M cariporide-sensitive  $pH_i$  dependences of (i) apical acid extrusion in the cilium-deficient monolayers (from Fig. 5B data), (ii) basolateral acid extrusion in the cilium-deficient monolayers (from Fig. 6C data), and (iii) basolateral acid extrusion in the cilium-competent monolayers (from Fig. 6D data). These cariporide-sensitive plots were generated by subtracting the plot of cariporide-insensitive acid extrusion from the corresponding plot of total acid extrusion obtained from either the apical or basolateral total acid extrusion (Fig. 7). Cariporide-sensitive acid extrusion on the basolateral side was best fit with the line,  $y = -341x + 2389$ , for the cilium-deficient cell monolayers and,  $y = -280x + 2017$  for the cilium-competent cell monolayers. Cariporide-sensitive acid extrusion on the apical side of cilium-deficient cell monolayers was best fit with the line  $y = -97x + 673$ . Cariporide-sensitive acid extrusion on the basolateral sides of the cilium-deficient and -competent monolayers were similar, but had a steeper  $pH_i$  dependency to that on the apical side of the cilium-deficient monolayer. Furthermore, cariporide-sensitive acid extrusion on the basolateral side of either monolayer was 3.5-4.5 fold greater than that on the apical side of the mutant monolayer in the  $pH_i$  range 6.23-6.68. In conclusion, apical NHE activity induced in the mutant monolayers is considerably less than basolateral NHE activity in both mutant and rescued monolayers.

***Figure 7:  $pH_i$  Dependencies of Cariporide-sensitive Acid Extrusion***

### ***Urinary and Blood pH Dysregulation in a Kidney-specific Conditional Cilium***

***Knockout Mouse*** To correlate our findings concerning the inappropriate appearance of an apical NHE and upregulated NHE function in well-polarized cilium-deficient cell monolayers studied *in vitro*, freshly voided urine and fresh blood samples were collected from HoxB7-Cre; Tg737<sup>flx/□</sup> kidney-specific conditional cilium knockout mice versus littermate controls at postnatal days 7, 14, 21 and 28. Loss of cilia in collecting ducts was confirmed by immunofluorescence analysis using antibodies against acetylated □-tubulin. Tubule identity was determined by positive DBA lectin staining (Vector Laboratories). HoxB7-Cre is expressed in the collecting duct epithelium and conditional mutant mice rapidly develop cysts during the perinatal period. A dilated collecting duct without cilia is observed in Fig. 8A, while a normal collecting duct with intact cilia is shown in Fig. 8B. The kidneys from a wild-type littermate are shown in Fig. 8C, while a cystic kidney is shown for this conditional cilium knockout animals in Fig. 8D. Taken together, this conditional cilium knockout mouse displays a renal cystic phenotype similar to the Tg737<sup>orp<sup>k</sup></sup> mouse.

If NHE activity is upregulated in the collecting duct *in vivo* and if an apical NHE was now present on the apical surface of collecting duct principal cells, one would expect to observe more acidic urine from mutant mice. Compared to littermate controls, mutant mice had significantly more acidic urine at each postnatal age studied (Fig. 8E) and became more pronounced with age. Compared to littermate urine, mutant urine was more acidic by a mean of 0.3 pH units at day 7, 0.7 pH units at day 14, 1.2 pH units at day 21, and 1.6 pH units at day 28. All differences were statistically significant. The acidic urine



of the mutant mice also influenced their blood pH. Compared to littermate urine, mutant blood was more alkaline by a mean of 1.1 pH units at day 28. Although not statistically significant, there was also a trend toward more alkaline blood of the mutant mice at the early postnatal days 7, 14, and 21. These data are consistent with the apical NHE dysregulation phenotype observed *in vitro*. The apical NHE-based acid-base disturbance is significant enough to affect urinary pH and cause metabolic alkalosis to develop in this mouse model of cystic kidney disease.

***Figure 8 Part A-D: Imaging of the Ciliary Status and the Cystic Nature of Kidneys in the HoxB7 Cre-Lox Kidney-specific Conditional Cilium knockout Mouse Model; Part E: Urinary and Blood pH. Metabolic Measurements of Fresh Urine and Plasma Samples Reveals Acid-Base Balance Anomalies in Cilium-deficient PKD Mouse Models***

## ***Discussion***

In summary, this study provides the first description to our knowledge of an acid-base transport abnormality and an acid-base disturbance within a primary organ or tissue affected by polycystic kidney disease. We have amassed a significant body of data in *in vitro* well-polarized renal cortical collecting duct principal cells demonstrating that functional NHE activity is inappropriately present on the apical surface of the renal collecting duct that are deficient in primary cilia. Analysis of these BCECF fluorescence-based experiments shows an upregulation of overall NHE activity in cilium-deficient renal principal cell monolayers. Of particular importance, we have urinary and blood pH measurements from fresh *in vivo* samples from mutant mice and their littermates in the first 4 weeks of age showing early-onset, enhanced and persistent urinary acidification and a development of metabolic alkalosis in mutant animals. It is our hope that this work prompts a new sub-field of polycystic kidney disease research focusing on acid-base transport and homeostasis in PKD.

Our work has implications for multiple issues regarding renal homeostasis as well as whole body physiology that may impact upon PKD pathophysiology. An important question arises, namely: How could acid-base transport anomalies contribute to PKD pathogenesis in the kidney and other tissues? Acid-base transport dysregulation has already been documented in the choroid plexus of the *Tg737<sup>orpk</sup>* mouse; this phenotype related to NaHCO<sub>3</sub> cotransporter function (Ref. 4). Chronic hyperacidification of the final urine may affect collecting duct and urinary tract physiology in ways that we do not yet appreciate. If NHE dysregulation is also present in bile duct and pancreatic duct, this

would acidify bile duct and exocrine pancreas secretions that are normally alkaline to neutralize acidic gastric juices. Such a phenotype would affect the breakdown of foods and absorption of essential nutrients at points downstream in the small intestine which require a neutral or alkaline environment. The development of metabolic alkalosis from excess  $H^+$  secretion and excretion necessitates compensation by the respiratory system as well as changes in the renal collecting duct system with regard to a switch from A-type to B-type intercalated cells (Ref. 20). In these cilium-deficient mouse models of PKD, we and others have not examined if such a switch does occur. Moreover, the reversion to an undifferentiated and hyper-proliferative phenotype for the cystic kidney epithelial cell in the collecting duct also evoked a re-visiting of the idea of a “progenitor cell” in the collecting duct that may give rise to principal versus intercalated cells (Ref. 1). Perhaps, the cystic epithelial cell regains a “progenitor cell-like status” in the renal collecting duct that provides a predisposition to remodeling as well as to transport abnormalities. In addition to the numerous studies and thoughts about NaCl and water transport and its roles in both forms of PKD, acid-base transport dysregulation should be examined. Moreover, an integrated review of proliferation together with dysregulated transport of ions, acids, bases and water might yield some groundbreaking results and ideas for ARPKD and ADPKD pathogenesis.

Our work revisits two fundamental questions in cell physiology in PKD. First, how does a disruption in the primary cilium lead to changes in apical membrane protein expression and function? Second, how does a disruption in the apical monocilium cause a disruption in the polarity of expression of a particular epithelial membrane protein? We

choose to examine these two questions together because our findings suggest that they are inter-related with respect to both a change in polarity and an upregulation in NHE function. The simplest and first possible explanation is that the apical membrane landscape (and the supporting cortical cytoskeleton beneath the apical cell surface) is completely changed without a primary cilium. With the emergence of conditional cilium knockout mice where the cilium is completely absent in tissues and cells derived from these mice, this question can now be examined. The loss of the primary cilium may also promote dysregulation of autocrine and paracrine signaling immediately above the apical cell surface. In previous work from our laboratory that is in press (Ref. 15), the loss of a primary cilium caused an attenuation of autocrine purinergic signaling and flow-induced calcium signaling. Moreover, we showed that apyrase, an ATP/ADP scavenger, attenuates this flow-induced calcium signal, as does gadolinium, a broad specificity calcium entry channel blocker (Ref. 15). Praetorius and coworkers have generated similar data in a recent publication generated in the same timeframe (Ref. 16). Interestingly, purinergic signaling, via phospholipase C products and intracellular calcium, modulates NHE activity (Refs. 3, 29). It may be the case that the cortical cytoskeleton beneath the apical membrane, autocrine extracellular signaling, and intracellular signaling may all change, leading to the dysregulation in NHEs, ENaC, NBCs, etc. observed in cilium-deficient cells. It is curious that Na-dependent transporters seem to be affected most prominently by a missing cilium (Refs. 4, 21). We continue to contend that Na-dependent channel and transporter upregulation is an underlying primary cause of the profound and early-onset hypertension in pediatric patients affected by ARPKD (Ref. 11) and may also

contribute to the hypertension that precedes a decline in renal failure in ADPKD (Ref. 22).

There is also a continual emergence of studies over the course of PKD investigation showing abnormal polarity of expression of epithelial membrane proteins in cystic versus non-cystic epithelia. Growth factor receptors and Na,K-ATPase pump subunits are normally, if not exclusively, basolateral membrane proteins in renal collecting duct epithelia. While it remains unclear and controversial whether functional Na,K-ATPase subunit complexes are in the apical membrane of cystic epithelial cells (Refs. 23, 24), individual pump subunits have been found in the apical membrane (Ref. 23). There is more uniform agreement that growth factor receptors appear on the apical surface as well as the basolateral surface of cystic epithelia. In this study, we have ample functional evidence demonstrating that an NHE subtype or subtypes are expressed in error on the apical surface of cilium-deficient principal cells derived from renal collecting duct. Most studies to date (Refs. 8, 10, 31, 32), save a few publications (Refs. 12, 14), show that NHEs are expressed exclusively on the basolateral surface of collecting duct cells.

What of the NHE subtypes that might be involved in this apical mislocalization and upregulation? Apical NHE function, found exclusively in mutant cilium-deficient cells, was markedly more sensitive to cariporide and HOE-694 at the inhibitory doses for NHE1 documented in studies within rat and rabbit. However, doses that also affect NHE2 abolished the remaining NHE activity in the apical membrane of mutant cell monolayers.

As such, we suggest that NHE1 and NHE2 trafficking may be confused in cilium-deficient polarized collecting duct epithelial cells derived from mutant mice. Our studies in these transgenic mice have raised two issues that have hampered our analysis of NHE function and expression. Most studies have been done in rat, rabbit and human, rather than mouse. Moreover, many laboratory and commercial antibodies to NHEs have been made in mice. In addition and in our hands, many “NHE-specific” antibodies have been imperfect and lack subtype specificity to allow a comprehensive assessment at the protein level for the NHE subtype superfamily. This work remains in progress. Rather, we have begun our assessment at the mRNA level using subtype-specific primers and multiple forms of RT-PCR. Our preliminary work in progress shows that NHE1, NHE2 and NHE4 are expressed in our cilium-deficient and cilium-competent cell models. These early data corroborate past work (Refs. 12, 14). Despite the use of at least 6 different primer pairs for NHE3, we could not amplify this apical subtype more predominantly expressed in the proximal tubule. However, we also have positive RT-PCR amplification for NHEs 5, 6, 7 and 8 in these principal cell models. As such, we have as many as 7 NHE subtypes to account for in our cells. Hence, we must be cautious about the interpretation of the pharmacological data until we have immunocytochemical data with appropriate and NHE-specific antibodies that confirm or extend the pharmacological studies. Our data do implicate NHE function in this aberrant phenotype, to the exclusion of other acid-base transport mechanisms. Analysis of the biochemistry and polarity of expression of these NHE subtypes *in vitro* and *in vivo* is beyond the scope of the present study where specific antibodies raised in animals other than mice are not yet available. We will address these issues in a future publication.

Taken together, our current work has demonstrated both mislocalized and inappropriate NHE expression and function in cilium-deficient principal cells derived from mouse models of polycystic kidney disease. In addition, there is overall upregulation of NHE function in cilium-deficient cell monolayers versus cilium-competent cell monolayers that is consistent with persistent urinary acidification in mutant mice and the development of metabolic alkalosis as the kidneys become more cystic over time. This dysregulation of NHE expression and function also cause the shared expression in the same apical membrane domain of principal cells of NHEs and ENaC. Not only do our data imply profound acid-base pathophysiology, an upregulated and inappropriate apical NHE may cause upregulation of ENaC directly. Studies of  $\delta$ ENaC have shown that extracellular acidification opens this particular ENaC subunit (Ref. 35). Apical acidification is present *in vitro* and *in vivo* in cilium-deficient models. Benos, Stanton and co-workers showed in *Xenopus* oocytes that intracellular acidification stimulated  $\alpha$ ENaC (Ref. 9). It remains possible that their shared presence in the apical membrane of cilium-deficient cells may exacerbate  $\text{Na}^+$  hyperabsorption in ARPKD and may be a primary cause of hypertension in either or both ARPKD and ADPKD.

### ***Acknowledgments***

A special thanks to Drs. Peter Komlosi and Darwin Bell (now at the Medical University of South Carolina in Charleston, SC) for the use of their custom sided flow chamber for our studies. We gratefully acknowledge the support of our PKD R01 NIH DK67343 to EMS. We also acknowledge the support of R01 DK65655 to BKY. We also acknowledge the support of our Recessive PKD Translational and Research Core Centers (P30 DK074038).



## ***References***

- 1      **Aigner J, Kloth S, Jennings ML and WW Minuth.** Transitional differentiation patterns of principal and intercalated cells during renal collecting duct development. *Epithelial Cell Biol.* 4(3):121-30, 1995.
- 2      **Bachmann O, Riederer B, Rossmann H, Groos S, Schultheis PJ, Shull GE, Gregor M, Manns MP and U Seidler.** The Na<sup>+</sup>/H<sup>+</sup> exchanger isoform 2 is the predominant NHE isoform in murine colonic crypts and its lack causes NHE3 upregulation. *Am J Physiol Gastrointest Liver Physiol.* 287(1):G125-33, 2004
- 3      **Bagorda A, Guerra L, Di Sole F, Helmle-Kolb C, Favia M, Jacobson KA, Casavola V, and SJ Reshkin.** Extracellular adenine nucleotides regulate Na<sup>+</sup>/H<sup>+</sup> exchanger NHE3 activity in A6-NHE3 transfectants by a cAMP/PKA-dependent mechanism. *J Membr Biol.* 188: 249–259, 2002
- 4      **Banizs B, Komlosi P, Bevensee MO, Schwiebert EM, Bell PD and BK Yoder.** Altered pH(i) regulation and Na(+)/HCO<sub>3</sub>(-) transporter activity in choroid plexus of cilia-defective Tg737(orpk) mutant mouse. *Am J Physiol Cell Physiol.* 292: C1409 - C1416, 2007.
- 5      **Bevensee MO and WF Boron.** Manipulation and regulation of cytosolic pH. In: *Methods in Neurosciences*, Vol. 27. Measurement and manipulation of intracellular ions. J Kraicer and SJ Dixon, eds. New York: Academic Press. p. 252-273, 1995.
- 6      **Boron WF and P De Weer.** Intracellular pH transients in squid giant axons caused by CO<sub>2</sub>, NH<sub>3</sub>, and metabolic inhibitors. *J Gen Physiol.* 67(1):91-112, 1976.

- 7      **Boyarsky G, Ganz MB, Sterzel RB and WF Boron.** pH regulation in single glomerular mesangial cells. I. Acid extrusion in absence and presence of HCO<sub>3</sub><sup>-</sup>. *Am J Physiol.* 255(6 Pt 1):C844-56, 1988.
- 8      **Chaillet JR, Lopes AG and WF Boron.** Basolateral Na-H exchange in the rabbit cortical collecting tubule. *J Gen Physiol.* 86(6):795-812, 1985.
- 9      **Chalfant, ML, Denton JS, Berdiev BK, Ismailov II, Benos DJ and BA Stanton.** Intracellular H<sup>+</sup> regulates the alpha-subunit of ENaC, the epithelial Na<sup>+</sup> channel. *Am J Physiol Cell Physiol* 276: C477-C486, 1999.
- 10     **Ford P, Rivarola V, Kierbel A, Chara O, Blot-Chabaud M, Farman N, Parisi M and C Capurro.** Differential role of Na<sup>+</sup>/H<sup>+</sup> exchange isoforms NHE-1 and NHE-2 in a rat cortical collecting duct cell line. *J Membr Biol.* 190(2):117-25, 2002.
- 11     **Guay-Woodford LM and RA Desmond.** Autosomal recessive polycystic kidney disease: the clinical experience in North America. *Pediatrics* 111: 1072–1080, 2003
- 12     **Guerra, L, Sole FD, Volenti G, Ronco PM, Perlino E, Casavola V and SJ Reshkin.** Polarized distribution of Na<sup>+</sup>/H<sup>+</sup> exchanger isoforms in rabbit collecting duct cells. *Kidney Int* 53: 1269-1277, 1998
- 13     **Haycraft CJ, Zhang Q, Song B, Jackson WS, Detloff PJ, Serra R and BK Yoder.** *Development.* 134(2):307-16, 2007.
- 14     **Hill C, Giesberts AN and SJ White.** Expression of isoforms of the Na<sup>(+)</sup>/H<sup>(+)</sup> exchanger in M-1 mouse cortical collecting duct cells. *Am J Physiol Renal Physiol.* 282(4):F649-54, 2002
- 15     **Hovater MB, Olteanu D, Hanson EL, Cheng NL, Siroky B, Fintha A, Komlosi P, Bell PD, Yoder BK, and EM Schwiebert.** Loss of apical monocilia on

collecting duct principal cells impairs apically-directed ATP release and flow-induced calcium signals in an integrated system. *Purinergic Signaling* 3(3): In Press, 2007

16 **Jensen ME, Odgaard E, Christensen MH, Praetorius HA and J Leipziger.** Flow-induced  $[Ca^{2+}]_i$  increase depends on nucleotide release and subsequent purinergic signaling in the intact nephron. *J Am Soc Nephrol.* 18(7):2062-70, 2007.

17 **Kizer, N. L., B. Lewis, and B. A. Stanton.** Electrogenic sodium absorption and chloride secretion by an inner medullary collecting duct cell line (mIMCD-K2). *Am. J. Physiol.* 268 (Renal Fluid Electrolyte Physiol. 37): F347-F355, 1995.

18 **Martinez JR and JJ Grantham.** Polycystic kidney disease: etiology, pathogenesis, and treatment. *Dis Mon.* 41(11):693-765, 1995.

19 **Masereel B, Pochet L and D Laeckmann.** An overview of inhibitors of  $Na^{+}/H^{+}$  exchanger. *Eur J Med Chem.* 38(6):547-54, 2003.

20 **Narbaitz R, Kapal VK and DZ Levine.** Induction of intercalated cell changes in rat pups from acid- and alkali-loaded mothers. *Am J Physiol.* 264(3 Pt 2):F415-20, 1993.

21 **Olteanu D, Yoder BK, Liu W, Croyle MJ, Welty EA, Rosborough K, Wyss JM, Bell PD, Guay-Woodford LM, Bevensee MO, Satlin LM and EM Schwiebert.** Heightened epithelial  $Na^{+}$  channel-mediated  $Na^{+}$  absorption in a murine polycystic kidney disease model epithelium lacking apical monocilia. *Am J Physiol Cell Physiol.* 290(4):C947-9, 2006

22 **Perrone RD and DC Miskulin.** Hypertension in individuals at risk for autosomal dominant polycystic kidney disease: to screen or not to screen? *Am J Kidney Dis.* 46(3):557-9, 2005.

- 23     **Rohatgi R, Greenberg A, Burrow CR, Wilson PD and LM Satlin.** Na transport in autosomal recessive polycystic kidney disease (ARPKD) cyst lining epithelial cells. *J Am Soc Nephrol.* 14(4):827-36, 2003.
- 24     **Schafer JA, Watkins ML, Li L, Herter P, Haxelmans S and E Schlatter.** A simplified method for isolation of large numbers of defined nephron segments. *Am J Physiol.* 273(4 Pt 2):F650-7, 1997
- 25     **Schild L.** The epithelial sodium channel: from molecule to disease. *Rev Physiol Biochem Pharmacol.* 151:93-107, 2004.
- 26     **Sullivan, LP, Wallace DP and JJ Grantham.** Epithelial transport in polycystic kidney disease. *Physiol Rev* 78: 1165-1191, 1998.
- 27     **Takahashi H, Calvet JP, Dittmore-Hoover D, Yoshida K, Grantham JJ, and VH Gattone 2nd.** A hereditary model of slowly progressive polycystic kidney disease in the mouse. *J Am Soc Nephrol* . 1: 980–989, 1991.
- 28     **Thomas JA, Buchsbaum RN, Zimniak A, and E. Racker.** Intracellular pH measurements in Ehrlich ascites tumor cells utilizing spectroscopic probes generated in situ. *Biochemistry.* 81:2210-2218, 1979.
- 29     **Urbach V, Hélix N, Renaudon B and BJ Harvey.** Cellular mechanisms for apical ATP effects on intracellular pH in human bronchial epithelium. *J Physiol.* 15;543(Pt 1):13-21, 2002.
- 30     **Wang T, Hropot M, Aronson PS and G Giebisch.** Role of NHE isoforms in mediating bicarbonate reabsorption along the nephron. *Am J Physiol Renal Physiol.* 281(6):F1117-22, 2001.

- 31     **Wang X and I Kurtz.** H<sup>+</sup>/base transport in principal cells characterized by confocal fluorescence imaging. *Am J Physiol.* 259(2 Pt 1):C365-73, 1990.
- 32     **Weiner ID and LL Hamm.** Regulation of intracellular pH in the rabbit cortical collecting tubule. *J Clin Invest.* 85(1):274-81, 1990.
- 33     **Wilson PD.** Polycystic kidney disease. *N Engl J Med* 350: 151–164, 2004
- 34     **Wilson PD, Sherwood AC, Palla K, Du J, Watson R and JT Norman.** Reversed polarity of Na<sup>+</sup>-K<sup>+</sup>-ATPase: mislocation to apical plasma membrane. *Am J Physiol.* 260:F420–F430, 1991
- 35     **Yamamura H, Ugawa S, Ueda T and S Shimada.** Protons activate the delta-subunit of the epithelial Na<sup>+</sup> channel in humans. *J Biol Chem.* 26;279(13):12529-34, 2004.
- 36     **Yu, J., Carroll, T. J. and AP McMahon.** Sonic hedgehog regulates proliferation and differentiation of mesenchymal cells in the mouse metanephric kidney. *Development.* 129,5301–5312, 2002.

## ***Figure Legends***

### ***Figure 1: Proton Pseudoflux Measurements and Calculations***

Typical trace recorded at the end of an experiment without inhibitor (Fig. 1A). Once monolayer was fully recovered from acid load protocol, a high- $K^+$ /nigericin solution in 0  $Na^+$  calibrated at different pH values (5.5-8.5) was perfused on both sides. To transform the BCECF fluorescence ratio in pH units, a steady state value was calculated for each  $pH_o$  evaluated. If we assume that high- $K^+$ /nigericin solution will set  $pH_i$  equal to  $pH_o$  we could plot the fluorescence data to a virtual  $pH_i$  (Fig. 1B) using the formula given in the text. The lower and upper asymptote found for rescued cilium-competent cells was 0.387 and 1.998, respectively, with a pK equal to 7.212. Calibration curve in the *orpk* cilium-deficient cells had a lower and upper asymptote equal with 0.420 and 1.722, respectively, and a pK of 7.095. Buffering power was necessary for conversion of  $pH_i$  to proton efflux (Fig. 1C). Stepwise removal of  $NH_4^+$  was used to determine the relationship between  $pH_i$  and intrinsic buffering capacity. These methods also showed that these cell monolayers were well polarized and of high resistance, lending themselves to be ideal for these measurements.

### ***Figure 2: Flow Chamber and Early $Na^+$ Removal and Re-Addition Protocols.***

The flow chamber used in all BCECF imaging studies was designed by Drs. Peter Komlosi and Darwin Bell. A schematic of this chamber is shown in Fig. 2A. Initial experiments involving  $Na^+$  removal and re-addition are shown below. The original traces in “rescued” cilium-competent cell monolayers and “mutant” cilium-deficient cell

monolayers are shown in Fig 2B and 2C respectively, and are representative of an  $n = 17$  for rescued cell monolayers and an  $n = 24$  for mutant cell monolayers. In Step 1 of the protocol, a Na-replete Ringer was perfused through both sides of the monolayer. In Step 2 of the protocol, a Na-free Ringer (Na replaced with equimolar N-methyl-D-glucamine (NMDG)) was perfused on both sides of the monolayer. In Step 3 of the protocol, a Na-replete Ringer was added to the apical side of the monolayer only. In Step 4 of the protocol, a Na-replete Ringer was also added to the basolateral side of the monolayer as well to re-achieve the beginning of the experiment; this maneuver allowed complete recovery of  $\text{pH}_i$ .

***Figure 3: Multiple Mutant Cell Clones Display this Mislocalized Apical NHE Activity in Addition to Normal Basolateral-exclusive NHE Activity Displayed in Multiple Rescued Cell Clones***

The flow chamber was also used for a more effective  $\text{NH}_4\text{Cl}$  “prepulse” protocol. Three rescued cell clones (A=Rescued 1, B=Rescued 2, C=Rescued B2) and three mutant cell clones (D=Mutant 1, E=Mutant 2, F=Mutant 3) were studied using the following protocol. Step 1 was measurement of resting  $\text{pH}_i$  with Na-replete Ringer on both sides of the monolayer. Step 2 was Na-free Ringer (replaced with NMDG) on both sides of the monolayer with 20 mM  $\text{NH}_4\text{Cl}$  to cause rapid alkalinization. Step 3 was  $\text{NH}_4\text{Cl}$  prepulse removal in Na-free Ringer on both sides of the monolayer, causing rapid and complete acidification. Step 4 was re-addition of Na-replete Ringer to the apical side of the monolayer. Step 5 was re-addition of Na-replete Ringer to the basolateral side of the monolayer as well; this maneuver allowed complete recovery of  $\text{pH}_i$ . None of the rescued

clones showed recovery with re-addition of Na on the apical side in Step 4 (Fig. 3 A-C). In contrast, each mutant displayed an apical recovery once sodium was added back on the apical side in Step 4 (Fig. 3 D-F).

***Figure 4: Lower and Faster Acidification, Higher Alkalinization and Higher Apical Acid Extrusion Capacity in Mutant versus Rescued Cells Monolayers***

Intracellular acidification was faster, reaching a lower value in the same amount of time, in cilium-deficient versus cilium-competent monolayers. After we recorded a resting  $\text{pH}_i$ , we simultaneously change the Na-containing solution on both sides with Na-free solution letting the monolayers to acidify over a period of time. Representative traces are shown together for comparison (Fig. 4A). Summarized data for alkalinization peak and acidification steady state recorded during the ammonium prepulse experiments revealed higher alkalinization followed by a lower acidification, both in respect to the resting  $\text{pH}_i$ , in mutant cell monolayers versus rescued cell monolayers (n=59 traces and 45 traces, respectively). Alkalinization peak in mutant versus rescued cell monolayers has a mean  $\pm$  SEM of  $8.13 \pm 0.05$  pH units and  $7.76 \pm 0.03$  pH units respectively. Acidification steady state in mutant versus rescued cell monolayers has a mean  $\pm$  SEM of  $5.79 \pm 0.073$  pH units and  $6.41 \pm 0.03$  pH units respectively. Statistical analysis was determined using ANOVA.  $P < 0.01$  was considered statistically significant. (Fig. 4B). No difference was found between rescued and mutant cells monolayer resting  $\text{pH}_i$ s (7.20 and 7.21 respectively) so for the sake of a close comparison we plot all the data in the same graph using the crossing point set for pH 7.2. Apical acid extrusion in both mutant and rescued



cells monolayers (n=27 traces for each) was calculated as the product of  $dpH_i/dt$  and intrinsic buffering power. The  $pH_i$  sensitivity of total acid extrusion in cilium-deficient monolayers is much greater than in cilium-component monolayers (Fig. 4C). These data suggest an inappropriate NHE activity on the apical cell membrane of CCD PC cells that lack a well-formed apical central cilium.

***Figure 5: Pharmacological Assessment of Apical NHE Activities***

Original traces in cilium-deficient cells in the absence and presence of HOE-694 demonstrate that apical recovery is sensitive to a low dose of this inhibitor (Fig. 5A). Values for 10  $\mu$ M HOE-694 inhibition of total acid extrusion on the apical side of the cilium-deficient monolayer are given in the original text. Apical total acid extrusion in the absence and presence of cariporide shows that 1  $\mu$ M inhibit the majority of the NHE activity (59-70%) whereas 50  $\mu$ M inhibits 20% more (79-89%) to a value very close to the minimal total acid extrusion observed in rescued monolayers (Fig. 5B). Together, these data show that total acid extrusion, inappropriately present on the apical membrane of cilium-deficient cells, is quite sensitive to low doses of these two more specific NHE inhibitors. Each plot represent summarized acid extrusion data from 27 traces.

***Figure 6: Pharmacological Assessment of Basolateral NHE Activities***

Original traces, in the absence and in the presence of inhibitor, were recorded during the ammonium prepulse protocol. Representative traces with and without cariporide are shown in Fig. 6A. Higher doses of HOE-694 was necessary to inhibit the basolateral total acid extrusion in mutant (Fig. 6B) and rescued cell monolayers (original traces not shown

but refer to the original text for summarized acid extrusion). Summarized data (n=27 traces) are shown for total acid extrusion in the presence and in the absence of inhibitor. In cilium-deficient monolayers, 1  $\mu$ M cariporide reduced basolateral acid extrusion by 49-59% in the  $\text{pH}_i$  range 6.03-7.18, and 50  $\mu$ M cariporide reduced acid extrusion by 91-93% in the  $\text{pH}_i$  range 6.18-6.78. Rescued cell monolayers present a similar profile, with 1  $\mu$ M and 50  $\mu$ M cariporide inhibiting basolateral NHE acid extrusion by 35-45% and 93-95%, respectively, over a  $\text{pH}_i$  range of 6.33-6.78 (Fig. 6D).

***Figure 7:  $\text{pH}_i$  Dependencies of Cariporide-sensitive Acid Extrusion***

These plots are generated by subtracting the plot of cariporide-insensitive acid extrusion from the corresponding plot of total acid extrusion obtained from either the apical or basolateral side. Data was fitted with a linear equation to determine the slope. Basolateral cariporide-sensitive acid extrusion in mutant and rescued cell monolayers has a slope of -340.53 and -280.35, respectively, whereas apical acid extrusion displayed a value equal to -96.881. Cariporide-sensitive acid extrusion on the basolateral side of either monolayer was 3.5-4.5 fold greater than that on the apical side of the mutant monolayer in the  $\text{pH}_i$  range 6.23-6.68. These data suggest that apical NHE activity induced in the mutant monolayers is considerably less than basolateral NHE activity in both mutant and rescued monolayers

***Figure 8 Part A-D: Imaging of the Ciliary Status and the Cystic Nature of Kidneys in the HoxB7 Cre-Lox Kidney-specific Conditional Cilium knockout Mouse Model; Part E: Urinary and Blood pH. Metabolic Measurements of Fresh Urine and Plasma***

### ***Samples Reveals Acid-Base Balance Anomalies in Cilium-deficient PKD Mouse Models***

Analysis of cilia and renal pathology in *Tg737* conditional cilia mutants. Cilia were analyzed by immunofluorescence using antibodies against acetylated  $\alpha$ -tubulin (green) in collecting ducts isolated from 7 day old (Fig. 8A) *Tg737<sup>flox/Δ</sup>*; *HoxB7-Cre* and (Fig. 8B) *Tg737<sup>flox/WT</sup>*; *HoxB7-Cre* mice. Nuclei are labeled with Hoechst (blue). Note the absence of cilia in the conditional mutant and the dilation of the tubule segment. Renal pathology was analyzed in paraffin sections. Shown is a section from a day 14 control (Fig. 8C) and mutant (Fig. 8D). Fresh urine and blood samples were collected from *HoxB7-Cre*; *Tg737<sup>flox/□</sup>* kidney-specific conditional cilium knockout mice versus littermate controls at 7, 14, 21 (19-23) and 28 days of life (Fig. 8E). The pH measurements from a total of 50 cilium knockout mice and 116 cilium competent mice are displayed comparatively for each time point. An average for each group of mice was calculated and it is shown together with the original data as a crossing line for a better comparison. We also set a secondary y axis to correlate for blood pH measurements. Urinary pH measurements in cilium knock out mice versus cilium competent mice express as mean  $\pm$  SEM: by Day 7:  $5.28 \pm 0.05$  pH units and  $5.59 \pm 0.04$  respectively; by Day 14:  $5.01 \pm 0.04$  pH units and  $5.72 \pm 0.04$  pH units respectively; by Day 21(19-23):  $5.05 \pm 0.07$  pH units and  $6.25 \pm 0.1$  pH units respectively; by Day 28:  $5.33 \pm 0.11$  pH units and  $6.9 \pm 0.2$  pH units. All separations were statistically significant. Blood pH measurements in cilium knock out mice versus cilium competent mice express as mean  $\pm$  SEM: by Day 7:  $7.66 \pm 0.04$  pH units and  $7.59 \pm 0.05$  pH units respectively; by Day 14:  $7.51 \pm 0.03$  pH units and  $7.44 \pm 0.03$  pH units respectively; by Day 21 (19-23):  $7.50 \pm 0.4$  pH units and  $7.45 \pm 0.03$  pH

units. These separations are not statistical significant. However, by Day 28:  $7.50 \pm 0.03$  pH units and  $7.32 \pm 0.02$  pH units measured in cilium knock out versus cilium competent mice respectively the difference became significant. Statistical analysis was determined using ANOVA.  $P < 0.01$  was considered statistically significant.

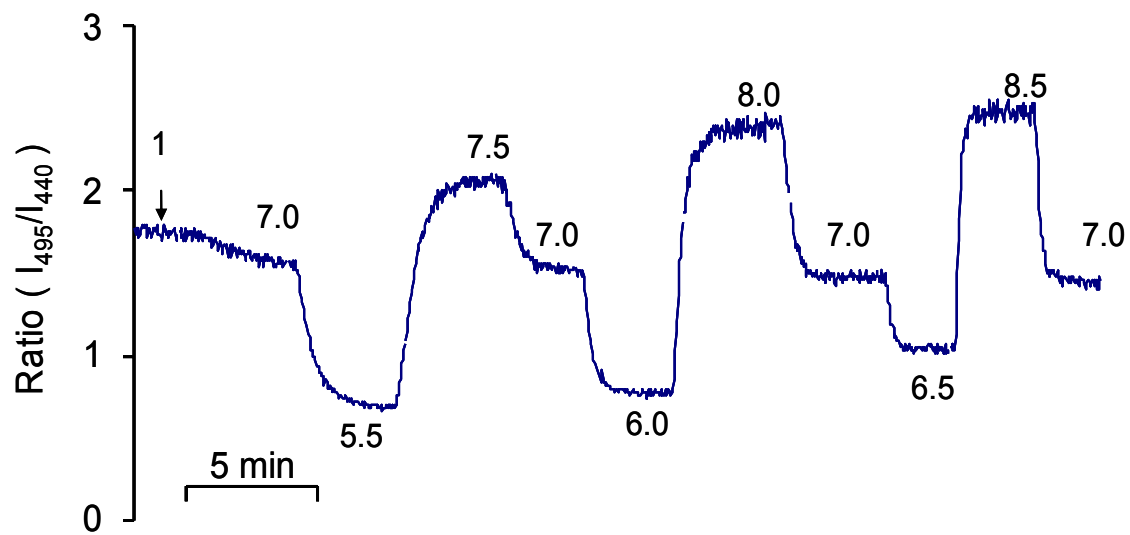


Figure 1A

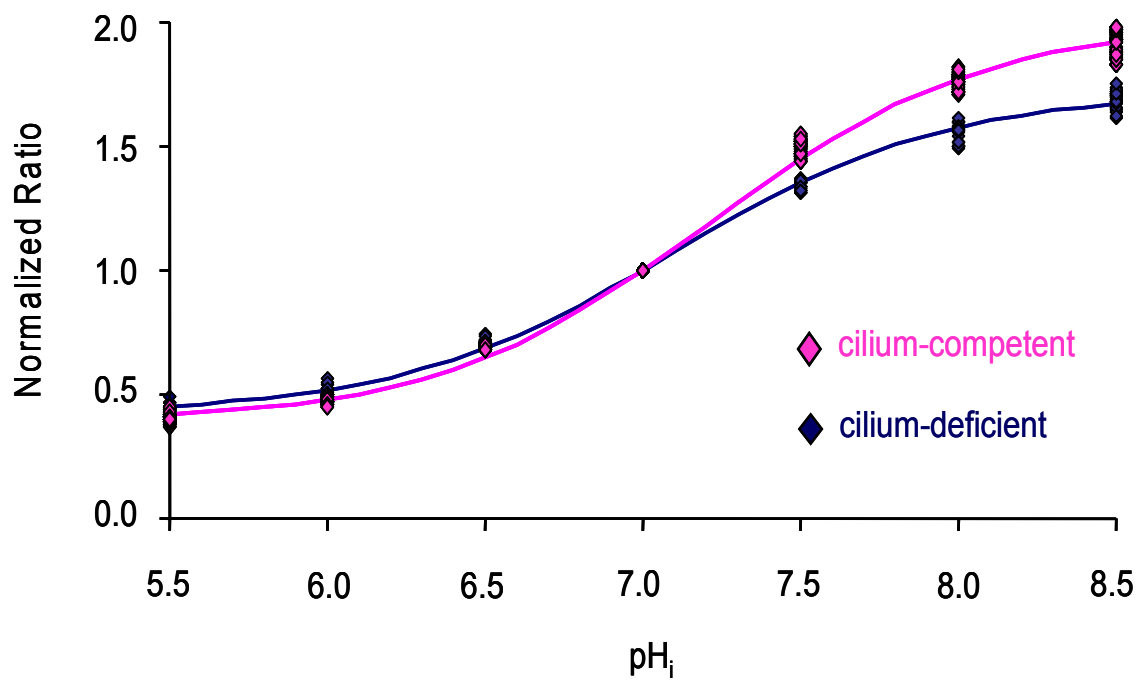


Figure 1B

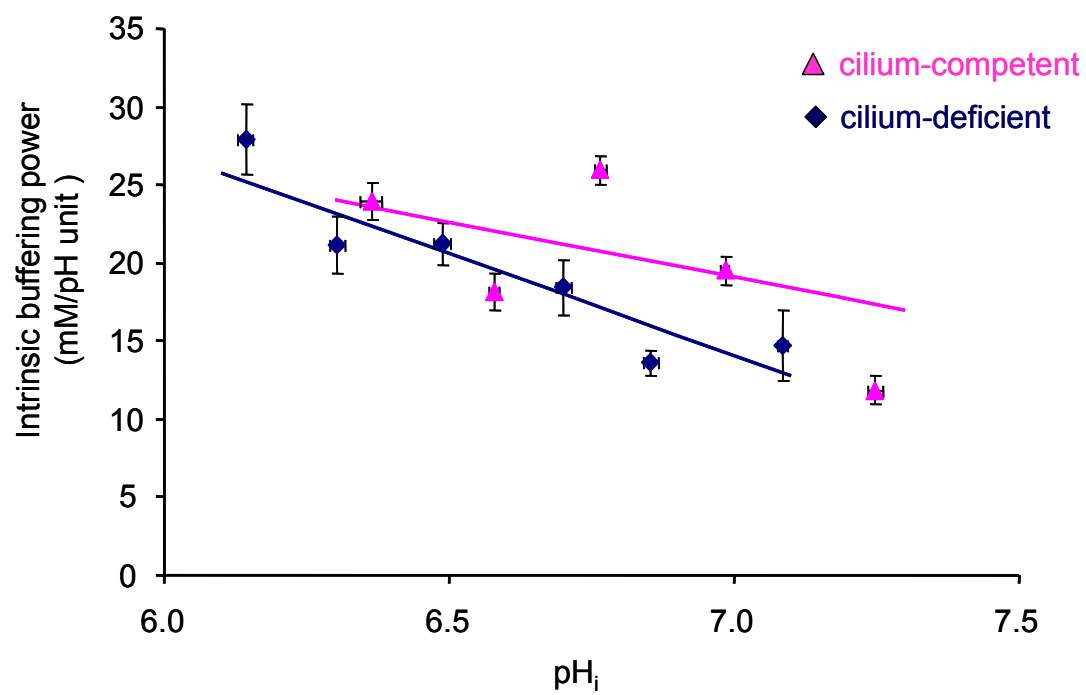
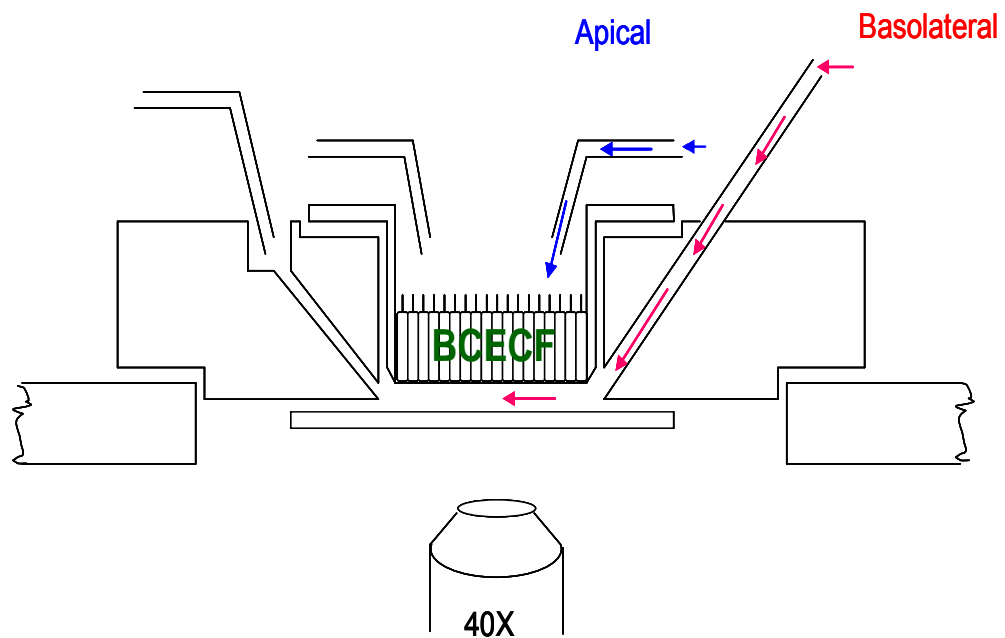
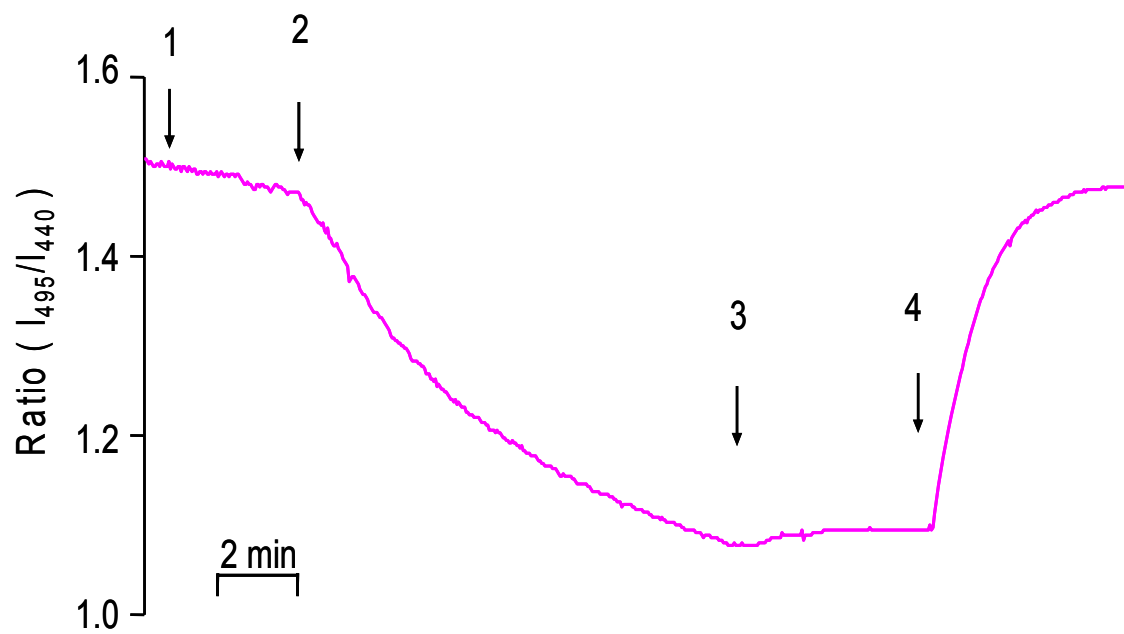


Figure 1C



**Figure 2A**



**Figure 2B**

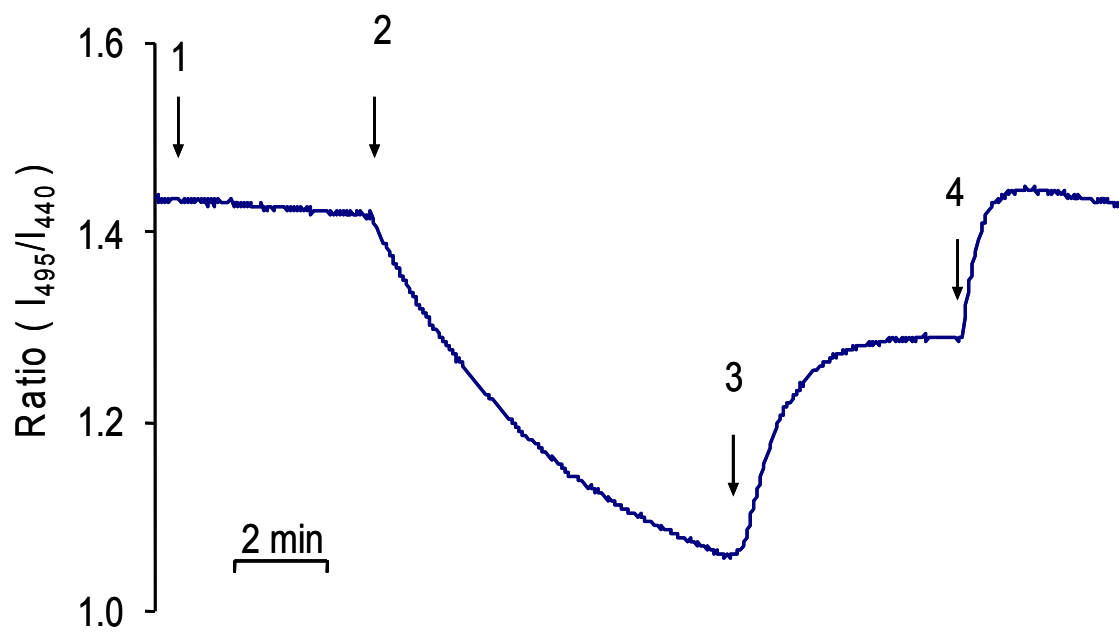


**Figure 2C**



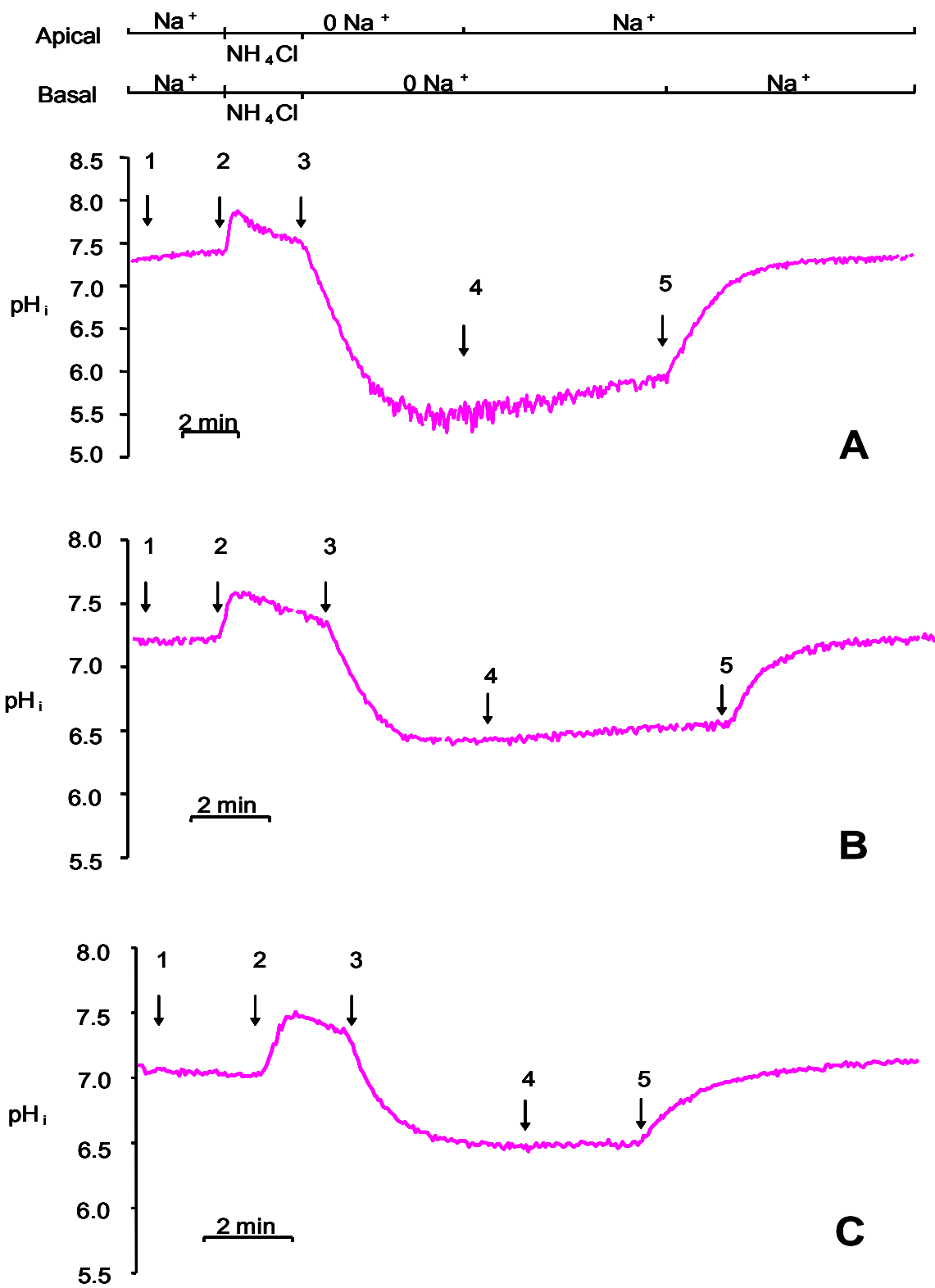


Figure 3 (A-C)

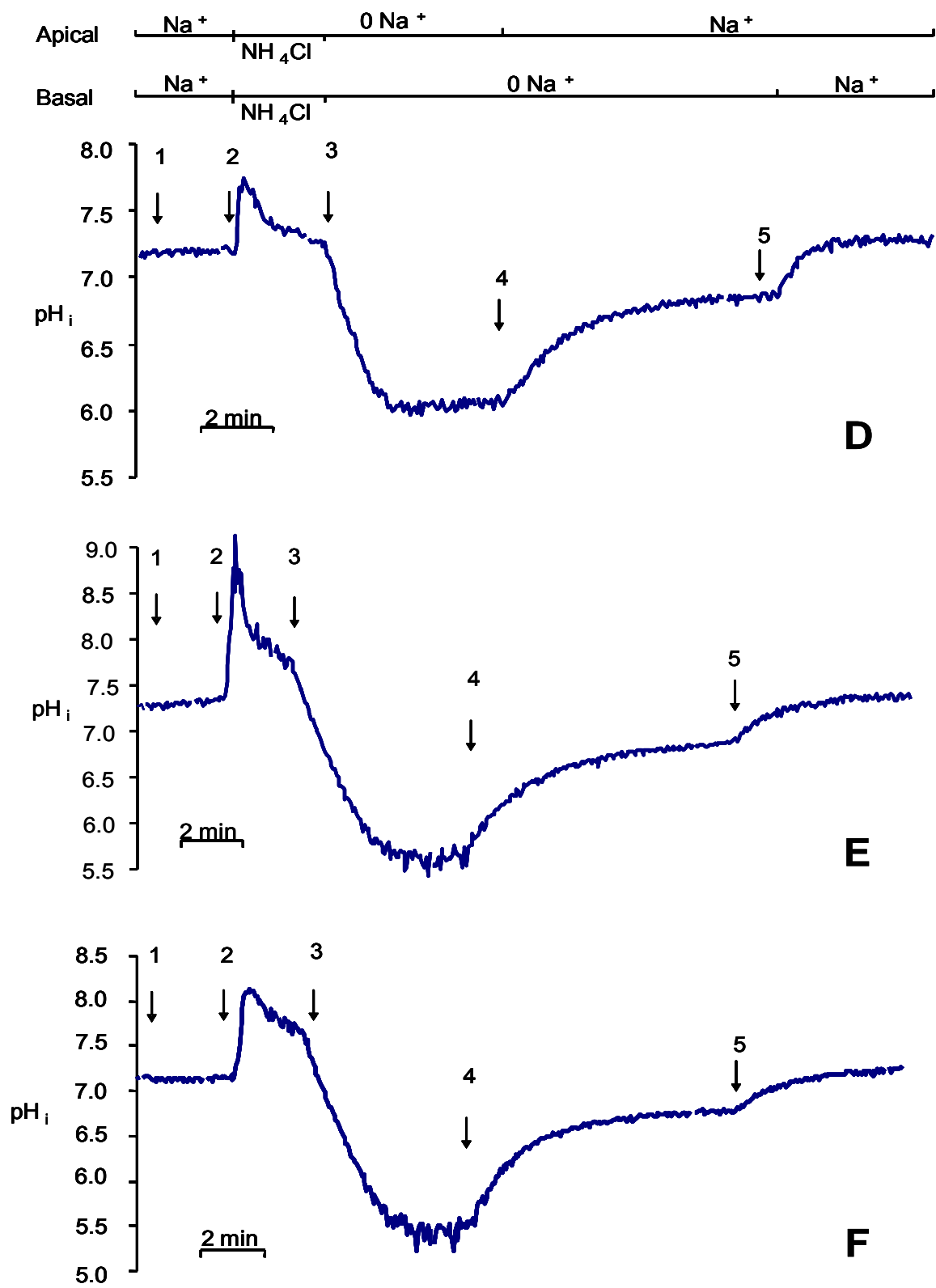
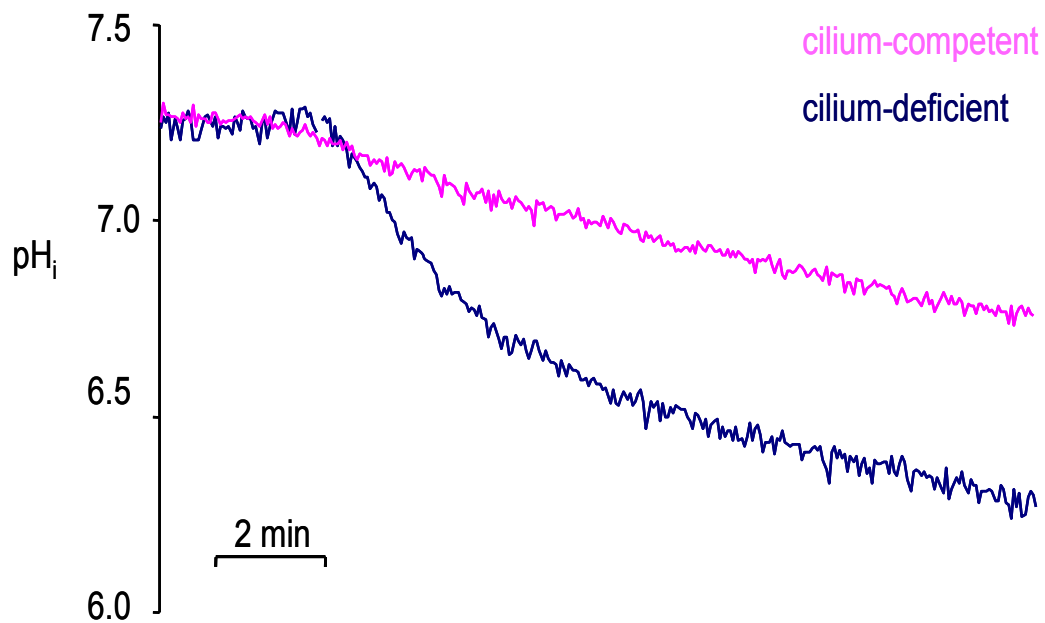
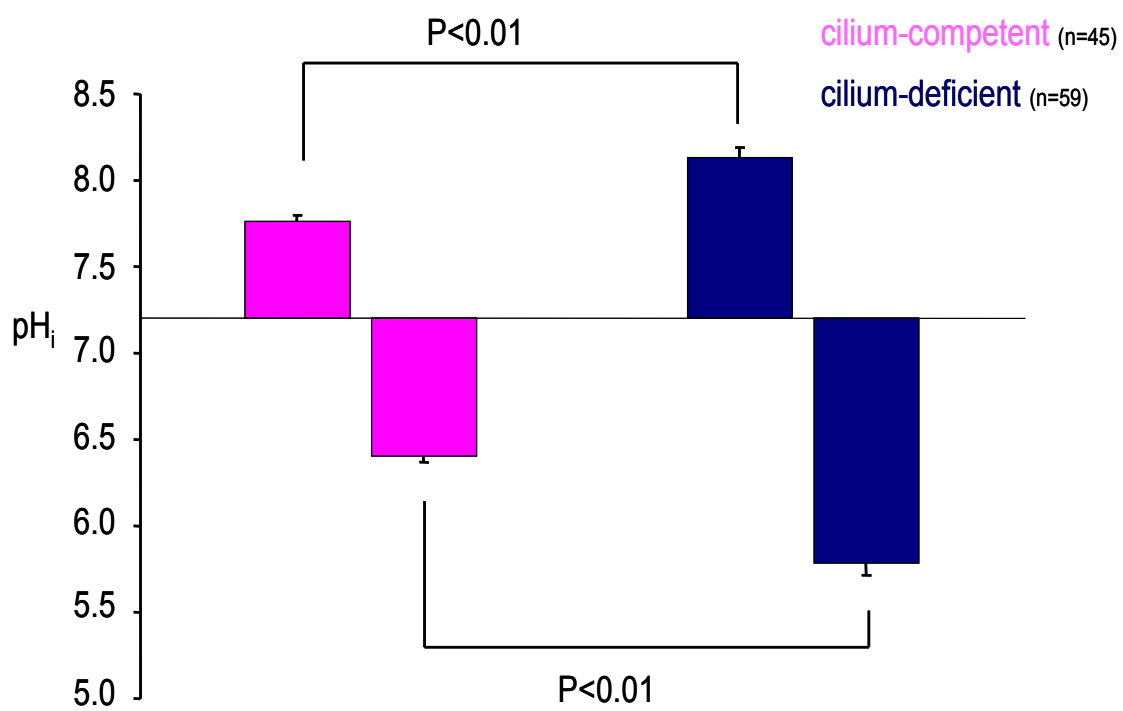


Figure 3 (D-F)



**Figure 4A**



**Figure 4B**

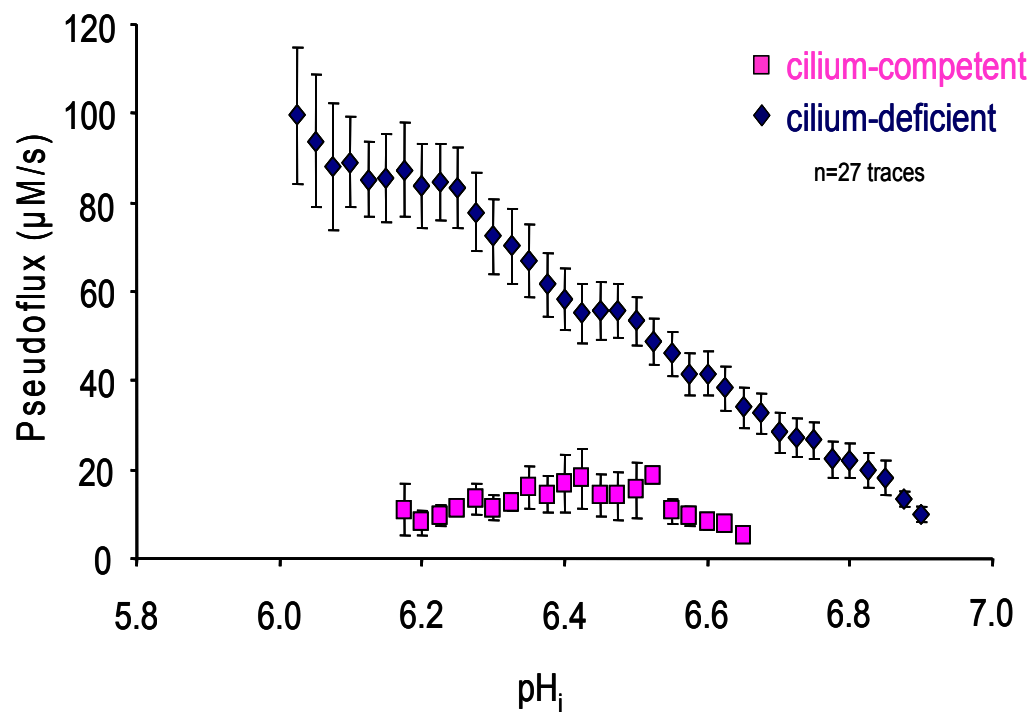


**Figure 4C**

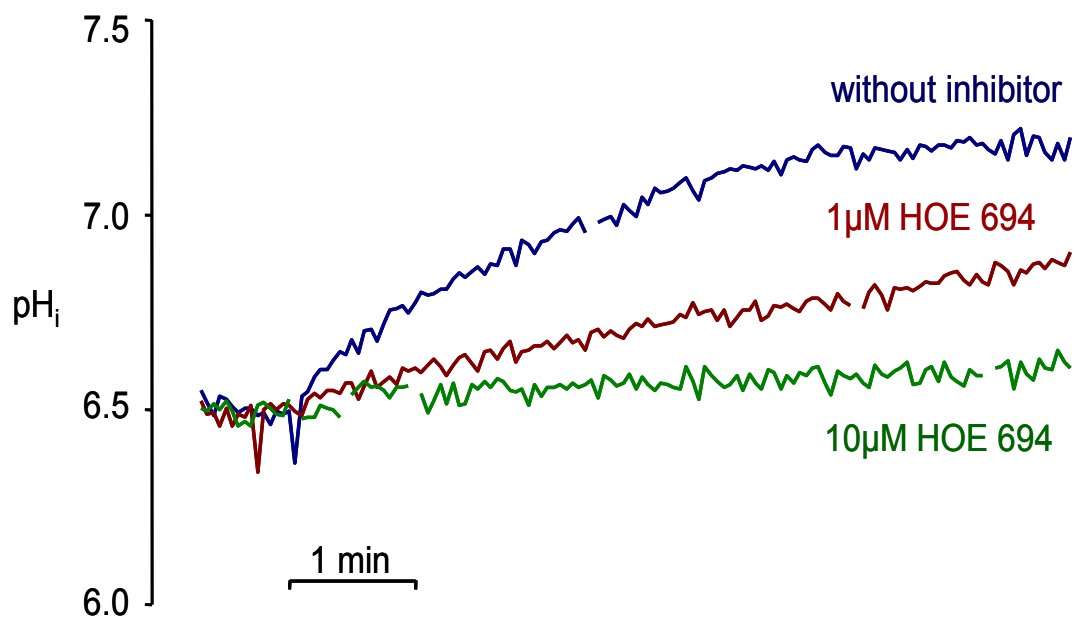


Figure 5A

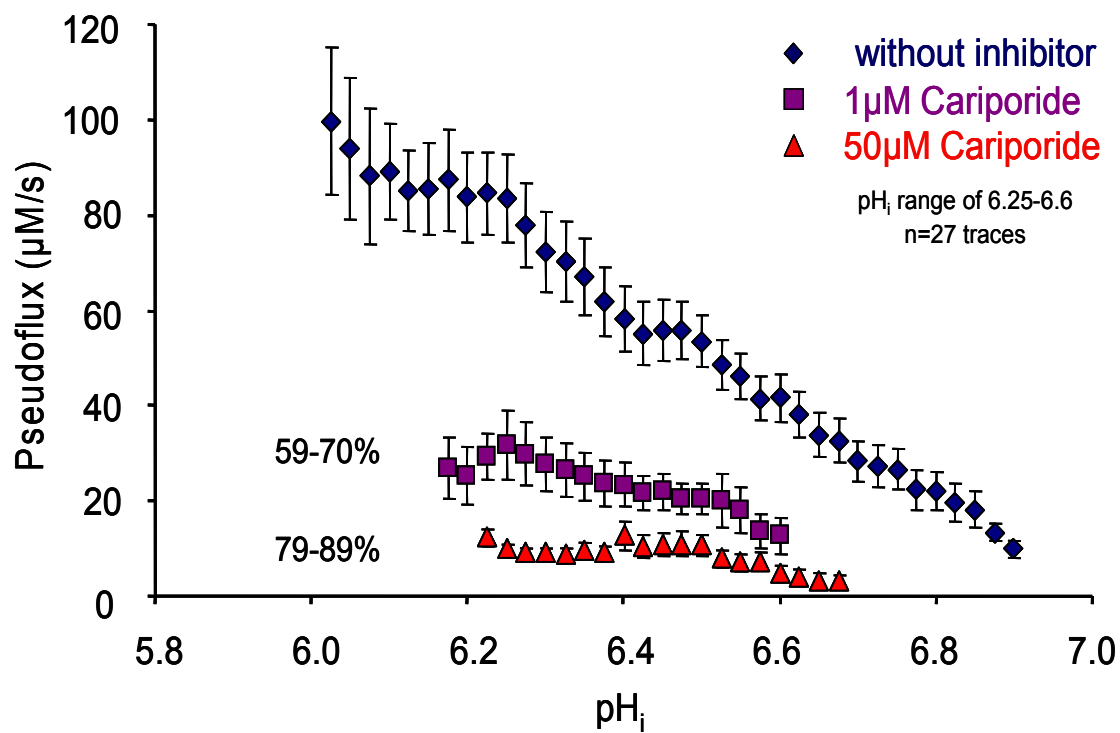
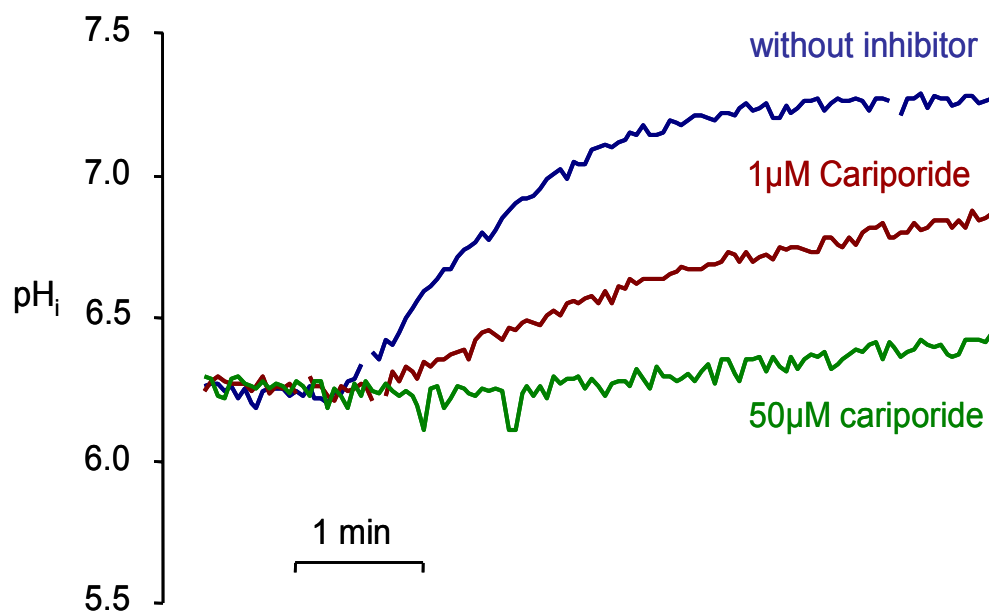
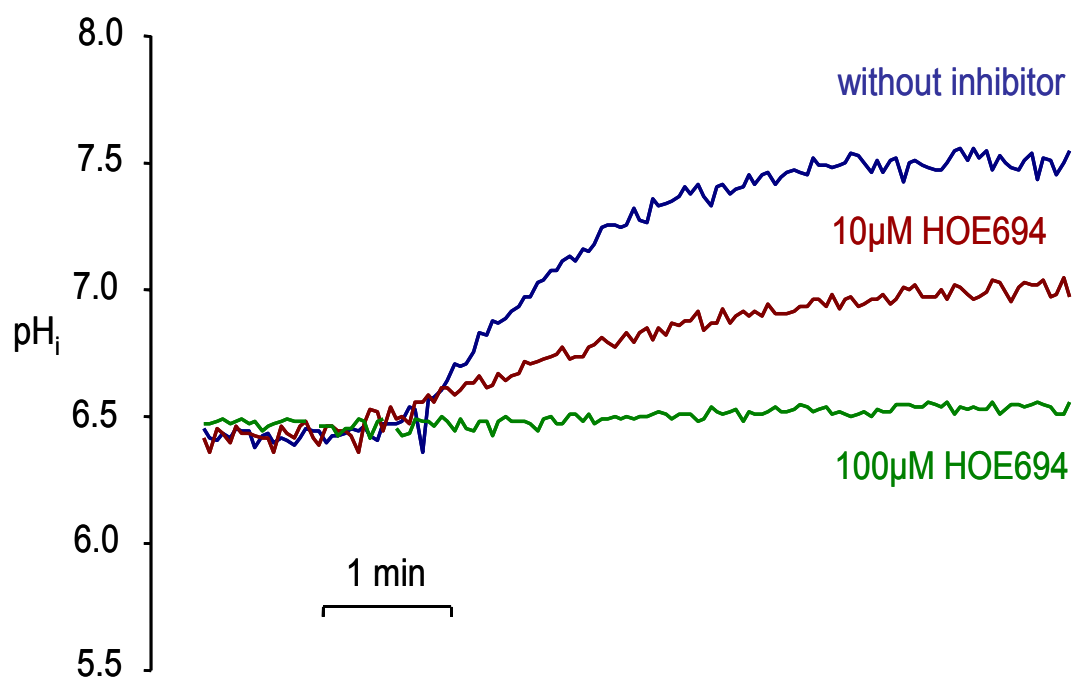


Figure 5B



**Figure 6A**



**Figure 6B**

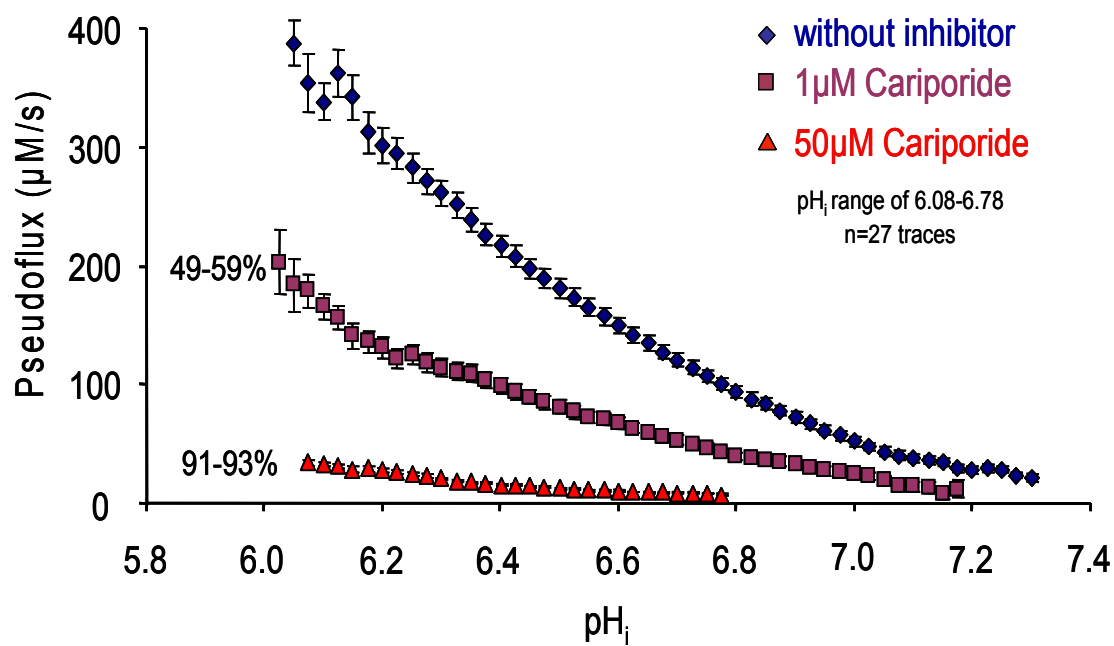


Figure 6 C

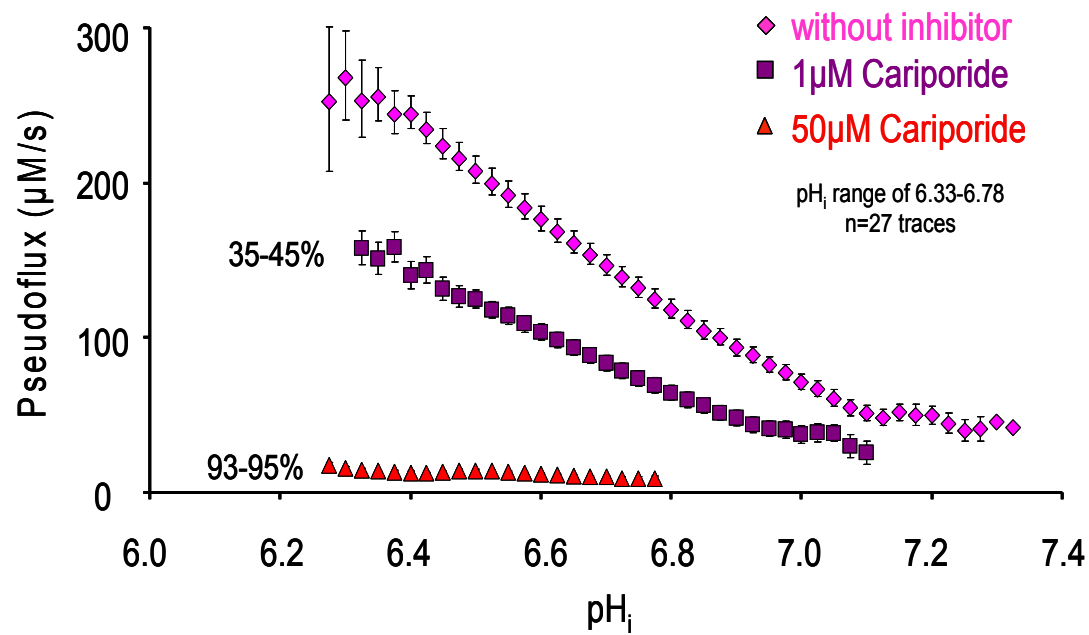
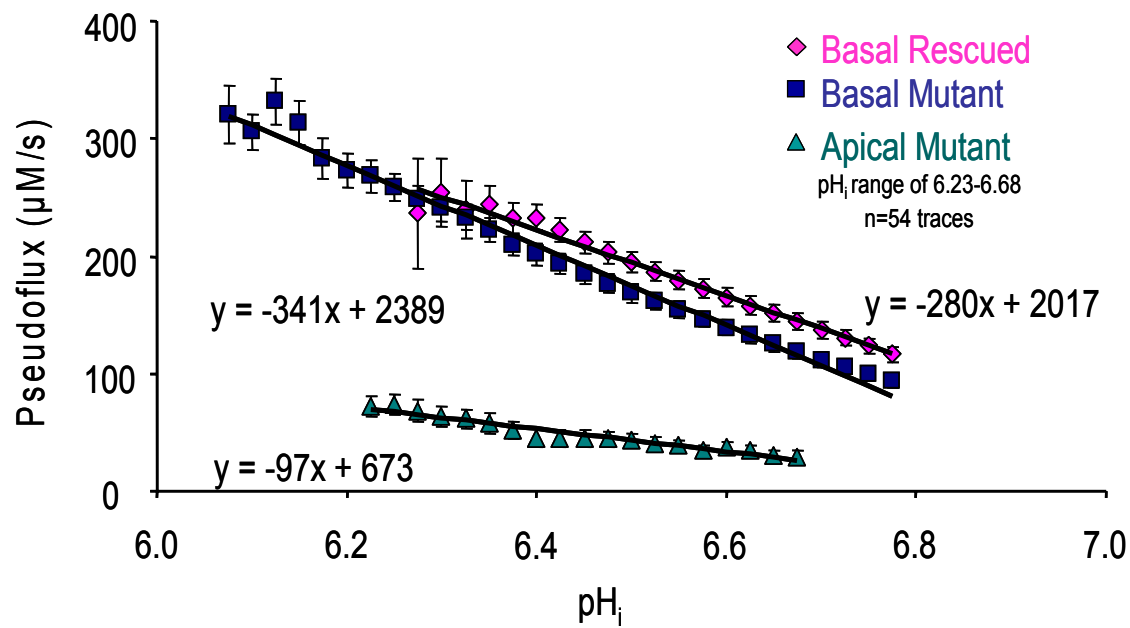
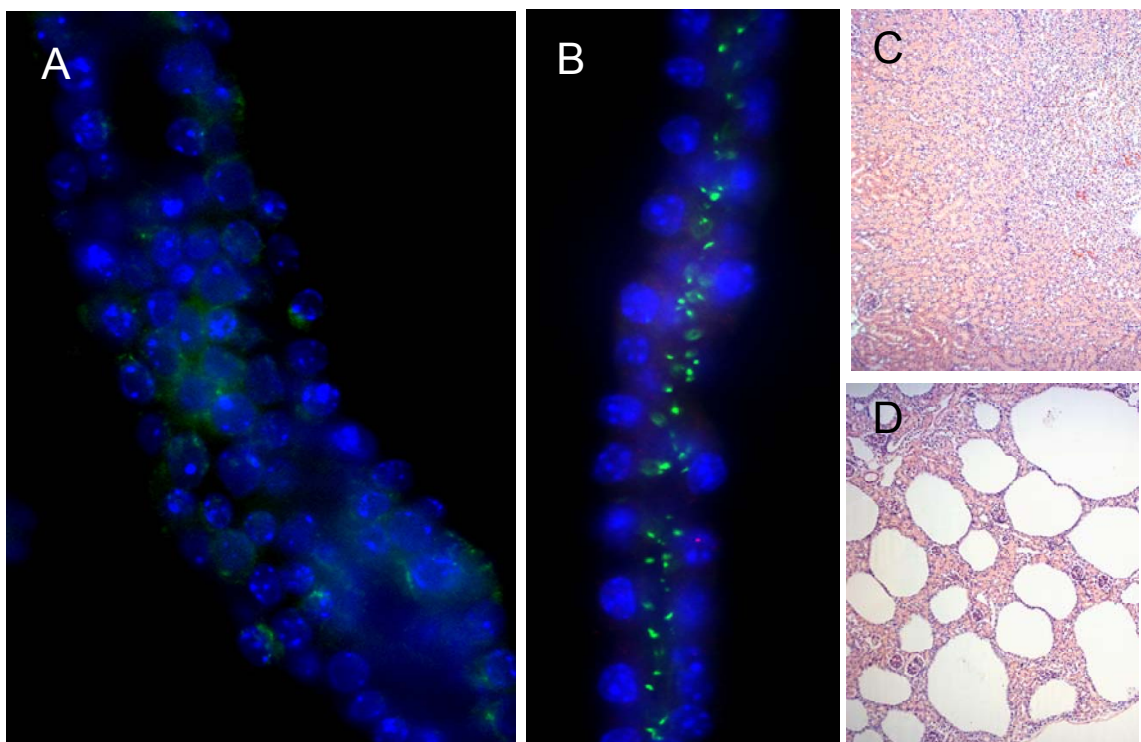


Figure 6D



**Figure 7**





**Figure 8 (A-D)**

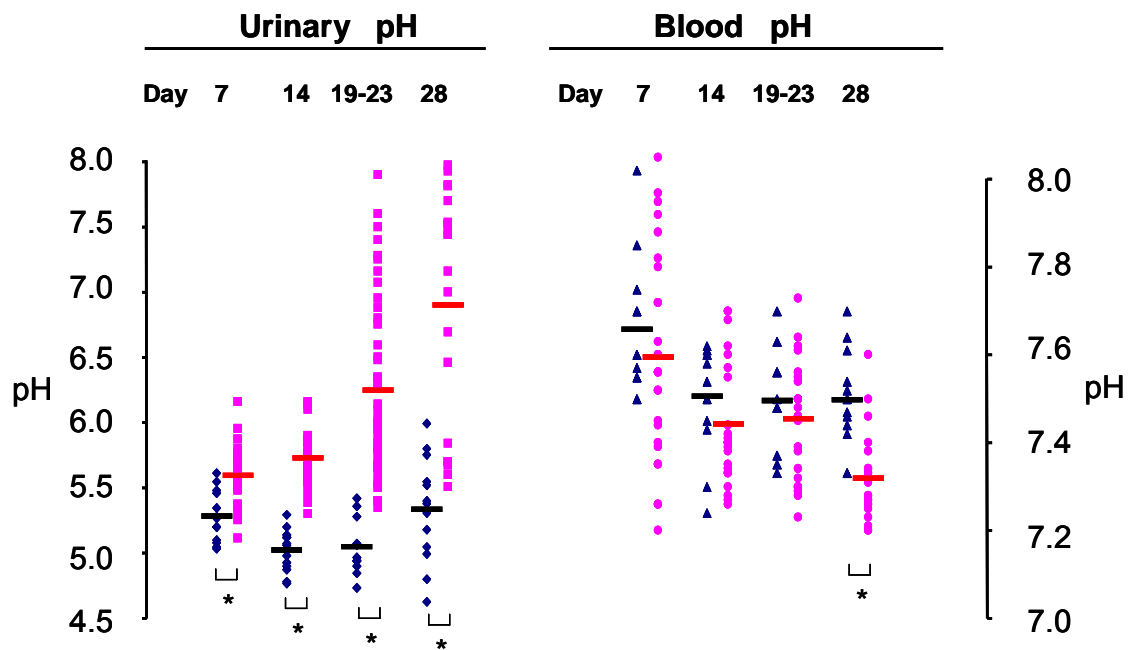


**Figure 8E**

## DISCUSSION

Chapters 2 and 3 summarize the work that I have performed on cell and mouse models of polycystic kidney disease generated and provided by our collaborator, Dr. Bradley Yoder. Our laboratory, in collaboration Dr. Mark Bevensee, have made rapid and substantive progress on the pathophysiological processes within these cell and mouse models as a consequence of a partial or complete loss in the apical membrane's primary and non-motile cilium.

To briefly summarize my results, I found an upregulation of ENaC-mediated  $\text{Na}^+$  absorption in cilium-deficient versus cilium-competent renal cortical collecting duct principal cell models derived from the  $\text{Tg737}^{orpK}$  mouse that have been developed and characterized in detail by Dr. Yoder's laboratory. The phenotype of the  $\text{Tg737}^{orpK}$  mouse seems to be consistent with the early onset and severe hypertension observed in ARPKD and significant hypertension that precedes the decline in renal function in ADPKD. During the course of this work, some of the NHE-selective amiloride analogs, e.g. EIPA and DMA, also inhibited the upregulated  $\text{Na}^+$  absorptive current observed in the cilium-deficient cell monolayers studied under open-circuit and short-circuit current conditions. In this light, I examined NHE function in cilium-deficient and cilium-competent cell monolayers by pH-sensitive BCECF imaging. I found a consistent and inappropriate expression of apical NHE function in these cilium-deficient models that was not observed in cilium-competent cell models or in wild-type principal cell models and has

not been described in the literature. From this novel observation, I also found overall upregulation in NHE function in these mutant cell models. Importantly, this *in vitro* pathophysiological phenotype was also present *in vivo* in conditional, kidney specific cilium knockout mice. These animals had consistently more acidic urine at weeks 1, 2, 3 and 4 of age and developed metabolic alkalosis at 4 weeks of age.

Figure 4. summarizes these findings. Upregulated NHE function in the apical membrane may also contribute to the development of hypertension in one or both forms of PKD. Acid-base transport dysregulation and defects in acid-base balance in PKD may have profound effects on kidney function and even more profound effects in the liver and pancreas which are also affected in the extra-renal manifestations of PKD.

## THE FUNDAMENTAL QUESTION

The following question is one that has been posed by countless investigators examining cilia biology and polycystic kidney disease and its related cystic disorders: *How does a loss of the primary cilium cause a dysregulation or change in a structural or functional endpoint in the cell?* My fundamental question is similar: *How does a loss of the primary cilium cause a dysregulation in apical membrane transport proteins in the cilium-deficient epithelial cell?* Several hypotheses presented below govern my future investigations regarding upregulation of ENaC and dysregulation and upregulation of NHEs in cilium-deficient cells. In the end, I will present a hypotheses where mislocalized apical NHE activity may fuel ENaC upregulation via two mechanisms that may be additive in triggering the profound  $\text{Na}^+$  hyperabsorption and resultant hypertension.

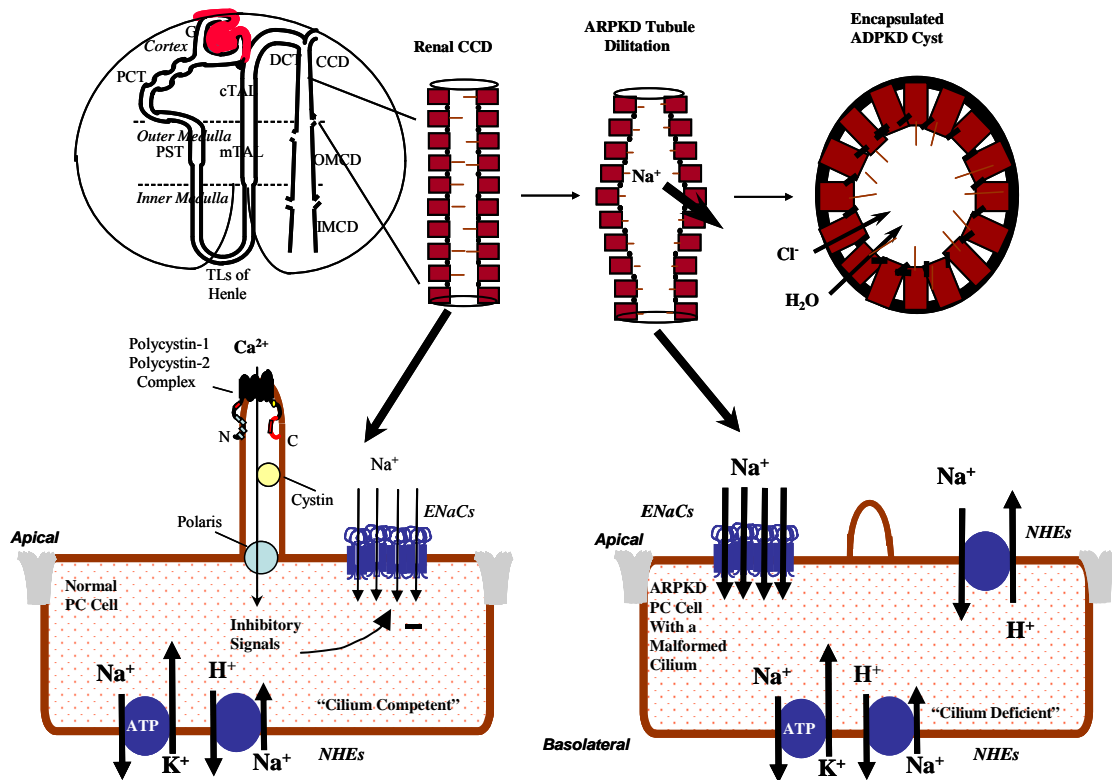


**Figure 4. Differences in Renal Tubule Re-Modeling in ARPKD versus ADPKD**

While the changes in transepithelial salt, acid-base and water transport are not fully appreciated in ARPKD pseudocystic epithelia versus ADPKD cystic epithelia versus normal or non-cystic epithelia, hypertension is a known and severe phenotype in both forms of PKD, especially ARPKD.

## HYPOTHESES

### *“Compensatory Upregulation” Hypothesis*

Figure 5. illustrates the concept that, without a primary central cilium in the apical or luminal membrane of CCD principal cells, the cell is not fully differentiated. The expression or elaboration of a cilium or cilia or villi or microvilli on the luminal surface of epithelial cells is widely thought to be the terminal step in epithelial cell differentiation and/or polarity (Refs. 2, 3, 276). In this light, apical and basolateral membrane proteins may not be appropriately expressed or localized. The cells themselves may have quality control mechanisms (heretofore unrecognized) that recognize when apical and basolateral expression is inappropriate or insufficient, signaling a need to overexpress membrane  $\text{Na}^+$  transporters such as ENaC channels and NHEs. In genomic analysis of whole kidney mRNA from multiple and different mouse models of ARPKD (Tg737<sup>orp</sup> and *cpk* mice versus littermate controls and on the same C57/Bl6 genetic background), Dr. Yoder's group found upregulation of several  $\text{Na}^+$ -dependent transporters (B.K. Yoder, privileged communication). As presented in the Future Directions, I have assessed whether individual or multiple ENaC subunits and/or NHE subtypes are upregulated at the mRNA level in cilium-deficient versus cilium-competent cells. At least one subunit for ENaC (the beta-ENaC subunit) and one for NHE (the NHE2 subtype) are upregulated at the mRNA level in cilium-deficient cells. Therefore, this mechanism may play a part in ENaC upregulation and NHE dysregulation observed in my studies.

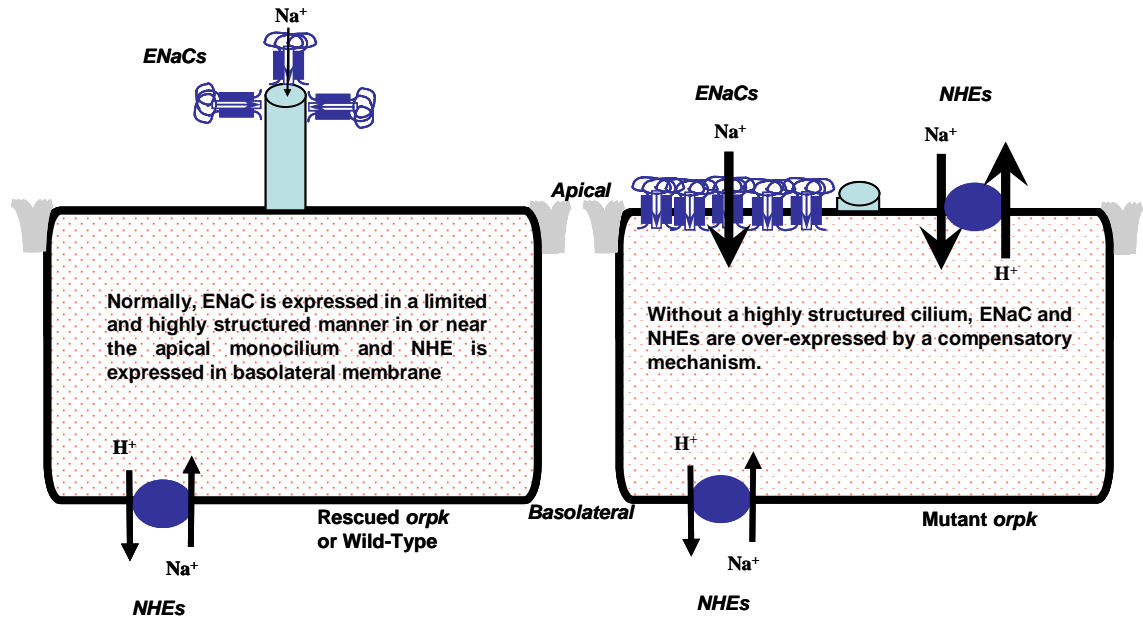


**Figure 5. Compensatory Overexpression and Redistribution**

Normally, ENaC and NHEs are expressed in a limited and highly structured manner in or near the apical monocilium. Without a highly structured cilium, ENaC and NHEs are over-expressed by a compensatory mechanism.

### *“Loss of Cilium-specific Signals” Hypothesis*

Figure 6 summarizes a mechanism that is more plausible to explain ENaC upregulation. However, this pathophysiological mechanism may also play a role in NHE dysregulation. An important caveat is that the same cellular mechanism may not hold for both ENaC upregulation and NHE dysregulation. With this hypothesis, cilium-specific signals are lost along with the cilium. These signals may emanate from the monocilium as intracellular signal transduction cascades. Alternatively and in addition, the monocilium may also influence secretion of autocrine and paracrine signaling ligands that are released into the lumen of the CCD and act on cell surface receptors on the same cell or on neighboring cells. My colleague, Michael Hovater, published a recent paper (Ref. 273) and mini-review (Ref. 277) assessing the secretion and signaling of purinergic ligands in the luminal microenvironment of the nephron of the kidney. My lab has also examined this signaling within the lumen of “pseudocysts” and encapsulated cysts in PKD (Ref. 278).

The paper by Hovater described the finding that basal ATP secretion is not different between cilium-deficient and cilium-competent cell monolayers grown and studied as polarized cell monolayers on filter supports. However, ATP secretion in response to calcium-driven, mechanically-induced, and hypotonic cell swelling-triggered signals was impaired in cilium-deficient cell monolayers versus cilium-competent cell monolayers. Purinergic ligands and signaling, via both P2X receptor  $\text{Ca}^{2+}$  entry channels (Ref. 279) and P2Y G protein-coupled receptors (Ref. 280), inhibits ENaC (Ref. 281) and may modulate NHEs (Refs. 282, 283) in epithelial cells from the kidney and other tissues. Because secretion of purinergic ligands like ATP and its metabolites is impaired



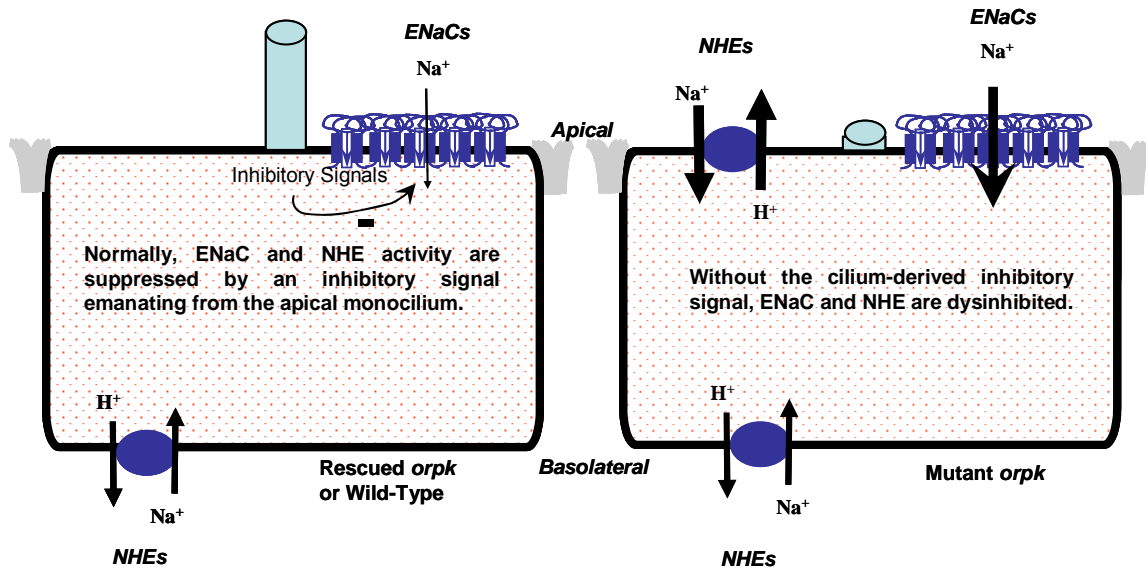


**Figure 6. Dysregulation due to Loss of Cilium-derived Signal**

Normally, ENaC and NHE activity are suppressed by an inhibitory signal emanating from the apical monocilium. Without the cilium-derived inhibitory signal, ENaC and NHE are dysinhibited.

in cilium-deficient cells, there may be a lack of a purinergic inhibitor that tonically attenuates  $\text{Na}^+$  absorption across principal cells in the CCD on a minute-to-minute basis. A future direction, that has become imperative as a result of this work, is the localization of key P2X and P2Y receptors on or near the monocilium. The  $\text{Ca}^{2+}$  entry and/or  $\text{Ca}^{2+}$  release triggered by P2X and P2Y receptors, respectively, as well as products of phospholipase-driven phosphoinositide turnover all attenuate ENaC and NHEs.

Secreted molecules that act as autocrine and paracrine ligands to affect ENaC and NHEs via receptors and/or affect ENaC and NHEs directly are not limited solely to purinergic ligands. There are many candidates for such local regulators that may be present at or near the apical surface of the renal collecting duct. I discuss a few candidates below that could play important roles in this pathophysiology.

Growth factors and their receptors are dysregulated in PKD. The growth factor signaling cascades in epithelial cells are hyperactive in PKD. Dominant negative EGF receptor mice were crossbred with  $\text{Tg737}^{orp/k}$  mice in an effort to probe the importance of this signaling cascade in PKD. This maneuver led to the attenuation of cystic disease in this mouse model. I did not include growth factors in my defined culture medium because of the hyperactivity of this cascade and its effect on cell proliferation. Inclusion of EGF in another study of ENaC in collecting duct epithelial cells derived from *bpk* mice played a prominent role in an observation that ENaC activity was reduced in cystic cells versus non-cystic cells. This was opposite to my results, to work of Satlin and coworkers in human ARPKD cells versus relevant controls, and to the hypertensive phenotype observed in human ARPKD patients. I maintain that EGF and other growth factors are inhibitors of ENaC and that this inhibition was stronger in cystic cells due to the

hyperactivity of the EGF receptor cascade. Indeed, unpublished observations from Michael Hovater's work in our laboratory showed that EGF was a strong inhibitor of ENaC currents in both mutant and rescued cell monolayers (Michael Hovater and Erik Schwiebert, unpublished observations). The same was true for TGFbeta. Intriguingly, however, these growth factors were only effective on the basolateral surface, despite reports that the receptors for growth factors are mislocalized to the apical surface in some models of PKD. I will continue to screen growth factors and their role in the ENaC and NHE dysregulation phenotypes.

It is also possible that there are apically secreted factors that stimulate apical ENaCs and NHEs and are more prevalent or more active in cilium-deficient preparations versus cilium-competent preparations. Defining the autacoids that are stimulatory versus inhibitory in mutant and rescued cell models of collecting duct principal cells is not a trivial enterprise. I continue to have an intriguing observation that remains critical to the observation of the ENaC upregulation and NHE dysregulation. These cell models appear to condition their apical medium to fuel ENaC activity and the inappropriate appearance of an apical NHE. Replacement of the apical medium makes amiloride-sensitive absorptive ENaC  $\text{Na}^+$  current disappear, only to re-appear 5-12 hours later. This result was presented in ENaC paper above. Basolateral medium replacement led to a slight augmentation in the currents likely due to addition of fresh supplemental hormones present in the medium such as insulin. This led me to perform Ussing chamber experiments in defined medium (without serum) because this conditioned medium is washed away in standard Ussing chamber studies. This led to complete disappearance of the short-circuit currents due to ENaC under basal conditions. Conditioned medium on

both sides of the Ussing chamber (devoid of serum) maintained ENaC current sufficiently to compare the currents in cilium-deficient versus cilium-competent cell monolayers. ENaC  $\text{Na}^+$  current is more robust when the apical medium volume is limited to a volume that is adequate enough to keep the monolayer covered. Limited experiments where the mutant conditioned medium has been collected and added to the rescued cell monolayers resulted in the transient stimulation of ENaC currents in the rescued cell monolayers. Intracellular, membrane-bound and secreted proteases have been shown to stimulate ENaC (Refs. 284-286). This is thought to occur via cleavage of the extracellular domain of ENaC subunits (Ref. 287). As such, secreted proteases may play an important role in this “conditioned medium” maintenance phenotype. Indeed, in ENaC paper, aprotinin and leupeptin inhibited ENaC  $\text{Na}^+$  currents under open-circuit and short-circuit current conditions. Trypsin stimulated these currents, although briefly and transiently. These results led me to conclude that there was already robust protease activity in these cell monolayers systems endogenously, fueling the system. I will continue to examine the role of proteases in my system as well as any possible role for protease-activated receptors (PARs), a type of G protein-coupled receptor, in this pathophysiology. Proteases and PARs and their possible regulation of NHEs have not been addressed. Purinergic and protease regulation of NHEs is a high priority for future experiments.

#### *“Dysregulation of the Apical Cortical Cytoskeleton” Hypothesis*

Figure 7 presents a hypothesis that attempts to explain the ENaC upregulation and apical NHE dysregulation from the point of view that loss of the cilium results in a disrupted cytoskeleton. The actin cytoskeleton is critical in maintaining cell polarity and

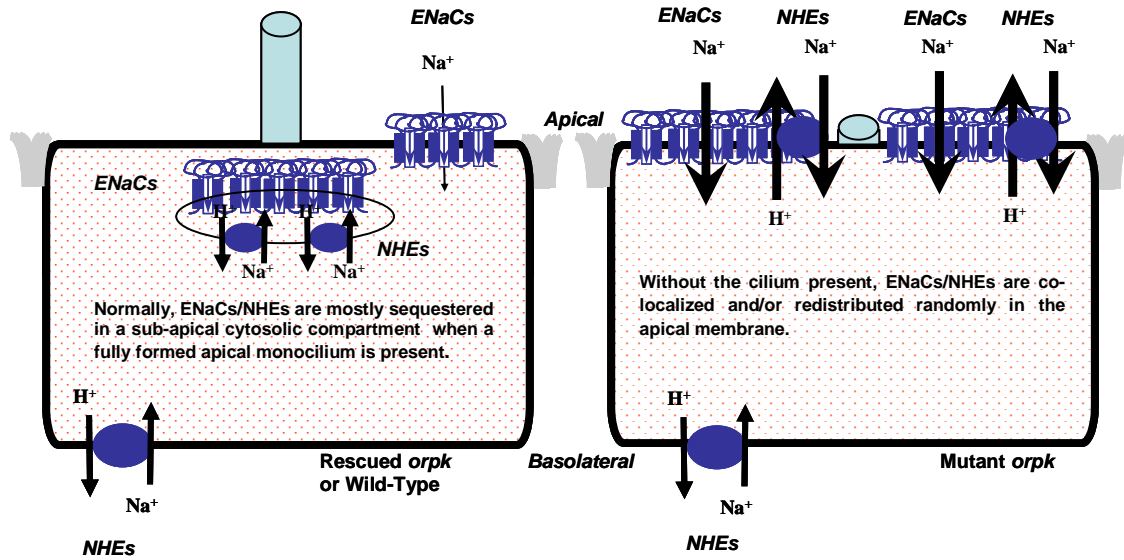


**Figure 7. Dysregulation due to a Change in Localization**

Normally, ENaCs/NHEs are mostly sequestered in a sub-apical cytosolic compartment when a fully formed apical monocilium is present. Without the cilium present, ENaCs/NHEs are co-localized and/or redistributed randomly in the apical membrane.

in the distribution and stability of membrane proteins (Refs. 2, 3, 276). The role of actin in cystic diseases was suggested by Wilson *et al.* (Ref. 288) who demonstrated that actin and polycystin-1 are part of a multiprotein complex involved in cell-cell and cell-matrix interactions. Interaction between alpha-actinin and a defective polycystin-2 may play an important role in cell adhesion and proliferation abnormalities found in ADPKD (Ref. 289). Abnormalities in actin cytoskeleton organization were found in IMCD cells where expression of the PKHD1 gene and fibrocystin/polyductin protein was silenced (Ref. 290). An increase in globular versus filamentous actin was found in principal cells from the Tg737<sup>orpk</sup> mouse (B Siroky and P. Darwin Bell, unpublished observations), indicating that the actin cytoskeleton is disrupted in cilium-deficient cells versus cilium-competent cells. The polycystin-2 protein expression pattern of localization is changed in the Tg737<sup>orpk</sup> mouse (Ref. 291).

A fraction of newly synthesized plasma membrane proteins may escape from sorting processes within the trans-Golgi network and be delivered to the incorrect membrane domain in normal kidney epithelial cells (Ref. 276). The misplaced proteins may be internalized and then sent via the endocytic/transcytotic pathway to the correct plasma membrane domain. Upon arrival to the correct location, other molecules (e.g. spectrin and E-cadherin) stabilize these misplaced proteins, linking them to the cytoskeleton (Ref. 276). A possible mis-sorting process, dysfunctional endocytosis/transcytosis processes and/or aberrant cytoskeletal interactions, due to a lost or dysfunctional cytoskeleton may explain the mislocalized proteins found in PKD (apical Na/K pump, apical-EGF receptor, basolateral Na/K/2Cl co-transporter). However, this process seems to be selective and is probably due to a specialized transport

mechanism that remains to be elucidated (Ref. 292). Abnormalities in E-cadherin localization (Ref. 292) and re-distribution of  $\beta$ -spectrin (Ref. 293) found in cultured ADPKD cells may explain why the mis-targeted proteins become destabilized and are present in the wrong membrane domain.

ENaC and several NHEs have been shown to interact with cytoskeleton (Refs. 28, 31, 136, 178). Upregulated ENaC may be due to abnormalities in cytoskeletal molecules that normally are required to remove ENaC and/or to mediate ENaC activity and expression at the apical membrane surface of the epithelial cell (e.g. clathrin-mediated endocytosis that help to remove ENaC from the cell surface. An inappropriate apical NHE expression may be explained by abnormalities in trafficking processes (e.g. vesicle transport, ER-Golgi trafficking) or internalization during the typical “re-direction” process. This explanation is most plausible for NHE1 that is normally expressed on the basolateral membrane or for NHE6 and NHE9 that are shown to be expressed transiently on the apical membrane during the maturation process (Ref. 105). NHE3 requires an intact cytoskeleton for its proper function (Ref. 178). It will be interesting to assess NHE3 function in the proximal tubule or in proximal tubule cells from mice shown to have a disrupted primary cilium and/or actin cytoskeleton. NHE5 is shown to be stimulated by actin disruption; however, it is highly restricted to neuronal tissue and it is not present in polarized kidney epithelial cells (Ref. 294).

#### *Favored Hypothesis to Explain Upregulation of ENaC Activity*

Figure 8. presents the hypothesis that I favor. It integrates the data of Michael Hovater in our laboratory with the data presented in Chapter 2 documenting ENaC

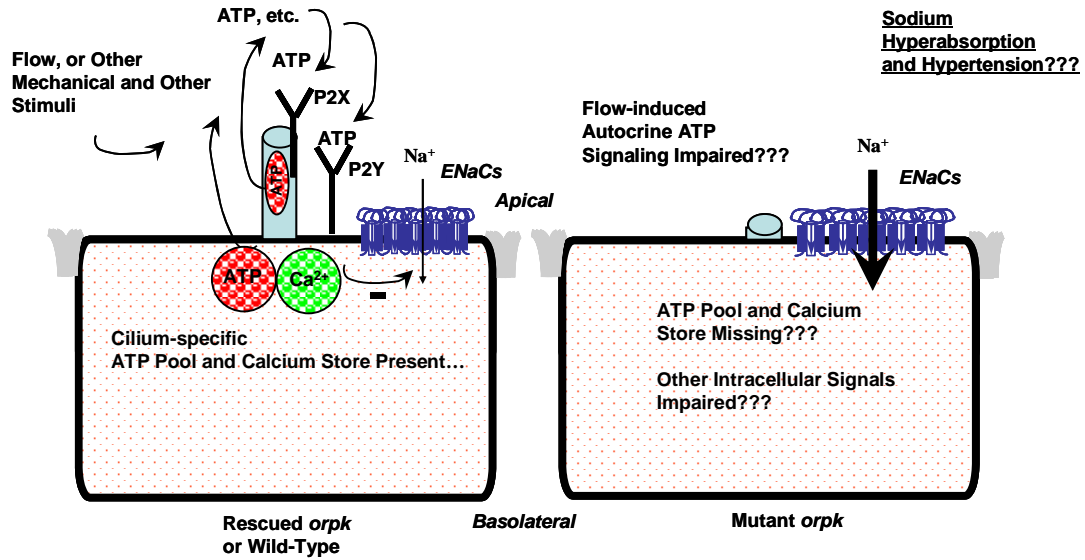


**Figure 8. The ENaC Upregulation Problem**

Wild type cells or rescued *orpk* cells with intact cilia on the apical membrane are characterized with defined ATP pools and intracellular  $\text{Ca}^{2+}$  stores which maintains ENaC inhibition. In the cilium deficient cell, these ATP pools and intracellular  $\text{Ca}^{2+}$  may be missing or undefined leading to upregulation of ENaC.



upregulation. Stimulation of ATP secretion by mechanical perturbations or other means is more robust in cilium-competent cells than in cilium-deficient cells. I hypothesize that local autocrine or paracrine purinergic signaling may be a tonic inhibitor of ENaC-mediated  $\text{Na}^+$  absorption on a minute-to-minute basis, only superceded by endocrine stimuli such as the renin-angiotensin-aldosterone system (RAS), glucocorticoids, and vasopressin. When purinergic and other cilium-driven inhibitory signals are lost, ENaC becomes upregulated or dysregulated, leading to  $\text{Na}^+$  hyperabsorption and hypertension.

#### *Favored Hypothesis to Explain NHE Dysregulation*

Figure 9. is based upon the work of Ullrich Hopfer and co-workers from the proximal tubule which has examined angiotensin receptor localization at or near the brush border in primary cilium-deficient versus primary cilium-competent cells (Ref. 196). In monolayers grown at 33 °C, there is a brush border without a primary cilium and angiotensin receptors are replete all through the brush border membrane. At 39°C, there is a monocilium present in the center of the brush border that extends beyond the brush border surface and the receptors are localized in a sub-cilium vesicle or endosome. Similarly, it is possible that NHE or NHEs are sequestered in sub-apical vesicles in close proximity of the cilium but excluded from the apical membrane of collecting duct principal cells of the distal nephron under normal or cilium-competent conditions. These vesicles may also be stabilized by the multi-protein complex found near the basal body or centrosome. In the absence of normal length cilia with a well-built system of scaffolds, the organization of proteins beneath this structure may dissipate in some respect, changing the normal interdependency between these molecules. This dysregulation may

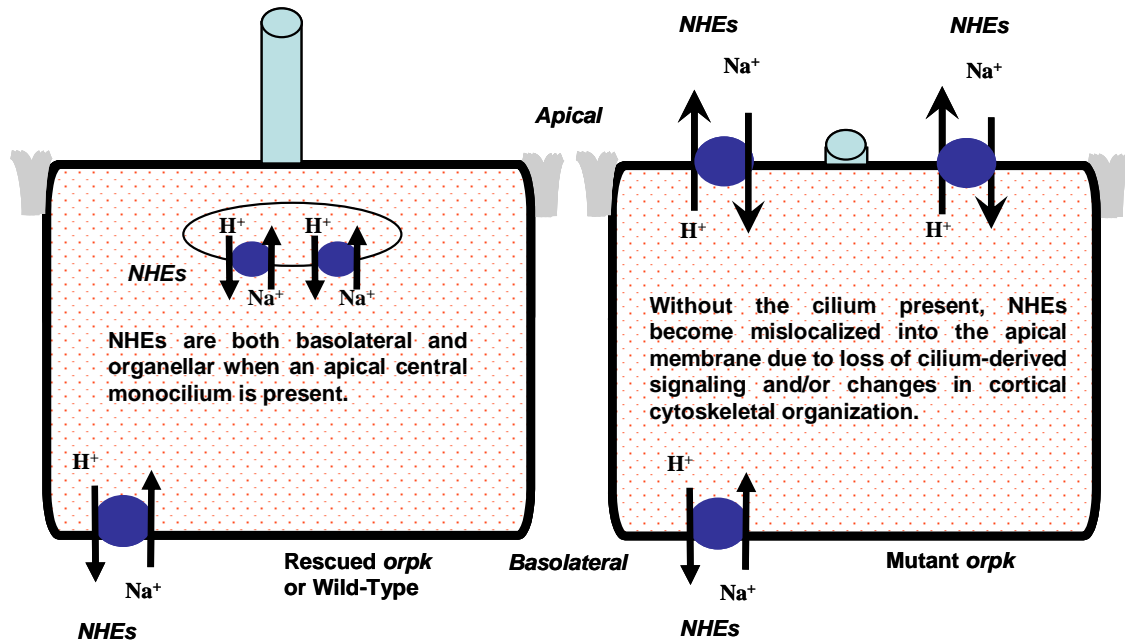


**Figure 9. The Apical NHE Problem**

Wild type cells or rescued *orpk* cells may express NHE's in the endosomes, sub apical vessicles along with the normal basolateral expression. In cilium deficient cells, the basal ciliary foundation is disorganized and without proper interaction with the sub apical vessicles, the vessicles may fuse with apical membrane.

affect the stability of the vesicles that are sequestered normally at this location. Little is known about the specific localization of intracellular NHEs and how cilia, the basal body and the cytoskeleton may change their expression on the apical surface.

An additional study, unrelated to PKD, corroborates this. NHE3 was found to be localized in the center of the apical membrane of polarized renal proximal tubule cells in the opossum kidney (Ref. 205). Modifications in the ultrafiltrate composition are sensed by the cilium that may send signals to the base of the cilium for docked vesicles to be released. Once the cilium is missing, those vesicles may become unstable, and they may be released to the apical membrane without proper regulation. This concept becomes more important in cells that normally do not express NHE on the apical surface (PC of the collecting duct, IMCD), because it may confer functional properties which are detrimental to health. Subtle modifications in the ciliary apparatus resulting in overexpressed NHE3 on the apical surface of the proximal tubule may also account for sodium hyperabsorption and onset of hypertension. However, this concept may become more valuable later when proximal tubule cell models with or without cilia impairment are available for study.

*Final Hypothesis: Can Inappropriate Apical Expression of NHEs Stimulate ENaC Hyperactivity and Na<sup>+</sup> Hyperabsorption in Cilium-deficient Principal Cells?*

In my thinking, considerable importance has been given to how an apical mislocalized NHE may influence ENaC activity. This logic is illustrated in Figure 10. Although there are no descriptions of normal co-localization of ENaC and NHE along the nephron, there is co-localization in epithelial cells from other tissues such as the distal

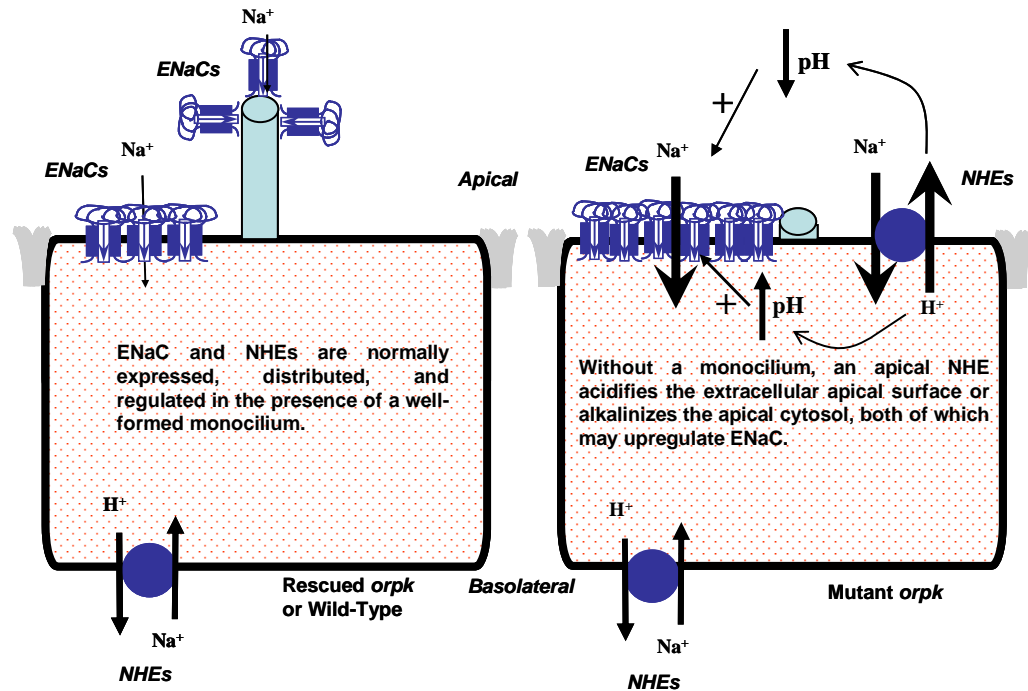


**Figure 10. The Apical NHE-ENaC Crosstalk Problem**

Mislocalized/inappropriate expression of an apical NHE in the cilium deficient cell upregulates ENaC by one action with two simultaneous effects: an extracellular acidification which is reported to stimulate alpha-ENaC and an intracellular alkalinization which is reported to stimulate delta-ENaC.

colon and, to a lesser degree, in the small intestine where colostomized animals show enhanced ENaC expression and function (Refs. 295, 296). Also, it should be noted that, in the respiratory epithelial cells from normal subjects and CF patients, there is primarily apical NHE activity (D. Olteanu, M.O. Bevensee, and E.M. Schwiebert, unpublished observations). Apical NHE is typically present in the proximal nephron, where it contributes to not only maintaining intracellular pH but also to  $\text{Na}^+$  and bicarbonate absorption (proximal tubule, thick ascending limb and distal tubule). ENaC has a more restricted function dedicated to fine tuning of  $\text{Na}^+$  reabsorption. What happens with ENaC activity/expression if a second  $\text{Na}^+$  reabsorption mechanism is present/mislocalized to the same apical membrane domain? One answer would be that ENaC will be shut off as a compensatory mechanism. Our first study shows actually that ENaC activity is upregulated in the same cell where NHE is present on the apical side. Chalfant *et al.* (Ref. 32) reported that intracellular alkalinization stimulates ENaC current and that this effect is mediated by the  $\alpha$ -ENaC subunit. An active apical NHE may exchange intracellular protons for extracellular  $\text{Na}^+$ , leading to an alkalinized environment just beneath the apical membrane in the vicinity of ENaC. I have preliminary data showing the presence of  $\alpha$ -ENaC subunit on RT-PCR in our cells. So I have a viable starting point, and I intend to test this hypothesis further (more will be discussed in Future Directions below).

Yamamura *et al.* (Ref. 33) reported that the ENaC channel, formed by monomeric human  $\delta$ -ENaC expressed in *Xenopus* oocytes, is activated by extracellular acidification. The apical NHE exchanger may create an extracellular acidic environment close to a  $\delta$ -ENaC-based heteromultimer to stimulate these absorptive epithelial  $\text{Na}^+$  channels (a

caveat here is that a mouse  $\delta$ ENaC gene has not been reported yet). The whole picture, where an inappropriate apical NHE may upregulate ENaC activity both by intracellular alkalization and extracellular acidification at the same time, is strengthened markedly by our *in vivo* measurements in mice (Chapter 3) and by preliminary *in vitro* observations where we measured pH in apical media of cilium-deficient and cilium-competent monolayers (D. Olteanu and E.M. Schwiebert, unpublished observations). Moreover, we have preliminary evidence that there is profound fluid absorption *in vitro* from mutant cilium-deficient cell monolayers versus rescued cilium-competent cell monolayers. In mutant monolayers left unfed for several days, the apical medium disappears and the monolayers are hydrated by the basolateral medium but devoid of apical medium (D. Olteanu and E.M. Schwiebert, unpublished observations). It is my intention to follow up on these observations while performing metabolic measurements of urinary and plasma  $\text{Na}^+$  (together with blood pressure measurements in the appropriate mouse models) in my postdoctoral work.

## FUTURE DIRECTIONS

### SUMMARY OF APPROACH

An important caveat to the above discussion of the different hypotheses is that more than one of them could contribute to the cellular pathophysiology that I have observed in cilium-deficient cell models to date. To begin to address the hypotheses outlined above, I first needed to undertake an inventory of the ENaC subunits and NHE subtypes that may be expressed in cilium-deficient and cilium-competent cell monolayers. With knowledge of the ENaC subunits and NHE subtypes expressed in my model systems, I can test the hypotheses above. Given that there have been notorious problems with raising antibodies to ENaC subunits and NHE isoforms, my initial work presented below has begun by with RT-PCR for  $\alpha\beta\gamma$ -ENaC and NHEs 1-10.

#### *RT-PCR Analysis of ENaC mRNA expression in our Cell Models*

Cells were seeded on 24 mm diameter filter supports (Corning Incorporated, Corning NY) and grown at 37 °C. Two weeks after the cells reached confluence and a high-resistance cell monolayer was formed, the membrane with the monolayer was cut out from the filter and used for RNA extraction with PureLink Micro-to-Midi Total RNA Purification System (Invitrogen, Carlsbad, CA). DNase I was also purchased from

Invitrogen. cDNA was synthesized using an iScript cDNA Synthesis Kit (Bio-Rad, Hercules, CA). Taq DNA Polymerase was obtained from Roche (Indianapolis, IN).

Primers for  $\alpha$ -ENaC (forward, 5'-AAG CCC AAG GGT GTA GAG T-3', and reverse, 5'-GAT GAG CCG AAC CAC AGG-3', expected product is 374 bp) and  $\delta$ -ENaC (forward, 5'-CCC AGC CAT AAA CTC-3', and reverse, 5'-ATC TCC ACC ATC AGC-3', expected product is 282 bp) were derived from a previous study (Ref. 297). However, there is no mouse  $\delta$ -ENaC nucleotide or protein complete sequence reported in any data base (Ref. 297). These authors used the human  $\delta$ -ENaC as a template to search the mouse genome data base (Ref. 297). Primers for  $\beta$ -ENaC were designed in our laboratory (forward, 5'-GAC CAC ATG ATC CGT AAC TG-3', and reverse, 5'-GCT TGA CAA TAC CCT TCC TG-3', expected product is 307 bp). Primers for  $\gamma$ -ENaC (forward 5'-CTC GTC TTC TCT TTC TAC AC-3', and reverse, 5'-GCA GAA TAG CTC ATG TTG-3', expected product is 557 bp) were derived from a study assessing ENaC expression in rat colon (Ref. 298) and were modified for the mouse sequence. All the products were sequenced.

With these methods and armed with these primers, I have begun amplifications of mRNA from cilium-deficient and cilium-competent cell monolayers. I am still defining the best RT-PCR conditions for  $\alpha$ -ENaC and  $\gamma$ -ENaC. Early results show that  $\alpha$ -ENaC and  $\gamma$ -ENaC are expressed in both the mutant and rescued cells. Preliminary data also suggest that the  $\beta$ -ENaC transcript is overexpressed in cilium-deficient cell monolayers when compared to cilium-competent cell monolayers (Figure 11). I have verified all ENaC PCR products by cDNA sequencing. I hope to detect  $\delta$ -ENaC in our cell models and perform semi-quantitative and real-time RT-PCR on the ENaC subunits that appear



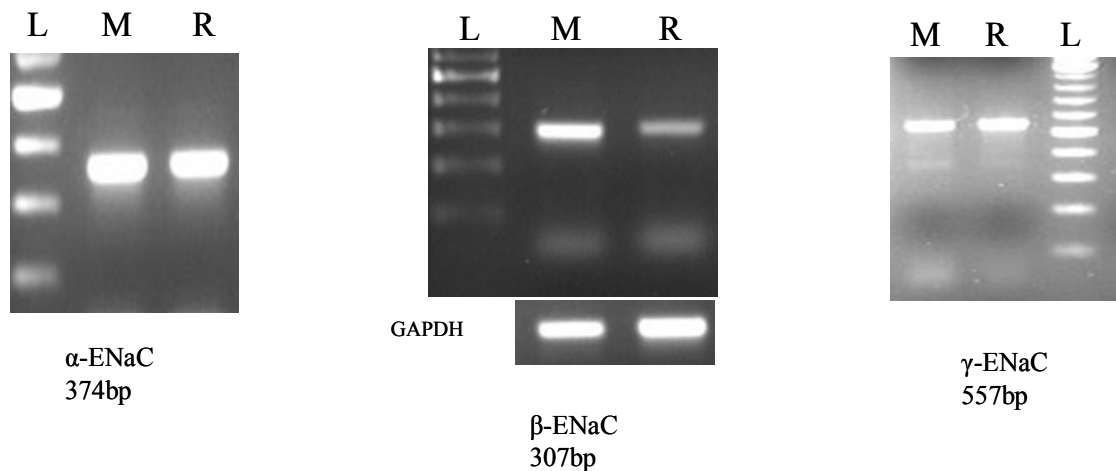


**Figure 11. ENaC RT-PCR Products**

In order to determine which ENaC subunits are expressed in our cell lines, I began by testing for different isoforms using RT-PCR. Preliminary results showed that alpha, beta and gamma isoforms are present in our cells, moreover that the beta ENaC transcript is overexpressed in cilium deficient cells. All products were sequenced. Work is being continued to refine the conditions for alpha and gamma ENaC. (L=Ladder) (M=Mutant/Cilium deficient cells) (R=Rescued/Cilium competent cells)

differentially expressed in mutant versus rescued cell monolayers, such as  $\beta$ -ENaC. I hope to complement this work using antibodies directed against endogenous ENaC protein subunits; however, these experiments have proved exceedingly difficult.

#### *RT-PCR Analysis of NHE Isoforms*

I performed RT-PCR analysis on all isoforms of the NHE gene superfamily to provide comprehensive examination of the NHE isoforms that are expressed in mutant and rescued cells. This complete analysis is essential, because mutant or “cystic” kidney epithelial cells have an enhanced rate of proliferation and can show re-programming in their gene expression profiles (Ref. 299). Primers for NHE 1, NHE 3 (set 1) and NHE 4 are derived from a study of NHE activity in an M-1 CCD cell line (Ref. 300). NHE3 isoform mRNA was not reported to be a transcript in principal cells of CCD. However, in order to be comprehensive (in case mutant cells express NHE3), I designed multiple primer sets to mouse NHE3. The second set of NHE3 primers were derived from a study of NHEs in colonic crypts (Ref. 301). These primers were adjusted for the mouse sequence. I also designed other 2 sets of primers for NHE3 in our laboratory. Results with all sets of primers were negative; NHE3 is not expressed in mutant or rescued cell monolayers at the mRNA level. Primers for NHE6, NHE7, NHE8, and NHE9 were derived from a study by Gillespie and coworkers from hair cells of the inner ear (Ref. 302). Their sizes and sequences were corrected for mouse. NHE2, NHE5 and NHE10 primer pairs were designed in our laboratory. I have positive RT-PCR results for NHE2 and NHE5, but I could not test the efficiency of NHE10 primers because they were not

tested with a positive control mRNA sample. For a listing of the NHE primers used, please refer to Table 1 below.

All NHE PCR products were sequenced. I have a total of 7 NHE isoforms expressed in mutant and rescued cell monolayers based upon my analysis. They are NHE1, NHE2, NHE4, and NHE5 through 8 (Figure 12). The isoforms expressed are both membrane-resident and organellar NHE isoforms, preliminary results show that, in cilium-deficient cells, transcription of NHE2 gene has a higher level of expression than in cilium-competent cells. However, this work is still in progress. Taken together, these results show that mouse principal cells from the CCD appear to be enriched with NHE subtypes and suggest that principal cells of the collecting duct may cooperate with intercalated cells for a higher order of acid-base balance regulation than heretofore recognized in renal physiology.

Mouse NHE primers	Sequence (5'-3')	Chromosome	Exon	Predicted Size (bp)
NHE1	Sense TCTGCCGTCTCAACTGTCTCTA Antisense CCCTTCAACTCCTCATTCACCA	4	8 12	422
NHE2	Sense GCGTTTACCACCCGTTTCAC Antisense AGACGAAAGCCCGAGTTCAC	1	3 4	295
NHE3	Sense GGAACAGAGCGGAGGAGCAT Antisense GAAGTTGTGTGCCAGATTCTC	13	12 14	321
first set	Sense CCACACACTGCAACAGTACC Antisense ATAGGCAGTTTCCCATTAGG	13	12 14	252
NHE3	Sense CTGCTGAATGATGCAGTGAC Antisense AGGAAGGCGAAGATAACACC	13	3 5	161
third set	Sense ACTTCATGCCCAATCGACTC Antisense TTCAGTTCACCCATCAAGCC	13	2 2&3	139
NHE4	Sense GGCTGGGATTGAAGATGTATGT Antisense GCTGGCTGAGGATTGCTGTAA	1	7 11	501
NHE5	Sense CTGGGATGTGTACTACAGACTC Antisense TCAACAGGTTGGTGACAGAG	8	10 11&12	145
NHE6	Sense TCTCTTCGGGGAAAGTGCCTCAAT Antisense TAACGTCAAAGGTGGCTGTTGTC	X	6 7	104
NHE7	Sense GCCCCATTTTCATCATCGGTG (crct) Antisense CCAATCTTATGCCTTCTGCCCA	X	10 11	106
NHE8	Sense GCCACTATTGCCGATTTTCAACGC Antisense TTGCCACCCACTGACATCTGACATA	2	8 9	156
NHE9	Sense TGAGTTCGCCGATGCTGGAGAC Antisense GGAATCTTCTGCTTTCTGCCCAG	9	8 11	366
NHE10	Sense AAAGGTCAAAACCACACCTG Antisense CAAGTCCGATTTTITGCCAC	16	21 22	261

**Table 1. NHE Primers**

To define which NHE subtypes may be expressed in our cells, we tested for all 10 known NHE isoforms. Primers sequences, chromosomal location, exons, and predicted size are shown.

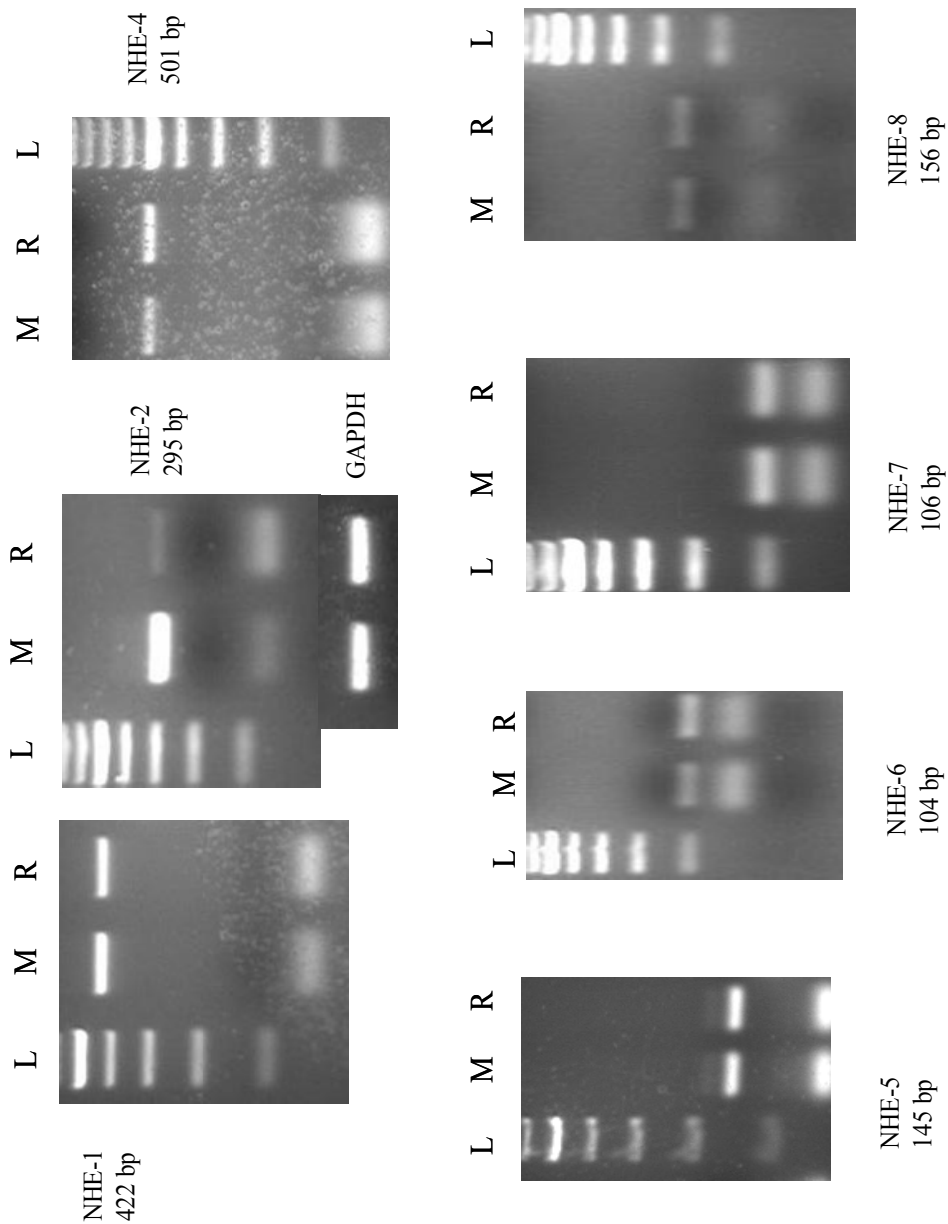


**Figure 12. NHE RT-PCR Products**

I have found that a total of 7 NHE isoforms can be detected in our mutant and rescued cell monolayers based upon RT-PCR analysis. I have found that NHE-2 transcript is upregulated in mutant/cilium deficient cells. All products were sequenced. (L=Ladder) (M=Mutant/Cilium deficient cells) (R=Rescued/Cilium competent cells)

## FUTURE LINES OF INVESTIGATION

### *Which NHEs are mis-targeted and apical?*

Taking into account that there are at least 7 isoforms present in our cells, it is hard to identify which NHEs are mislocalized on the apical side because most of these isoforms, especially NHE5 through 8, have yet to be characterized thoroughly. Pharmacological data suggest that one or more NHEs with relatively high affinity for selective inhibitors may be mislocalized to the apical surface. I have attempted to detect which NHE proteins are expressed in our cells, but commercial antibodies were not selective and provided false positive results. Because I know which NHE subtype transcripts are more likely to be expressed in our cells and because I already have a large body of functional experiments, an elegant experiment would be to test the apical/basolateral NHE activities in cells where expression of a specific NHE isoform is inhibited. I will use siRNA constructs specific designed for each prominent isoform to “knockdown” or diminish their expression. I will then test both mutant and rescued cell monolayers for changes in NHE activities. Another experiment would be to test control cell monolayers and mutant and rescued cell monolayers transfected with siRNA in hypertonic media. NHE1 and 4 are known to be acutely stimulated by hypertonicity, whereas NHE3 and NHE5 are inhibited. Other experimental maneuvers will also be designed and performed in the absence and presence of siRNA “knockdown” of specific NHE isoforms to define more specifically which NHE subtypes are most prominent.

*Do apical and basolateral NHEs engage in crosstalk or feed each other's activity in the mutant cells?*

A compelling experiment would be to test if inhibition of apical NHEs would influence the activity of the basolateral NHE and vice versa. In the same experiment, I can compare the rate of intracellular acidification due to inhibition of basolateral NHE in the presence or in the absence of an NHE inhibitor on the apical side. Theoretically, the rate of acidification in the absence of apical inhibitor should be lower than the rate of acidification in the presence of inhibitor. That is because, if it is not inhibited, apical NHE may contribute to acid extrusion and may attenuate the intracellular acidification slope. In other words, inhibition of the NHE function in one membrane domain should stimulate NHE function on the opposite membrane by a compensatory mechanism. This mechanism is based on the fact that inhibition of NHE will decrease the  $\text{pH}_i$  by  $\text{H}^+$  accumulation and will also decrease intracellular  $\text{Na}^+$ . However, in a similar experiment done by Good *et al.* (Ref. 141), it was suggested that, in rat medullary thick ascending limb, inhibition of basolateral NHE activity results subsequently in the inhibition of an apical membrane NHE.

*Positive and negative regulators of ENaCs and NHEs influenced by the cilium: Purinergic and protease regulation?*

I will test the effect of protease inhibitors (aprotinin, leupeptin), ATP scavengers (apyrase, hexokinase), and ATP receptor antagonists (suramin, PPADS) in a standard experimental preparation to determine if endogenous secretion of proteases and/or ATP as extracellular stimuli affect NHE function in either or both membranes. I also need to

perform open-circuit experiments to assess effects on amiloride-sensitive transepithelial voltage. These studies will be complemented by adding exogenous proteases and purinergic ligands if the scavenging/inhibition/antagonism studies are fruitful.

*Extracellular apical acidification and/or intracellular alkalinization upregulate amiloride-sensitive ENaC currents.*

Preliminary observations of ENaC current measurements (once filters were taken out of the incubator) showed that, once the apical pH became more alkaline due to CO<sub>2</sub> evaporation, the ENaC current decreased markedly. I wish to increase apical acidification by adding H<sup>+</sup> versus other acids to determine whether it is protons that specifically activate ENaCs or whether it is acidic pH. There is a subfamily of acid-sensing ion channels (ASICs) in the ENaC superfamily of cation channels in which protons modulate channel function. Such regulation has been suggested for  $\delta$ -ENaC (Ref. 33). P2X receptor channels have similar topology to ENaCs and ASICs and are modulated by extracellular pH as well (Ref. 303).

I will also do an “ammonium chloride” pre-pulse maneuver to alter pH<sub>i</sub>. I will measure ENaC current across monolayers in the absence and presence of 20 mM NH<sub>4</sub>Cl to both sides. I will immediately measure the transepithelial voltage. Based on the fact that  $\alpha$ -ENaC is stimulated by intracellular alkalinization, I would expect to see an increase in amiloride-sensitive current, followed shortly by a slow decrease given the time course of NH<sub>3</sub>/NH<sub>4</sub><sup>+</sup>-induced pH<sub>i</sub> changes.



*Upregulation of ENaCs and NHEs: Metabolic and blood pressure measurements that confirm hypertension in these animal models.*

In order to measure blood pressure in mice, I will focus on the conditional cilium-knockout mouse models developed by Dr. Yoder. Tg737<sup>orpk</sup> mice and Hoxb7-Cre mice are too small to study and cysts develop quite fast. A careful interpretation of blood pressure measurement would have to be made. Blood pressure is affected rapidly once the kidney function is destroyed. Also, large cysts in kidneys without renal failure can produce hypertension due to compression, diminish TG filtrate and secondary activation of RAS.

I will first study normal mature wild-type mice that are not treated with tamoxifen, and I would implant the blood telemetry probe. I will wait for a few days to allow the mice to recover from surgery as well as to be sure that the mouse has reached equilibrium in terms of electrolytes. Then, I will begin to measure blood pressure for several days as a base line. Once completed, tamoxifen will be added in the drinking water. Blood pressure will be measured constantly. I will then remove tamoxifen from the drinking water and assess blood pressure. I would optimize our protocol on wild-type mice. Then, in mice of large enough size that have Cre-Lox conditional cilium “knockout” genetics, I would repeat this protocol on mutant mice to compare to their littermates. From our *in vitro* studies and from *in vivo* pH measurements, I speculate that I will observe the development of marked hypertension in the absence of primary cilium globally and specific to the kidney. This result would agree with the human condition in which hypertension precedes renal failure in both ARPKD and ADPKD.

*Upregulation of ENaCs and NHEs in the developing respiratory epithelium: Cause of respiratory hypoplasia and insufficiency in ARPKD?*

Possible implications of upregulated ENaC and NHEs in respiratory tract will also be tested in mice treated with tamoxifen and in control mice with nothing added in drinking water. I will test if there is any difference in nasal potential difference experiments between mice which are treated with or without tamoxifen. If the results are encouraging, our lab plans to develop an immortalized cell line from mouse trachea of mutant and control cilium knockout mice to verify our findings. These cell lines will help us understand more about how cilium engages in “crosstalk” with different channels and transporter found on or close to the apical membrane.

*Cytoskeletal alterations in the regulation of apical ENaCs and NHEs*

Studies done by Brian Siroky and Darwin Bell (unpublished observations) showed that treatment with BAPTA-AM, a cell-calcium chelator, attenuated the change in the actin cytoskeletal network observed with a loss of the primary cilium. In addition, treatment of cilium-competent cells with cytochalasin D disrupted the actin microfilaments, leading to an increase in proliferation, a characteristic found in cilium-deficient cells. To test if cytoskeleton reconstruction in mutant cells and/or cytoskeleton disorganization in rescued cells may influence ENaC and NHE expression and/or function, I will perform similar experiments with the appropriate doses of BAPTA-AM, cytochalasin D, and other drugs to assess the influence of the actin cytoskeleton on these endpoints.

## CONCLUSIONS

Taken together, dysregulation of ENaCs and NHEs in the apical membrane of cilium-deficient cell monolayers has provided novel insights into polycystic kidney disease and the development of hypertension in this debilitating renal disease. With such seminal findings, new questions emerge. Central to these questions is how the emerging sensory organelle, the primary cilium, regulates the expression, function and distribution of Na<sup>+</sup>-dependent channels and transporters in ductal epithelia.

## GENERAL LIST OF REFERENCES

- 1 Pazour GJ. Intraflagellar transport and cilia-dependent renal disease: The ciliary hypothesis of polycystic kidney disease J. Am. Soc. Nephrol. 15(10): 2528 – 2536, 2004.
- 2 Davenport JR and BK Yoder. An incredible decade for the primary cilium: a look at a once-forgotten organelle. Am J Physiol Renal Physiol. 289(6):F1159-69, 2005.
- 3 Nauli SM and J Zhou. Polycystins and mechanosensation in renal and nodal cilia. Bioessays. 26(8):844-56, 2004.
- 4 Gabow PA, Chapman AB, Johnson AM, Tangel DJ, Duley IT, Kaehny WD, Manco-Johnson M, and RW Schrier. Renal structure and hypertension in autosomal dominant polycystic kidney disease. Kidney Int 38: 1177–1180, 1990.
- 5 Chapman AB and RW Schrier. Pathogenesis of hypertension in autosomal dominant polycystic kidney disease. Semin Nephrol 11: 653–660, 1991
- 6 Guay-Woodford LM and RA Desmond. Autosomal recessive polycystic kidney disease: the clinical experience in North America. Pediatrics 111(5): 1072-1080, 2003.
- 7 Freis ED. Salt, volume and the prevention of hypertension. Circulation. 53(4):589-95, 1976.
- 8 Schafer JA. Renal Physiology. Essential Medical Physiology by Johnson LR. Third Edition. Elsevier (USA), 2003.

- 9 Palmer BF, Alpern RJ, and DW Seldin. Physiology and pathophysiology of sodium retention. The Kidney. Lippincott Williams and Wilkins. Third Edition, 2000.
- 10 Konrad M and S. Weber. Recent advances in molecular genetics of hereditary magnesium-losing disorders. J Am Soc Nephrol. 14(1):249-60, 2003.
- 11 Hummler E, Barker P, Talbot C, Wang Q, Verdumo C, Grubb B, Gatzky J, Burnier M, Horisberger JD, Beermann F, Boucher R and BC Rossier. A mouse model for the renal salt-wasting syndrome pseudohypoaldosteronism. Proc Natl Acad Sci U S A. 14;94(21):11710-5, 1997.
- 12 Klusmann E, Maric K and W. Rosenthal. The mechanisms of aquaporin control in the renal collecting duct. Rev Physiol Biochem Pharmacol. 141:33-95, 2000.
- 13 Kellenberger S and L Schild. Epithelial sodium channel/degenerin family of ion channels: a variety of functions for a shared structure. Physiol. Rev. 82: 735-767, 2002.
- 14 Drummond HA, Abboud FM, and MJ Welsh. Localization of beta and gamma subunits of ENaC in sensory nerve endings in the rat foot pad. Brain Res 884: 1-12, 2000.
- 15 Drummond HA, Price MP, Welsh MJ, and FM Abboud. A molecular component of the arterial baroreceptor mechanotransducer. Neuron 21: 1435-1441, 1998.
- 16 Drummond HA, Gebremedhin D, and DR Harder. Degenerin/epithelial Na<sup>+</sup> channel proteins: components of a vascular mechanosensor. Hypertension. 44(5):643-8, 2004.
- 17 Canessa CM, Schild L, Buell G, Thorens B, Gautschi I, Horisberger JD, and BC Rossier. Amiloride-sensitive epithelial Na<sup>+</sup> channel is made of three homologous subunits. Nature. 367(6462):463-7, 1994.

- 18 Firsov D, Gautschi I, Merillat AM, Rossier BC, and L Schild. The heterotetrameric architecture of the epithelial sodium channel (ENaC). *EMBO J.* 17(2):344-52, 1998.
- 19 Kosari F, Sheng SH, Li JQ, Mak DD, Foskett JK, and TR Kleyman. Subunit stoichiometry of the epithelial sodium channel. *J Biol Chem* 273: 13469 –13474, 1998.
- 20 Cheng C, Prince LS, Snyder PM, and MJ Welsh. Assembly of the epithelial Na<sup>+</sup> channel evaluated using sucrose gradient sedimentation analysis. *J Biol Chem.* 273(35):22693-700, 1998.
- 21 Eskandari S, Snyder PM, Kreman M, Zampighi GA, Welsh MJ, and EM Wright. Number of subunits comprising the epithelial sodium channel. *J Biol Chem.* 274(38):27281-6, 1999.
- 22 Snyder PM, Cheng C, Prince LS, Rogers JC, and MJ Welsh. Electrophysiological and biochemical evidence that DEG/ENaC cation channels are composed of nine subunits. *J Biol Chem.* 273(2):681-4, 1999.
- 23 Waldmann R, Champigny G, Bassilana F, Voilley N, and M Lazdunski. Molecular cloning and functional expression of a novel amiloride-sensitive Na<sup>+</sup> channel. *J Biol Chem.* 270(46):27411-4, 1995.
- 24 Giraldez T, Afonso-Oramas D, Cruz-Muros I, Garcia-Marin V, Pagel P, Gonzalez-Hernandez T, and DA de la Rosa. Cloning and functional expression of a new epithelial sodium channel delta subunit isoform differentially expressed in neurons of the human and monkey telencephalon. *J Neurochem.* 102(4):1304-15, 2007.

- 25 Brockway LM, Zhou ZH, Bubien JK, Jovov B, Benos DJ, and KT Keyser. Rabbit retinal neurons and glia express a variety of ENaC/DEG subunits. *Am J Physiol Cell Physiol*. 283(1):C126-34, 2002.
- 26 Babini E, Geisler HS, Siba M, and S Gründer. A new subunit of the epithelial Na<sup>+</sup> channel identifies regions involved in Na<sup>+</sup> self-inhibition. *J Biol Chem*. 278(31):28418-26, 2003.
- 27 Renard S, Lingueglia E, Voilley N, Lazdunski M, and P Barbry. Biochemical analysis of the membrane topology of the amiloride-sensitive Na<sup>+</sup> channel. *J Biol Chem*. 269(17):12981-6, 1994.
- 28 Rotin D, Bar-Sagi D, O'Brodovich H, Merilainen J, Lehto VP, Canessa CM, Rossier BC, and GP Downey. An SH3 binding region in the epithelial Na<sup>+</sup> channel (alpha rENaC) mediates its localization at the apical membrane. *EMBO J*. 13(19):4440-50, 1994.
- 29 Shimkets RA, Lifton RP, and CM Canessa. The activity of the epithelial sodium channel is regulated by clathrin-mediated endocytosis. *J Biol Chem*. 272(41):25537-41, 1997.
- 30 Copeland, SJ, Berdiev BK, Ji HL, Lockhart J, Parker S, Fuller CM, and DJ Benos. Regions in the carboxy terminus of alpha-bENaC involved in gating and functional effects of actin. *Am J Physiol Cell Physiol* 281: C231-C240, 2001.
- 31 Mazzochi C, Bubien JK, Smith PR, and DJ Benos DJ. The carboxyl terminus of the alpha-subunit of the amiloride-sensitive epithelial sodium channel binds to F-actin. *J Biol Chem*. 281(10):6528-38, 2006.

- 32 Chalfant, ML, Denton JS, Berdiev BK, Ismailov II, Benos DJ, and BA Stanton. Intracellular H<sup>+</sup> regulates the alpha-subunit of ENaC, the epithelial Na<sup>+</sup> channel. *Am J Physiol Cell Physiol* 276: C477-C486, 1999.
- 33 Yamamura H, Ugawa S, Ueda T, and S Shimada. Protons activate the delta-subunit of the epithelial Na<sup>+</sup> channel in humans. *J Biol Chem.* 279(13):12529-34, 2004.
- 34 Palmer LG and OS Andersen. Interactions of amiloride and small monovalent cations with the epithelial sodium channel. Inferences about the nature of the channel pore. *Biophys J* 55: 779-787, 1989.
- 35 McNicholas CM and CM Canessa. Diversity of channels generated by different combinations of epithelial sodium channel subunits. *J Gen Physiol* 109: 681-692, 1997.
- 36 Garty H and LG Palmer. Epithelial sodium channels: function, structure, and regulation. *Physiol Rev* 77: 359-396, 1997.
- 37 Palmer LG and G Frindt. Gating of Na channels in the rat cortical collecting tubule: effects of voltage and membrane stretch. *J Gen Physiol.* 107(1):35-45, 1996.
- 38 Ismailov II, Berdiev BK, Shlyonsky VG, and DJ Benos. Mechanosensitivity of an epithelial Na<sup>+</sup> channel in planar lipid bilayers: release from Ca<sup>2+</sup> block. *Biophys J.* 72(3):1182-92, 1997.
- 39 Morimoto T, Liu W, Woda C, Carattino MD, Wei Y, Hughey RP, Apodaca G, Satlin LM, and TR Kleyman. Mechanism underlying flow stimulation of sodium absorption in the mammalian collecting duct. *Am J Physiol Renal Physiol.* 291(3):F663-9, 2006.
- 40 Satlin LM, Sheng S, Woda CB, and TR Kleyman TR. Epithelial Na<sup>+</sup> channels are regulated by flow. *Am J Physiol Renal Physiol.* 280(6):F1010-8, 2001.



- 41 Komwatana P, Dinudom A, Young JA, and DI Cook. Cytosolic Na<sup>+</sup> controls and epithelial Na<sup>+</sup> channel via the Go guanine nucleotide-binding regulatory protein. *Proc Natl Acad Sci U S A*. 93(15):8107-11, 1996.
- 42 Silver RB, Frindt G, Windhager EE, and LG Palmer. Feedback regulation of Na<sup>+</sup> channels in rat CCT. I. Effects of inhibition of Na pump. *Am J Physiol*. 264 (3 Pt 2):F557-64, 1993.
- 43 Hille, B. Elementary properties of ions in solution. In *Ionic Channels of Excitable Membranes*, 2nd edn, pp. 261-290. Sinauer Associates, Inc., Sunderland, MA, USA. 1992.
- 44 Askwith, C.C., C.J. Benson, M.J. Welsh, and P.M. Snyder. DEG/ENaC ion channels involved in sensory transduction are modulated by cold temperature. *Proc. Natl. Acad. Sci. USA*. 98:6459–6463, 2001.
- 45 Chraïbi A and JD Horisberger. Na self inhibition of human epithelial Na channel: temperature dependence and effect of extracellular proteases. *J Gen Physiol*. 120(2):133-45, 2002
- 46 Frindt G, Masilamani S, Knepper MA, and LG Palmer. Activation of epithelial Na channels during short-term Na deprivation. *Am J Physiol Renal Physiol*. 280(1):F112-8, 2001.
- 47 Frindt G, McNair T, Dahlmann A, Jacobs-Palmer E, and LG Palmer. Epithelial Na channels and short-term renal response to salt deprivation. *Am J Physiol Renal Physiol*. 283(4):F717-26, 2002.
- 48 Vuagniaux G, Vallet V, Jaeger NF, Pfister C, Bens M, Farman N, Courtois-Coutry N, Vandewalle A, Rossier BC, and E Hummler. Activation of the amiloride-

sensitive epithelial sodium channel by the serine protease mCAP1 expressed in a mouse cortical collecting duct cell line. *J Am Soc Nephrol* 11: 828–834, 2000.

49 Vallet V, Chraïbi A, Gaeggeler HP, Horisberger JD, and BC Rossier. An epithelial serine protease activates the amiloride-sensitive sodium channel. *Nature* 389: 607–610, 1997.

50 Caldwell RA, Boucher RC, and MJ Stutts. Neutrophil elastase activates near-silent epithelial Na<sup>+</sup> channels and increases airway epithelial Na<sup>+</sup> transport. *Am J Physiol Lung Cell Mol Physiol* 288: L813–L819, 2005.

51 Tong Z, Illek B, Bhagwandin VJ, Verghese GM, and GH Caughey. Prostatic, a membrane-anchored serine peptidase, regulates sodium currents in JME/CF15 cells, a cystic fibrosis airway epithelial cell line. *Am J Physiol Lung Cell Mol Physiol* 287: L928–L935, 2004.

52 Shen JP and CU Cotton. Epidermal growth factor inhibits amiloride-sensitive sodium absorption in renal collecting duct cells. *Am J Physiol Renal Physiol* 284: F57–F64, 2003.

53 Vehaskari V, Hering-Smith K, Moskowitz D, Weiner I, and L Hamm. Effect of epidermal growth factor on sodium transport in the cortical collecting tubule. *Am J Physiol Renal Fluid Electrolyte Physiol* 256: F803–F809, 1989

54 Ma HP, Saxena S, and DG Warnock. Anionic phospholipids regulate native and expressed epithelial sodium channel (ENaC). *J Biol Chem*. 277(10):7641-4, 2002.

55 Ma HP, Chou CF, Wei SP, and DC Eaton. Regulation of the epithelial sodium channel by phosphatidylinositides: experiments, implications, and speculations. *Pflugers Arch*. Epub Ahead of Print Jun 29 2007.

- 56 Peti-Peterdi J, Warnock DG, and PD Bell. Angiotensin II directly stimulates ENaC activity in the cortical collecting duct via AT1 receptors. *J Am Soc Nephrol* 13: 1131–1135, 2002.
- 57 Blazer-Yost BL, Liu X, and SI Helman. Hormonal regulation of ENaCs: insulin and aldosterone. *Am J Physiol Cell Physiol* 274: C1373–C1379, 1998.
- 58 Ecelbarger CA, Kim GH, Wade JB, and MA Knepper. Regulation of the abundance of renal sodium transporters and channels by vasopressin. *Exp Neurol* 171: 227–234, 2001.
- 59 Light DB, Corbin JD, and BA Stanton. Dual ion-channel regulation by cyclic GMP and cyclic GMP-dependent protein kinase. *Nature*. 344(6264):336-9, 1990.
- 60 Wang W, Li C, Nejsum LN, Li H, Kim SW, Kwon TH, Jonassen TE, Knepper MA, Thomsen K, Frøkier J, and S. Nielsen. Biphasic effects of ANP infusion in conscious, euvolumic rats: roles of AQP2 and ENaC trafficking. *Am J Physiol Renal Physiol*. 290(2):F530-41., 2006.
- 61 Alvarez de la Rosa D, Canessa CM. Role of SGK in hormonal regulation of epithelial sodium channel in A6 cells. *Am J Physiol Cell Physiol*. 284(2):C404-14, 2003.
- 62 Loffing J, Zecevic M, Feraille E, Kaissling B, Asher C, Rossier BC, Firestone GL, Pearce D, and F Verrey. Aldosterone induces rapid apical translocation of ENaC in early portion of renal collecting system: possible role of SGK. *Am J Physiol Renal Physiol* 280: F675-F682, 2001.
- 63 Masilamani S, Kim GH, Mitchell C, Wade JB, and MA Knepper. Aldosterone-mediated regulation of ENaC alpha, beta, and gamma subunit proteins in rat kidney. *J Clin Invest* 104: R19-R23, 1999.

- 64 Shigaev A, Asher C, Latter H, Garty H, and E Reuveny. Regulation of sgk by aldosterone and its effects on the epithelial Na<sup>+</sup> channel. *Am J Physiol Renal Physiol* 278: F613–F619, 2000.
- 65 Alvarez de la Rosa D, Zhang P, Naray-Fejes-Toth A, Fejes-Toth G, and CM Canessa. The serum and glucocorticoid kinase sgk increases the abundance of epithelial sodium channels in the plasma membrane of *Xenopus* oocytes. *J Biol Chem* 274: 37834 – 37839, 1999.
- 66 Naray FT, Canessa C, Cleaveland ES, Aldrich G, Fejes-Toth G: Sgk is an aldosterone-induced kinase in the renal collecting duct—Effects on epithelial Na<sup>+</sup> channels. *J Biol Chem* 274: 16973 –16978, 1999.
- 67 Chen SY, Bhargava A, Mastroberardino L, Meijer OC, Wang J, Buse P, Firestone GL, Verrey F, and D Pearce. Epithelial sodium channel regulated by aldosterone-induced protein sgk. *Proc Natl Acad Sci USA* 96: 2514 –2519, 1999
- 68 Diakov A and C Korbmacher. A novel pathway of epithelial sodium channel activation involves a serum- and glucocorticoid-inducible kinase consensus motif in the C terminus of the channel's alpha-subunit. *J Biol Chem* 279: 38134 –38142, 2004
- 69 Debonneville C, Flores SY, Kamynina E, Plant PJ, Tauxe C, Thomas MA, Munster C, Chraïbi A, Pratt JH, Horisberger JD, Pearce D, Loffing J, and O Staub. Phosphorylation of Nedd4-2 by Sgk1 regulates epithelial Na<sup>+</sup> channel cell surface expression. *EMBO J* 20: 7052 –7059, 2001.
- 70 Snyder PM, Olson DR, and BC Thomas. Serum and glucocorticoid-regulated kinase modulates Nedd4-2-mediated inhibition of the epithelial Na<sup>+</sup> channel. *J Biol Chem* 277: 5 –8, 2002.

- 71 Staub O, Gautschi I, Ishikawa T, Breitschopf K, Ciechanover A, Schild L, and D Rotin. Regulation of stability and function of the epithelial Na<sup>+</sup> channel (ENaC) by ubiquitination. *EMBO J.* 16(21):6325-36, 1997.
- 72 Shimkets RA, Lifton RP, and CM Canessa. The activity of the epithelial sodium channel is regulated by clathrin-mediated endocytosis. *J Biol Chem.* 272(41):25537-41, 1997.
- 73 Inoue T, Nonoguchi H, and K Tomita. Physiological effects of vasopressin and atrial natriuretic peptide in the collecting duct. *Cardiovasc Res* 51: 470-80, 2001.
- 74 Willmann JK, Bleich M, Rizzo M, Schmidt-Hieber M, Ullrich KJ, and R Greger. Amiloride inhibitable Na<sup>+</sup> conductance in rat proximal tubule. *Pflügers Arch* 434: 173-78, 1997.
- 75 Duc C, Farman N, Canessa CM, Bonvalet JP, and BC Rossier. Cell-specific expression of epithelial sodium channel alpha, beta, and gamma subunits in aldosterone-responsive epithelia from the rat: localization by in situ hybridization and immunocytochemistry. *J Cell Biol.* 127(6 Pt 2):1907–1921, 1994.
- 76 Renard, S, Voillet, N, Bassilana, F, Lazdunski, M, and P Barbry. Localization and regulation by steroids of the subunits of the amiloride-sensitive Na<sup>+</sup> channel in colon, lung and kidney. *Pflügers Arch* 430:299–307, 1995.
- 77 Volk KA, Sigmund RD, Snyder PM, McDonald FJ, Welsh MJ, and JB Stokes. rENaC is the predominant Na<sup>+</sup> channel in the apical membrane of the rat renal inner medullary collecting duct. *J Clin Invest.* 96(6): 2748-57, 1995.
- 78 Hager H, Kwon TH, Vinnikova AK, Masilamani S, Brooks HL, Frøkiaer J, Knepper MA and S. Nielsen. Immunocytochemical and immunoelectron microscopic

localization of alpha-, beta-, and gamma-ENaC in rat kidney. *Am J Physiol Renal Physiol.* 280(6):F1093-106, 2001.

79 Liddle, G. W., Bledsoe, T., and WS. Coppage, Jr. A familial renal disorder simulating primary aldosteronism but with negligible aldosterone secretion. *Trans. Assoc. Am. Phys.* 76: 199-213, 1963.

80 Shimkets, R. A., Warnock, D. G., Bositis, C. M., Nelson-Williams, C., Hansson, J. H., Schambelan, M., Gill, J. R., Jr., Ulick, S., Milora, R. V., Findling, J. W., Canessa, C. M., Rossier, B. C., and R.P. Lifton. Liddle's syndrome: heritable human hypertension caused by mutations in the beta subunit of the epithelial sodium channel. *Cell* 79: 407-414, 1994.

81 Hansson, J. H., Nelson-Williams, C., Suzuki, H., Schild, L., Shimkets, R., Lu, Y., Canessa, C., Iwasaki, T., Rossier, B., and R.P. Lifton. Hypertension caused by a truncated epithelial sodium channel gamma subunit: genetic heterogeneity of Liddle syndrome. *Nature Genet.* 11: 76-82, 1995.

82 Abriel H, Loffing J, Rebhun JF, Pratt JH, Schild L, Horisberger JD, Rotin D, and O Staub. Defective regulation of the epithelial Na<sup>+</sup> channel by Nedd4 in Liddle's syndrome. *J Clin Invest.* 103(5):667-73, 1999.

83 Staub O, Dho S, Henry PC, Correa J, Ishikawa T, McGlade J, and D Rotin. WW domains of Nedd4 bind to the proline-rich PY motifs in the epithelial Na<sup>+</sup> channel deleted in Liddle's syndrome. *EMBO J* 15: 2371 –2380, 1996

84 Shimkets RA, Lifton RP, and CM Canessa. The activity of the epithelial sodium channel is regulated by clathrin-mediated endocytosis. *J Biol Chem* 272: 25537 –25541, 1997.

- 85 Chang, S. S., Grunder, S., Hanukoglu, A., Rosler, A., Mathew, P. M., Hanukoglu, I., Schild, L., Lu, Y., Shimkets, R. A., Nelson-Williams, C., Rossier, B. C., and R.P. Lifton, R. P. Mutations in subunits of the epithelial sodium channel cause salt wasting with hyperkalaemic acidosis, pseudohypoaldosteronism type 1. *Nature Genet.* 12: 248-253, 1996.
- 86 Boucher RC. Relationship of airway epithelial ion transport to chronic bronchitis. *Proc Am Thorac Soc.* 1(1):66-70, 2004.
- 87 Morales MM, Falkenstein D and AG Lopes. The cystic fibrosis transmembrane regulator (CFTR) in the kidney. *An Acad Bras Cienc.* 72(3):399-406, 2000.
- 88 Boucher, R. C., Cotton, C. U., Gatzky, J. T., Knowles, M. R., and J.R. Yankaskas. Evidence for reduced Cl<sup>-</sup> and increased Na<sup>+</sup> permeability in cystic fibrosis human primary cell cultures. *J Physiol* 405:77-103, 1988.
- 89 Kunzelmann K, Kathöfer S, and R Greger. Na<sup>+</sup> and Cl<sup>-</sup> conductances in airway epithelial cells: increased Na<sup>+</sup> conductance in cystic fibrosis. *Pflugers Arch.* 431(1):1-9, 1995.
- 90 Kerem, E., Bistrizer, T., Hanukoglu, A., Hofmann, T., Zhou, Z., Bennett, W., MacLaughlin, E., Barker, P., Nash, M., Quittell, L., Boucher, R., and M.R. Knowles. Pulmonary epithelial sodium channel dysfunction and excess airway liquid in pseudohypoaldosteronism. *N. Engl. J. Med.* 341: 156-162, 1999.
- 91 Talbot CL, Bosworth DG, Briley EL, Fenstermacher DA, Boucher RC, Gabriel SE, and PM Barker. Quantitation and localization of ENaC subunit expression in fetal, newborn, and adult mouse lung. *Am J Respir Cell Mol Biol* 20: 398-406, 1999

- 92 Harding R, Pinkerton KE and CG Plopper. The Lung: Development, Aging and the Environment. Elsevier, 2003.
- 93 Orłowski J and S Grinstein. Diversity of the mammalian sodium/proton exchanger SLC9 gene family. *Pflügers Arch.* 447(5):549-65, 2004.
- 94 Pouyssegur J, Sardet C, Franchi A, L'Allemain G, and S Paris. A specific mutation abolishing Na<sup>+</sup>/H<sup>+</sup> antiport activity in hamster fibroblasts precludes growth at neutral and acidic pH. *Proc Natl Acad Sci USA* 81: 4833–4837, 1984.
- 95 Putney LK and DL Barber. Na-H exchange-dependent increase in intracellular pH times G2/M entry and transition. *J Biol Chem* 278: 44645–44649, 2003.
- 96 Rentsch ML, Ossum CG, Hoffmann EK, and SF Pedersen. Roles of Na(+)/H (+) exchange in regulation of p38 mitogen-activated protein kinase activity and cell death after chemical anoxia in NIH3T3 fibroblasts. *Pflügers Arch.* 454(4):649-62, 2007.
- 97 Donowitz M, Janecki A, Akhter S, Cavet ME, Sanchez F, Lamprecht G, Zizak M, Kwon WL, Khurana S, Yun CH, and CM Tse. Short-term regulation of NHE3 by EGF and protein kinase C but not protein kinase A involves vesicle trafficking in epithelial cells and fibroblasts. *Ann NY Acad Sci* 915: 30–42, 2000.
- 98 Gekle M, Serrano OK, Drumm K, Mildenerger S, Freudinger R, Gassner B, Jansen HW, and EI Christensen. NHE3 serves as a molecular tool for cAMP-mediated regulation of receptor-mediated endocytosis. *Am J Physiol Renal Physiol* 283: F549–F558, 2002.
- 99 Gekle M, Volker K, Mildenerger S, Freudinger R, Shull GE, and M Wiemann. NHE3 Na<sup>+</sup>/H<sup>+</sup> exchanger supports proximal tubular protein reabsorption in vivo. *Am J Physiol Renal Physiol* 287: F469–F473, 2004.



- 100 Nakamura N, Tanaka S, Teko Y, Mitsui K, H Kanazawa. Four Na<sup>+</sup>/H<sup>+</sup> exchanger isoforms are distributed to Golgi and post-Golgi compartments and are involved in organelle pH regulation. *J Biol Chem.* 280(2):1561-72, 2005.
- 101 Janecki AJ, Montrose MH, Zimniak P, Zweibaum A, Tse CM, Khurana S and M Donowitz. Subcellular redistribution is involved in acute regulation of the brush border Na<sup>+</sup>/H<sup>+</sup> exchanger isoform 3 in human colon adenocarcinoma cell line Caco-2. Protein kinase C-mediated inhibition of the exchanger. *J Biol Chem.* 10;273(15):8790-8, 1998.
- 102 Szaszi K, Paulsen A, Szabo EZ, Numata M, Grinstein S and J Orlowski. Clathrin-mediated endocytosis and recycling of the neuron-specific Na<sup>+</sup>/H<sup>+</sup> exchanger NHE5 isoform. Regulation by phosphatidylinositol 3'-kinase and the actin cytoskeleton. *J Biol Chem.* 8;277(45):42623-32, 2002.
- 103 Brett CL, Wei Y, Donowitz M, and R Rao. Human Na<sup>+</sup>/H<sup>+</sup> exchanger isoform 6 is found in recycling endosomes of cells, not in mitochondria. *Am J Physiol Cell Physiol* 282: C1031–C1041, 2002.
- 104 Miyazaki E, Sakaguchi M, Wakabayashi S, Shigekawa M, and K Mihara. NHE6 protein possesses a signal peptide destined for endoplasmic reticulum membrane and localizes in secretory organelles of the cell. *J Biol Chem* 276: 49221–49227, 2001.
- 105 Hill JK, Brett CL, Chyou A, Kallay LM, Sakaguchi M, Rao R and PG Gillespie. Vestibular Hair Bundles Control pH with (Na<sup>+</sup>, K<sup>+</sup>)/H<sup>+</sup> Exchangers NHE6 and NHE9. *J Neurosci.* 27;26(39):9944-55, 2006.
- 106 Numata M and J Orlowski. Molecular cloning and characterization of a novel (Na<sup>+</sup>,K<sup>+</sup>)/H<sup>+</sup> exchanger localized to the trans-Golgi network. *J Biol Chem* 276: 17387–17394, 2001.

- 107 Goyal S, Vanden Heuvel G, and PS Aronson PS. Renal expression of novel Na<sup>+</sup>/H<sup>+</sup> exchanger isoform NHE8. *Am J Physiol Renal Physiol* 284: F467–F473, 2003.
- 108 Wang D, Hu J, Bobulescu IA, Quill TA, McLeroy P, Moe OW, and DL Garbers. A sperm-specific Na<sup>+</sup>/H<sup>+</sup> exchanger (sNHE) is critical for expression and in vivo bicarbonate regulation of the soluble adenylyl cyclase (sAC). *Proc Natl Acad Sci U S A* 104(22):9325-30, 2007.
- 109 Wang D, King SM, Quill TA, Doolittle LK, and DL Garbers. A new sperm-specific Na<sup>+</sup>/H<sup>+</sup> exchanger required for sperm motility and fertility. *Nat Cell Biol.* 5(12):1117-22, 2003.
- 110 Brett CL, Donowitz M, and R Rao. Evolutionary origins of eukaryotic sodium/proton exchangers. *Am J Physiol Cell Physiol.* 288(2):C223-39, 2005.
- 111 Szabó EZ, Numata M, Shull GE, and J Orlowski. Kinetic and pharmacological properties of human brain Na<sup>(+)</sup>/H<sup>(+)</sup> exchanger isoform 5 stably expressed in Chinese hamster ovary cells. *J Biol Chem.* 275(9):6302-7, 2000.
- 112 Chambrey R, St John PL, Eladari D, Quentin F, Warnock DG, Abrahamson DR, Podevin RA, and M Paillard. Localization and functional characterization of Na<sup>+</sup>/H<sup>+</sup> exchanger isoform NHE4 in rat thick ascending limbs. *Am J Physiol Renal Physiol.* 281(4):F707-17, 2001.
- 113 Bookstein C., Musch, M. W., DePaoli, A., Xie, Y., Rabenau, K., Villereal, M., Rao, M. C., and E.B. Chang. Characterization of the rat Na<sup>+</sup>/H<sup>+</sup> exchanger isoform NHE4 and localization in rat hippocampus *Am. J. Physiol.* 271(5 Pt 1):C1629-38, 1996.

- 114 Zhang J, Bobulescu IA, Goyal S, Aronson PS, Baum MG, and OW Moe. Characterization of Na<sup>+</sup>/H<sup>+</sup> Exchanger NHE8 in cultured renal epithelial cells. *Am J Physiol Renal Physiol*. Epub Ahead of Print June 20, 2007.
- 115 Counillon L. and J Pouyssegur. The expanding family of eucaryotic Na<sup>+</sup>/H<sup>+</sup> exchangers. *J Biol Chem* 275:1-4, 2000.
- 116 Chow CW. Regulation and intracellular localization of the epithelial isoforms of the Na<sup>+</sup>/H<sup>+</sup> exchangers NHE2 and NHE3. *Clin Invest Med* 22(5):195-206, 1999.
- 117 Masereel B, Pochet L and D Laeckmann. An overview of inhibitors of Na<sup>(+)</sup>/H<sup>(+)</sup> exchanger. *Eur J Med Chem*. 38(6):547-54, 2003.
- 118 Zachos NC, Tse M and M Donowitz. Molecular physiology of intestinal Na/H exchange. *Annu Rev Physiol*.;67:411-43, 2005.
- 119 Nath SK, Hang CY, Levine SA, Yun CH, Montrose MH, Donowitz M, and CM Tse. Hyperosmolarity inhibits the Na<sup>+</sup>/H<sup>+</sup> exchanger isoforms NHE2 and NHE3: an effect opposite to that on NHE1. *Am J Physiol*. 270(3 Pt 1):G431-41, 1996.
- 120 Attaphitaya S, Nehrke K, and JE Melvin. Acute inhibition of brain-specific Na<sup>+</sup>/H<sup>+</sup> exchanger isoform 5 by protein kinases A and C and cell shrinkage. *Am J Physiol Cell Physiol* 281: C1146-C1157, 2001.
- 121 Soleimani M, Singh G, Bizal GL, Gullans SR, and JA McAteer. Na<sup>+</sup>/H<sup>+</sup> exchanger isoforms NHE-2 and NHE-1 in inner medullary collecting duct cells. Expression, functional localization, and differential regulation. *J. Biol. Chem*. 269: 27973 – 27978, 1994.
- 122 Chow CW, Woodside M, Demaurex N, Yu FH, Plant P, Rotin D, Grinstein S, and J Orlowski. Proline-rich motifs of the Na<sup>+</sup>/H<sup>+</sup> exchanger 2 isoform. Binding of Src

homology domain 3 and role in apical targeting in epithelia. *J Biol Chem.* 274(15):10481-8, 1999.

123 Kapus, A., S. Grinstein, S. Wasan, R. Kandasamy, and J. Orlowski. Functional characterization of three isoforms of the Na<sup>+</sup>/H<sup>+</sup> exchanger stably expressed in Chinese hamster ovary cells. ATP dependence, osmotic sensitivity, and role in cell proliferation. *J. Biol. Chem.* 269:23544-23552, 1994.

124 Bachmann O, Riederer B, Rossmann H, Groos S, Schultheis PJ, Shull GE, Gregor M, Manns MP, and U Seidler. The Na<sup>+</sup>/H<sup>+</sup> exchanger isoform 2 is the predominant NHE isoform in murine colonic crypts and its lack causes NHE3 upregulation. *Am J Physiol Gastrointest Liver Physiol.* 287(1):G125-33, 2004.

125 Kapus A, Grinstein S, Wasan S, Kandasamy R, and J. Orlowski. Functional characterization of three isoforms of the Na<sup>+</sup>/H<sup>+</sup> exchanger stably expressed in Chinese hamster ovary cells. ATP dependence, osmotic sensitivity, and role in cell proliferation. *J Biol Chem.* 269(38):23544-52, 1994.

126 Coupaye-Gerard B, Bookstein C, Duncan P, Chen XY, Smith PR, Musch M, Ernst SA, Chang EB and TR Kleyman. Biosynthesis and cell surface delivery of the NHE1 isoform of Na<sup>+</sup>/H<sup>+</sup> exchanger in A6 cells. *Am J Physiol.* 271(5 Pt 1):C1639-45, 1996.

127 Noel, J., Roux, D., and J Pouyssegur. Differential localization of Na<sup>+</sup>/H<sup>+</sup> exchanger isoforms (NHE1 and NHE3) in polarized epithelial cell lines. *J. Cell Sci.* 109, 929-939, 1996.

- 128 Khan S, Wu KL, Sedor JR, Abu Jawdeh BG and JR Schelling. The NHE1 Na<sup>+</sup>/H<sup>+</sup> exchanger regulates cell survival by activating and targeting ezrin to specific plasma membrane domains. *Cell Mol Biol (Noisy-le-grand)*. 30;52(8):115-21, 2006.
- 129 Lagana A, Vadnais J, Le PU, Nguyen TN, Laprade R, Nabi IR, and J Noël. Regulation of the formation of tumor cell pseudopodia by the Na<sup>(+)</sup>/H<sup>(+)</sup> exchanger NHE1. *J Cell Sci*. 113:3649-62, 2000.
- 130 Allen DG and XH Xiao. Role of the cardiac Na<sup>+</sup>/H<sup>+</sup> exchanger during ischemia and reperfusion. *Cardiovasc Res* 57: 934–941, 2003.
- 131 Hove MT, Jansen MA, Nederhoff MG, and CJ Van Echteld. Combined blockade of the Na<sup>+</sup> channel and the Na<sup>+</sup>/H<sup>+</sup> exchanger virtually prevents ischemic Na<sup>+</sup> overload in rat hearts *Mol Cell Biochem*. 297(1-2):101-10, 2007.
- 132 Wakabayashi S, Ikeda T, Iwamoto T, Pouyssegur J, and M Shigekawa. Calmodulin-binding autoinhibitory domain controls "pH-sensing" in the Na<sup>+</sup>/H<sup>+</sup> exchanger NHE1 through sequence-specific interaction. *Biochemistry* 36(42):12854-61, 1997.
- 133 Pang T, Su X, Wakabayashi S, and M Shigekawa. Calcineurin homologous protein as an essential cofactor for Na<sup>+</sup>/H<sup>+</sup> exchangers. *J Biol Chem*. 276(20):17367-72, 2001.
- 134 Li X, Alvarez B, Casey JR, Reithmeier RA, and L Fliegel. Carbonic anhydrase II binds to and enhances activity of the Na<sup>+</sup>/H<sup>+</sup> exchanger. *J Biol Chem*. 277(39):36085-91, 2002.

- 135 Aharonovitz O, Zaun HC, Balla T, York JD, Orlowski J, and S Grinstein. Intracellular pH regulation by Na(+)/H(+) exchange requires phosphatidylinositol 4,5-bisphosphate. *J Cell Biol.* 150(1):213-24, 2000.
- 136 Denker, S.P. Huang, D.C., Orlowski, J., Furthmayr, H., and D.L. Barber. Direct binding the Na-H exchanger NHE1 to ERM proteins regulates the cortical cytoskeleton and cell shape independently of H<sup>+</sup> translocation. *Mol. Cell* 6:1425-1436, 2000.
- 137 Kusuhara M, Takahashi E, Peterson TE, Abe J, Ishida M, Han J, Ulevitch R, and BC Berk. p38 Kinase is a negative regulator of angiotensin II signal transduction in vascular smooth muscle cells: effects on Na<sup>+</sup>/H<sup>+</sup> exchange and ERK1/2. *Circ Res.* 83(8):824-31, 1998.
- 138 Liaw YS, Yang PC, Yu CJ, Kuo SH, Luh KT, Lin YJ, and ML Wu. PKC activation is required by EGF-stimulated Na(+)-H<sup>+</sup> exchanger in human pleural mesothelial cells. *Am J Physiol.* 274(5 Pt 1):L665-72, 1998.
- 139 Karmazyn M. The sodium-hydrogen exchange system in the heart: its role in ischemic and reperfusion injury and therapeutic implications. *Can J Cardiol.* 12(10):1074-82, 1996.
- 140 Sauvage M, Maziere P, Fathallah H, and F Giraud. Insulin stimulates NHE1 activity by sequential activation of phosphatidylinositol 3-kinase and protein kinase C zeta in human erythrocytes. *Eur J Biochem.* 267(4):955-62, 2000.
- 141 Good DW, T George and BA Watts, III. Basolateral membrane Na<sup>+</sup>/H<sup>+</sup> exchange enhances HCO<sub>3</sub><sup>-</sup> absorption in rat medullary thick ascending limb: Evidence for functional coupling between basolateral and apical membrane Na<sup>+</sup>/H<sup>+</sup> exchangers. *Proc. Nat. Acad. Sci. USA* 92: 12525-12529, 1995.

- 142 Watts BA 3rd, George T, and DW Good. The basolateral NHE1  $\text{Na}^+/\text{H}^+$  exchanger regulates transepithelial  $\text{HCO}_3^-$  absorption through actin cytoskeleton remodeling in renal thick ascending limb. *J Biol Chem.* 280(12):11439-47, 2005.
- 143 Good DW, Watts BA 3rd, George T, Meyer JW, and GE Shull. Transepithelial  $\text{HCO}_3^-$  absorption is defective in renal thick ascending limbs from  $\text{Na}^+/\text{H}^+$  exchanger NHE1 null mutant mice. *Am J Physiol Renal Physiol.* 287(6):F1244-9, 2004.
- 144 Siffert W and R Düsing. Sodium-proton exchange and primary hypertension. *Hypertension.* 26:649-655, 1995.
- 145 Kuro-o, M., K. Hanaoka, Y. Hiroi, T. Noguchi, Y. Fujimori, S. Takewaki, M. Hayasaka, H. Katoh, A. Miyagishi, R. Nagai, Y. Yazaki, and Y. Nabeshima. Salt-sensitive hypertension in transgenic mice overexpressing  $\text{Na}^+$ -proton exchanger. *Circ. Res.* 76: 148-153, 1995.
- 146 Kelly, M. P., P. A. Quinn, J. E. Davies, and L. L. Ng. Activity and expression of  $\text{Na}^+/\text{H}^+$  exchanger isoform 1 and 3 in kidney proximal tubules of hypertensive rats. *Circ. Res.* 80: 853-860, 1997.
- 147 Dudley, C. R. K., D. J. Taylor, L. L. Ng, G. L. Kemp, P. J. Ratcliffe, G. K. Radda, and J. G. G. Ledingham. Evidence for abnormal  $\text{Na}^+/\text{H}^+$  antiport activity detected by phosphorus nuclear magnetic resonance spectroscopy in exercising skeletal muscle of patients with essential hypertension. *Clin. Sci.* 79: 491-497, 1990.
- 148 Orlov SN, Adragna NC, Adarichev VA, Hamet P. Genetic and biochemical determinants of abnormal monovalent ion transport in primary hypertension. *Am J Physiol.* 276(3 Pt 1):C511-36, 1999.

- 149 Sun AM, Liu Y, Dworkin LD, Tse CM, Donowitz M, and KP Yip. Na<sup>+</sup>/H<sup>+</sup> exchanger isoform 2 (NHE2) is expressed in the apical membrane of the medullary thick ascending limb. *J Membr Biol.* 160(1):85-90, 1997.
- 150 Chambrey R, Warnock DG, Podevin RA, Bruneval P, Mandet C, Belair MF, Bariety J, and M Paillard. Immunolocalization of the Na<sup>+</sup>/H<sup>+</sup> exchanger isoform NHE2 in rat kidney. *Am J Physiol.* 275(3 Pt 2):F379-86, 1998.
- 151 Peti-Peterdi J, Chambrey R, Bebok Z, Biemesderfer D, St John PL, Abrahamson DR, Warnock DG, and PD Bell. Macula densa Na<sup>(+)</sup>/H<sup>(+)</sup> exchange activities mediated by apical NHE2 and basolateral NHE4 isoforms. *Am J Physiol Renal Physiol.* 278(3):F452-63, 2000.
- 152 Choi, JY, Shah M, Lee MG, Schultheis PJ, Shull GE, Muallem S, and M Baum. Novel amiloride-sensitive sodium-dependent proton secretion in the mouse proximal convoluted tubule. *J Clin Invest* 105:1141-1146, 2000.
- 153 Wang, T, Yang CL, Abbiati T, Schultheis PJ, Shull GE, Giebisch G, and PS Aronson. Mechanism of proximal tubule bicarbonate absorption in NHE3 null mice. *Am J Physiol Renal Physiol* 277: F298-F302, 1999.
- 154 Biemesderfer, D, Rutherford PA, Nagy T, Pizzonia JH, Abu-Alfa AK, and PS Aronson. Monoclonal antibodies for high-resolution localization of NHE3 in adult and neonatal rat kidney. *Am J Physiol Renal Physiol* 273: F289-F299, 1997.
- 155 Qian, F., F. J. Germino, Y. Cai, X. Zhang, S. Somlo, and G. G. Germino. PKD1 interacts with PKD2 through a probable coiled-coil domain. *Nat. Genet.* 16:179-183, 1997.



- 156 Nath SK, Kambadur R, Yun CH, Donowitz M, and CM Tse. NHE2 contains subdomains in the COOH terminus for growth factor and protein kinase regulation. *Am J Physiol.* 276(4 Pt 1):C873-82, 1999.
- 157 Ghisan, F. K., S. Knobel, J. A. Barnard, AND M. Breyer. Expression of a novel sodium-hydrogen exchanger in the gastrointestinal tract and kidney. *J. Membr. Biol.* 144: 267-271, 1995.
- 158 Bailey MA, Giebisch G, Abbiati T, Aronson PS, Gawenis LR, Shull GE, and T Wang. NHE2-mediated bicarbonate reabsorption in the distal tubule of NHE3 null mice. *J Physiol* 561:765–775, 2004.
- 159 Kapus, A., Grinstein, S., Wasan, S., Kandasamy, R. A., and J. Orłowski. *J. Biol. Chem.* 269, 23544-23552, 1994.
- 160 Gens JS, Du H, Tackett L, Kong SS, Chu S, and MH Montrose. Different ionic conditions prompt NHE2 and NHE3 translocation to the plasma membrane. *Biochim Biophys Acta.* 1768(5):1023-35, 2007.
- 161 Schultheis, PJ, Clarke LL, Meneton P, Harline M, Boivin GP, Stemmermann G, Duffy JJ, Doetschman T, Miller ML, and GE Shull. Targeted disruption of the murine Na<sup>+</sup>/H<sup>+</sup> exchanger isoform 2 gene causes reduced viability of gastric parietal cells and loss of net acid secretion. *J Clin Invest* 101: 1243-1253, 1998.
- 162 Amemiya, M, Loffing J, Lotscher M, Kaissling B, Alpern RJ, and OW Moe. Expression of NHE-3 in the apical membrane of rat renal proximal tubule and thick ascending limb. *Kidney Int* 48: 1206-1215, 1995.

- 163 Biemesderfer, D, Pizzonia J, Abu-Alfa A, Exner M, Reilly R, Igarashi P, and PS Aronson. NHE3: a Na<sup>+</sup>/H<sup>+</sup> exchanger isoform of renal brush border. *Am J Physiol Renal Fluid Electrolyte Physiol* 265: F736-F742, 1993.
- 164 Shugrue, CA, Obermuller N, Bachmann S, Slayman CW, and RF Reilly. Molecular cloning of NHE3 from LLC-PK1 cells and localization in pig kidney. *J Am Soc Nephrol* 10: 1649-1657, 1999.
- 165 Li X, Galli T, Leu S, Wade JB, Weinman EJ, Leung G, Cheong A, Louvard D, and M. Donowitz. Na<sup>+</sup>-H<sup>+</sup> exchanger 3 (NHE3) is present in lipid rafts in the rabbit ileal brush border: a role for rafts in trafficking and rapid stimulation of NHE3. *J Physiol* 537: 537–552, 2001.
- 166 Geibel J, Giebisch G, and WF Boron. Angiotensin II stimulates both Na/H exchange and Na/HCO<sub>3</sub> cotransport in the rabbit proximal tubule. *Proc Natl Acad Sci USA* 87: 7919 -7920, 1990.
- 167 Eiam-Ong S, Hilden SA, King AJ, John CA, and NE Madias. Endothelin-1 stimulates the Na/H and Na/HCO<sub>3</sub> transporters in rabbit renal cortex. *Kidney Int* 42: 18 - 24, 1992.
- 168 Gesek FA, and AC Schoolwerth AC. Insulin increases Na/H exchange activity in proximal tubules from normotensive and hypertensive rats. *Am J Physiol* 260: F695 - F703, 1991.
- 169 Felder CC, Campbell T, Albrecht F, and P Jose. Dopamine inhibits Na/H exchange activity in renal BBMVs by stimulation of adenylate cyclase. *Am J Physiol* 259: F297 -F303, 1990.

- 170 Kahn AM, Dolson GM, Hise MK, Bennet SC, and EJ Weinman. Parathyroid hormone and dibutyryl cAMP inhibit Na/H exchange in renal brush border vesicles. *Am J Physiol* 248:F212 -F218, 1985.
- 171 Cho JH, Musch MW, Bookstein CM, McSwine RL, Rabenau K and EB Chang. Aldosterone stimulates intestinal Na<sup>+</sup> absorption in rats by increasing NHE3 expression of the proximal colon. *American Journal of Physiology Cell Physiology* 274:C586–C594, 1998.
- 172 Gekle M, Serrano OK, Drumm K, Mildenerger S, Freudinger R, Gassner B, Jansen HW, and EI Christensen. NHE3 serves as a molecular tool for cAMP-mediated regulation of receptor-mediated endocytosis. *Am J Physiol Renal Physiol* 283: F549–F558, 2002. 156. Drumm K, Gassner B, Silbernagl S, and M Gekle. Inhibition of Na<sup>+</sup>/H<sup>+</sup> exchange decreases albumin-induced NF- $\kappa$ B activation in renal proximal tubular cell lines (OK and LLC-PK1 cells). *Eur J Med Res* 6: 422–432, 2001.
- 173 Drumm K, Gassner B, Silbernagl S, and M Gekle. Inhibition of Na<sup>+</sup>/H<sup>+</sup> exchange decreases albumin-induced NF- $\kappa$ B activation in renal proximal tubular cell lines (OK and LLC-PK1 cells). *Eur J Med Res* 6: 422–432, 2001.
- 174 Lee EM, Pollock CA, Drumm K, Barden JA, and P Poronnik. Effects of pathophysiological concentrations of albumin on NHE3 activity and cell proliferation in primary cultures of human proximal tubule cells. *Am J Physiol Renal Physiol* 285: F748–F757, 2003.
- 175 Levine SA, Nath SK, Yun CH, Yip JW, Montrose M, Donowitz M, and CM Tse. Separate C-terminal domains of the epithelial specific brush border Na<sup>+</sup>/H<sup>+</sup> exchanger

isoform NHE3 are involved in stimulation and inhibition by protein kinases/growth factors. *J Biol Chem.* 270(23):13716-25, 1995.

176 Zizak M, Lamprecht G, Steplock D, Tariq N, Shenolikar S, Donowitz M, Yun CH, and EJ Weinman. cAMP-induced phosphorylation and inhibition of Na(+)/H(+) exchanger 3 (NHE3) are dependent on the presence but not the phosphorylation of NHE regulatory factor. *J Biol Chem.* 274(35):24753-8, 1999.

177 Weinman EJ, Steplock D, Donowitz M, and S Shenolikar. NHERF associations with sodium-hydrogen exchanger isoform 3 (NHE3) and ezrin are essential for cAMP-mediated phosphorylation and inhibition of NHE3. *Biochemistry* 39:6123–6129, 2000.

178 Wang T. Flow-activated transport events along the nephron. *Molecular cell biology and physiology of solute transport. Current Opinion in Nephrology & Hypertension.* 15(5):530-536, 2006.

179 Hayashi, M., T. Yoshida, T. Monkawa, Y. Yamaji, S. Sato, and T. Saruta. Na<sup>+</sup>/H<sup>+</sup>-exchanger 3 activity and its gene in the spontaneously hypertensive rat kidney. *J. Hypertens.* 15: 43-48, 1997.

180 Lapointe MS, Sodhi C, Sahai A, and D Batlle. Na<sup>+</sup>/H<sup>+</sup> exchange activity and NHE-3 expression in renal tubules from the spontaneously hypertensive rat. *Kidney Int.* 62(1): 157-65, 2002.

181 Yang LE, Leong PK, Ye S, Campese VM, and AA McDonough. Responses of proximal tubule sodium transporters to acute injury-induced hypertension. *Am J Physiol Renal Physiol* 284: F313-F322, 2003.

- 182 Leong PK, Yang LE, Landon CS, McDonough AA and Yip KP. Phenol injury-induced hypertension stimulates proximal tubule  $\text{Na}^+/\text{H}^+$  exchanger activity. *Am J Physiol Renal Physiol* 290: F1543-F1550, 2006.
- 183 Woo AL, Noonan WT, Schultheis PJ, Neumann JC, Manning PA, Lorenz JN, and GE Shull. Renal function in NHE3-deficient mice with transgenic rescue of small intestinal absorptive defect. *Am J Physiol Renal Physiol* 284: F1190–F1198, 2003.
- 184 Schultheis PJ, Clarke LL, Meneton P, Miller ML, Soleimani M, Gawenis LR, Riddle TM, Duffy JJ, Doetschman T, Wang T, Giebisch G, Aronson PS, Lorenz JN, and GE Shull. Renal and intestinal absorptive defects in mice lacking the NHE3  $\text{Na}^+/\text{H}^+$  exchanger. *Nat Genet* 19: 282–285, 1998.
- 185 Chambrey, R, Achard JM, St John PL, Abrahamson DR, and DG Warnock. Evidence for an amiloride-insensitive  $\text{Na}^+/\text{H}^+$  exchanger in rat renal cortical tubules. *Am J Physiol Cell Physiol* 273:C1064-C1074, 1997.
- 186 Pizzonia, JH, Biemesderfer D, Abu-Alfa AK, Wu MS, Exner M, Isenring P, Igarashi P, and PS Aronson. Immunochemical characterization of  $\text{Na}^+/\text{H}^+$  exchanger isoform NHE4. *Am J Physiol Renal Physiol* 275: F510-F517, 1998.
- 187 Gawenis LR, Greeb JM, Prasad V, Grisham C, Sanford LP, Doetschman T, Andringa A, Miller ML, and GE Shull. Impaired gastric acid secretion in mice with a targeted disruption of the NHE4  $\text{Na}^+/\text{H}^+$  exchanger. *J Biol Chem.* 280(13):12781-9, 2005.
- 188 Attaphitaya S, Park K, and JE Melvin. Molecular cloning, genomic organization, and functional expression of  $\text{Na}^+/\text{H}^+$  exchanger isoform 5 (NHE5) from human brain. *J Biol Chem*, 274: 4377-4382, 1999.

- 189 Szaszi K, Paulsen A, Szabo EZ, Numata M, Grinstein S and J Orlowski. Clathrin-mediated endocytosis and recycling of the neuron-specific Na<sup>+</sup>/H<sup>+</sup> exchanger NHE5 isoform. Regulation by phosphatidylinositol 3'-kinase and the actin cytoskeleton. *J Biol Chem.* 8;277(45):42623, 2002.
- 190 Baum M. Developmental changes in proximal tubule NaCl transport. *Pediatr Nephrol.* Epub Ahead of Print Aug 8 2007.
- 191 Becker AM, Zhang J, Goyal S, Dwarakanath V, Aronson PS, Moe OW, and M Baum. Ontogeny of NHE8 in the rat proximal tubule. *Am J Physiol Renal Physiol.* 293(1):F255-61, 2007.
- 192 Pulakat L, Cooper S, Knowle D, Mandavia C, Bruhl S, Hetrick M, and N Gavini. Ligand-dependent complex formation between the Angiotensin II receptor subtype AT2 and Na<sup>+</sup>/H<sup>+</sup> exchanger NHE6 in mammalian cells. *Peptides* 26(5):863-73, 2005.
- 193 Nonaka S, Tanaka Y, Okada Y, Takeda S, Harada A, Kanai Y, Kido M, and N Hirokawa. Randomization of left-right asymmetry due to loss of nodal cilia generating leftward flow of extraembryonic fluid in mice lacking KIF3B motor protein. *Cell* 95: 829–837, 1998.
- 194 Singla V and JF Reiter. The primary cilium as the cell's antenna: signaling at a sensory organelle. *Science.* 4;313(5787):629-33, 2006.
- 195 Paintrand M, Moudjou M, Delacroix H, Bornens M. Centrosome organization and centriole architecture: their sensitivity to divalent cations. *J. Struct. Biol.* 108:107–128, 1992.

- 196 Kolb RJ, Woost PG, and U Hopfer. Membrane trafficking of angiotensin receptor type-1 and mechanochemical signal transduction in proximal tubule cells. *Hypertension*. 44(3):352-9, 2004.
- 197 Andrews PM and KR Porter. A scanning electron microscopic study of the nephron. *Am J Anat*. 140(1):81-115, 1974.
- 198 Bulger RE, Siegel FL, and R Pendergrass. Scanning and transmission electron microscopy of the rat kidney. *Am J Anat* 139: 483–502, 1974.
- 199 Astrinidis A, Senapedis W, Henske EP. Hamartin, the tuberous sclerosis complex 1 gene product, interacts with polo-like kinase 1 in a phosphorylation-dependent manner. *Hum Mol Genet*. 15;15(2):287-97, 2006.
- 200 Shillingford JM, Murcia NS, Larson CH, Low SH, Hedgepeth R, et al. The mTOR pathway is regulated by polycystin-1, and its inhibition reverses renal cystogenesis in polycystic kidney disease. *Proc Nat Acad Sci USA* 103:5466–71, 2006.
- 201 Brook-Carter PT, Peral B, Ward CJ, Thompson P, Hughes J, Maheshwar MM, Nellist M, Gamble V, Harris PC, and JR Sampson. Deletion of the TSC2 and PKD1 genes associated with severe infantile polycystic kidney disease--a contiguous gene syndrome. *Nat Genet*. 8(4):328-32, 1994.
- 202 Wilson PD. Polycystic kidney disease. *N Engl J Med*. 8;350(2):151-64, 2004.
- 203 Raychowdhury MK, McLaughlin M, Ramos AJ, Montalbetti N, Bouley R, Ausiello DA, and HF Cantiello. Characterization of single channel currents from primary cilia of renal epithelial cells. *J Biol Chem*. 280(41):34718-22, 2005.
- 204 Resnick A and U Hopfer. Force-response considerations in ciliary mechanosensation. *Biophys. J*. 93: 1380-1390, 2007.

- 205 Akhter S, Kovbasnjuk O, Li X, Cavet M, Noel J, Arpin M, Hubbard AL, and M Donowitz. Na(+)/H(+) exchanger 3 is in large complexes in the center of the apical surface of proximal tubule-derived OK cells. *Am J Physiol Cell Physiol.* 283: C927–C940, 2002.
- 206 Sullivan, LP, Wallace DP and JJ Grantham. Epithelial transport in polycystic kidney disease. *Physiol Rev* 78: 1165-1191, 1998.
- 207 Rohatgi R, Greenberg A, Burrow CR, Wilson PD, and LM Satlin. Sodium transport in autosomal recessive polycystic kidney disease (ARPKD) cyst lining epithelial cells *J. Am. Soc. Nephrol.* 14(4):827-36, 2003.
- 208 Hildebrandt F and W Zhou. Nephronophthisis-associated ciliopathies. *J Am Soc Nephrol.* 18(6):1855-71, 2007.
- 209 Harnett JD, Green JS, Cramer BC, Johnson G, Chafe L, McManamon P, Farid NR, Pryse-Phillips W, and PS Parfrey. The spectrum of renal disease in Laurence-Moon-Biedl syndrome. *N Engl J Med.* 319(10):615-8, 1988.
- 210 Croft JB and M Swift. Obesity, hypertension, and renal disease in relatives of Bardet-Biedl syndrome sibs. *Am J Med Genet* 36: 37–42, 1990.
- 211 Croft JB, Morrell D, Chase CL, and M Swift. Obesity in heterozygous carriers of the gene for the Bardet-Biedl syndrome. *Am J Med Genet* 55: 12–15, 1995.
- 212 Michel JM, Diggle JH, Brice J, Mellor DH, and P Small. Two half-siblings with tuberous sclerosis, polycystic kidneys and hypertension. *Dev Med Child Neurol.* 25(2):239-44, 1993.



- 213 Grantham JJ, Nair V, and F Winklhofer. Cystic diseases of the kidney. In: Brenner BM, ed. Brenner & Rector's The Kidney. Vol. 2. 6th ed. Philadelphia: W.B. Saunders Company; 1699–1730, 2000.
- 214 PKD Foundation  
([http://www.pkdcure.org/site/PageServer?pagename=pkdabt\\_feature\\_testimonylg03](http://www.pkdcure.org/site/PageServer?pagename=pkdabt_feature_testimonylg03))
- 215 Fick GM, Johnson AM, Strain JD, Kimberling WJ, Kumar S, Manco-Johnson ML, Duley IT, and PA Gabow. Characteristics of very early onset autosomal dominant polycystic kidney disease. *J Am Soc Nephrol.* 3(12):1863-70, 1993.
- 216 Blyth H and BG Ockenden. Polycystic disease of kidneys and liver presenting in childhood. *J Med Genet.* 8(3):257-84, 1971.
- 217 Proesmans W, Van Damme B, Casaer P, Marchal, and G. Marchal. Autosomal dominant polycystic kidney disease in the neonatal period: association with a cerebral arteriovenous malformation. *Pediatrics.* 70(6):971-5, 1982.
- 218 Pei Y, Paterson AD, Wang KR, He N, Hefferton D, Watnick T, Germino GG, Parfrey P, Somlo S, and P St George-Hyslop. Bilineal disease and trans-heterozygotes in autosomal dominant polycystic kidney disease. *Am J Hum Genet.* 68(2):355-63, 2001
- 219 Igarashi P and S. Somlo. Genetics and pathogenesis of polycystic kidney disease. *J Am Soc Nephrol.* 13(9):2384-98, 2002.
- 220 Tsiokas, L., E. Kim, T. Arnould, V. P. Sukhatme, and G. Walz. Homo- and heterodimeric interactions between the gene products of PKD1 and PKD2. *Proc. Natl. Acad. Sci. USA* 94:6965-6970, 1997.
- 221 Mochizuki T, Wu G, Hayashi T, Xenophontos SL, Veldhuisen B, Saris JJ, Reynolds DM, Cai Y, Gabow PA, Pierides A, Kimberling WJ, Breuning MH, Deltas CC,

Peters DJ, and S Somlo. PKD2, a gene for polycystic kidney disease that encodes an integral membrane protein. *Science* 272(5266):1339-42, 1996.

222 Schneider MC, Rodriguez AM, Nomura H, Zhou J, Morton CC, Reeders ST, and S Weremowicz. A gene similar to PKD1 maps to chromosome 4q22: a candidate gene for PKD2. *Genomics*. 38(1):1-4, 1996.

223 Nilius B. Store-operated  $\text{Ca}^{2+}$  entry channels: still elusive! *Sci STKE*. 27;2004(243):pe36, 2004.

224 Nauli SM, Alenghat FJ, Luo Y, Williams E, Vassilev P, Li X, Elia AE, Lu W, Brown EM, Quinn SJ, Ingber DE, and J Zhou. Polycystins 1 and 2 mediate mechanosensation in the primary cilium of kidney cells. *Nat Genet* 33:129–137, 2003.

225 Roscoe JM, Brissenden JE, Williams EA, Chery AL, and M Silverman. Autosomal dominant polycystic kidney disease in Toronto. *Kidney Int*. 1993 Nov;44(5):1101-8.

226 Fick GM, Johnson AM, Hammond WS, and PA Gabow. Causes of death in autosomal dominant polycystic kidney disease. *J Am Soc Nephrol*. 5(12):2048-56, 1995.

227 Harrap SB, Davies DL, Macnicol AM, Dominiczak AF, Fraser R, Wright AF, Watson ML, and JD Briggs. Renal, cardiovascular and hormonal characteristics of young adults with autosomal dominant polycystic kidney disease. *Kidney Int*. 40:501 -508, 1991.

228 Torres VE, Wilson DM, Burnett JC, Johnson CM, and KP Offord. Effect of inhibition of converting enzyme on renal hemodynamics and sodium management in polycystic kidney disease. *Mayo Clin Proc* 66:1010-1017, 1991.

- 229 Iversen J, Frandsen H, Norgaard N, and S Strandgaard. Sympathetic nervous activity in adult polycystic kidney disease. *Hypertension* 28:692, 1996.
- 230 Cerasola G, Vecchi ML, Mule G, Cottone S, Mangano MT, Andronico G, Contorno A, Parrino I, Renda F, and G Pavone. Sympathetic activity and blood pressure pattern in autosomal dominant polycystic kidney disease hypertensives. *Am J Nephrol* 18: 391 -398, 1998.
- 231 Hoher B, Zart R, Schwarz A, Vogt V, Braun C, Thone-Reineke C, Braun N, Neumayer H-H, Koppenhagen K, Bauer C, and P Rohmeiss. Renal endothelin system in polycystic kidney disease. *J Am Soc Nephrol* 9: 1169-1177, 1998.
- 232 Giusti R, Neri M, Angelini D, Carlini A, Fiorini I, Bigongiari P, and A Antonelli. Plasma concentration of endothelin and arterial pressure in patients with ADPKD. *Contrib Nephrol* 115: 118-121, 1995.
- 233 Torres VE. Water for ADPKD? Probably, yes. *J. Am. Soc. Nephrol.* 17(8):2089-91, 2006.
- 234 Torres VE, Wilson DM, Offord KP, Burnett JC Jr, and JC Romero. Natriuretic response to volume expansion in polycystic kidney disease. *Mayo Clin Proc.* 64(5):509-15, 1989.
- 235 Torres VE, Donovan KA, Scicli G, Holley KE, Thibodeau SN, Carretero OA, Inagami T, McAteer JA, and CM Johnson. Synthesis of renin by tubulocystic epithelium in autosomal-dominant polycystic kidney disease. *Kidney Int.* 42(2):364-73, 1992.
- 236 Loghman-Adham M, Soto CE, Inagami T, and L Cassis. The intrarenal renin-angiotensin system in autosomal dominant polycystic kidney disease. *Am J Physiol Renal Physiol.* 287(4):F775-88, 2004.

- 237 Casarini DE, Boim MA, Stella RC, Krieger-Azzolini MH, Krieger JE, and N Schor. Angiotensin I-converting enzyme activity in tubular fluid along the rat nephron. *Am J Physiol.* 272: F405–F409, 1997.
- 238 van Kats JP, Schalekamp MA, Verdouw PD, Duncker DJ, and AH Danser. Intrarenal angiotensin II: interstitial and cellular levels and site of production. *Kidney Int.* 60(6):2311-7, 2001.
- 239 Navar LG, Harrison-Bernard LM, Nishiyama A, and H Kobori. Regulation of intrarenal angiotensin II in hypertension. *Hypertension.* 39(2 Pt 2):316-22, 2002.
- 240 Harris, P. J., and J. A. Young. Dose-dependent stimulation and inhibition of proximal tubular sodium reabsorption by angiotensin II in the rat kidney. *Pfluegers Arch.* 367: 295-297, 1977.
- 241 Chatsudthipong V and YL Chan. Inhibitory effect of angiotensin II on renal tubular transport. *Am J Physiol.* 260(3 Pt 2):F340-6, 1991.
- 242 Gardner, K.D., Jr. Composition of fluid in twelve cysts of a polycystic kidney. *N. Engl. J. Med.* 281:985-988, 1969.
- 243 Schwab S, Hinthorn D, Diederich D, Cuppage F, and JJ Grantham. pH-dependent accumulation of clindamycin in a polycystic kidney. *Am J Kidney Dis.* 3(1):63-66, 1983.
- 244 Huseman R, Grady A, Welling D, and JJ Grantham. Macropuncture study of polycystic disease in adult human kidneys. *Kidney Int.* 18(3):375-85, 1980.
- 245 Gardner, K. D.. JR., J. S. Burnside, B. J. Skipper, S. K. Swan, W. M. Bennett, B. A. Connors, and A. P. Evan. On the probability that kidneys are different in autosomal dominant polycystic disease. *Kidney Int.* 42: 1199-1206, 1992.

- 246 Huseman, R., A. Grady, D. Welling, and J.J. Grantham. Macropuncture study of polycystic disease in adult human kidneys. *Kidney Int.* 18: 375-385, 1980.
- 247 Wang T and G Giebisch. Effects of angiotensin II on electrolyte transport in the early and late distal tubule in rat kidney. *Am J Physiol-Renal Physiol.* 271: F143–F149, 1996.
- 248 Barreto-Chaves MLM and M Mello-Aires. Effect of luminal angiotensin II and ANP on early and late cortical distal tubule HCO<sub>3</sub><sup>-</sup> reabsorption. *Am J. Physiol. Renal Physiol.* 271: F977–F984, 1996.
- 249 Ye M and JJ Grantham. The secretion of fluid by renal cysts from patients with autosomal dominant polycystic kidney disease. *N Engl J Med.* 329(5):310-3, 1993.
- 250 Grantham JJ, M Ye, VH Gattone 2nd, and LP Sullivan. In vitro fluid secretion by epithelium from polycystic kidneys. *J. Clin. Invest.* 95(1): 195-202, 1995.
- 251 Perrone, R. D. In vitro function of cyst epithelium from human polycystic kidney. *J. Clin. Invest.* 76: 1688-1691, 1985.
- 252 Gallego MS and BN Ling. Regulation of amiloride-sensitive Na<sup>+</sup> channels by endothelin-1 in distal nephron cells. *Am J Physiol Renal Physiol* 271(2 Pt 2):F451-60, 1996.
- 253 Ecelbarger CA, Kim GH, Terris J, Masilamani S, Mitchell C, Reyes I, Verbalis JG, and MA Knepper. Vasopressin-mediated regulation of epithelial sodium channel abundance in rat kidney. *Am J Physiol Renal Physiol.* 279(1):F46-53, 2000.
- 254 Wilson PD, Sherwood AC, Palla K, Du J, Watson R and JT Norman. Reversed polarity of Na<sup>+</sup>-K<sup>+</sup>-ATPase: mislocation to apical plasma membrane. *Am J Physiol.* 260:F420–F430, 1991.

- 255 Du J and PD Wilson. Abnormal polarization of EGF receptors and autocrine stimulation of cyst epithelial growth in human ADPKD. *Am J Physiol*. 269(2 Pt 1):C487-95, 1995.
- 256 Hua X, JF Collins, L Bai, PR Kiela, RM Lynch, and FK Ghishan. Epidermal growth factor regulation of rat NHE2 gene expression. *Am J Physiol Cell Physiol* 281: C504-C513, 2001.
- 257 Shenolikar S and EJ Weinman. NHERF: targeting and trafficking membrane proteins. *Am J Physiol Renal Physiol*. 280(3):F389-95, 2001.
- 258 Ward CJ, Yuan D, Masyuk TV, Wang X, Punyashtiti R, Whelan S, et al. Cellular and subcellular localization of the ARPKD protein; fibrocystin is expressed on primary cilia. *Hum Mol Genet* 12: 2703-2710, 2003.
- 259 Wang S, Luo Y, Wilson PD, Witman GB, and J Zhou. The autosomal recessive polycystic kidney disease protein is localized to primary cilia, with concentration in the basal body area. *J Am Soc Nephrol* 15: 592-602, 2004.
- 260 Zhang MZ, Mai W, Li C, Cho SY, Hao C, Moeckel G, et al. PKHD1 protein encoded by the gene for autosomal recessive polycystic kidney disease associates with basal bodies and primary cilia in renal epithelial cells. *Proc Natl Acad Sci USA* 101: 2311-2316, 2004.
- 261 Sweeney WE Jr. and ED Avner. Functional activity of epidermal growth factor receptors in autosomal recessive polycystic kidney disease. *Am J Physiol* 275: F387-F394, 1998.

- 262 Hogan MC, Griffin MD, Rossetti S, Torres VE, Ward CJ, and PC Harris. PKHDL1, a homolog of the autosomal recessive polycystic kidney disease gene, encodes a receptor with inducible T lymphocyte expression. *Hum Mol Genet.* 12(6):685-98, 2003.
- 263 Menezes LF, Cai Y, Nagasawa Y, Silva AM, Watkins ML, Da Silva AM, et al. Polyductin, the PKHD1 gene product, comprises isoforms expressed in plasma membrane, primary cilium, and cytoplasm. *Kidney Int* 66:1345-1355, 2004.
- 264 Lin F, Hiesberger T, Cordes K, Sinclair AM, Goldstein LS, Somlo S, and P Igarashi. Kidney-specific inactivation of the KIF3A subunit of kinesin-II inhibits renal ciliogenesis and produces polycystic kidney disease. *Proc Natl Acad Sci USA* 100: 5286–5291, 2003.
- 265 Jiang ST, Chiou YY, Wang E, Lin HK, Lin YT, Chi YC, Wang CK, Tang MJ, and H Li. Defining a link with autosomal-dominant polycystic kidney disease in mice with congenitally low expression of Pkd1. *Am J Pathol.* 168(1):205-20, 2006.
- 266 Hjelle JT, Waters DC, Golinska BT, Steidley KR, Burmeister V, Caughey R, Ketel B, McCarroll DR, Olsson PJ, Prior RB, et al. Autosomal recessive polycystic kidney disease: characterization of human peritoneal and cystic kidney cells in vitro. *Am J Kidney Dis.* 15(2):123-36, 1990.
- 267 Rohatgi R, Zavilowitz B, Vergara M, Woda C, Kim P, and LM Satlin. Cyst fluid composition in human autosomal recessive polycystic kidney disease. *Pediatr Nephrol.* 20(4):552-3, 2005.
- 268 Veizis EI, Carlin CR, and CU Cotton. Decreased amiloride-sensitive Na<sup>+</sup> absorption in collecting duct principal cells isolated from BPK ARPKD mice. *Am J Physiol Renal Physiol*, 286:244-54, 2004.

- 269 Vehaskari VM, Hering-Smith KS, Moskowitz DW, Weiner ID, and LL Hamm. Effect of epidermal growth factor on sodium transport in the cortical collecting tubule. *Am J Physiol Renal Fluid Electrolyte Physiol* 256: F803–F809, 1989.
- 270 Shen JP and CU Cotton. Epidermal growth factor inhibits amiloride-sensitive sodium absorption in renal collecting duct cells. *Am J Physiol Renal Physiol* 284: F57–F64, 2003.
- 271 Loghman-Adham M, Soto CE, Inagami T, and C Sotelo-Avila. Expression of components of the renin-angiotensin system in autosomal recessive polycystic kidney disease. *J Histochem Cytochem.* 53(8):979-88, 2005.
- 272 Banizs B, Komlosi P, Bevensee MO, Schwiebert EM, Bell PD, and BK Yoder. Altered pH(i) regulation and Na(+)/HCO<sub>3</sub>(-) transporter activity in choroid plexus of cilia-defective Tg737(orpk) mutant mouse. *Am J Physiol Cell Physiol.* 292:C1409 - C1416, 2007.
- 273 Hovater MB, Olteanu D, Hanson EL, Cheng NL, Siroky B, Fintha A, Komlosi P, Bell PD, Yoder BK, and EM Schwiebert. Loss of apical monocilia on collecting duct principal cells impairs apically-directed ATP release and flow-induced calcium signals in an integrated system. *Purinergic Signaling* 3(3): In Press, 2007.
- 274 Wakabayashi S, Bertrand B, Ikeda T, Pouyssegur J, and M Shigekawa. Mutation of calmodulin-binding site renders the Na<sup>+</sup>/H<sup>+</sup> exchanger (NHE1) highly H<sup>+</sup>-sensitive and Ca<sup>2+</sup> regulation-defective. *J Biol Chem.* 269:13710-13715, 1994.
- 275 Mazzochi C, Benos DJ, and PR Smith. Interaction of epithelial ion channels with the actin-based cytoskeleton. *Am J Physiol Renal Physiol.* 291(6):F1113-22, 2006.



- 276 Simons, K. and SD Fuller. Cell surface polarity in epithelia. *Annu. Rev. Cell Biol.* 1:243-288, 1985.
- 277 Hovater MB, Olteanu D, Welty EA, and EM Schwiebert. Purinergic signaling in the lumen of a normal nephron and in remodeled PKD encapsulated cysts. *Purinergic Signaling* 3 (3): In Press, 2007.
- 278 Wilson PD, Hovater JS, Casey CC, Fortenberry JA and EM Schwiebert. ATP release mechanisms in primary cultures of epithelia derived from the cysts of polycystic kidneys. *J Am Soc Nephrol.* 10(2):218-29, 1999.
- 279 Rembold CM, Weaver BA and J. Linden. Adenosine triphosphate induces a low  $[Ca^{2+}]_i$  sensitivity of phosphorylation and an unusual form of receptor desensitization in smooth muscle. *J Biol Chem.* 25;266(9):5407-11, 1991.
- 280 Dubyak, G. R., and C. El-Moatassim. Signal transduction via P2-purinergic receptors for extracellular ATP and other nucleotides. *Am. J. Physiol.* 265 (Cell Physiol. 34): C577-C606, 1993
- 281 Leipziger J. Control of epithelial transport via luminal P2 receptors. *Am J Physiol Renal Physiol.* 284(3):F419-32, 2003.
- 282 Bagorda A, Guerra L, Di Sole F, Helmle-Kolb C, Favia M, Jacobson KA, Casavola V, and SJ Reshkin. Extracellular adenine nucleotides regulate  $Na^+/H^+$  exchanger NHE3 activity in A6-NHE3 transfectants by a cAMP/PKA-dependent mechanism. *J Membr Biol* 188: 249–259, 2002.
- 283 Urbach V, Hélix N, Renaudon B and BJ Harvey. Cellular mechanisms for apical ATP effects on intracellular pH in human bronchial epithelium. *J Physiol.* 15;543(Pt 1):13-21, 2002.

- 284 Vallet V, Chraibi A, Gaeggeler HP, Horisberger JD and BC Rossier. An epithelial serine protease activates the amiloride-sensitive sodium channel. *Nature*. 389(6651):607-10, 1997.
- 285 Chraibi A, Vallet V, Firsov D, Hess SK and JD Horisberger. Protease modulation of the activity of the epithelial sodium channel expressed in *Xenopus* oocytes. *J Gen Physiol*. 111(1):127-38, 1998.
- 286 Rossier BC. The epithelial sodium channel: activation by membrane-bound serine proteases. *Proc Am Thorac Soc*. 1(1):4-9, 2004.
- 287 Hughey RP, Bruns JB, Kinlough CL, Harkleroad KL, Tong Q, Carattino MD, Johnson JP, Stockand JD and TR Kleyman. Epithelial sodium channels are activated by furin-dependent proteolysis. *J Biol Chem*. 30;279(18):18111-4, 2004.
- 288 Geng L, Burrow CR, Li HP and PD Wilson PD. Modification of the composition of polycystin-1 multiprotein complexes by calcium and tyrosine phosphorylation. *Biochim Biophys Acta*.1535(1):21-35, 2000.
- 289 Li Q, Montalbetti N, Shen PY, Dai XQ, Cheeseman CI, Karpinski E, Wu G, Cantiello HF and XZ Chen. Alpha-actinin associates with polycystin-2 and regulates its channel activity. *Hum Mol Genet*. 14(12):1587-603, 2005.
- 290 Mai W, Chen D, Ding T, Kim I, Park S, Cho SY, Chu JS, Liang D, Wang N, Wu D, Li S, Zhao P, Zent R and G Wu. Inhibition of Pkhd1 impairs tubulomorphogenesis of cultured IMCD cells. *Mol Biol Cell*. 16(9):4398-409.0, 2005.
- 291 Pazour GJ, San Agustin JT, Follit JA, Rosenbaum JL and GB Witman. Polycystin-2 localizes to kidney cilia and the ciliary level is elevated in orpk mice with polycystic kidney disease. *Curr Biol*.12(11):R378-80, 2002.

- 292 Charron AJ, Nakamura S, Bacallao R and A Wandering-Ness A. Compromised cytoarchitecture and polarized trafficking in autosomal dominant polycystic kidney disease cells. *J Cell Biol.* 149(1):111-24, 2000.
- 293 Charron AJ, Bacallao RL and A. Wandering-Ness. ADPKD: a human disease altering Golgi function and basolateral exocytosis in renal epithelia. *Traffic.* 1(8):675-86, 2000.
- 294 Szaszi K, Paulsen A, Szabo EZ, Numata M, Grinstein S and J Orłowski. Clathrin-mediated endocytosis and recycling of the neuron-specific Na<sup>+</sup>/H<sup>+</sup> exchanger NHE5 isoform. Regulation by phosphatidylinositol 3'-kinase and the actin cytoskeleton. *J Biol Chem.* 277(45):42623-32, 2002.
- 295 Koyama K, Sasaki I, Naito H, Funayama Y, Fukushima K, Unno M, Matsuno S, Hayashi H and Y Suzuki. Induction of epithelial Na<sup>+</sup> channel in rat ileum after proctocolectomy. *Am J Physiol.* 276(4 Pt 1):G975-84, 1999.
- 296 Iordache C and M Duszyk. Sodium 4-phenylbutyrate upregulates ENaC and sodium absorption in T84 cells. *Exp Cell Res.* 15;313(2):305-11, 2007.
- 297 Hernández-González EO, Sosnik J, Edwards J, Acevedo JJ, Mendoza-Lujambio I, López-González I, Demarco I, Wertheimer E, Darszon A and PE Visconti. Sodium and Epithelial Sodium Channels Participate in the Regulation of the Capacitation-associated Hyperpolarization in Mouse Sperm *J Biol Chem.* 281(9):5623-33, 2006.
- 298 Inagaki A, Yamaguchi S and T Ishikawa. Amiloride-sensitive epithelial Na<sup>+</sup> channel currents in surface cells of rat rectal colon. *Am J Physiol Cell Physiol.* 286(2):C380-90, 2004.

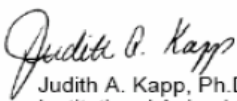
- 299 Lee JE, Park MH and JH Park. The gene expression profile of cyst epithelial cells in autosomal dominant polycystic kidney disease patients. *J Biochem Mol Biol.* 30;37(5):612-7, 2004.
- 300 Hill C, Giesberts AN and SJ White. Expression of isoforms of the Na(+)/H(+) exchanger in M-1 mouse cortical collecting duct cells. *Am J Physiol Renal Physiol.* 282(4):F649-54, 2002.
- 301 Bachmann O, Riederer B, Rossmann H, Groos S, Schultheis PJ, Shull GE, Gregor M, Manns MP and U. Seidler. The Na<sup>+</sup>/H<sup>+</sup> exchanger isoform 2 is the predominant NHE isoform in murine colonic crypts and its lack causes NHE3 upregulation. *Am J Physiol Gastrointest Liver Physiol.* 287(1):G125-33, 2004.
- 302 Hill JK, Brett CL, Chyou A, Kallay LM, Sakaguchi M, Rao R and PG Gillespie. Vestibular hair bundles control pH with (Na<sup>+</sup>, K<sup>+</sup>)/H<sup>+</sup> exchangers NHE6 and NHE9. *J Neurosci.* 26(39):9944-55, 2006.
- 303 Schwiebert EM and A Zsembery. Extracellular ATP as a signaling molecule for epithelial cells. *Biochim Biophys Acta.* 2;1615(1-2):7-32, 2003.

APPENDIX A  
MEMORANDUM

MEMORANDUM

DATE: November 22, 2006

TO: Bradley K. Yoder, Ph.D.  
MCLM-652 0005  
FAX: 934-0950

FROM:   
Judith A. Kapp, Ph.D., Chair  
Institutional Animal Care and Use Committee

SUBJECT: **NOTICE OF APPROVAL - Please forward this notice to the appropriate granting agency.**

---

The following application was reviewed and approved by the University of Alabama at Birmingham Institutional Animal Care and Use Committee (IACUC) on November 22, 2006.

Title of Application: Cilia and Cystic Kidney Disease  
Fund Source: NIH

This institution has an Animal Welfare Assurance on file with the Office of Laboratory Animal Welfare (OLAW) (Assurance Number A3255-01) and is registered as a Research Facility with the United States Department of Agriculture. The animal care and use program is accredited by the Association for Assessment and Accreditation of Laboratory Animal Care (AAALAC International).

**Institutional Animal Care and Use Committee**  
B10 Volker Hall  
1670 University Boulevard  
205.934.1294  
FAX 205.975.7886


Mailing Address:  
VH B10  
1530 3RD AVE S  
BIRMINGHAM AL 35294-0019

APPENDIX B  
NOTICE OF APPROVAL

**NOTICE OF APPROVAL**

**DATE:** November 22, 2006

**TO:** Bradley K. Yoder, Ph.D.  
MCLM-652 0005  
FAX: 934-0950

**FROM:**   
Judith A. Kapp, Ph.D., Chair  
Institutional Animal Care and Use Committee

**SUBJECT:** Title: Cilia and Cystic Kidney Disease  
Sponsor: NIH  
Animal Project Number: 061106733

---

On November 22, 2006, the University of Alabama at Birmingham Institutional Animal Care and Use Committee (IACUC) reviewed the animal use proposed in the above referenced application. It approved the use of the following species and numbers of animals:

Species	Use Category	Number in Category
Mice	B	400
Mice	A	1360

Animal use is scheduled for review one year from November 2006. Approval from the IACUC must be obtained before implementing any changes or modifications in the approved animal use.

**Please keep this record for your files, and forward the attached letter to the appropriate granting agency.**

Refer to Animal Protocol Number (APN) 061106733 when ordering animals or in any correspondence with the IACUC or Animal Resources Program (ARP) offices regarding this study. If you have concerns or questions regarding this notice, please call the IACUC office at 934-7692.

**Institutional Animal Care and Use Committee**  
B10 Volker Hall  
1670 University Boulevard  
205.934.1294  
FAX 205.975.7886

Mailing Address:  
VH B10  
1530 3RD AVE S  
BIRMINGHAM AL 35294-0019